Faculty of Resource Science and Technology

Molecular Docking, ADME Evaluation and Synthesis of Thiourea Derivatives and Their Metal Complexes as Potential Antibacterial Agents

Brandon Sanday Anak Mominn

Master of Science
2025

Molecular Docking, ADME Evaluation and Synthesis of Thiourea Derivatives and Their Metal Complexes as Potential Antibacterial Agents

Brandon Sanday Anak Mominn

A thesis submitted

In fulfillment of the requirements for the degree of Master of Science

(Chemistry)

Faculty of Resource Science and Technology

UNIVERSITI MALAYSIA SARAWAK

2025

DECLARATION

I declare that the work in this thesis was carried out in accordance with the regulations of Universiti Malaysia Sarawak. Except where due acknowledgements have been made, the work is that of the author alone. The thesis has not been accepted for any degree and is not concurrently submitted in candidature of any other degree.

……

Signature

Name: Brandon Sanday Anak Mominn

Matric No.: 21020152

Faculty of Resource Science and Technology

Universiti Malaysia Sarawak

Date: 20th October 2025

ACKNOWLEDGEMENT

First and foremost, I would like to thank my parents Mr. Mominn Jenta Gem and Madam Sweether Anak Nuri for giving me their supports be it morally or financially while finishing this project. Thank you for believing in me and for your unconditional love.

Special thanks to my supervisor, Dr. Maya Asyikin binti Mohamad Arif for guiding me throughout this project. Thank you for your supervision and sharing your impeccable ideas with me. I am grateful to be able to work with you. Thank you for your patience and for your unwavering support.

To the staff of the faculty, the science officers, Mr. Leo Bulin Anak Unting and Mr. Wahap bin Warni, thank you for teaching me and giving me permission to operate the laboratory instruments. I truly learned a lot from handling those machines. Likewise, to the lab assistants, Mr. Ismadi bin Rosli, Madam Leida Anak Anthony, Madam Dayang Fatimawati binti Awg Alli and Madam Norhayati binti Bujang, many thanks for your assistance and helpful gesture. Without all of you, it would be difficult to complete this research.

I would also like to express my gratitude to those from the Biology Department, lecturer Madam Fazia binti Mohamed Sinang and fellow postgraduates Sabella binti Justin, Nur Azzah binti Osman, Emmanuelle Usun Stephen and Scholastica Ramih Bunya for teaching me and guiding me especially to conduct the latter part of this research. It has been an amazing journey thanks to you guys. To my senior, Mr. Faris Danish, thank you for your words of encouragement and sharing your knowledge with me, your wisdom and perseverance really inspired me to finish my Master's degree.

To the Centre of Graduate Studies UNIMAS, a sincere thank you for the assistance and guidance all this time. To Yayasan Sarawak, thank you for awarding me the scholarship during the pursuit of this Master's degree. It is such an honour to be one of the scholarship recipient. To my closest friend, Mr. Saravanan Mohandas, thank you for believing in me and encouraging me to complete my studies. Finally, to any individual who directly and indirectly contributed to this project, I thank you from the depth of my heart. This project is specially dedicated to all of you.

ABSTRACT

Antibacterial resistance has become a major threat worldwide. Due to lack of discovery of new antibiotics and increasing cases of resistance, there is an urgent need to discover novel classes of antibiotics with improved activity and less toxicity with the help of computational tools. Twelve amino acid bearing thiourea compounds had been docked using AutoDock Vina 1.5.6 against DNA Gyrase Enzyme (PDB ID: 1KZN) and pharmacologically evaluated using SwissADME software to look for potential antimicrobial agent. The cinnamoyl derivatives (compound **1-3**) demonstrated high docking scores between -5.7 and 7.1 kJ/mol along with good pharmacokinetic profiles with the adherence to the Lipinski's Rule of Five. Subsequently, the docking of Cu(II), Zn(II) and Co(II) complexes of compound **1-3** recorded higher docking scores between -6.9 and -8.3 kJ/mol compared to its free ligand despite violation of the Lipinski's Rule. Thus, compound **1-3** and its complexes were selected for synthesis. The formation of compound **1-3** was confirmed by the presence of NH and C=S groups at 3165 – 3056 cm^{-1} and 1293 – 1269 cm^{-1} respectively, based on Fourier Transform Infrared (FTIR) spectra as well as -CONH and -CSNH signals at δ_H 11.4 - 11.2 ppm from ^1H Nuclear Magnetic Resonance (NMR) data. The formation of complexes were confirmed by the shifting of C=O of the carboxylate group at 1731-1716 cm^{-1} to a lower frequency. The biological evaluation of compound **1-3** and complexes **1a-3c** against *E. coli* ATCC 25922 strain by agar well method indicated that compound **2**, complex **1a** and **2a** were potentially active antimicrobial agents with inhibition zone 11 – 13 mm. This study offers a computer-driven discovery of novel thiourea compound and its complexes as antibacterial agent.

Keywords: Thiourea, metal complex, antibacterial, molecular docking, ADME

Pengedokan, Penilaian ADME dan Sintesis Terbitan Tiourea dan Kompleks Logam Sebagai Ejen Antibakteria yang Berpotensi

ABSTRAK

*Rintangan bakteria merupakan ancaman yang besar di peringkat global. Kekurangan penemuan antibiotik baharu dan peningkatan kes-kes rintangan telah menggesa penciptaan antibiotik yang lebih berkesan dan kurang kesan sampingan dengan bantuan komputer. Dua belas sebatian tiourea yang mengandungi asid amino telah direka dan menjalani simulasi pengedokan terhadap protein DNA gyrase (ID Protein:1KZN) dan dinilai dari ciri farmakologi. Terbitan sinamoil (sebatian **1-3**) mencatatkan skor tenaga dari -5.7 hingga -7.1 kJ/mol serta mempunyai ciri farmakokinetik yang memenuhi syarat Lipinski. Seterusnya, pengedokan kompleks logam Cu(II), Zn(II) dan Co(II) bagi sebatian **1-3** mencatatkan skor tenaga yang lebih tinggi berbanding ligand bebas iaitu sebanyak -6.9 kJ/mol hingga -8.3 kJ/mol walaupun melanggar prinsip Lipinski. Oleh itu, sebatian **1-3** dan logam kompleks tersebut dipilih untuk disintesis. Pembentukan sebatian **1-3** telah disahkan dengan kehadiran kumpulan fungsi -NH dan -C=S di 3165 – 3056 cm^{-1} dan 1293 – 1269 cm^{-1} berdasarkan Spektroskopi Inframerah Transformasi Fourier serta signal -CONH dan -CSNH di δ_H 11.4-11.2 ppm daripada data ^1H Resonans Magnetik Nuklear. Pembentukan kompleks logam pula disahkan dengan peralihan kumpulan fungsi C=O karbosilat di 1731-1716 cm^{-1}ke frekuensi yang lebih rendah. Penilaian biologi terhadap strain ATCC 25922 bakteria* E. coli *melalui kaedah peresapan agar menunjukkan yang sebatian **2**, **1a** and **2a** berpotensi sebagai ejen bakteria dengan zon perencatan 11 – 13 mm. Projek ini memaparkan potensi sebatian tiourea dan logam kompleksnya sebagai ejen antibakteria.*

Kata kunci: *Tiourea, logam kompleks, antibakteria, pengedokan, penilaian ADME*

TABLE OF CONTENTS

LIST OF TABLES

LIST OF FIGURES

LIST OF ABBREVIATIONS

AMR	Antimicrobial resistance
ADME	Absorption, distribution, metabolism and excretion
AME	Aminoglycoside modifying enzyme
AR	Androgen receptor
ATR-IR	Attenuated Total Reflectance Infrared Spectroscopy
BBB	Blood brain barrier
CA	Carbonic anhydrase
CADD	Computer aided drug design
CDK	Cyclin dependent kinase
CL	Chain length
CNS	Central nervous system
COX-2	Cyclooxygenase-2
CRPC	Castration-resistant prostate cancer
CTGF	Connective tissue growth factor
CuNP	Copper nanoparticle
DCM	Dichloromethane
DMSO	Dimethylsulfoxide
ENR	Enrofloxacin
EP	Efflux pump
FDA	Food and Drug Administration
FTIR	Fourier transform infrared spectra
GI	Gastrointestinal
GLASS	Global Antimicrobial Resistance and Use Surveillance System
Hertz	Hz
IR	Infrared spectra
LOX	Lipoxygenase
mCRPC	Metastatic castration-resistant prostate cancer
MD	Molecular dynamic
MDR	Multi-drug resistant
MIC	Minimum inhibitory concentration
MMP-2	Matrix metalloproteinase-2

MOE	Molecular operating environment
MRSA	Methicillin-resistant *Staphylococcus aureus*
NAL	Nalidixic acid
NCE	New chemical entities
NMR	Nuclear magnetic resonance
NMT	N-myristoyltransferase
NP	Natural product
PAINS	Pan Assay Interference Compounds
PBP	Penicillin-binding proteins
PDB	Protein Data Bank
P-pg	P-glycoprotein
QRDR	Quinolone-resistance determining region
QSAR	Quantitative structure-activity relationship
RMSD	Root mean square deviation
Ro5	Rule of five
ROS	Reactive oxygen species
SAR	Structure activity relationship
THF	Tetrahydrofuran
TMS	Tetramethylsilane
TNF-α	Tumour necrosis factor alpha
UTI	Urinary tract infections
WHO	World Health Organization
XDR	Extensively-drug resistant

CHAPTER 1

INTRODUCTION

1.1 Study background

According to the World Economic Forum (2020), antibiotic resistance (AMR) poses a serious threat to the healthcare system. This statement is further supported by a review by O'neill, (2014) which estimated 10 million deaths worldwide by 2050 as a result of drug-resistant diseases that will give a disastrous impact to the economy in that vein of the 2008-2009 financial crisis and put up to 24 million people into extreme poverty by 2030 (World Bank Document, 2017). According to Institute for Health Metrics and Evaluation (n.d.), 3 500 deaths due to AMR and 14 000 deaths linked to AMR were reported in Malaysia in 2019. Bernama (2024) projected 87 000 deaths from 2020 to 2030 if this situation is not tackled. In modern medicine, antibiotics had reduced the mortality and morbidity rates while the global consumption of antibiotics surged from 21.1 billion to 34.8 billion doses from 2000 to 2015 proving the increase in its demand in the health industry (Klein et al., 2018). The excessive usage of antimicrobials however speeds up the AMR process which subsequently led to the emergence of multi-drug resistant (MDR) and extensively drug-resistant (XDR) bacteria such as *Mycobacterium tuberculosis* and methicillin-resistant *Staphylococcus aureus* (MRSA) (Yam et al., 2019). Thus, there is an urgent need to develop new antibiotic and a completely new classes of compound that do not develop resistance easily (Sovari & Zobi, 2020).

Escherichia coli is a gram negative bacteria belonging to the family of *Enterobacteriaceae* commonly found in the gastrointestinal tract and warm blooded animals

as well as in soil and water (Monisha et al., 2022; Denamur et al., 2021; Pakbin et al., 2023). It is the common cause of bacterial meningitis (Pelkonen et al., 2020), urinary tract infections (UTI) (Haley et al., 2024; Sokhn et al., 2020) and food borne diseases (Pakbin et al., 2023). Unlike gram-positive bacteria, gram-negative bacteria are coated with another bilayer outside of its peptidoglycan layer which offers special protection from not only polar molecules but also some lipophilic compound (Henderson et al., 2016). Therefore, gram-negative bacteria are always considered to be more difficult to kill due to the low penetration of compound across the additional membrane. *E. coli* had been listed in World Health Organization (WHO) list of Priority Pathogen list in 2017 (WHO, 2024). According to Global Antimicrobial Resistance and Use Surveillance System (GLASS) Report by WHO (2022), the resistance rate of *E. coli* against third-generation cephalosporin was reported at 42% in 76 countries while one-fifth of UTI cases due to *E. coli* was found to be less susceptible against common drugs such as ampicillin, co-trimoxazole and fluoroquinolones in 2020. A study conducted in Bangladesh demonstrated high prevalence rate of *E. coli* resistance against antibiotic Ciprofloxacin (Das et al., 2023). Furthermore, it was expected that by 2050, *E. coli* resistance will account for 30% of the total 10 million cases of MDR annually (O'neill, 2014).

Thiourea or thiocarbamide is a white crystalline solid containing sulphur and nitrogen atoms (Mohapatra et al., 2019). The molecular structure was reported as analogous of urea by Puzzarini (2012), with the replacement of its C=O group into C=S group (Figure 1.1). The application of thiourea for medicinal purposes are well documented in literature such as anticancer (Kirishnamaline et al., 2021), antimicrobial (Ghorab et al., 2017), as potential treatment of Alzheimer's diseases (Ujan et al., 2021) as well as ion recognition and

sensor in biological media (Mitrea & Cîrcu, 2021). In addition, thiourea derivatives as ionophore for metal detection for application in environmental remediation had been reported by Khairul et al., (2016a) thanks to the presence of π-conjugated system and multiple ligand binding site with metal ions. The preparation of substituted thiourea derivatives can be done by condensation of primary or secondary amine with isothiocyanate groups (Fakhar et al., 2018; Hou et al., 2023) although synthesis using carbon disulphide had been reported by Naz et al., (2020). In addition, thiourea makes an attractive candidate as a potential candidate of antibiotic due to the presence of C=S, C=O and NH functionality that can be easily protonated under acidic condition thus able to react with the phosphate and carboxylate groups of the bacterial membrane to exert its antibacterial activity (Shalas et al., 2023). Several studies had demonstrated that thiourea derivatives were particularly active against Gram negative strains such as *K. Pneumoniae* and *E. coli* (Ramaswamy et al., 2022; Xu et al., 2024). Moreover, the presence of these functional groups which is similar to that of urea is reported to have excellent cytotoxicity thus makes them as potential anticancer candidate (Makeen & Albratty, 2023).

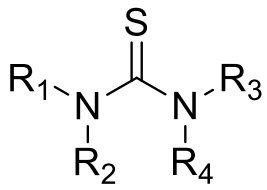

Figure 1.1: General structure of thiourea

Meanwhile, coordination chemistry of urea and thiourea had received tremendous response by various researchers over the years owing to its various application (Mohapatra et al., 2019). Thiourea moieties containing O, N and S atoms have gained interest due to their various coordination modes and it can exist in both neutral and anionic state (Cunha et

al., 2018; Wei et al., 2017). The increasing metal-based therapies advancing through the clinical trials had opened the door for more metal-containing drugs as a potential treatment of various diseases (Boros et al., 2020). The versatility of transition metal compound offer new and improved compounds for medicinal application and the history of metal-based drugs could be traced all the way back in 1978 when cisplatin (Figure 1.2) was approved as anticancer drugs which subsequently renewed interest in the study of metal complexes for medicinal applications (Cirri et al., 2021). Furthermore, the variable in its oxidation state allows metal centre to coordinate with different ligands which lead to the design of better novel compound with improved efficacy and reduced side effects along with better physical properties (Khan et al., 2020).

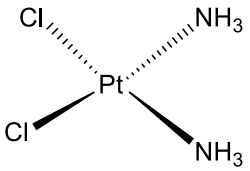

Figure 1.2: Molecular structure of metal-based anticancer drug, Cisplatin

As of July 2019, there were only 42 antibiotic drugs advancing into clinical trials (The Pew Charitable Trust, 2019). Although this number looks rather impressive on its own, it is still subpar when compared to anticancer drugs which amassed a total of 1100 drugs for clinical trials in 2018 (Powaleny, 2018). Furthermore, 75% of antimicrobial drugs are simply derivatives of already existing compounds therefore there are tendency of microorganisms developing resistance towards them (Roope et al., 2019). This lukewarm numbers might be driven by the fact that companies unwilling to invest on its research and development on finding new antibiotics due to low return (Roope et al., 2019). In addition, most antimicrobials being studied are purely organic with metal being neglected due to the association with toxicity (Frei et al., 2020). However, Frei et al. (2020) reported that metal

based compound had higher hit rate against fungi as well as *Enterococcus faecium, S.aureus, Klebsiella pneumoniae, Acinetobacter baumannii, Pseudomonas aeruginosa* and *Enterobacter species* or collectively known as the ESKAPE pathogens suggesting an imminent potential of metal complex compound as new class of antibiotic in the future.

Bringing a new drug to a market is a complicated process that costs millions. Many potential compounds despite the efficacy were discontinued along the way due to severe side effects. Furthermore, the hurdle process to get the FDA approval is making the process even more complex. Computational method such as molecular docking and ADME evaluation offers a useful approach in designing new and potent drugs which helps to save time and cost by focusing only on the potentially active lead molecules. Molecular docking helps to study the binding interaction of molecules on specific target enzyme, which could improve the selectivity of a candidate molecule and subsequently reduce the potential side effects (Labute et al., 2014). DNA gyrase enzyme is an enzyme that command the negative supercoiling in bacterial DNA enzyme during cell replication. Targeting this enzyme as main target in designing antibacterial agents help to improve the selectivity of a drug molecule due to the enzyme being solely present in bacteria cell (Rajakumari et al., 2024). Many studies have documented the potential of thiourea derivatives as the inhibitors of gyrase enzyme, thus it could be a new potential molecule to tackle the AMR issues (Hashem et al., 2020; Rana et al., 2024). Additionally, ADME evaluation offers the pharmacological assessment of designed compound by predicting the pharmacokinetic properties such as bioavailability, physicochemical properties as well as the permeability in the blood brain barrier (BBB) (M Honório et al., 2013). These information are valuable as it gives insight on how drugs are being distributed, metabolized and excreted in the body. It also helps to

predict the possible drug-drug interaction and potential side effects.

Herein this study, computational tools such as AutoDock Vina and SwissADME had been utilized to design twelve amino acid thioureas and their metal complexes as potential antibacterial agents. Subsequently, the most potentially active thiourea and its complexes were then synthesised and characterized with various spectroscopic methods such FTIR, NMR, CHNS elemental analysis and UV-Vis spectra. The antibacterial activities were then evaluated using agar well diffusion method against *E. coli* ATCC 25922 strain.

1.2 Problem statement

AMR refers to a situation when common drugs are no longer effective in killing bacteria (Murray et al., 2022). When this happens, common diseases caused by bacterial infections can no longer be treated with existing antibiotics while surgical procedures or chemotherapy among cancer patients for instance can no longer be performed without putting these patients at risk of acquiring bacterial infections (Nanayakkara et al., 2021; Teillant et al., 2015). Consequently, diseases are becoming difficult to treat, patients will experience longer hospitalization period and it will enforce economic burden to the humanity (Kumar et al., 2024; Mayito et al., 2024; World Bank, 2017). *E. coli* is a common gram-negative bacterial that is found in the intestinal microflora. The resistance of *E. coli* against antibiotics were frequently reported and posed as a serious threat to the healthcare community (Babines-Orozco et al., 2024; Hassuna et al., 2024). Most of the existing antibiotic drugs, while effectively kills bacteria, suffer from how easily it is to develop resistance against bacteria. Furthermore, the antibiotic pipeline is experiencing a major drawback because of big pharmaceutical companies refusing to take part in antibiotic research leading to discovery void for many years as there is no new compound approved for the treatment of infections (Dutescu & Hillie, 2021). To address this issue, it is critical to design and develop new classes of compound as potential candidates of antibiotics that do not develop resistance easily. Computer aided drug design (CADD) such as molecular docking and ADME evaluation should be incorporated in designing novel compounds to study the binding interaction and predict the pharmacokinetic behaviors of novel compounds. Thiourea and its complexes represent a promising class of compounds to combat antibacterial resistance. While thioureas were reported to have antibacterial potential, some of the reported structures were too bulky (Fakhar et al., 2018), limited by the

number of alkyl chains (Abd Halim and Ngaini, 2016), long reaction time (Lalmangaihzuala et al., 2024) or is less or completely ineffective against *E.coli* strain (Tagiling et al., 2024). Therefore, small and less bulky cinnamoyl thioureas with amino acids side chains were designed as an antibacterial agent. Amino acids side chains were incorporated in the structure to improve the antibacterial properties, as well as its solubility (Alsalhi et al., 2022; Idrees et al., 2020). Furthermore, metal complex compound are sought after to be the next generation of antibiotics owing to their structural diversity, less toxicity and ligand exchange ability (Kamalov et al., 2024; King et al., 2024; Meier-Menches et al., 2018). Thus, by combining the antibacterial properties of thiourea and metal centers , a new and improved drug will be introduced in the future that could possibly defy resistance.

1.3 Objectives

This research was conducted with the following objectives:

i. To design twelve novel thiourea and its metal complexes as potent antibacterial agent using computational tools such as Autodock Vina and Biovia Discovery Studio software.

ii. To evaluate the pharmacokinetic profiles of designed compounds using SwissADME software.

iii. To synthesize and characterize novel cinnamoyl thiourea compounds along with its Cu(II), Zn(II) and Co(II) complexes using FTIR, ^{1}H NMR, ^{13}C NMR, UV-Vis spectra and CHNS elemental analysis.

iv. To investigate the antibacterial properties of cinnamoyl thiourea and its complexes against *E. coli* (ATCC25922) strain using agar well diffusion method.

CHAPTER 2

LITERATURE REVIEW

2.1 Antimicrobial resistance (AMR)

Thanks to the antibiotics, treatment of life-threatening infections are made possible, securing the health of many patients worldwide. However, the emergence of antimicrobial resistance due to the uncontrolled antibiotic usage posed an alarming global health challenge. Murray et al., (2022) estimated 4.95 million deaths associated with AMR in 2019. Of that sum, 1.27 million deaths were attributed to AMR. Furthermore, it was estimated that by 2050, 10 million deaths will be caused by AMR with an estimated loss of US$100 trillion (O'neill et al., 2014). However, it is notable that these estimations were made before the Covid-19 pandemic hits in 2019 whereby a significant increase was observed in antibiotics consumption in the period of 2019-2020 (Hussein et al., 2022). In Malaysia, 1190 AMR cases were reported from 2017 until 2020 from 146 Ministry of Health hospital with a reported cost of admission increased from RM 3.7 million in 2017 to a whopping RM 9.7 million in 2019 (Abdul Rassip et al., 2025). Drug resistance pathogens hinder the effort to treat infectious disease as drugs became ineffective for treatment of diseases on top of increasing the severity of the condition and higher rate of transmittance (Micoli et al., 2021).

One of the most important strategies in tackling AMR is to discover and develop potent antimicrobial agents (Hou et al., 2023). However, many big pharmaceutical companies such as Novartis, Astrazeneca and Allergan had drawn out of their antibiotic research. The difficulty and the complex clinical and regulatory procedure as well as low return led to many companies to disinvest from research and development of antibiotic

(Gajdács, 2019; Singer et al., 2020). For instance, in the US, the number of new antibiotics approved decreased significantly from 1980 to 2014 (Figure 2.1) while at the same tracking period the number of anticancer drugs went up (Plackett, 2020). The future of antibiotic pipelines are looking very bleak right now therefore it is important that we develop new classes of compound that could tackle this issue. Furthermore, as seen from the SARS-CorV-2 pandemic, the effect of infectious disease is nothing to be reckoned with as it could cause catastrophic effect on economy and rate of mortality.

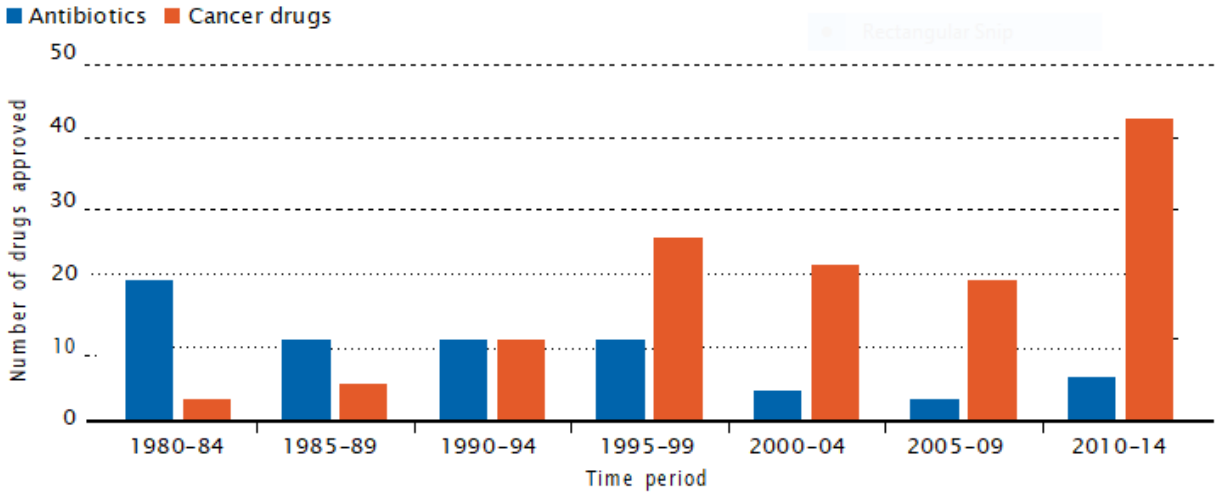

Figure 2.1: Comparison of number of approved antibiotics and cancer drugs in the US in the period of 1980-2014 (Plackett, 2020).

Similarly in Malaysia the country is also suffering from the same burden with reported resistance of some common bacteria towards antibiotics. According to the latest report in 2024, bacteria such as *Staphylococcus* and *Salmonella* had increasing resistance towards antibiotics. Additionally, from the report, *E. coli* samples had account for one of the most collected samples with 60 438 samples compared to other bacteria. Although the percentage of resistance was taking a dip in 2024, the previous years showed continuous

upwards trend in some antibiotics which is alarming especially Ciprofloxacin which consistently falls within 25%-30% range (Institute for Medical Research, 2024).

2.1.1 Mechanisms of AMR

Bacteria develop several mechanisms to resist the anti-microbial action of drugs. It is known that bacteria produce a specific enzyme to inactivate and modify drugs. An example of modifying enzyme is the aminoglycoside modifying enzyme (AMEs) that modifies aminoglycoside molecules through the alteration of hydroxyl or amino molecules (Munita & Arias, 2016). A study by Bordeleau et al., (2021) demonstrated that ApmA is an acetyltransferase enzyme which induced acetylation at the $N2'$ position of the octadiose element of the common antibiotic in veterinary known as apramycin (Figure 2.2). This process reduced the overall affinity of the molecule against its target and in turn promoting the resistance against this drug (Figure 2.3). In addition, a similar mechanism is also observed in β-lactam drugs. This class of antibiotic primarily targets transpeptidase enzyme also known as penicillin-binding proteins (PBPs) (Fakhriravari et al., 2022). Unfortunately, the acquisition of penicillinase via *blaZ* gene develops a resistance against the β-lactam drugs (Thomas et al., 2022). In MRSA, the acquisition of penicillin-binding protein 2′ ($PBP2'$) makes the MRSA strains resistant to almost all β-lactams due to the low affinity this group of antibiotics (Nomura et al., 2020).

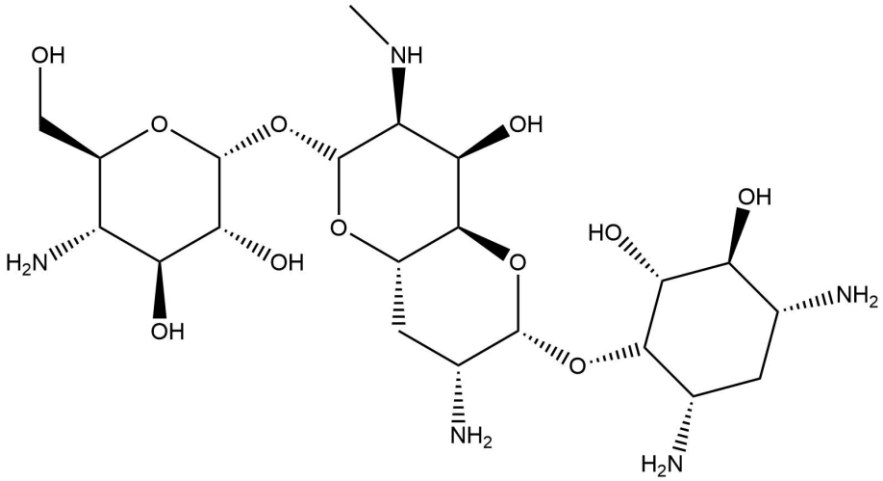

Figure 2.2: Molecular structure of Apramycin, an aminoglycoside antibiotic used in veterinary.

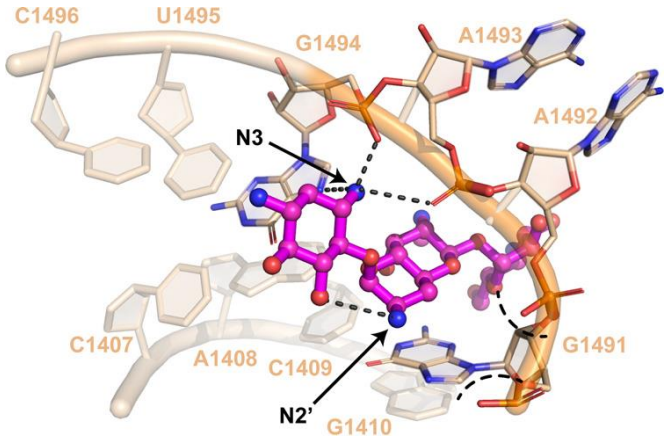

Figure 2.3: An image depicting the interaction of apramycin with ribosome [Protein Data Bank (PDB) ID: 4AQY (Bordeleau et al., 2021)

Study shown that the presence of efflux pumps (EPs) such as AcrAB-TolC in *E. coli*, NorA pump in *S. aureus* as well as the MexAB-OprM efflux pump of *P. aeruginosa* are the driving forces behind the resistance to their respective antibiotic (Chowdhury et al., 2019; Pesingi et al., 2019; Yu et al., 2022). EPs are transport proteins present in the plasma membrane of bacteria, flushing out toxic substances out of the cell including preventing the antibiotic reaching its target thus leading to antimicrobial resistance (Puzari & Chetia, 2017;

Santos et al., 2013). These transport proteins (Figure 2.4) actively pump out antibiotics out of the cell thus giving rise to the intrinsic resistance of Gram-negative bacteria to many of the drugs that can be used to treat Gram-positive bacterial infections. Consequently, overexpression of efflux pumps can lead to high levels of resistance to previously clinically useful antibiotics. In addition, low substrate specificity such as Tet pump allow it to pump out different substrates thus contributing to MDR efflux pumps (Blair et al., 2015).

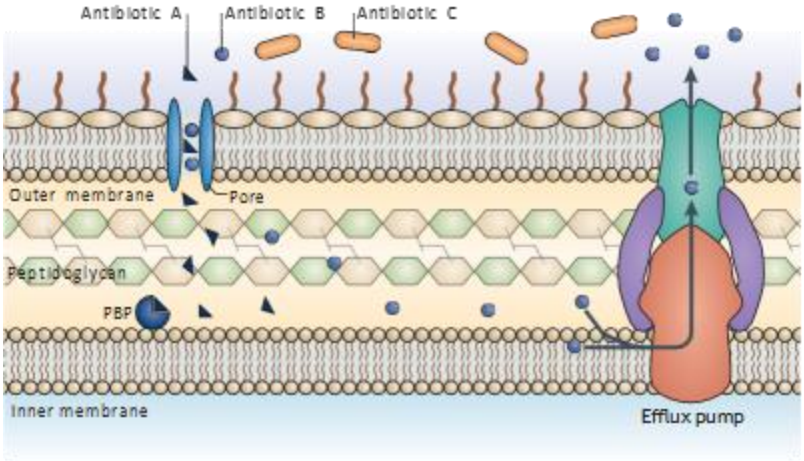

Figure 2.4: A visual depicting an efflux pump transporting antibiotics out of the cell membrane (Blair et al., 2015).

Another mechanism commonly employed by bacteria to resist antibiotics is through modification of the target enzymes. In a study by Morais et al., (2023), it was observed that 25.2% of *Staphylococcus pseudintermedius* were resistant against fluoroquinolones. Further investigation was carried out on the occurrence of mutations in the quinolone resistance-determining region (QRDR) of the target protein GrlA and GyrA. It was believed that double mutations GrlA:S80I/GyrA:S84L was linked to fluoroquinolones resistance in 36 out of 39 isolates. In another study by Villumsen et al. (2023), their work attempted to investigate the molecular mechanism that mediated *Gallibacterium anatis* resistance against

fluoroquinolones. DNA Gyrase enzyme comprising of *gyrA* and *gyrB* was studied to look for any point of mutations. They found some notable shifts in the position of a total of nine amino acids across all the subunits which influences the minimum inhibitory concentrations (MIC) values of nalidixic acid (NAL) and enrofloxacin (ENR) antibiotics against the bacteria strains. Gene mutations were also observed in PBPs, an enzyme involved in the synthesis of bacterial peptidoglycan layer (Tshibangu-Kabamba & Yamaoka, 2021). Kuo et al., (2023) presented a study on amino acids substitution in the PBP-1A protein of *Helicobacter pylori* (*H. pylori)* which was found to be resistant towards amoxicillin. There were 38 amino acid substitutions occurred in the isolates that were susceptible to this antibiotic. The authors postulated that the P623L substitutions was associated with the resistance, which was seen in nearly all of the resistant isolates.

2.2 Computer-aided drug design

Drug discovery and development is a complex process that began with discovery of diseases, followed by the identification of target receptor protein and lead compound (Figure 2.5) (Bisht & Singh, 2018). The traditional method is very time consuming and costly process taking between 12-15 years with an estimated 2.8 billion dollar cost to bring a new drug to the market (DiMasi, 2020; Singh et al., 2023). Computer-aided drug design in modern drug discovery combines computational tools along with biological knowledge to bring new potential drug candidate to the market (Niazi & Mariam, 2023). This modern and interdisciplinary method had contributed to significant cost reduction and lowered the rate of failures in drug discovery process (Yu & Mackerell, 2017). According to Dorahy et al., (2023), CADD can be divided into ligand-based and structure-based methods. The first method, ligand-based methods involved determination of structure activity relationships (SARs) which studies the relationship of a chemical structure of a drug to its biological

activity to predict novel and improved compounds. On the other hand, structure-based drug design studies the binding behaviour of compounds inside the 3D structure of a target receptor. These include molecular docking studies and molecular dynamic (MD) simulations (Batool et al., 2019).

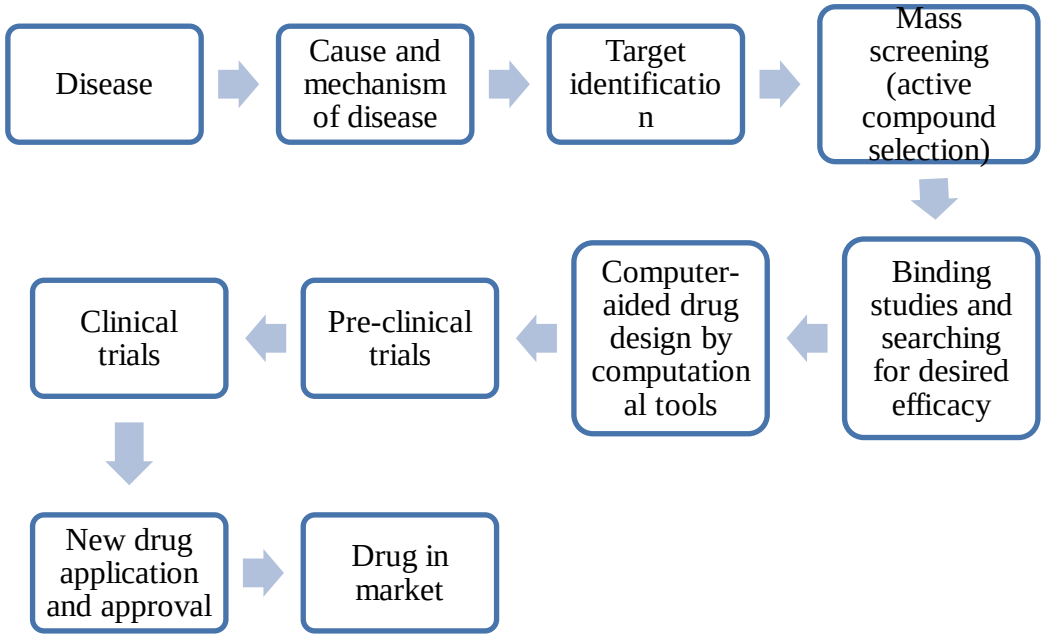

Figure 2.5: Process of drug discovery and development, from identification of diseases to its availability in the market

2.2.2 Molecular docking studies of thiourea

Molecular docking is a structural-based virtual screening method which had been vastly utilized in drug discovery process (Caballero, 2021). It is a technique to find the best conformation of a molecule to fit inside the binding cavity of a target receptor to form a stable-complex (Bassani & Moro, 2023). Based on the bar chart in Figure 2.6, molecular docking related searches had increased exponentially since the 2000s. For instance, Web of Science searches on molecular docking went from over 472 titles in the 2000s to well over 19 000 articles in 2024. The dramatic increase suggested the advancement of molecular docking tools in drug discovery process as well as the willingness of researchers to

incorporate modern method in drug design. Generally, a molecular docking simulation is generally based off two algorithms; that is the conformational search algorithm and the scoring function (Meng et al., 2011). The first algorithm is to find the best orientation of a molecule to fit in the active site cavity of a target protein to achieve an 'induced-fit' conformation. The second algorithm ranked all these conformations based on the docking score derived from an equation that factor in the conformational strain, electrical charges and stearic hindrance in order to find the most reliable and stable binding pose (Pavan et al., 2022). Some of the most used docking softwares by researchers in their studies are shown in Table 2.1 below.

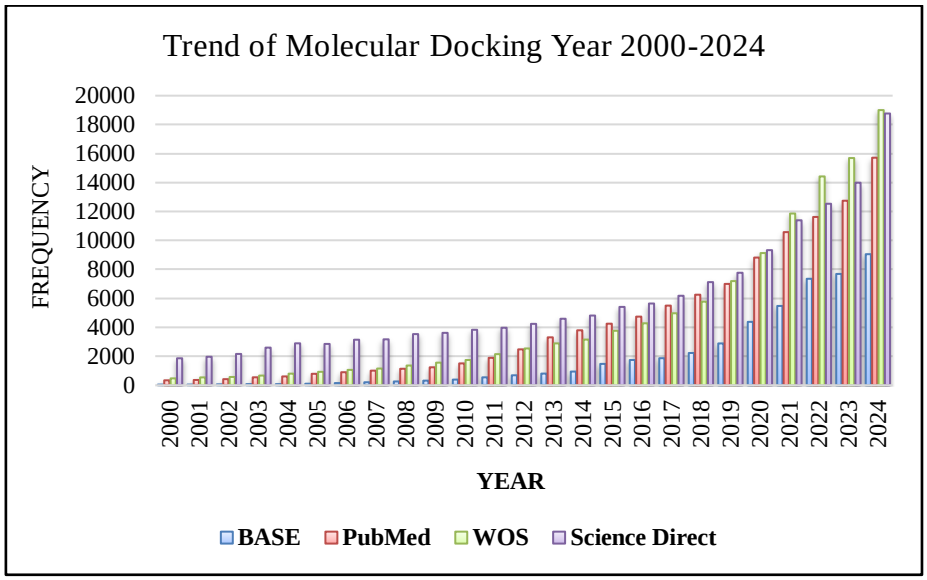

Figure 2.6: Trend of molecular docking studies from 2000-2024

Table 2.1: Examples of molecular docking softwares

Programs	Developers	Search algorithms	Scoring functions	Advantage(s)
Autodock	The Scripps Research Institute (Ivanova & Karelson, 2022)	Monte Carlo, Genetic algorithm, Lamarckian genetic algorithm (Malpani et al., 2020)	Lennard-Jones potential,hydrogen bond terms, coulomb potential desolvation & Entropic term (Gaillard, 2018)	Open-source
Autodock Vina	The Scripps Research Institute (Trott & Olson, 2010)	Monte Carlo (Tang et al., 2022)	Gaussian, linear hydrophobic, hydrogen-bond interaction and entropic term (Gaillard, 2018)	Easy to use Fast Speed Open- source
GOLD	Cambridge Crystallographic Data Center (CCDC)	Genetic algorithm (Chalmers, 2022)	Free energy calculations and molecular mechanic simulations (Vu et al., 2024)	Better accuracy than FleXx and Dock (Pagadala et al., 2017) Better pose prediction (Wang et al., 2016)
Glide	Schrödinger Maestro (Ivanova & Karelson, 2022)	Monte carlo (Vu et al., 2024)	Glidescore and EModel (Herbst et al., 2024)	Simple procedures (Ivanova & Karelson, 2022) Files preparation with minimal effort and time requirement. (Ivanova & Karelson, 2022)

There are a few examples of molecular docking studies of thiourea against various targeted enzymes through different molecular docking tools in research. Maalik et al., (2019) investigated the binding interaction of 3-trifluoromethyl benzoic acid thiourea with urease enzyme [Protein Data Bank (PDB) ID: 4ubp] using Molecular Operating Environment (MOE). Urease enzyme is an enzyme that is responsible to breakdown urine into ammonia

and carbon dioxide which in turns lead to urinary tract and gastrointestinal infections. It is commonly produced by *H. pylori* bacteria in the stomach. Good docking scores were often explained by valuable interactions between the ligand and targeted proteins. Molecular docking studies revealed that *N*-(3-triflouromethylphenyl)-*N′*-(2,6-diclorophenyl) as the top ranked compound, which was also the most active compound as obtained through experimental procedures. The interactions as shown in Figure 2.7 revealed an H-pi interaction between the trifluorophenyl group and amino acid residue His323. Hydrogen acceptor interactions were observed between Arg339 and Ala166 with trifluorophenyl groups of thiourea. Besides, the oxygen of the carbonyl group binds to the Cys322 while fluorine of trifluorophenyl groups showed metal-ion interaction with Ni(II) ion. These interactions allowed thiourea to be bound deeply inside the active pocket of the urease enzyme leading to high docking scores which explains its inhibitory effect.

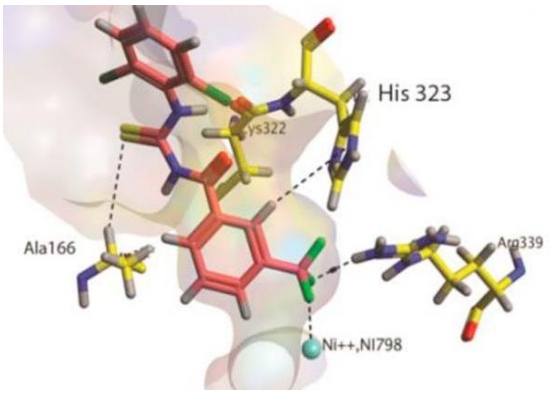

Figure 2.7: A 3D representation of binding interaction of N-(3-triflouromethylphenyl)-N′-(2,6-diclorophenyl)with the active site residues of urease enzyme (PDB ID: 4ubp) (Maalik et al., 2019).

On the other hand, Zullkiplee et al., (2021) evaluated the interaction between *bis*-thiourea derivatives with DNA gyrase enzyme of *E.coli* (PDB ID:4DUH) using Autodock Vina software. Compound *N1*,*N3*-bis((2-bromophenyl)carbamothioyl) benzene-1,3-tricarboxamide showed hydrogen bond interaction with GLY101 through C=O of thiourea

(Figure 2.8). Then, an electrostatic interaction was seen between aromatic group of the compound and HIS83 while hydrophobic interactions were noted for the residues GLY102, ALA100, VAL93, ALA90, ILE94 and PRO79. On the contrary, *N1,N4*-bis((2-bromophenyl)carbamothioyl) benzene-1,3-tricarboxamide amassed six hydrogen bonds interactions (Figure 2.9). C=S group formed three hydrogen bonds with amino acid residues HIS99, GLY117 and ASP49 (Firdausiah et al., 2020). The rest of the hydrogen bond interactions were seen between NH and LYS103; C=O with ASN46 and aromatic groups with VAL120. Between the two compounds, 1,4-*bis* thiourea had better docking score than *1,3-bis* thiourea. This is because 1,4-*bis* thiourea had greater negative values which correlated to stronger binding interaction with targeted protein (Uzzaman et al., 2019).

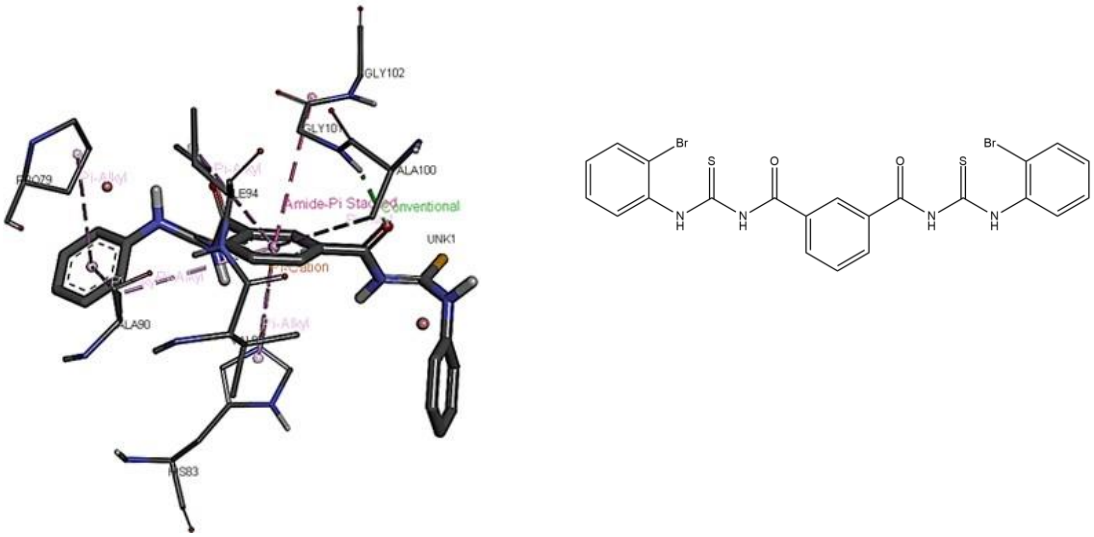

Figure 2.8: Visual representation (left) of the docking results of 1,3-*bis* thiourea (right) with 4DUH enzyme (Zullkiplee et al., 2021)

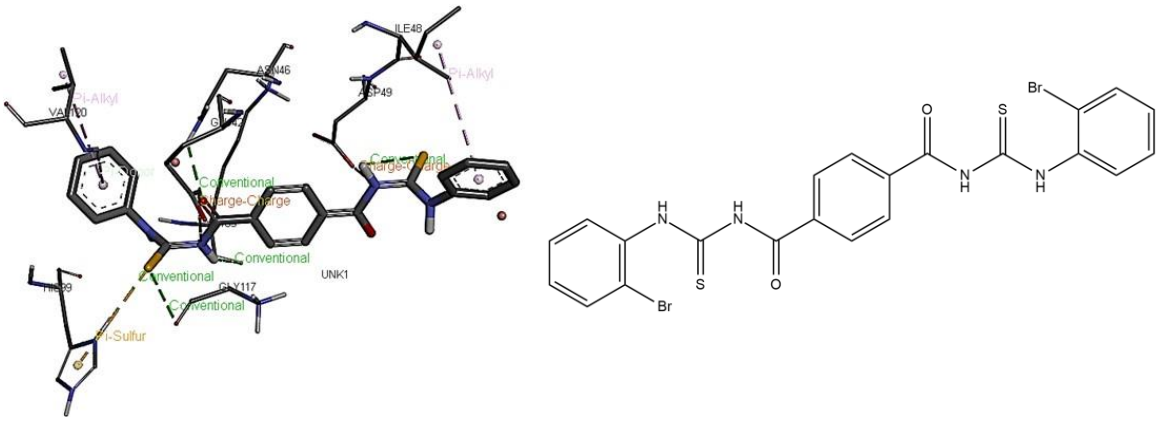

Figure 2.9: Molecular docking study visualization (left) of 1,4-*bis* thiourea (right) with 4DUH enzyme (Zullkiplee et al., 2021)

Hashem et al., (2020) also studied the binding interaction of novel thiourea derivatives with DNA gyrase and Toposiomerase IV enzymes using MOE. In this study, the binding interaction was compared with novobiocin. Compound 1-(2-Cyanoacetyl)-4-phenylacetylthiosemicarbazide was observed to be bound nicely to the DNA gyrase B with binding energy -12.23 kcal/mole as well as showing binding interaction similar to Novobiocin. For instance, the NH group of thiourea showed hydrogen bond interaction with Asp73 (Figure 2.10). Hydrogen bonding is crucial in stabilizing the three-dimensional structures of target macromolecules such as proteins and RNA and is also a key factor for the determination of binding affinity of drugs with their target (Costales et al., 2020; Kenny, 2022). As such, the hydrogen bond interaction originated from thioureas may explained the overall docking score of the compound. As for Topoisomerase IV, the only interaction that is similar to Novobiocin is the two hydrogen bond acceptors interaction between nitrogen and oxygen of cyanoacetyl group (Figure 2.11).

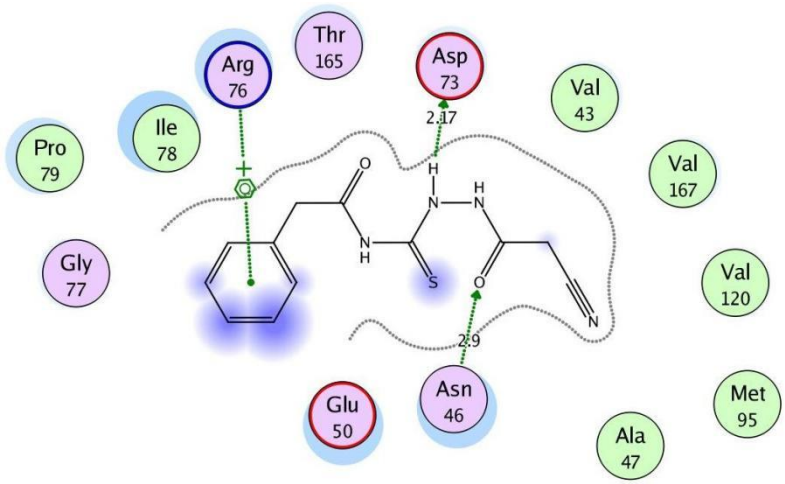

Figure 2.10: 2D representations of binding interactions of 1-(2-Cyanoacetyl)-4-phenylacetylthiosemicarbazide with DNA gyrase enzyme (Hashem et al., 2020)

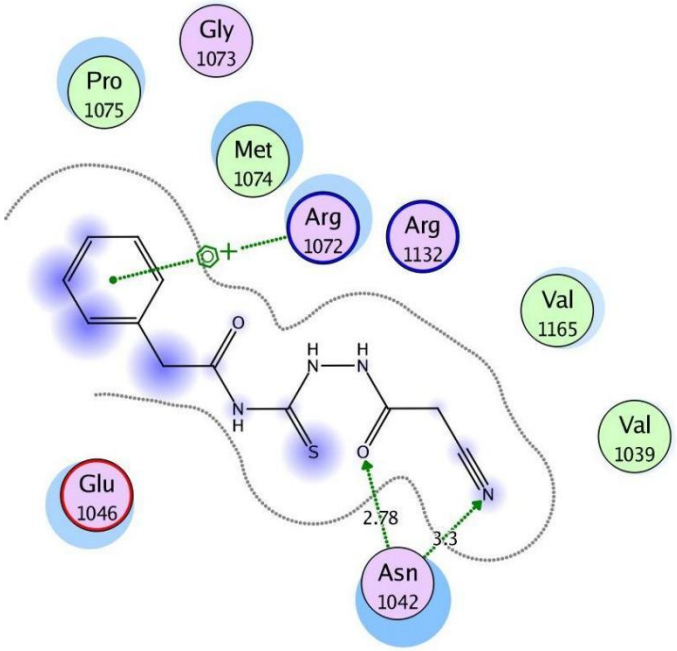

Figure 2.11: 2D representation of binding interactions of 1-(2-Cyanoacetyl)-4-phenylacetylthiosemicarbazide with Topoisomerase IV (Hashem et al., 2020)

Antypenko et al. (2019) utilized the Autodock 1.5.6 docking tool to observe the binding interactions of acyl thioureas with 14α-demethylase (NYP51) and N-myristoyltransferase (NMT). Some of the interactions observed between N-(2-Benzoylhydrazine-1-carbonothioyl)cyclopropane-carboxamide and NYP51 (Figure 2.12) were hydrogen bonding between sulfur and MET A:508; π-alkyl bonds of cyclopropyl fragment and TYR A:132 and A:118 as well as van der waals interactions with GLY A:307

and LEUA:376. On the other hand, the compound *N*-(2-(2-phenoxyacetyl)hydrazine-1-carbonothioyl)-cyclopropanecarboxamide was predicted to have further hydrogen bonding with NYP51 (Figure 2.13) between nitrogen and GLY A:307; π-alkyl bonds with LEU A:121 as well as Van der waals interactions with VAL A:509, PHE A:228 and LEU A:376.

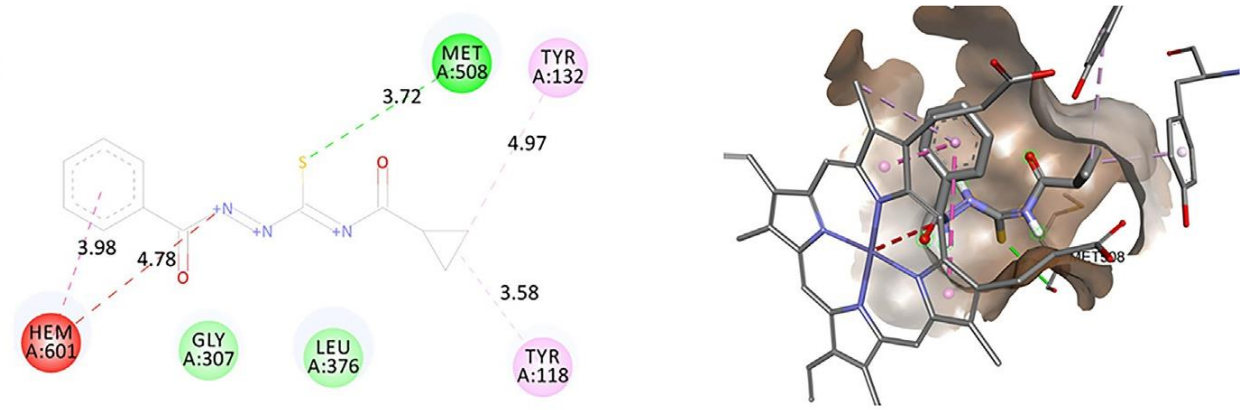

Figure 2.12: 2D (left) and 3D (right) representations of the binding interaction of *N*-(2-benzoylhydrazine-carbonothioyl)cyclopropane-carboxamide with 14α-demethylase enzyme (Antypenko et al. 2019)

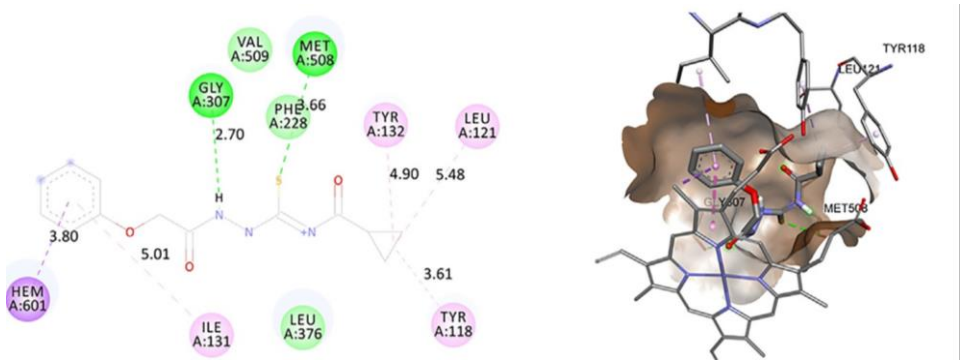

Figure 2.13: 2D (left) and 3D (right) representations of *N*-(2-(2-phenoxyacetyl)hydrazine-1-carbonothioyl)-cyclopropanecarboxamide with 14α-demethylase enzymes (Antypenko et al. 2019)

2.2.3 ADME evaluation of thioureas

In another aspect of CADD, the evaluation of its drug-likeness properties or pharmacokinetic profile of a potential target drug is a very critical process before the drug is approved for clinical use. The cost of drug discovery process increases yearly and currently stood at US$2.6B (Chan et al., 2019). While bringing a new drug to the market is a very tough process, approximately 90% of drugs failing at its final stage were due to its poor pharmacokinetics profiles (Bocci et al., 2017; Pantaleão et al., 2022). The inclusion of Absorption, Distribution, Metabolism and Excretion (ADME) evaluation studies in early drug discovery was proven to reduce the failure rate of drugs (Siramshetty et al., 2021). While experimental setting remains the best option for the determination of pharmacokinetic profiles, it is almost unrealistic to screen millions of compounds as it is very time consuming and costly. Therefore, an *in silico* approach of determining the ADME of molecule is another widely employed procedure in today's process of drug discovery (Padole et al., 2022).

SwissADME tool is commonly employed to predict the pharmacokinetic profiles of thioureas. For instance, Soomro et al., (2023) predicted the pharmacokinetic and physicochemical properties of thioureas (Figure 2.14) using the online software SwissADME and Pre-ADMET as well as the webtool ProTox II to analyse its toxicity. It was predicted that the compounds can be absorbed in the gastrointestinal tract (GI) and can permeate the BBB. Besides, the compounds have good bioavailability score and do not inhibit the metabolizing enzyme. Additionally, the compounds are non-toxic to the liver and have a high lethal dose therefore could be a future candidate for clinical trials and subsequent use for *in vivo* studies.

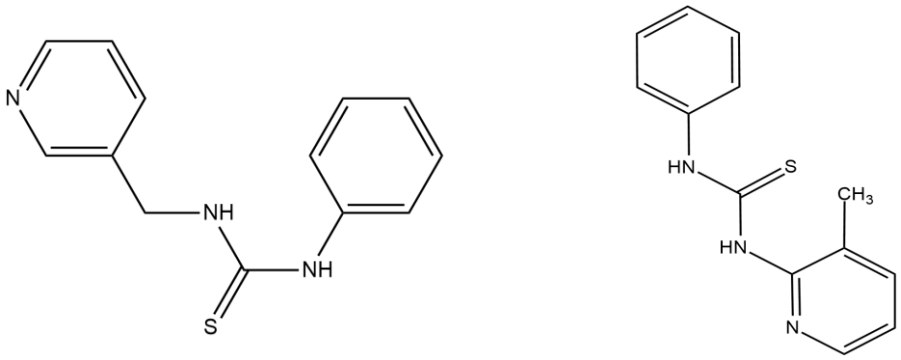

Figure 2.14: Molecular structure of thioureas

Similarly, Hussain et al., (2022) also made use of the SwissADME tool to conduct an ADME evaluation on novel amide and thiourea derivatives as potential CA inhibitors. Based on boiled-egg plot diagram (Figure 2.15), all the synthesized compounds were predicted to not cross the blood brain barrier but were permeable in the gastrointestinal tract. Furthermore, most compounds showed no Pan Assay Interference Compounds (PAINS) alert thus could serve as potential oral treatment of overexpression of carbonic anhydrase.

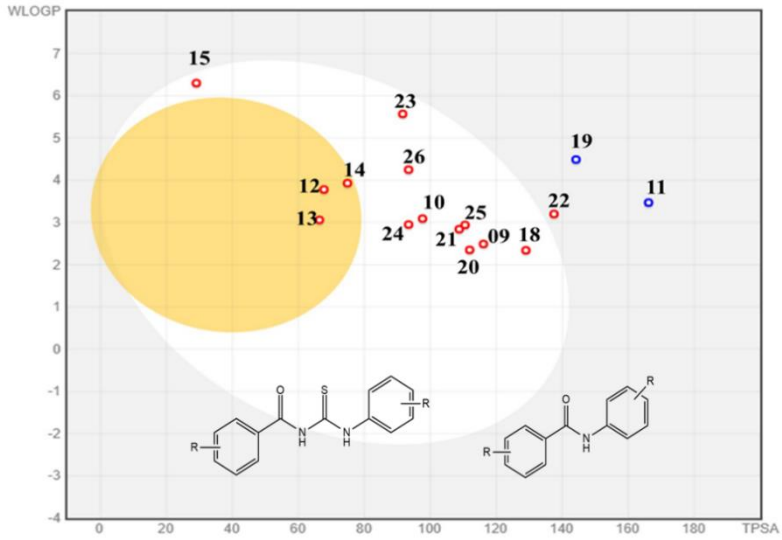

Figure 2.15: Hard-boiled egg diagram of amide and thiourea derivatives as obtained from SwissADME software (Yellow region suggested that molecules permeate BBB while white region represented gastrointestinal absorption of molecules; Red dot means molecules are not affected by P-glycoprotein while blue dot means vice versa) (Hussain et al., 2022)

Another *in silico* study was published by Makeen & Albratty, (2023) using various derivatives of thiourea and urea as tankyrase inhibitors in search for potent anticancer agent. Likewise, SwissADME software was used to predict the ADME properties alongside Autodock Vina to run its molecular docking against the tankyrase receptor (TNKS2) (PDB ID: 6KRO). Additionally, 2D quantitative structure-activity relationship (QSAR) modelling was used to study the relationship of chemical structures with biological activities. The prediction tools revealed that the compounds such as compound 18 (Figure 2.16) fulfilled the Lipinski's rules although some highlighted compounds violated the rules due to molecular weight being larger than 500. Besides, the compounds also portrayed good bioavailability and high GI absorption. It was also indicated that the compounds do not cross the blood brain barrier therefore minimizing the side effects on central nervous system (CNS).

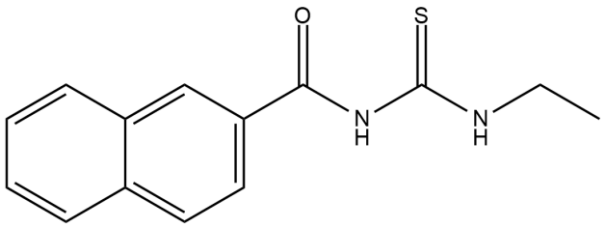

Figure 2.16: Molecular structure of thiourea derivative

It is evidenced that thiourea and its complexes had been shown to possess remarkable biological potential, from anticancer to antibacterial activities. Furthermore, with improved biological properties and low toxicity, metal complexes are proving to be a promising area in medicinal chemistry. By leveraging artificial intelligence (AI), computational tools such as docking and SwissADME software may be utilized to accelerate the process of drug discovery by narrowing down the choice of potentially active compound and eliminating the compounds that are likely to cause toxicity in human through simulation studies with target enzyme and assessment of pharmacokinetic profiles.

2.3 Significance of sulphur-containing compounds in medicinal chemistry

The sulphur motifs represent an important pharmacophore in medicinal chemistry. Sulphur is universally known as antimicrobial agent and had been used in many treatments of bacterial infected skin conditions (Teng et al., 2019). In fact, sulfonamide drug (a sulphur containing compound derived from sulfanilamides) were the earliest to be used as antibiotics (Feng et al., 2016; Petkar & Jagtap, 2021). There are currently 362 sulphur containing drugs that had been approved by FDA and is available in the market such as celecoxib for the treatment of pain, cefazolin for bacterial infection and dorzolamide as carbonic anhydrase (CA) inhibitors for the treatment of glaucoma (Feng et al., 2016; Scott & Njardarson, 2019). The biological activity of celecoxib for instance was defined by the presence of sulfonamide group which participate in hydrogen bonding within the active site of cyclooxygenase-2 (COX2) enzyme to reduce the production of prostaglandin, the sources of inflammation (Hassan et al., 2014; Wang et al., 2019).

Due to its various pharmacological properties, sulphur moieties had been an interesting motif in designing new potent active compound for different purposes. An example of sulphur-containing compound is the synthesis of thiophene-based derivatives (Figure 2.17) by Shah & Verma (2019) for its anti-microbial, antioxidant, anticorrosion and anticancer properties. Compound S_1 were found to be the most potent compound against bacterial strains such as *Bacillus subtilis*, *S. aureus*, *E. coli* and *Salmonella typhi* with MIC value 0.81 µM/mL. Meanwhile, compound S_4 could inhibit the growth of fungal strains *Aspergillus niger* and *Candida albican* with MIC value 0.91 µM/mL. On the other hand, the antioxidant activity of the most active compound recorded an IC_{50} values 48.45 and 45.33

which were portrayed by compound S_4 and S_6 respectively. Furthermore, thiophene derivatives were observed to possess anticorrosion as well as anticancer activity. The screening of compound S_8 against human cancer cell line (A-549) revealed that the compound inhibited cancer cell at 10^{-4}M dosage. The authors acknowledged the presence of the electron withdrawing group as the contributor to the significant anticancer properties.

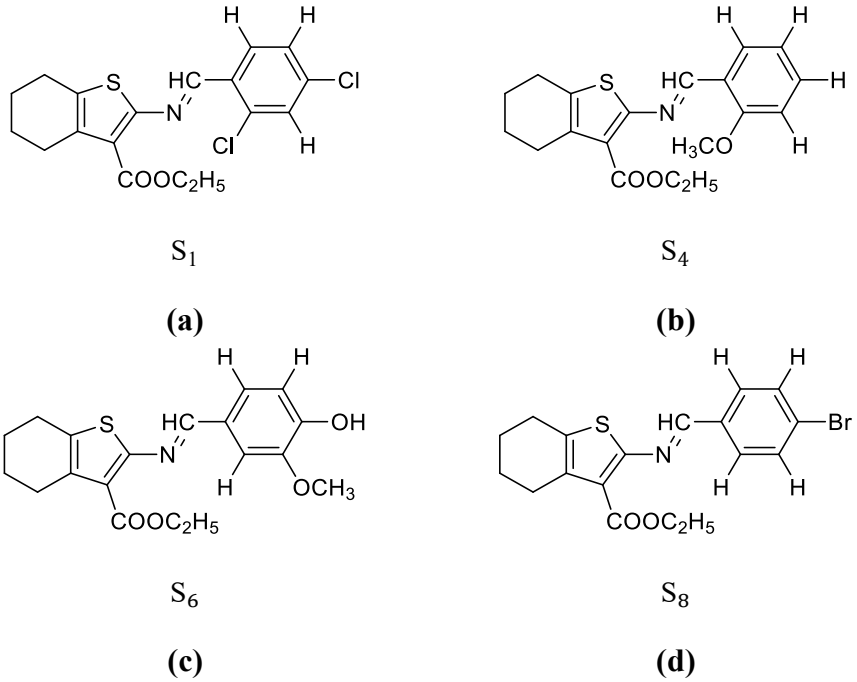

Figure 2.17(a)-(d): Thiophene-based derivatives

Trotsko et al., (2018) designed and synthesized another sulphur-containing molecule, novel thiazolidine compound (Figure 2.18) in search for potent antimicrobial agent. In their study, the authors used the broth dilution method to investigate the antimicrobial properties against both gram positive and gram negative bacterial strains such as *S. aureus, B. subtilis, E. coli* and *P. aeruginosa.* Novel thiazolidine compounds were ineffective against the negative strains except for *Pseudomonas mirabilis.* In contrast, the compounds were observed to be more potent against positive strains. In addition, the presence of electron withdrawing group at the phenyl rings gave a boost on the antibacterial activity of the compound. Furthermore, the authors observed the presence of electron donating group

increases the antibacterial activity in one of the synthesised compound while increasing the methyl chain would diminished its antibacterial effect.

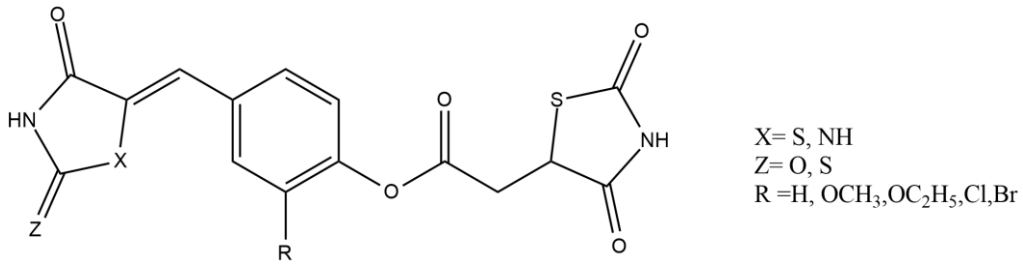

Figure 2.18: General structures novel thiazolidine compound

A new set of thiazole-based derivatives (Figure 2.19) had been produced by Omer et al., (2024) and tested against *S. aureus*, *E. coli* and *C. albicans* by growth turbidity method accompanied by molecular docking evaluation for elucidation of its possible mechanism. The results showed that the compounds inhibited the growth of *C. albican* strains. Subsequently, molecular docking simulation suggested strong interaction between the compound with 8JZN protein including lower energy scores indicating strong affinity inside the protein cavity.

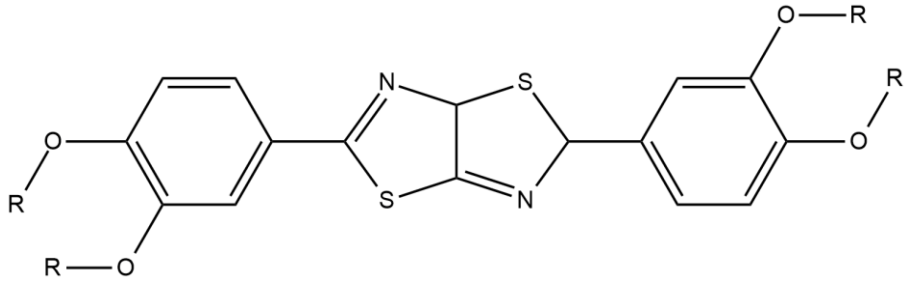

Figure 2.19: Novel thiazole derivatives as antifungal agent

Table 2.2: Summary of sulphur-based compound for pharmacological purposes

Compound	Advantages	Disadvantages
Thiophene derivatives (Shah and Verma, 2019)	Effective as anti-microbial, anti-corrosion, anti-oxidant and anti-cancer	Broad spectrum, compound lack selectivity
	Low reaction time, high yield	As it kills more bacteria, the chances of developing resistance are high
	Effective against Gram positive and Gram negative bacteria	
Thiazolidine derivatives (Trotsko et al., 2018)	Effective against the Gram positive bacterial strains	Synthesis of compound consist of multiple steps hence more reagents, time and costs are required.
	Compound has high melting point, indicating its stability	Compounds are ineffective against Gram negative strains
Thiazole derivatives (Omer et al., 2024)	Effective against fungal strains (*C. albican*)	Ineffective against bacterial strains.
	Compound embedded nicely inside the pocket of 8JZN enzyme	

2.3.1 Thiourea compounds

Continuing the significance of sulphur-containing compound, thiourea is another widely studied functionality for various applications. Thiourea, $SC(NH_2)_2$ is an organosulfur compound with a general formula $(R_1R_2N)(R_3R_4N)C=S$ (Favre and Powell, 2013). It is an urea analogue compound with S atom replacing the O atom instead and the presence of C, S, N and H atom makes them a versatile building blocks in a synthetic reaction (Fakhar et al., 2018). Some of the applications of thiourea include in gold leaching process (Sheel & Pant, 2021), herbicides (Li et al., 2021) and as chemosensor (Khan et al., 2020). Furthermore, due to its good coordination ability, it is used as intermediate in the synthesis of heterocyclic products (Limban et al., 2018). Besides, Singh and Tiwari (2018) stated that thioureas and their derivatives gained attention due to their physicochemical properties, synthesis accessibility, various applications and inexpensive use of chemicals and reagents.

Thiourea is a white crystalline solid also known as thiocarbamide or sulforia (Khan et al., 2020). It exists in two tautomeric forms as shown in Figure 2.20 and plays an important role in drug research (Agili, 2024; Kirishnamaline et al., 2021). Thioureas had been studied as anticancer (Arshad et al., 2021; Kirishnamaline et al., 2021; Parmar et al., 2021); anti-inflammatory (Mohamed et al., 2021); antimicrobial and antioxidant (Maalik et al., 2019). Besides, thiourea also has been reported to possess aromatase inhibitory activity (Pingaew et al., 2018) as well as carbonic anhydrase (CA) inhibitors (Qaiser et al., 2021) and cyclin dependent kinase (CDK) inhibitors (Shawky et al., 2021)

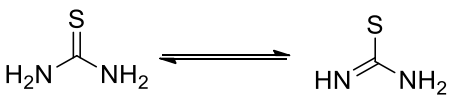

Figure 2.20: Tautomeric forms of thiourea

2.3.2 Drugs containing thiourea moiety

Thiourea functionality have been found in several Food and Drug Administration (FDA) approved drugs. Carbimazole is an anti-thyroid drug to treat hyperthyroidism and Grave's Diseases (Scarperi et al., 2023). It is a pro-drug and is transformed into methimazole (Figure 2.21) about 15-30 minutes after oral administration (Khan et al., 2023). Carbimazole falls into a category of drugs called thionamide which refers to classes of compound with five or six membered ring structure containing sulfur and is also a member of thiourea derivatives. Its active form inhibits thyroid hormones production by oxidizing iodide in the presence of thyroid peroxidase (Burch & Cooper, 2018). In Malaysia, carbimazole is marketed and trademarked as Camazol ™ by Xepa.

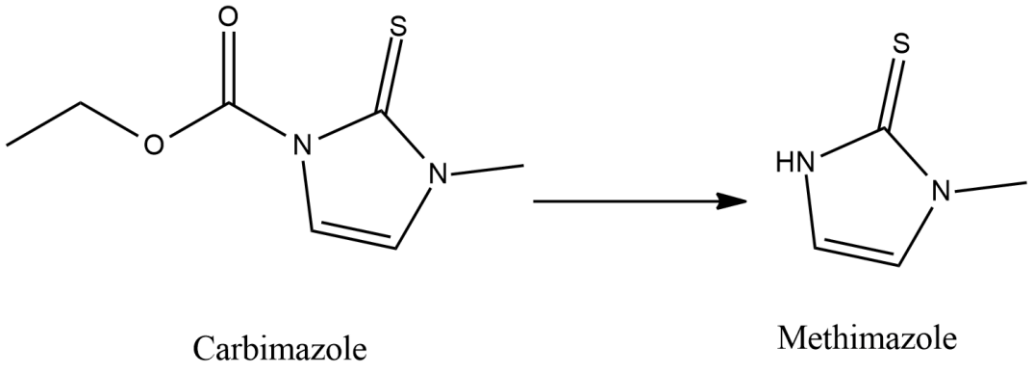

Figure 2.21: Structural conversion of carbimazole to methimazole after oral administration

Similarly, propylthiouracil (Figure 2.22) also belong to the group of drugs called thionamide. According to a large study conducted on thyroid storm in critically ill patients, there is no significant difference in mortality rate between two group of patients treated with either methimazole or propylthiouracil (Lee et al., 2023). Furthermore, a meta-analysis study also finds that the usage of propylthiouracil among pregnant women is safer than methimazole (Liu et al., 2023). Therefore, propylthiouracil is chosen as the first-line treatment option for pregnant women in their early pregnancy, in the case of thyroid storm,

as well as if patients are experiencing acute side effects to methimazole according to American Thyroid Association Guidelines 2016 (Ross et al., 2016). As for Japan Thyroid Association, either propylthiouracil or methimazole could serve as a candidate for the first-line therapy to treat hyperthyroidism (Satoh et al., 2016).

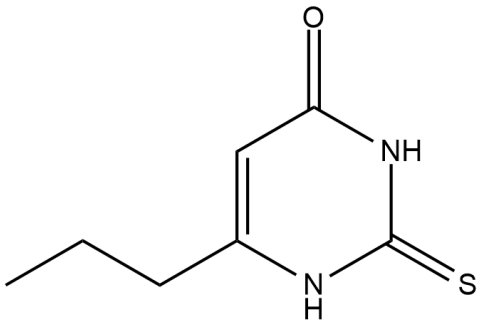

Figure 2.22: Molecular structure of propylthiouracil

Another example of thiourea containing drug is enzalutamide (Figure 2.23) which is a prostate cancer drug targeting the Androgen Receptor (AR) (Beer et al., 2017) It is marketed as XTANDI ® by Astellas Pharma Inc. and had been approved for castration-resistant prostate cancer (CRPC) and metastatic castration-sensitive prostate cancer at 160mg daily dose (FDA, 2023). It is a second-generation prostate cancer drug and exert its anticancer activity though binding of androgen to AR, nuclear translocation of AR and and AR with DNA interaction (Tran et al., 2009; Scott et al., 2018). The efficacy and safety of this drug was first evaluated in Phase I-II clinical trials where 140 patients with mCRPC was enrolled followed by Phase III trial involving over 1000 patients across 15 countries in 2012 (Scher et al., 2010, 2012).

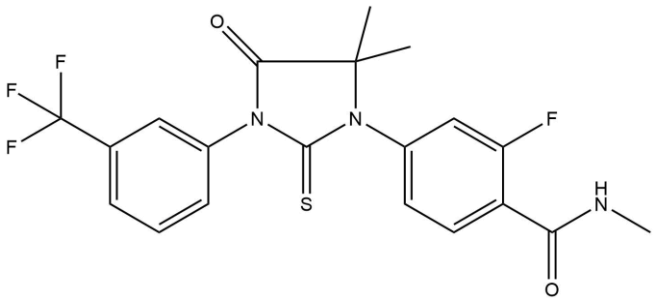

Figure 2.23: Molecular structure of enzalutamide

As of today, there is no FDA approved drugs with thiourea moiety that target antibacterial resistance. In fact, thiourea-based medications are still limited when compared to those containing urea (Ghosh & Brindisi, 2020; Ronchetti et al., 2021). Furthermore, some drugs based-off thiourea are no longer priority such as thioacetazone for treatment of tuberculosis or converted to safer drug such as cimetidine for the treatment of peptic ulcer (metiamide was deemed too toxic and generate undesirable side effects) (Ronchetti et al., 2021; WHO, 2019). However, thiourea serves as a great candidate as the next potential antibiotics thanks to many studies that had reported on its great antibacterial properties. In the next section, examples of numerous recent studies will be discussed regarding the antimicrobial potential of various thiourea derivatives.

2.3.3 Antimicrobial properties of thiourea derivatives

Thiourea derivatives are widely synthesised and studied in the quest of novel biologically active compound to combat antimicrobial resistance. The presence of C=S, C=O and NH functionality were reported to contribute to good antimicrobial effect thanks to the interaction with the receptor site of bacteria (Fakhar et al., 2018). Ibrahim et al. (2021) reported the synthesis of benzoyl and halobenzoyl thiourea bearing α and β- alanine amino acids from the reaction of aroylchlorides and ammonium thiocyanates in acetone (Figure 2.24). According to their observation, all halobenzoyl derivatives showed moderate to strong antibacterial properties against *Bacillus subtilis, S. aureus* and *E. coli* with zone of inhibition ranging from 8.8 - 19.0 mm. The bromo substituent was observed to be effective against

gram positive bacteria while fluorine substituent enhanced the inhibition against gram negative bacteria due to lipophilicity against the cell wall of gram-negative bacteria (Li et al., 2013). Besides, the author also highlighted the significant role of amino acids towards enhancing the antibacterial properties of thiourea as evidenced by 4-fluorobenzoyl thiourea bearing α-alanine (Figure 2.25) exhibiting better antimicrobial activity compared to 4-flurobenzoyl thiourea β-alanine (4Fβ).

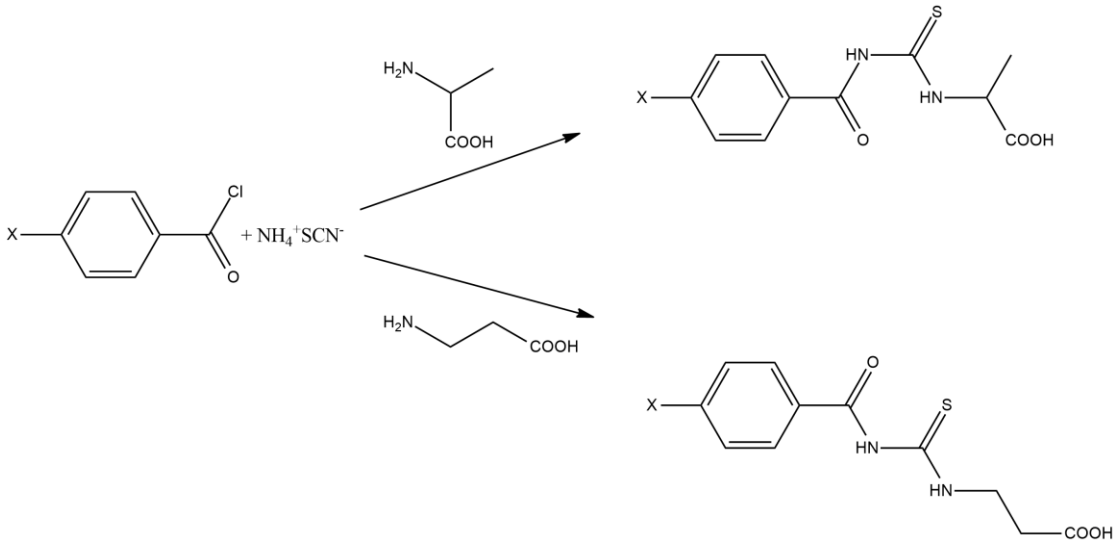

Figure 2.24: Preparation of benzoyl and halobenzoyl thiourea derivatives

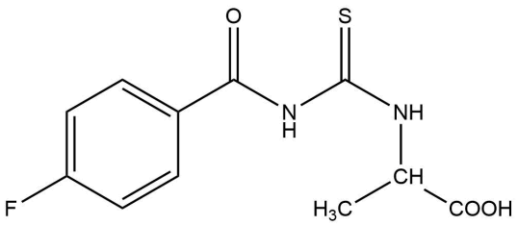

Figure 2.25: Molecular structure of 4-fluorobenzoyl thiourea α-alanine (4Fα)

In another study exploring the antibacterial properties of thiourea derivatives bearing amino acids side chains, Zullkiplee et al., (2021) synthesised novel *bis*-thiourea derivatives as potential antimicrobial against gram negative *E. coli*. The synthetic procedure was done through a reaction of isophthaloyl chloride and terephthaloyl chloride with various aniline derivatives. It was observed that 1,4-*bis*-thiourea displayed overall better performance

against bacteria compared to 1,3-*bis*-thiourea derivatives. This could be due to the stearic hindrance that resulted in less binding interaction with the bacteria cell wall (Pramilla et al., 2015; Zullkiplee et al., 2014). Therefore, it could be deduced that the position of substituent could play a role in enhancing antibacterial activities. Furthermore, although compound *N1,N3*-bis((2-bromophenyl)carbamothioyl)benzene-1,3-tricarboxamide (Figure 2.26) had the lowest MIC value at 228 ppm, the diameter of zone of inhibition was rather weak, only 7 mm as opposed to its positive control ampicillin at 12 - 16 mm. On the contrary, a similar work done by Fakhar et al. (2018) in exploring the antibacterial activities of *bis*-thiourea (Figure 2.27) with 2-methyl amino ethanol side chain did not yield a significant result against multiple strains of bacteria such as *Lysinibacillus* sp., *Vibrio owensii* and *Vibrio alginolyticus*. This is because the non-planarity of the compound led to steric hindrance which subsequently interrupted the interaction with bacteria receptor.

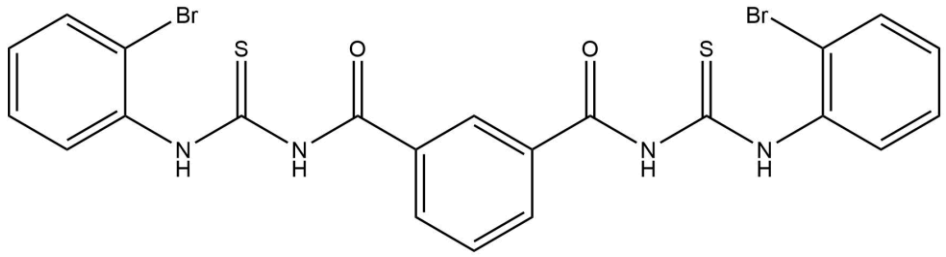

Figure 2.26: Molecular structure of *N1, N3*-bis((2-bromophenyl)carbamothioyl)benzene-1,3-tricarboxamide

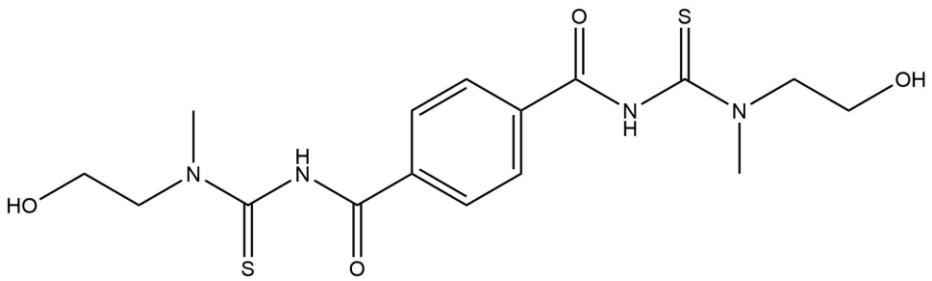

Figure 2.27: Molecular structure of *N1,N4*- Bis((2 hydroxyethyl)(methyl)carbamothioyl)terephthalamide

Naz et al., (2020) conducted a study on multiple biological properties of thiourea derivatives such as antibacterial, antioxidant, anticholinesterase as well as anti-diabetic activity. Novel thiourea derivatives were synthesised from carbon disulphide and reacted with different anilines derivatives and one aminobenzoate. Among five compounds, 1,3-bis(4-nitrophenyl)thiourea (Figure 2.28) was observed to be the most potent compound when tested with different strains of bacteria such as *K. pneumoniae*, *P. aeruginosa*, *S. typhi* and *Enterococcus faecalis* with 19 mm – 30 mm clear zones. Furthermore, MIC value was recorded to be at 40 - 50 µg/mL suggesting high antibacterial potential of the compounds against the bacterial strains.

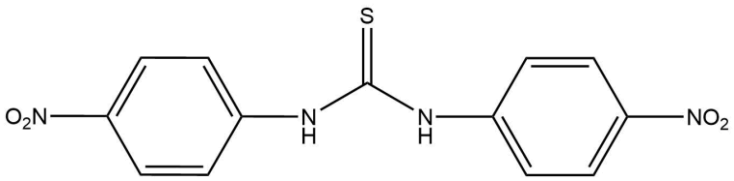

Figure 2.28: Molecular structure of 1,3-bis(4-nitrophenyl)thiourea

Researchers will typically combine a few scaffolds together during the design process of new drugs aiming to improve its biological activities, reduce its toxicity or to enhance its solubility. For example, a recent work by Kumar et al., (2023) incorporated thiourea/urea pharmacophores into β-lactams, an existing antibiotics to design a new set of biologically active compounds against a set of gram-positive (*S. aureus* and *B. cereus*) and gram-negative (*P. aeruginosa* and *E. coli*) bacterial strains. Compound as shown in Figure 2.29-2.31 showed the best antibacterial effect against all tested bacteria although the urea derivatives were seen as more active overall compared to its thiourea counterparts. Similar observations were also seen against fungal strains. Molecular docking tool was utilized to

study the binding interaction of compounds against targeted enzymes such as the PBPs enzyme (1VQQ) and CYP51 (5TZ1) enzyme.

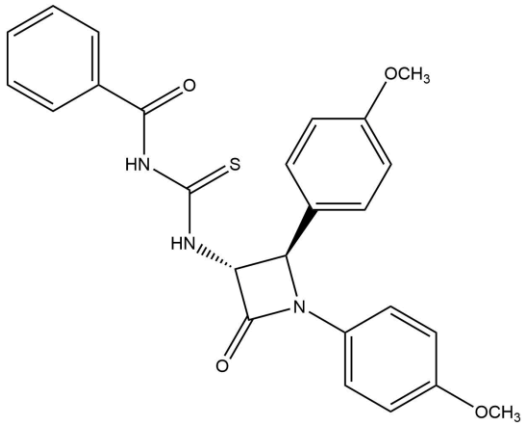

Figure 2.29: Molecular structure of 1-Benzoyl-3-[1,2-bis-(4-methoxy-phenyl)-4-oxo-azetidin-3-yl]-thiourea

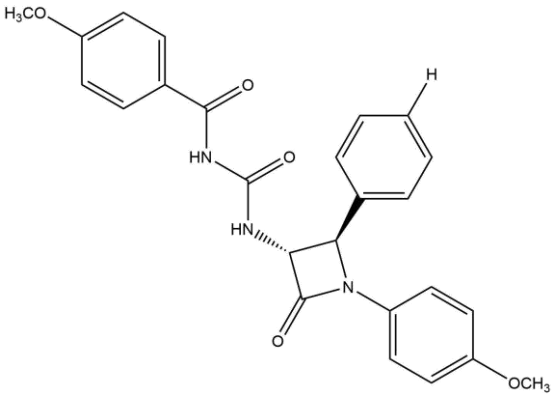

Figure 2.30: Molecular structure of 1-(4-Methoxy-benzoyl)-3-[1-(4-methoxy-phenyl)-2-oxo-4-phenyl-azetidin-3-yl]-urea

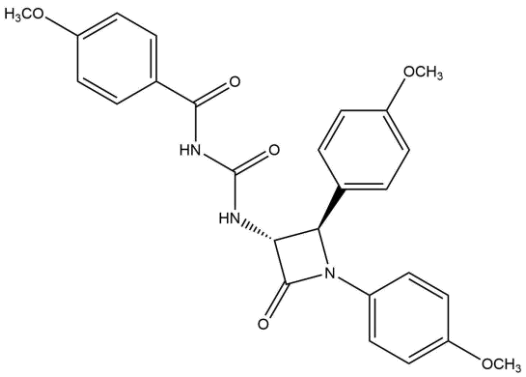

Figure 2.31: Molecular structure of 1-[1,2-Bis-(4-methoxy-phenyl)-4-oxo-azetidin-3-yl]-3-(4-methoxy-benzoyl)-urea

2.4 Medicinal importance of copper(II), zinc(II) and cobalt(II) as transition metal complexes

Transition metals are important elements in the periodic table with many uses. Having characteristics such as being able to conduct electricity and heat as well as malleable, transition metals have found its ways into various of the household products. Transition metals and their complexes play a crucial role in medicine and pharmaceutical sciences (Luo et al., 2021). According to Sodhi & Paul (2019), metals possessed specific properties such as redox potential, multiple binding mode and interactions with organic molecules that sparked interest as medicine. Furthermore, there is a significant advancement of application of metal complexes as drugs for the treatment of human diseases as transition metals with multiple charges can interact with negatively charged molecules leading to the development of metal-based drugs. Besides, study showed that the incorporation of metal was associated with increased biological properties (Khater et al., 2019). As biological molecules preferred to bind to softer metal, it was expected that the interaction may lead to better biological activities (Damena et al., 2022).

The research on metal-based drugs was catalyzed after the discovery of anticancer metal-based drugs cisplatin back in the 1960s (Dasari & Tchounwou, 2014). The drug, which had platinum (Pt) metal center was approved by the FDA in 1978 and is credited to renew interest of metal-based compound as drugs (Cirri et al., 2021). Another interesting metal-based drug is auranofin. It is a gold (Au) bearing metal-complexes used to treat rheumatoid arthritis (Deben et al., 2024). This drug had been studied as antimicrobial drugs and had since undergone seven clinical trials as an anticancer candidate (Cirri et al., 2021). Copper (Cu), zinc (Zn) and cobalt (Co) have been utilized in the synthesis of various metal

complexes for different biological purposes such as antiviral, antibacterial, antifungal and anticancer candidate (Aprajita & Choudhary, 2022; Ahamad et al., 2020; Naureen et al., 2021). These metals which are usually present as micronutrients in our body is crucial for normal body functions and had since gained special attention in the mission of creating new drugs.

2.4.1 Copper(II) complexes

The antimicrobial properties of copper are known since ancient times (Ghazy et al., 2021). It is known as solely solid surface material that kill MRSA, vancomycin-resistant *Enterococcus, A. baumannii* and *E. coli* owing to its broad antimicrobial spectrum and ability to act as electron acceptor or donor (Bruna et al., 2012). Besides, copper nanoparticles (CuNPs) are applied as antimicrobial coatings in dentistry and killing of virus SARs-CoV2 owing to its ability to penetrate across bacterial surface, thanks to its large surface area to volume ratio (Poggio et al., 2020). However, the synthesis of Cu(II) complexes have also been proven to have similar remarkable effects. The synthesis of Cu(II) complexes had been successfully done with mixed-ligand by Rostas et al., (2020) which afforded five-coordinated complex arranged in trigonal bipyramidal geometry. The MIC values revealed that complexes were better than ligands in inhibiting growth of several bacteria cell strains such as *E .coli, P. aeruginosa* and *S. aureus* along with their resistant strains. The most active compound, complex 2 (Figure 2.32) recorded an MIC values between 0.01 - 0.09 mM against all strains which was significantly lower than one of the ligand, bipyridine which had MIC values between 4.00 - 8.00 mM. Complex 2 also showed an efficient DNA-scavenging activity thanks to intercalation with DNA strands, presence of fused aromatic system, easily substituted ligands and the presence of hydrophobic groups.

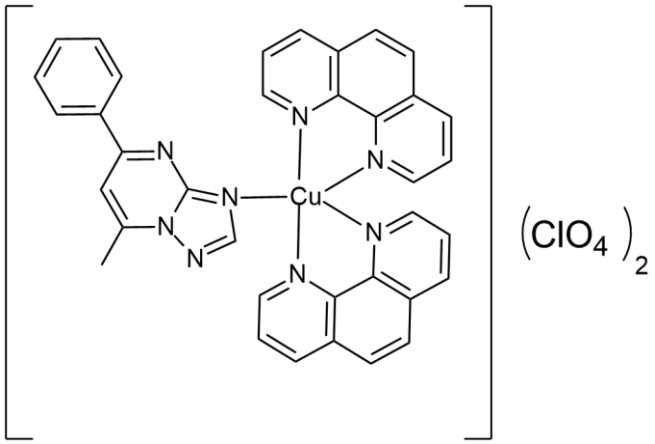

Figure 2.32: Molecular structure of copper(II) complex with mixed heterocycle ligand (Rostas et al., 2022)

Studies on the anticancer effects of Cu(II) complexes were extensively reported. It was shown in one study that complexation with copper may induced cancer cell apotosis through generation of reactive oxygen species (ROS), disruption of bacterial mitochondria cells and activation of capase 8 and 9 signaling pathways (Mariani et al., 2021). The complex [Cu(HPClNOL)Cl]Cl (Figure 2.33) was determined to exert more cytotoxicity than cisplatin against human breast cancer cell lines (MCF7) while showing equal toxicity against lung cancer cell lines (A549) without harming the non-cancer cells. This implied the less toxicity effects of Cu(II) complex. In addition, this study shown that drug treatment combining both cisplatin and the complex may promote cell specific synergistic or additive effects.

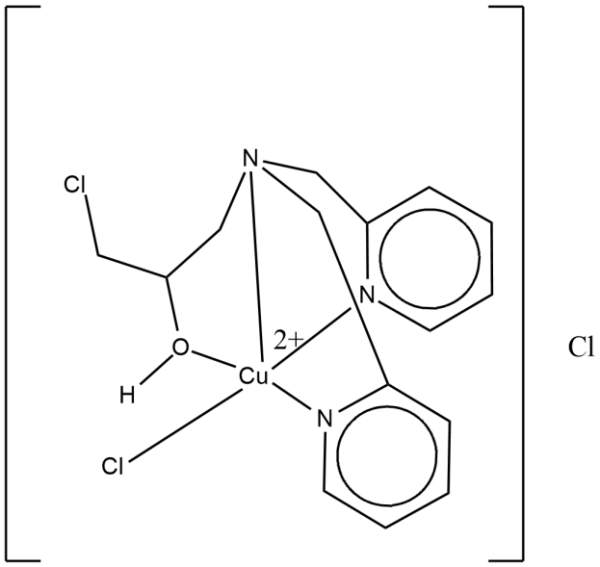

Figure 2.33: Molecular structure of complex [Cu(HPClNOL)Cl]Cl

Studies shown that Cu(II) complexes may have inhibitory effects against lipoxygenase (LOX) and cyclooxygenase-2 (COX-2), enzymes which are responsible for inflammatory response (Boulsourani et al., 2019; Hussain et al., 2019). Cu(II) complexes were reported to inhibit the activation of NF-κB/AP-1 cell and reduced tumour necrosis factor alpha (TNF-α) secretion which induced body inflammatory conditions (Vančo et al., 2021). In addition, free radicals are also associated with inflammation in our body and chronic inflammation produces a lot of free radicals which leads to more inflammation and caused body damage (Biswas et al., 2017). The complexes synthesised by Malis et al., (2021) exhibited significant ability to reduce hydrogen peroxide which are commonly associated with body inflammatory conditions (Wittmann et al., 2012). [Cu(clon)2(neoc)] (Figure 2.34) demonstrated the highest hydrogen peroxide reducing ability at 94.62% ± 0.94 which was comparable to ascorbic acid at 95.89% ± 2.14.

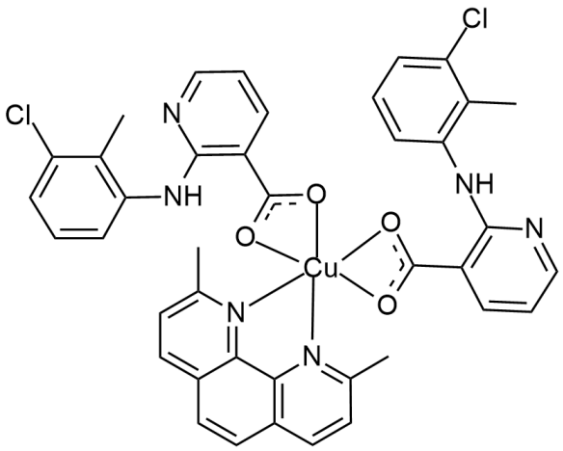

Figure 2.34: Molecular structure of [Cu(clon)2(neoc)] (Malis et al., 2021)

2.4.2 Zinc(II) complexes

Zinc is another essential micronutrient needed by the body and the second most abundant following iron (Solano, 2018). It is crucial for maintaining body processes such as auto-immune process, production of melanin and to curb oxidative stress (Kaczmarek et al., 2023). Zinc deficiency is associated with several health conditions such as alopecia areata, acne vulgaris and male infertility (Al-fagieh et al., 2023; Lalosevic et al., 2023; Yee et al., 2020).

In bacteria, Zn(II) ion is crucial in bacteria pathogenesis and virulence behaviour. It has been shown that the disruption to the Zn^{2+}uptake systems, will influence the bacteria's disease-causing ability as deletion of zinc uptake system gene were associated to poor growth in the enterotoxigenic *E. coli* strain as well as reducing the bacteria adhesion onto the host cell (Quan et al., 2020). Nevertheless, it was established that zinc on its own possessed specific ability to inhibit bacterial cell growth especially at high concentrations which was shown to induce toxicity in bacterial cell (McDevitt et al., 2011; Zhang et al., 2021).

Extensive research have been conducted to explore the antibacterial activities of Zn(II) complexes with different types of ligands as study demonstrated that the antibacterial efficacy of Zn (II) complexes were better than zinc(II) ion alone (Zhang et al., 2021). For instance, a series of Fe(III), Co(II), Ni(II), Cu(II) and Zn(II) mixed-ligand complexes were produced by Lateef et al., (2024) according to 1:1:1 ratio for antimicrobial analysis. The synthesised complexes were elucidated as octahedral structure, and the coordination occurred through N atom and the deprotonated OH groups. Metal complexes exhibited better antibacterial activity compared to their free ligands, which is consistent with the results reported in various studies. The chelation process reduced the polarity of the metal ions because of electron delocalisation with the donor groups which eventually increase the lipophilicity of the complexes and rendered them more permeable in penetrating the bacterial membrane (Uddin et al., 2012). ZnLQ complex (Figure 2.35) was shown as the most promising compound against all strains of bacteria and fungi such as *P. aeruginosa* and *A. flavus.* Furthermore, molecular docking data implied that this complex had a strong affinity against the targeted protein in its pocket site.

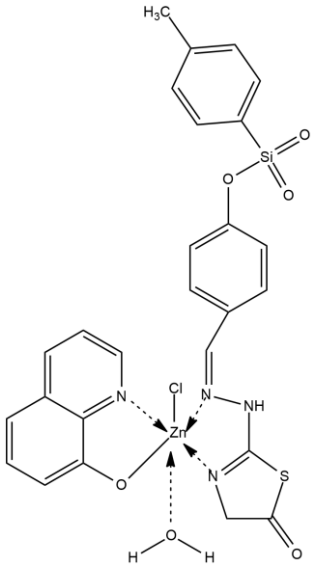

Figure 2.35: Molecular structure of ZnLQ complex

Zn(II) ion is a diamagnetic Lewis acid that can afford various coordination as well as being redox inactive according to Porchia et al., (2020). In the biological system, zinc can coordinate to N, O or S donor atoms present in histidine, glutamate/aspartate, and cysteine residues in four, five and six coordination system. It also supported tetrahedral, pyramidal, or octahedral coordination geometry with water molecules as well as favors the tetrahedral or in distorted trigonal bipyramidal shape with protein. The choice of metal strongly influenced the biological activities of a metal complex. Babgi et al., (2021) who synthesised dichloro(diamine) complexes of Zn(II) ion (Figure 2.36) found that the Zn(II) complexes had better anticancer activities than the platinum(II) complexes. Furthermore, it was demonstrated that the complexes had strong binding affinity towards CT-DNA via intercalation. In addition, the IC_{50} values suggested that the complexes had comparable cytotoxic activity compared to Sunitinib and Cisplatin as well as higher selectivity index against cancer cell lines than the reference drug which highlighted the strong potential of Zn(II) complexes as anticancer agent.

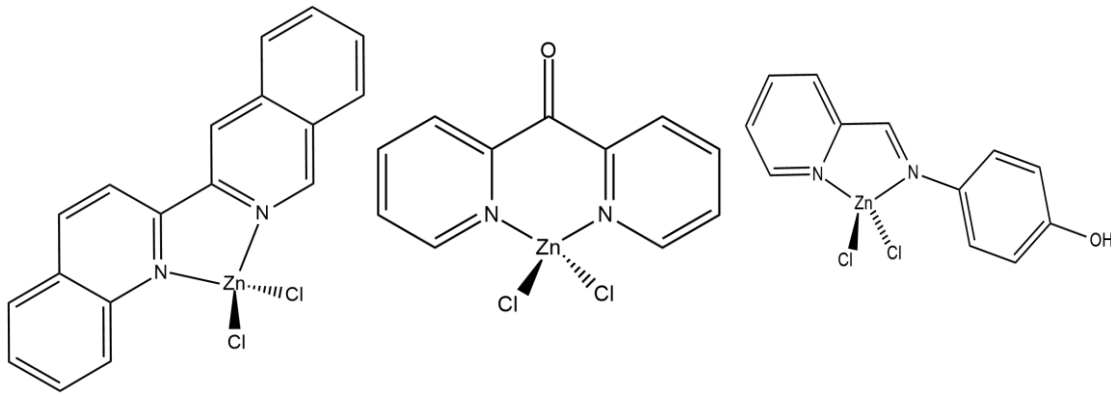

Zn-1 Zn-2 Zn-3

Figure 2.36: Zinc(II) complexes with dichloro(diimine) ligands

Designing new drugs by including metal had been proven to improve drug efficiency. Zinc is a d^{10} transition metal that maintained and stabilised molecules with nitrogen, oxygen and sulfur groups by forming a tetrahedral geometrical structure (Pace & Weerapana, 2014). Subsequently, Martinez et al., (2023) have designed a modified version of angiotensin II receptor blockers (ARB), candesartan with zinc(II) metal centers to improve its anti-hypertensive drug efficacy. An *in vivo* experiment revealed that ZnCand (Figure 2.37) reduced hypertension and cardiac hypertrophy in rats models. Furthermore, experimental data showed that ZnCand had stronger interaction than candesartan with angiotensin II receptor, type I as a result of more rigid structure produced upon complexation. Besides, the study also demonstrated that Zn(II) complex reduced the connective tissue growth factor (CTGF) and matrix metalloproteinase-2 (MMP-2) secretions, protein that is often associated with heart failures (Buckley et al., 2023; Yagi et al., 2012).

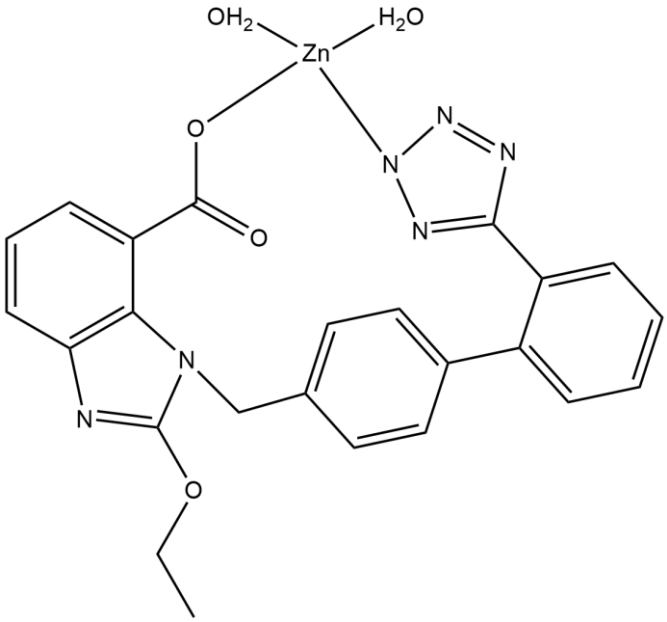

Figure 2.37: Molecular structure of ZnCand

2.4.3 Cobalt(II) complexes

Cobalt is present in our bodies as metal centers surrounded by corrin rings known as vitamin B_{12} and is crucial for maintaining healthy nervous systems (Calderón-Ospina & Nava-Mesa, 2017; Kennedy, 2016; Wienhausen et al., 2022). Similar to Cu(II) and Zn(II) complexes, Co(II) complexes had been the subject of attention due to its wide biological potential. In many cases, the geometrical structure of cobalt(II) complexes were determined as six-coordinated octahedral complex as supported by the magnetic moment value (Derafa et al., 2024; Kumar et al., 2024).

It is widely reported that complexation of ligands leads to significant improvement of the biological activities of a compound. In a study by Rani et al., (2023) it was reported that thiosemicarbazone-based of Ni(II), Zn(II), Ni(II) and Cu(II) metal complexes had better anti-oxidant and anti-inflammatory activities than its free ligands. The antimicrobial activities of the complexes however varied, but Co(II) complex (Figure 2.38) in particular

demonstrated remarkable potential against gram-negative bacteria *E. coli* strain as well as appreciable effect against *P. aeruginosa*. Electron delocalization in the complex compound was believed to increase the lipophilicity and the permeability of the compound which facilitated the movement of the complex across the cell bacteria membrane leading to killing of bacteria cells.

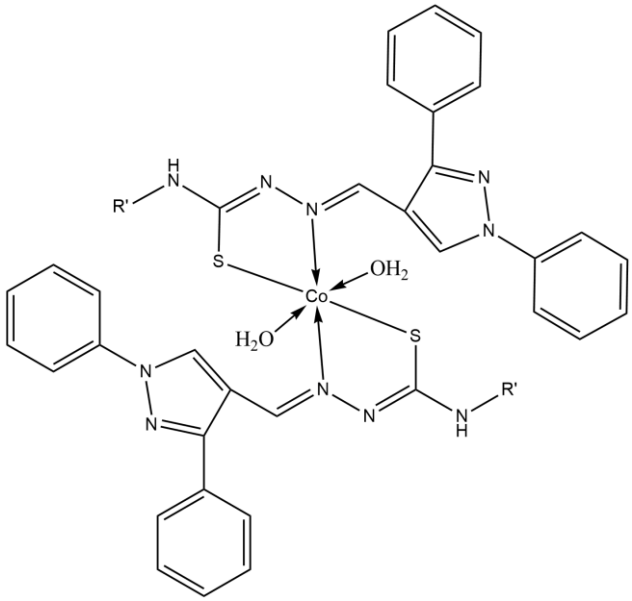

Figure 2.38: Thiosemicarbazone based cobalt(II) complex

In 2022, Damena et al. investigated the antioxidant and and anti-bacterial potential of Co(II) and vanadium (Va)(II) complexes synthesized with quinolines ligands. The results showed that the metal complexes were more active than its free ligands. Co(II) complexes (Figure 2.39) showed more potent antibacterial potential than vanadium(II) complexes with 10.78 ± 0.24 to 18.62 ± 0.19 mm clear zones at 150 and 300 µg/mL concentration.

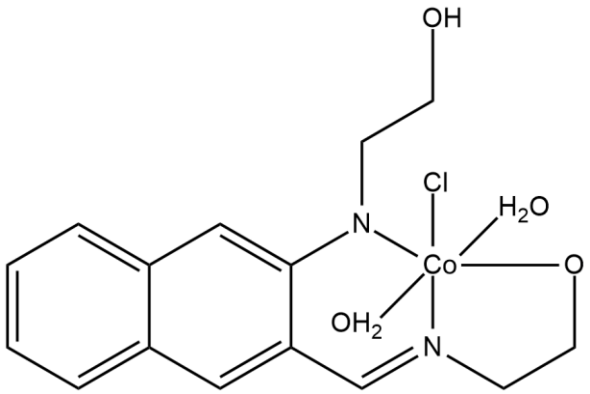

Figure 2.39: Molecular structure of $Co(L)(H_2O)_2Cl$

Besides, the anticancer potential of cobalt(II) complexes have also been investigated in a study by Yılmaz et al., (2019). Eighteen compound consisting of cobalt(II) and zinc(II) complexes (Figure 2.40) of benzimidazole ligands had been studied for its anticancer activity against human ovarian (A-2780) and prostate (Du-145) cancer cells. Out of eighteen complexes, two of the cobalt(II) shown values higher than the standard docetaxel against A-2790 cancer cell lines at 0.1 µM. Compound 18 (Figure 2.41) also demonstrated high antitumor activity against DU-145 and overall, the anticancer activity of the metal complexes were better than its free ligands against human ovarian cancer cell.

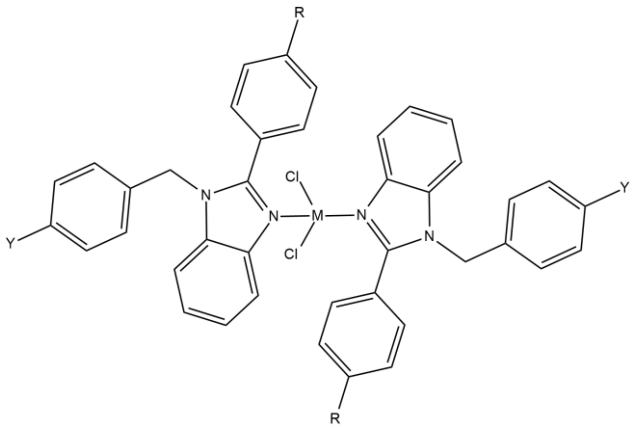

Figure 2.40: General structure of Co(II) and Zn(II) complexes of bendimidazole

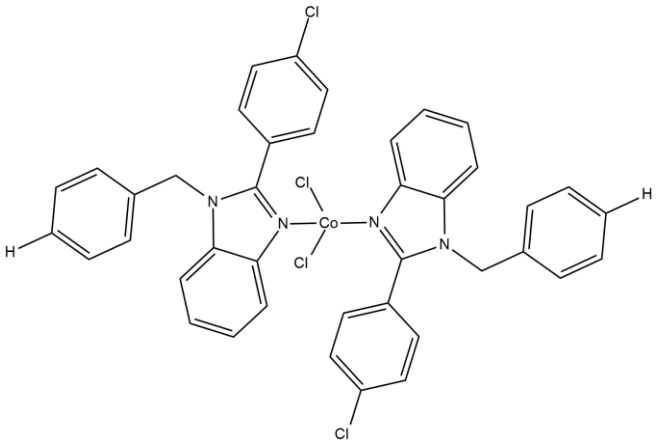

Figure 2.41: Molecular structure of dichlorobis(1-benzyl)-2-(4-chlorophenyl)-1H-benzimidazole-kN^3)cobalt(II)

2.4.4 Thiourea complexes as potential therapeutic agents

Thiourea is a versatile ligand due to the ability to coordinate with various metal to form stable metal complexes. The presence of electron rich heteroatoms such as sulfur and nitrogen are important for hydrogen bonding interaction and act as coordination site in metal complexation (Khan et al., 2020). The versatility is driven by the fact that it can act as a monodentate, bidentate and polydentate ligand through coordination with oxygen, nitrogen and sulfur atoms thus makes them an interesting choice as a ligand (Cunha et al., 2018; Rilak et al., 2015). Currently, various studies had reported on the pharmacological properties of thiourea complex including those incorporating Cu(II) and Zn(II) metals.

In one study by Bielenica et al., (2018), the synthesised Cu(II) complex of 1-(3,4-dichlorophenyl)-3-[3-(trifluoromethyl)phenyl]thiourea (Figure 2.42) displayed the broadest antimicrobial activity against standard *Staphylococcal* strains. The inhibitory activities of the complex were seen to be better than the parent ligand and the standard reference drug especially against the clinical isolates of *S. aureus* and *Staphylococcus epidermis*. The interaction of the parent ligand and the DNA gyrase enzyme was determined as the main

mechanism of the antibacterial activities; whereby hydrogen bond interaction between the -NH group of the thiourea functionality and amino acid Asp81 was determined as the key interaction.

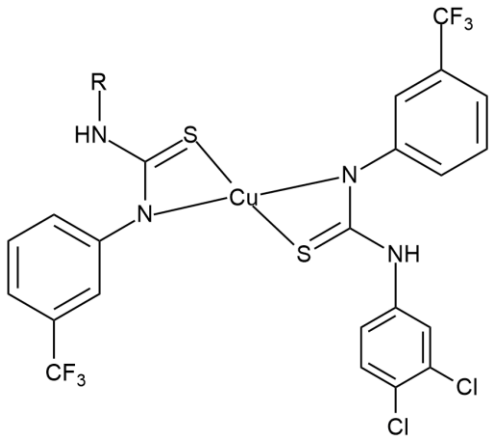

Figure 2.42: Geometrical structure of Cu(II) complex of 1-(3,4-dichlorophenyl)-3-[3-(trifluoromethyl)phenyl]thiourea

Rakhshani et al., (2018) prepared some novel bidentate thiourea complexes (Figure 2.43) which bonded through O and S atom using Ni(II) and Cu(II) as metal centers. The complexes were prepared in hot ethanolic solution according to 1:2 ratio between the ligands and metal salt solution. The antibacterial assays of these compounds revealed that the complexes were more potent against gram-negative bacteria *E. coli* than the gram-positive *S. aureus*. The difference in the compound efficacy can be explained in terms of the polarity of the cell wall membrane; where the gram-negative cell wall is infused with a peptidoglycan layer and an outer membrane consisting of protein, phospholipid and lipopolysaccahrides that are very polar hence facilitate the movement of the compound across cell membrane (Khosravi & Mansouri-Torshizi, 2018). Furthermore, the Cu(II) complex was revealed to be the most potent compound.

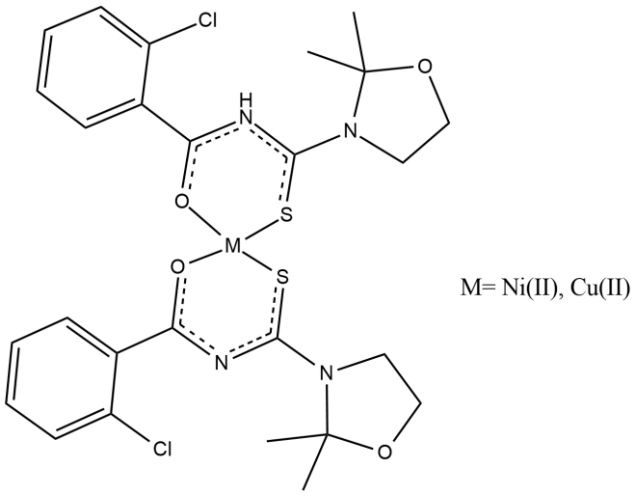

Figure 2.43: Geometrical structure of Cu(II) and Ni(II) complexes of benzoylthiourea

A series of Cu(II) thiourea benzamide complexes (Figure 2.44) were synthesised to an octahedral structure by Al-Salim & Al-Asadi, (2023). The Cu(II) complexes were shown to exert anticancer activity against MCF-7 breast cancer cell lines with IC_{50} values 4.03 and 4.66, which were more potent than its parent ligands. The complexes, which were synthesised according to 1:2 ratio with the metal salt solution saw the thiourea derivatives behaving as bidentate ligand with the metal centers.

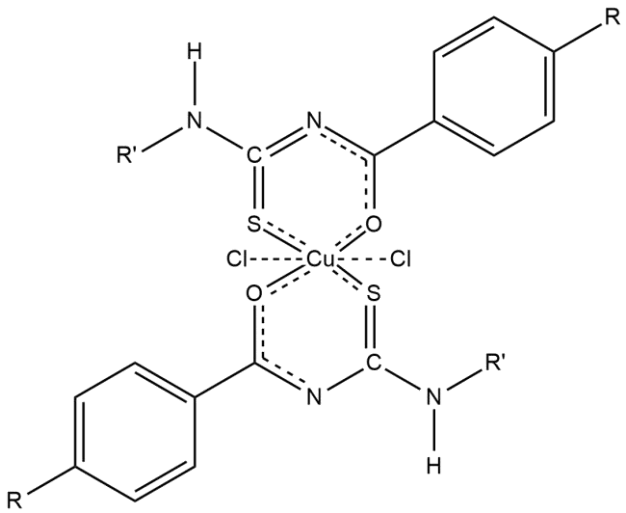

Figure 2.44: Cu(II) complexes of thiourea benzamide derivatives

Hassan et al., (2020) synthesised a series of Co(II), Ni(II), Zn(II) and Cu(II)

complexes of *N*-(2-Chlorophenyl)-*N'*-Benzoyl thiourea ligand. The synthesised complexes were determined to coordinate through the O and S atom of thiourea, with geometrical structure elucidated as tetrahedral and octahedral respectively. The Zn(II) complex of the thiourea derivative (Figure 2.45) showed potent antibacterial activity with diameter of the inhibition zone ranging from 16 – 33 mm against several bacterial and fungal strains including *S. aureus*, *E. coli* and *C. albican*.

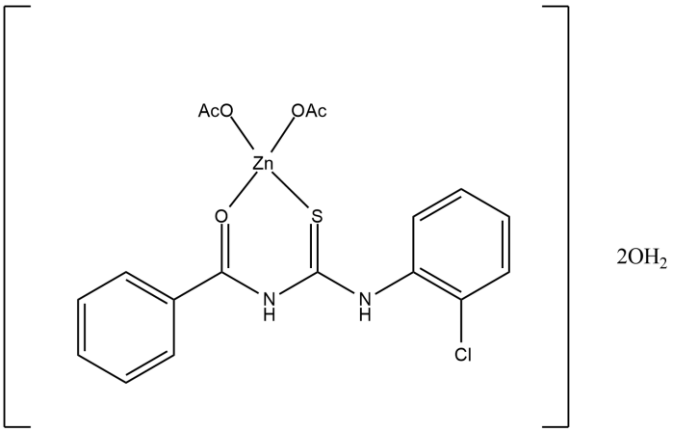

Figure 2.45: Zn(II) complex of N-(2-Chlorophenyl)-N'-benzoylthiourea

In a nutshell, metal complex compound holds a promising potential as a future antibiotic candidate. As a relatively new area in medicinal chemistry, metal complex specialized design redefines a new era of antibiotic, leading the way in targeting AMR. Its versatility, owing to its multiple charges, different coordination mode, and interaction with various ligands offer endless possibilities of creating new drugs with improved efficacy, dose reduction and defy resistance.

CHAPTER 3

METHODOLOGY

3.1 Molecular docking of thiourea and its complexes

Molecular docking simulations were performed using AutoDock Vina Sofware version 1.5.6 (Trott & Olson, 2010) to screen for compound with the highest docking energies. The 2D structures of compound **1-12** and complexes **1a-1c, 2a-2c, 3a-3c** were drawn using ChemDraw Professional 15.0 Software. Consequently, energy minimization was carried out by ChemDraw 3D using the MM2 forcefield and the energetically favourable conformations was eventually saved as pdb files. Using AutoDock tools, the structures of the compounds were converted from pdb to pdbqt files. Next, by assessing the PDB website, the 3D structure of target protein along with its co-crystallized ligand was downloaded as sdf files (PDB code: 1KZN) (Figure 3.1). Subsequently, by utilizing the PyMOL software, the co-crystallized ligand and water molecules were removed from the protein structures and the structure was eventually saved as pdb file. Then, using the AutoDock Vina Software, hydrogen atoms and Kollman charges were added to the protein and the final structures were saved as pdbqt file.

Molecular docking of compound **1-3** and complex **1a-3c** were performed after both protein and ligands had been converted to pdbqt format. Before carrying out any docking simulations, validation of the docking protocol were done by re-docking of the co-crystallized ligand onto the target protein. The re-docked protein-ligand complex was superimposed onto the original structure and the root mean square deviation (RMSD) value was calculated. Generally, an RMSD value of less than 2Å indicated that the method was

valid and docking of ligands can be proceeded (de Oliveira et al., 2023). From the docking validation, the grid size (x,y,z) was selected as (40,40,40), grid centre was set at (19.54, 19.167, 43.283) while the energy range and exhaustiveness was set at 4 and 10 respectively. These settings were applied to both ligands and complexes. Subsequently, the result files were saved as log.txt and pdbqt files respectively. Finally, Discovery Studio was used to visualize the ligand interaction.

Figure 3.1: Crystal structure of DNA Gyrase Enzyme (PDB ID:1KZN)

3.2 ADME Evaluation of thiourea and its complexes

To evaluate the *in silico* ADME and drug-likeness properties of compound **1-12** and complexes **1a-c, 2a-c and 3a-c,** SwissADME software was used to predict the physicochemical characteristics and their pharmacokinetic profiles. Figure 3.2 depicted the steps of ADME profiling of compound **1-3** and its complexes.

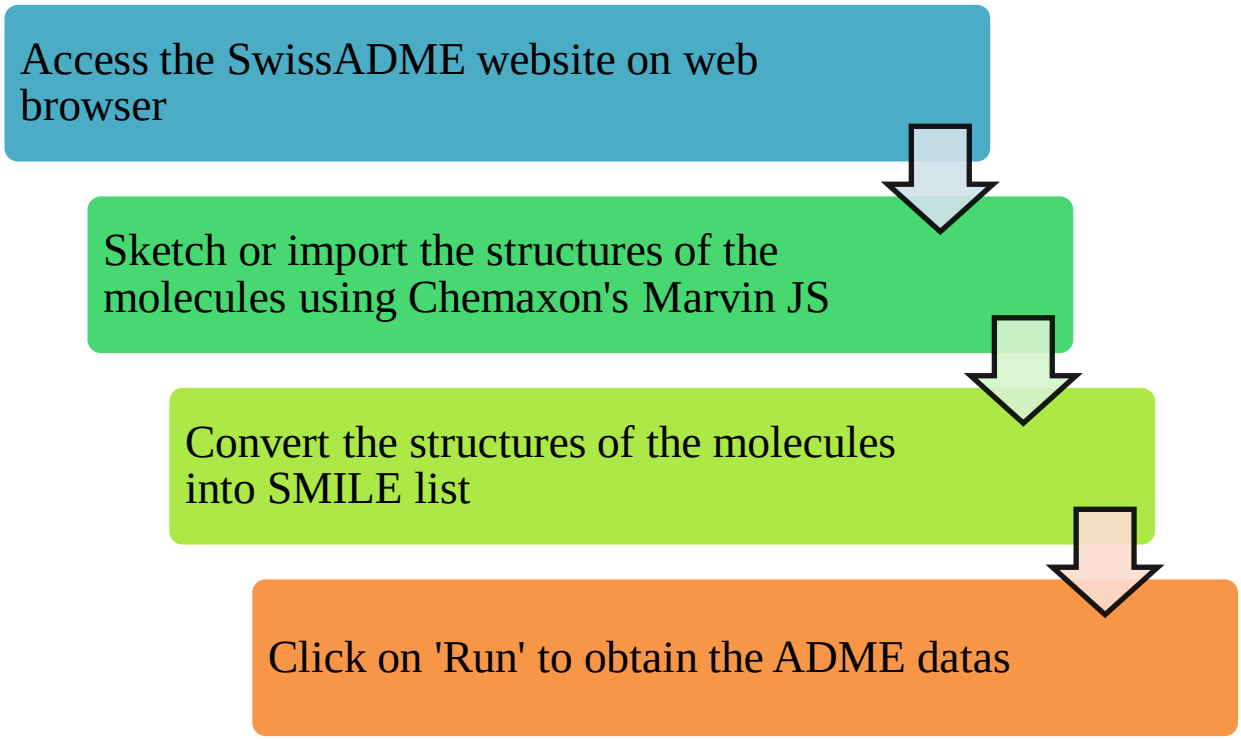

Figure 3.2: Flows in ADME screening of compounds

3.3 General experimental procedures

3.3.1 Chemical, reagents and solvents

All chemicals and reagents were used as purchased without further purification except for acetone. Acetone was obtained from Bendosen and were distilled prior to use to remove water. During distillation, the mixture of acetone was heated under reflux at 56 ℃ until evaporated. The heated vapors were allowed to flow into a Liebig condenser where it cooled down then condensed back into liquid and collected as pure acetone. All other solvents were of analytical grade; Dimethylsulfoxide (DMSO) was purchased from R&M chemicals, ethanol was purchased from HmbG chemicals, methanol and dichloromethane (DCM) was obtained from Emsure and used as received.

Additionally, reagents such as potassium hydroxide (KOH) was purchased from QRëc. Potassium thiocyanate (KSCN), cinnamoyl chloride as well as a series of amino acids such as methionine, valine and leucine from were all obtained from Mercks without purification and finally metal salt solution copper(II) chloride $CuCl_2 \cdot 2H_2O$ solution, cobalt(II) chloride $CoCl_2 \cdot 2H_2O$ solution and zinc(II) sulphate $ZnSO_4 \cdot 7H_2O$ solution were all purchased from HmbG chemicals and used as received.

3.3.2 Instrumentation

The melting point of compounds were determined using melting point apparatus Stuart SMP10. FTIR were used to identify the functional group in the solid compound (Khan et al., 2018). The infrared spectra of the synthesized compounds were recorded using Attenuated Total Reflectance Infrared Spectroscopy (ATR-IR) Spectroscopy Thermo

Nicolet Is10 FTIR Spectrometer at UNIMAS at resolution of 4 cm^{-1}. The absorption band were determined in the infrared region ranging from 4000-500 cm^{-1}. CHNS elemental analysis was carried out using ThermoScientific CHN Elemental Analyzer Flash EA1112 Series to determine the percentage of carbon, hydrogen, nitrogen and sulphur in the compound. UV-Vis spectra were obtained at 200-450 nm range using Agilent Cary 60 UV-Vis. It is a useful technique used to measure the absorption band of molecules in the UV-visible range to give picture on energy gap and the electronic transition (Mohammed et al., 2025). Meanwhile, ^{1}H and ^{13}C NMR spectra were recorded using JNM-ECA 500 at UNIMAS to further elucidate the structures of the compounds based on their chemical shifts. Tetramethysilane (TMS) was used as the standard internal reference while DMSO-d_6 was used as a solvent to dissolve the compounds. The chemical shifts were given in ppm values (δ) while the coupling constants (*J* values) were given in Hertz (Hz).

3.4 Synthesis of thiourea

3.4.1 Synthesis of (cinnamoylcarbamothioyl)methionine (1)

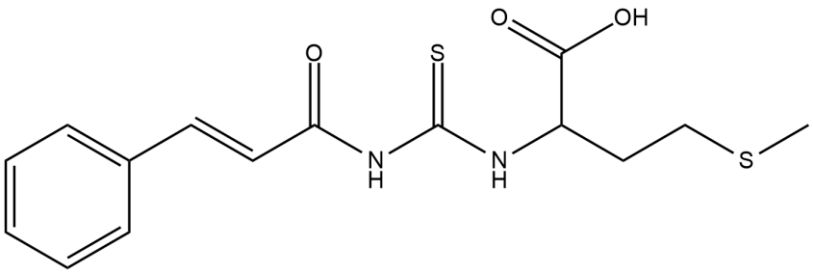

The synthesis of cinnamoyl thiourea was adopted from the method by Yusaini et al. (2022) with little modification. Initially, potassium thiocyanate KSCN (1.461 g, 0.015 mol) was added to a solution of cinnamoyl chloride (2.502 g, 0.015 mol) according to 1:1 ratio in dried acetone (120 mL). The mixture was then stirred for an hour at room temperature and the resulting white precipitate formed was filtered off the mixture. Subsequently, amino acid methionine (2.239 g, 0.015 mol) was added in 1:1 ratio into the filtrate solution and the mixture was stirred under reflux for 18 hrs at 60 ℃ to afford compound **1**. The following day, the mixture was cooled down and the filtrate was left to evaporate at room temperature for a few days to crystallize. The precipitate formed then recrystallized in a mixture of Ethanol: DCM at 1:1 ratio. Final product: yellowish solid (3.82 g, 75.3% yield)

MP: 160-163 ℃; UV-Vis. Spectrum, λ_{max}, nm: 290, FT-IR (cm^{-1}): 3056 (NH), 1716 (C=OOH), 1677(C=ONH), 1496 (C=C), 1269 (C=S), 1164 (C-N); ^{1}H NMR (500 MHz, DMSO -d_6): δ_H 11.44 (1H, s, NH), 11.20 (1H,d, *J*=7.5, NH), 7.70 (1H, d, *J*=16, Ar-H), 7.58 (2H, dd, *J*=7.5, Ar-H), 7.43 (2H, dd, *J*=5, Ar-H), 6.97 (1H, d, *J*=16, CH), 4.92 (1H, q, *J*= 7, CH), 2.02 (3H, s, CH_3); ^{13}C NMR (125MHz, DMSO -d_6: δ_C 180.9 (C=S), 172.4 (C=OOH), 166.8 (C=ONH), 145.0-120.4 (Ar-C), 57.0 (CH) , 39.9-39.7 (CH_2), 15.2 (CH_3); Cald for ($C_{15}H_{18}N_2O_3S_2$); C: 53.23% H:5.36% N:8.28% S: 18.95%. Found C: 52.94% H:5.56% N: 6.86% S: 17.3%.

3.4.2 Synthesis of (cinnamoylcarbamothioyl)valine (2)

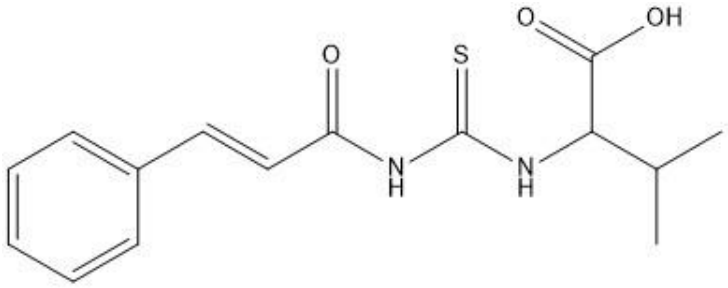

In a similar manner, compound **2** was afforded by the reaction of the intermediate produced through the initial reaction with valine (1.758 g, 0.015 mol). The yellowish solid was purified through slow recrystallization method using a mixture of Ethanol: DCM at 1:1 ratio. Final product: yellowish solid (3.82 g, 83.1% yield)

MP: 155-158 °C; UV-Vis. Spectrum, λ_{max}, nm: 287; FT-IR (cm^{-1}): 3165 (NH), 1732 (C=OOH), 1659(C=ONH), 1528 (Ar-C), 1293 (C=S), 1147 (C-N); ^{1}H NMR (500 MHz, DMSO -d_6): δ_H 11.47 (1H, s, NH), 11.28 (1H,d, *J*=8, NH), 7.72 (1H, d, *J*=16, Ar-H), 7.58 (2H, dd, *J*=7.5, Ar-H), 7.44 (2H, dd, *J*=5, Ar-H), 7.00 (1H, d, *J*=16, CH), 4.780 (1H, q, *J*= 4, CH), 0.919 (7H, d, *J*=14, CH_3); ^{13}C NMR (125 MHz, DMSO -d_6: δ_C 181.4 (C=S), 172.0 (C=OOH), 167.1 (C=ONH), 145.1-120.3 (Ar-C), 62.9 (CH), 19.3-18.4 (CH_3); Cald for ($C_{15}H_{18}N_2O_3S$); C: 58.08% H:5.92% N:9.14% S: 10.45%. Found C: 59.06% H:5.96% N: 8.23% S: 10.08%.

3.4.3 Synthesis of (cinnamoylcarbamothioyl)leucine(3)

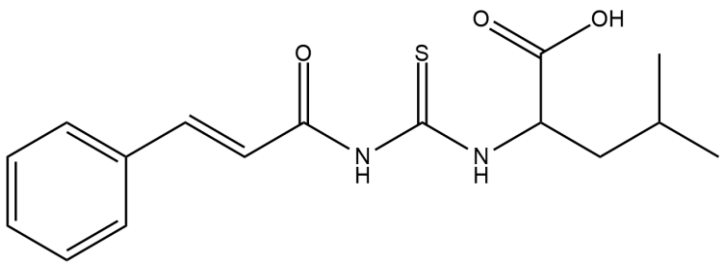

In a similar manner, compound **3** was synthesized by the reaction of the intermediate produced through the initial reaction with leucine (1.969 g, 0.015 mol). The white solid was purified through slow recrystallization method using a mixture of methanol: DCM at 1:1 ratio. Final product: white solid (3.57 g, 74.3% yield)

MP: 190-192 °C ; UV-Vis. Spectrum, λ_{max}, nm: 295; FT-IR (cm^{-1}): 3146 (NH), 1731 (C=OOH), 1660 (C=ONH), 1519 (Ar-C), 1281 (C=S), 1143 (C-N); ^{1}H NMR (500 MHz, DMSO -d_6): δ_H 11.43 (1H, s, NH), 11.13 (1H,d, *J*=8, NH), 7.70 (1H, d, *J*=15.5, Ar-H), 7.57 (2H, dd, *J*=7.5, Ar-H), 7.43 (2H, dd, *J*=3, Ar-H), 6.95 (1H, d, *J*=15.5, CH), 4.83 (1H, q, *J*= 7, CH), 0.88 (7H, q, *J*=6.5, CH_3); ^{13}C NMR (125 MHz, DMSO -d_6: δ_C 180.9 (C=S), 173.1 (C=OOH), 166.9 (C=ONH), 145.0-120.3 (Ar-C), 56.5 (CH), 25.2-22.5 (CH_3); Cald for ($C_{16}H_{20}N_2O_3S$); C: 59.98% H:6.29% N:8.74% S: 10.01%. Found C: 60.39% H:6.33% N: 8.52% S: 10.14%.

3.5 Synthesis of metal complexes

3.5.1 Synthesis of [bis(cinnamoylcarbamothioyl)methionine]Cu(II) (1a)

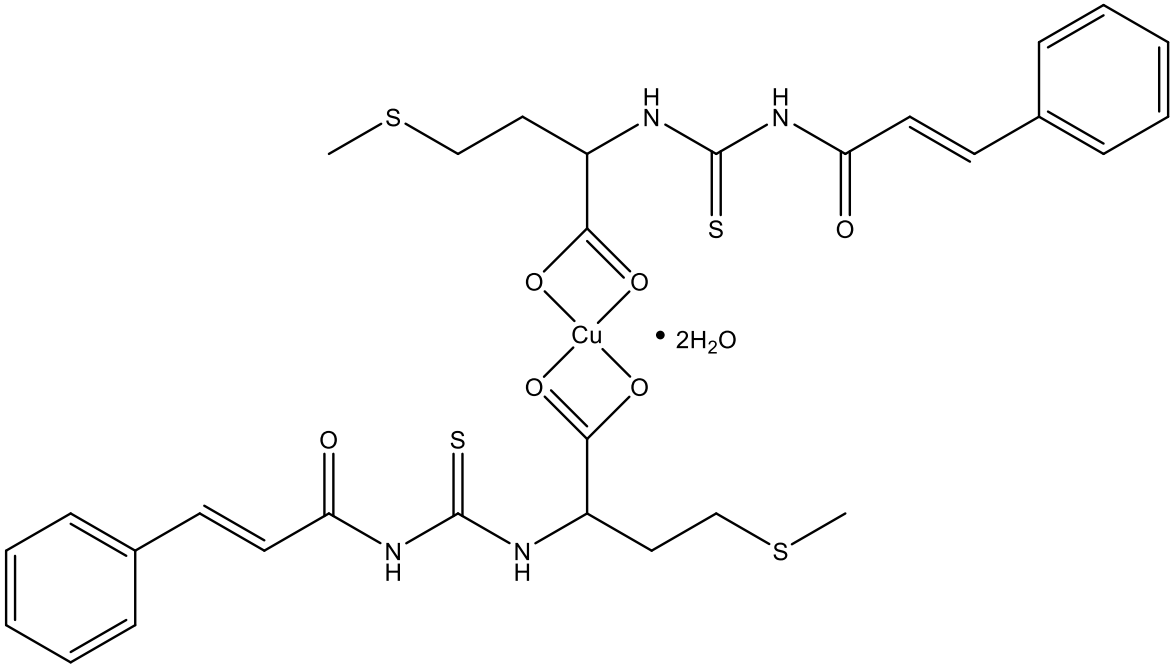

The procedure for the synthesis of thiourea complexes were adopted from Khan et al. (2020) with slight modification. Potassium hydroxide, KOH solution (0.056 g, 0.001 mol) was added dropwise into a solution of ligand **1** (0.338 g, 0.001 mol) previously dissolved in 9 mL ethanol inside a round bottomed flask. The resulting mixture was stirred for half an hour forming white precipitate. Consequently, copper salt solution, $CuCl_2 \cdot 2H_2O$ (0.085g, 0.0005 mol) dissolved in 0.5 mL of distilled water was added in 1:2 ratio (metal: ligand) which instantly form a green precipitate. The mixture was stirred for a further 2 hrs to allow the reaction to take place completely. After two hrs, the resulting solution was filtered to remove excess solvent. Green precipitate was collected on the filter paper and dried in the oven at 70°C for 18 hrs. Final product: Green precipitate (0.31 g, 40.56%).

MP: 166-168 °C; UV-Vis. Spectrum, λ_{max}, nm: 294; FT-IR (cm^{-1}): 3061 (NH), 1680 (C=ONH), 1572 (Ar-C), 1243 (C=S), 1176 (C-N). Cald for ($C_{30}H_{36}CuN_4O_6S_4 \cdot 2H_2O$); C: 46.49% H:4.65% N:7.23% S: 16.56%. Found C: 46.48% H:4.17% N: 7.43% S: 16.76%.

3.5.2 Synthesis of [bis(cinnamoylcarbamothioyl)valine]Cu(II) (2a)

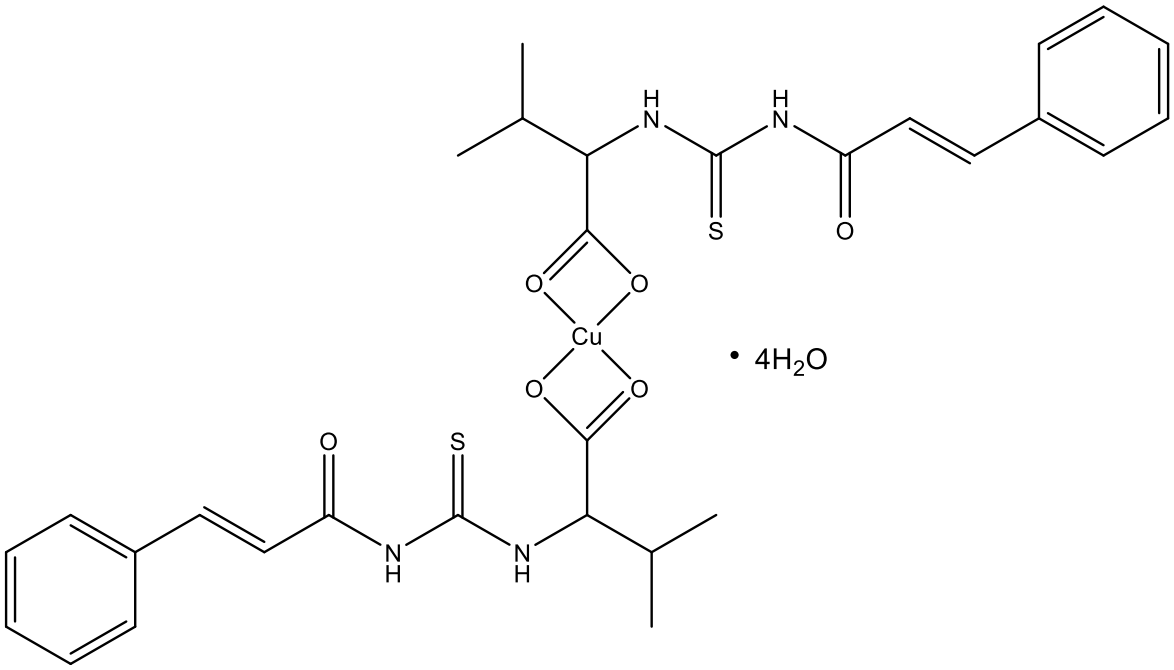

In a similar manner, complex **2a** was afforded from the reaction of ligand **2** (0.306 g, 0.001 mol) and $CuCl_2 \cdot 2H_2O$ (0.085 g, 0.0005 mol). Green precipitate was collected on the filter paper and dried in the oven at 70°C for 18 hrs. Final product: Green precipitate (0.12 g, 41.00%)

MP: 198 ℃; UV-Vis. Spectrum, λ_{max}, nm: 287; FT-IR (cm^{-1}): 3061 (NH), 1681 (C=ONH), 1573 (Ar-C), 1243 (C=S), 1175 (C-N). Cald for ($C_{30}H_{36}CuN_4O_6S_2 \bullet 4H_2O$); C: 48.24% H:4.82% N:7.51% S: 8.59%. Found C: 48.08% H:4.17% N: 7.65% S: 8.39%.

3.5.3 Synthesis of [bis(cinnamoylcarbamothioyl)leucine]Cu(II) (3a)

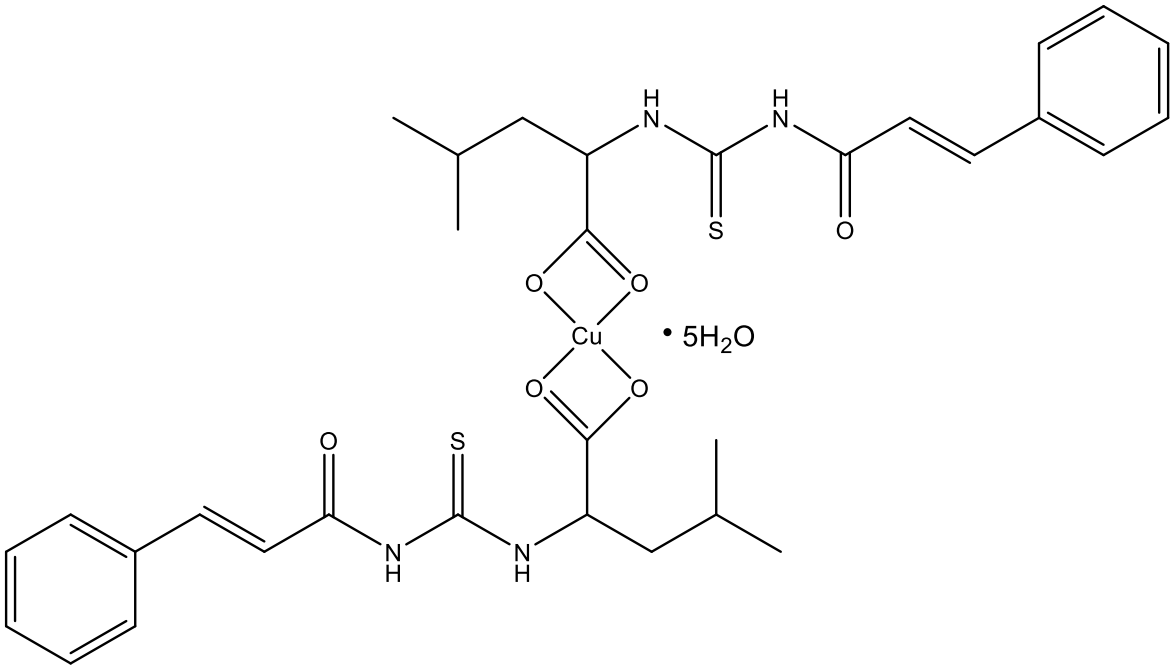

In a similar manner, Complex **3a** was afforded from the reaction of ligand **3** in methanol (0.320 g, 0.001 mol) and $CuCl_2 \cdot 2H_2O$ in distilled water. Green precipitate was collected on the filter paper and dried in the oven at 70°C for 18 hrs. Final product: Dark green precipitate (0.30 g, 37.7%).

MP: 205 °C; UV-Vis. Spectrum, λ_{max}, nm: 287 FT-IR (cm^{-1}): 3060 (NH), 1681 (CONH), 1573 (Ar-C), 1243 (C=S), 1176 (C-N). Cald for ($C_{32}H_{40}CuN_4O_6S_2 \cdot 5H_2O$); C: 48.46% H:5.05% N:7.07% S: 8.09%. Found C: 48.09% H:4.98% N: 7.04% S: 7.71%.

3.5.4 Synthesis of [bis(cinnamoylcarbamothioyl)methionine]Zn(II) (1b)

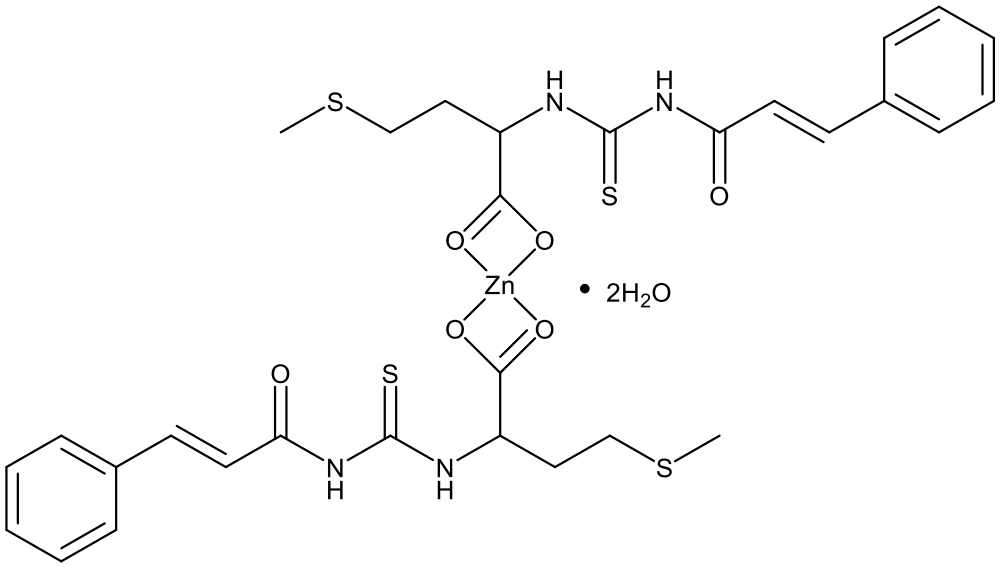

Potassium hydroxide, KOH solution (0.056 g, 0.001 mol) was added dropwise into a solution of ligand **1** (0.338 g, 0.001 mol) previously dissolved in 9 mL ethanol inside a round bottomed flask. The resulting mixture was stirred for half an hour forming white precipitate. Consequently, zinc(II) salt solution, $ZnSO_4 \cdot 2H_2O$ (0.144 g, 0.0005 mol) dissolved in 0.5 mL of distilled water was added in 1:2 ratio (metal:ligand). The mixture was stirred for a further 2 hrs to allow the reaction to take place completely to afford complex **1b**. After two hrs, the resulting solution was filtered to remove excess solvent. White precipitate was collected on the filter paper and dried in the oven at 70°C for 18 hrs. Final product: White precipitate (0.27 g, 34.14%).

MP: 224-227 °C; UV-Vis. Spectrum, λ_{max}, nm: 294; FT-IR (cm^{-1}): 3060 (NH), 1681 (C=ONH), 1593 (Ar-C), 1243 (C=S), 1176 (C-N). Cald for ($C_{30}H_{36}ZnN_4O_6S_4 . 2H_2O$); C: 46.38% H:4.64% N:7.22% S: 16.52%. Found C: 46.4% H:2.67% N: 5.16% S: 16.11%.

3.5.5 Synthesis of [bis(cinnamoylcarbamothioyl)valine]Zn(II) (2b)

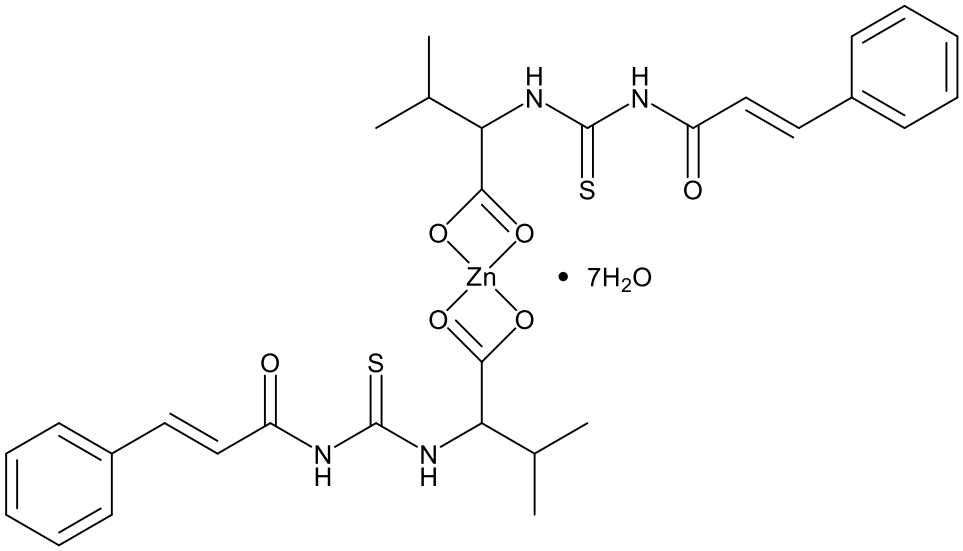

In a similar manner, complex **2b** was afforded from the reaction of ligand **2** (0.306 g, 0.001 mol) and $ZnSO_4 \cdot 7H_2O$ (0.144 g, 0.0005 mol) dissolved in 0.5 mL of distilled water added in 1:2 ratio (metal:ligand). White precipitate was collected on the filter paper and dried in the oven at 70°C for 18 hrs. Final product: White precipitate (0.36 g, 89.76%)

MP: 211-213 °C; UV-Vis. Spectrum, λ_{max}, nm: 294 FT-IR (cm^{-1}): 3060 (NH), 1681 (C=ONH), 1573 (Ar-C), 1243 (C=S), 1176 (C-N). Cald for ($C_{30}H_{36}ZnN_4O_6S_2 \bullet 7H_2O$); C: 44.88% H:4.49% N:6.98% S: 7.99%. Found C: 45.68% H:3.89% N: 6.95% S: 5.85%

3.5.6 Synthesis of [bis(cinnamoylcarbamothioyl)leucine]Zn(II) (3b)

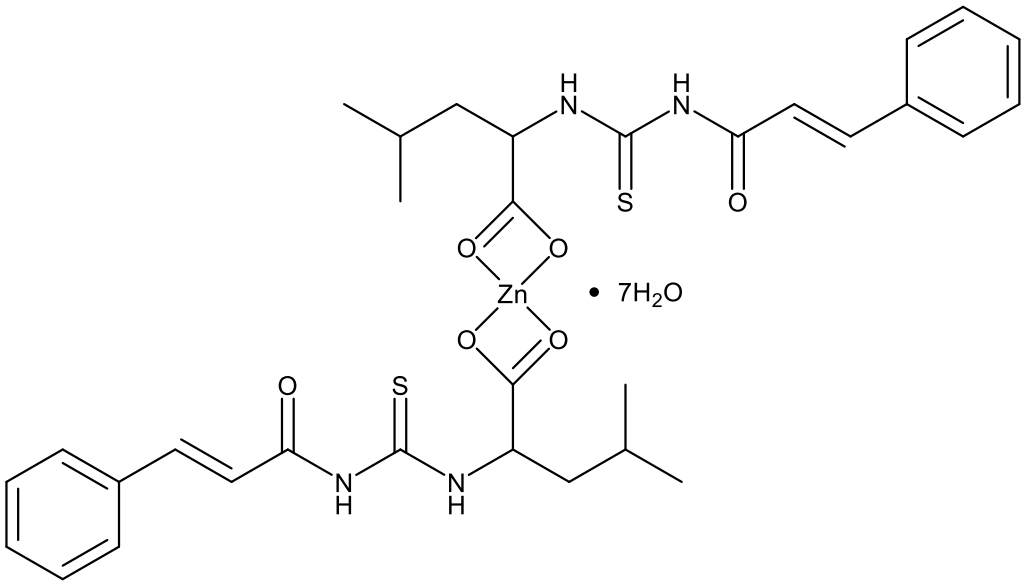

In a similar manner, complex **3b** was afforded from the reaction of ligand **3** (0.320 g, 0.001 mol) and $ZnSO_4 \cdot 7H_2O$ (0.144 g, 0.0005 mol) dissolved in 0.5 mL of distilled water added in 1:2 ratio (metal:ligand). White precipitate was collected on the filter paper and dried in the oven at 70°C for 18hrs. Final product: White precipitate (0.29 g, 26.39%)

MP: 237-242 °C; UV-Vis. Spectrum, λ_{max}, nm: 296; FT-IR (cm^{-1}): 3060 (NH), 1680 (C=ONH), 1558 (Ar-C), 1242 (C=S), 1175(C-N). Cald for ($C_{32}H_{40}ZnN_4O_6S_2.7H_2O•5CH_3OH$); C: 35.35% H:3.68% N:5.16% S: 5.90%. Found C: 35.29% H:3.75% N: 5.35% S: 6.51%

3.5.7 Synthesis of [bis(cinnamoylcarbamothioyl)methionine]Co(II) (1c)

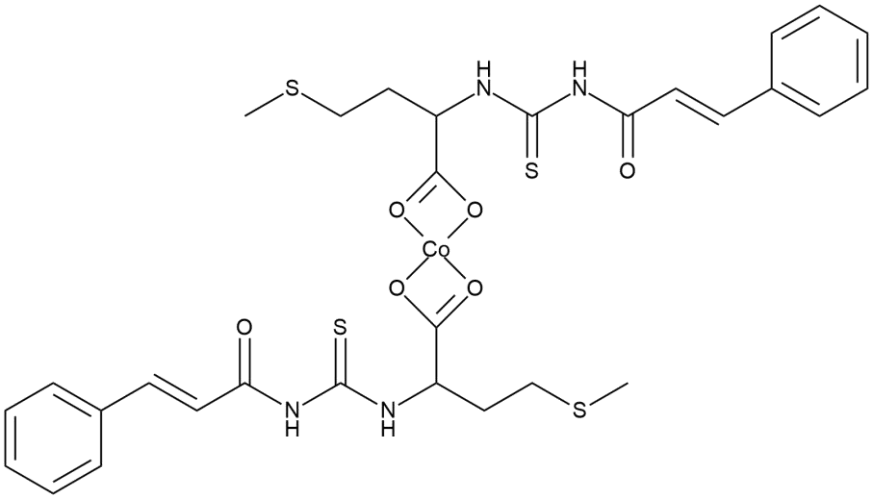

Potassium hydroxide, KOH solution (0.056 g, 0.001 mol) was added dropwise into a solution of ligand **1** (0.338 g, 0.001 mol) previously dissolved in 9 mL ethanol inside a round bottomed flask. The resulting mixture was stirred for half an hour forming white precipitate. Consequently, cobalt(II) salt solution, $CoCl_2 \cdot 2H_2O$ (0.121 g, 0.0005 mol) dissolved in 0.5 mL of distilled water was added in 1:2 ratio (metal:ligand) which instantly form a purple precipitate. The mixture was stirred for a further 2 hrs to allow the reaction to take place completely. After two hrs, the resulting solution was filtered to remove excess solvent. Purple precipitate was collected on the filter paper and dried in the oven at 70°C for 18 hrs. Final product: Purple precipitate (0.15 g, 39.7%).

MP: 255-258 °C; UV-Vis. Spectrum, λ_{max}, nm: 295; FT-IR (cm^{-1}): 3060 (NH),1660 (C=ONH), 1530 (Ar-C), 1220 (C=S), 1169 (C-N). Cald for ($C_{30}H_{36}CoN_4O_6S_4$); C: 49.06% H:4.91% N: 7.64% S: 17.48%. Found C: 48.97% H:3.02% N:7.61% S: 17.43%.

3.5.8 Synthesis of [bis(cinnamoylcarbamothioyl)valine]Co(II) (2c)

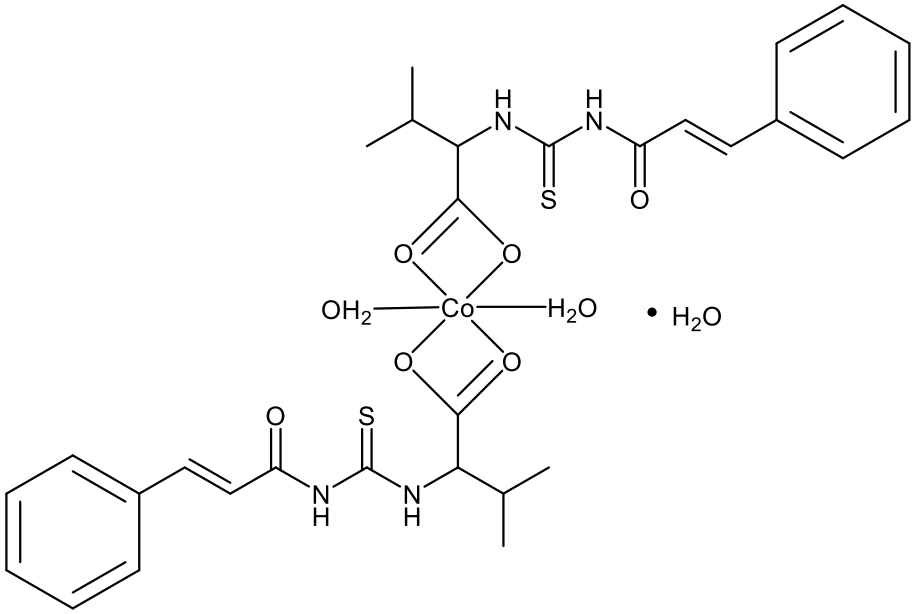

In a similar manner, complex **2c** was synthesized from the reaction of ligand **2** (0.306 g, 0.001 mol) and $CoCl_2 \cdot 2H_2O$ (0.121 g, 0.0005 mol) metal salt solution dissolved in 0.5 mL ethanol according to 1:2 ratio (metal:ligand). A purple precipitate was collected on the filter paper and dried in the oven at 70°C for 18 hrs. Final product: Purple precipitate (0.11 g, 24.67%)

MP: 253-256 °C; UV-Vis. Spectrum, λ_{max}, nm: 295; FT-IR (cm^{-1}): 3062 (NH), 1662 (C=ONH), 1574 (Ar-C), 1220 (C=S), 1167 (C-N). Cald for ($C_{30}H_{36}CoN_4O_6S_2 \bullet 3H_2O$); C: 39.65% H:3.96% N: 5.73% S: 7.06%. Found C: 39.67% H:3.71% N:5.78% S: 3.26%

3.5.9 Synthesis of [bis(cinnamoylcarbamothioyl)leucine]Co(II) (3c)

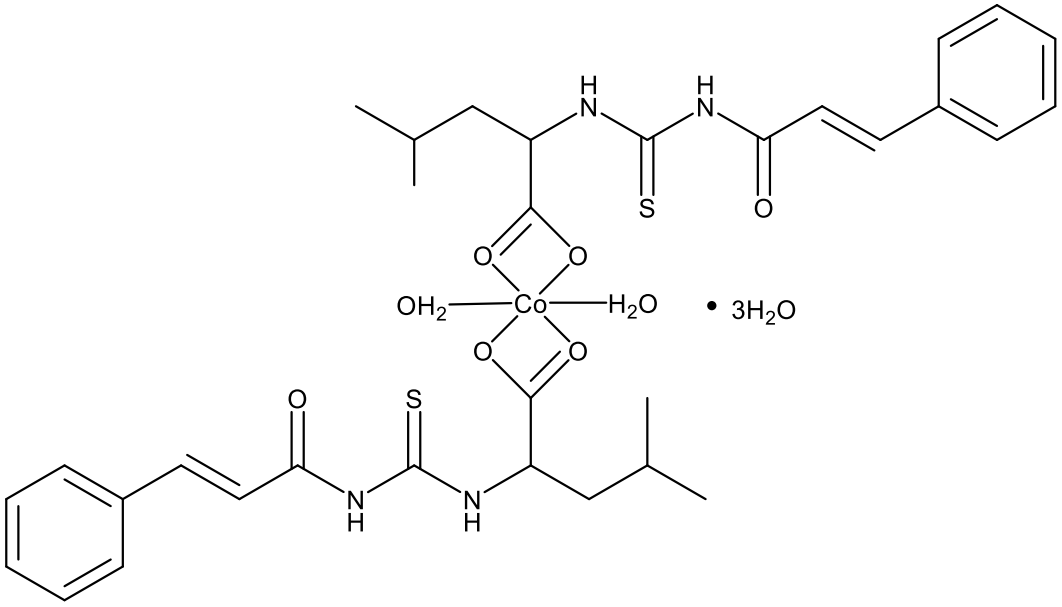

In a similar manner, complex **3c** was synthesized from the reaction of ligand **3** (0.320 g, 0.001 mol) and $CoCl_2 \cdot 2H_2O$ (0.121 g, 0.0005 mol) metal salt solution dissolved in 0.5 mL methanol according to 1:2 ratio (metal:ligand). A purple precipitate was collected on the filter paper and dried in the oven at 70°C for 18 hrs. Final product: Purple precipitate (0.24 g, 30.72%)

MP: 211-215 °C; UV-Vis. Spectrum, λ_{max}, nm: 295; FT-IR (cm^{-1}): 3207 (NH), 1668 (C=ONH), 1559 (Ar-C), 1278 (C=S), 1187 (C-N). Cald for ($C_{32}H_{40}CoN_4O_6S_2 \bullet 5H_2O$); C: 48.75% H:5.08% N: 7.11% S: 8.14%. Found C: 48.73% H:5.55% N:6.95% S: 4.78%

3.6 Antibacterial Evaluation of Thiourea and Its Complexes

3.6.1 Agar-well diffusion method

Compound **1-3** and its respective complexes (complex **1a-1c**, **2a-2c** and **3a-3c**) were screened against the standard *E. coli* strain ATCC 25922 using agar-well diffusion method following the standard method developed by American Society for Microbiology (Hudzicki, 2009) . Generally, this method involves the inoculation of bacterial on the surface of the agar followed by pipetting approximately 20-100 µL of extract solution into the well dug using a sterile cork borer or a tip. Then, the agar plate would be incubated according to a suitable condition and the antibacterial agent would diffuse accordingly to inhibit the growth of bacteria (Balouiri et al., 2016). This method is an easy and inexpensive method for bacterial testing. Additionally, the datas are straightforward and large sample testing can be conducted (Balouiri et al., 2016). A fresh bacterial culture was used in each of the experimental procedures prepared by the inoculation of bacterial culture in a nutrient broth medium for 18 hrs. After 18 hrs, the bacterial culture was adjusted according to 0.5 Mcfarland standard, which was examined using the UV-Vis Spectrophotometer Shimadzu UV-1900i. When the bacterial culture was successfully adjusted to 0.5 McFarland standard, it was then ready to be inoculated onto the agar media.

Antibacterial assays were conducted using Muller-Hinton agar medium by referring to the procedure by Ghorab et al. (2017) but with self-modifications. About 0.2 µL of nutrient broth containing bacterial cell culture was inoculated onto the agar medium using a sterile cotton bud. A 6 mm well was dug using a sterile straw with a diameter of 6 mm on the agar media. Then, 20 µL of the standard solution containing compound was pipetted into each of the agar well. The stock solution of the tested compound was prepared previously

by dissolving the compounds in DMSO. However, metal complexes were insoluble when prepared at higher concentrations (i.e more than 500 ppm) therefore 500 ppm was chosen as the highest concentration, followed by dilution to lower concentration. The final concentrations of the tested compound were prepared in 150 ppm, 250 ppm and 500 ppm respectively. For this experiment, DMSO act as the negative control while Ciprofloxacin was the positive control. After the solution was allowed to properly diffuse, the agar plates were incubated overnight at 37 ℃. After 18 hrs, the diameter of the zone of inhibition was measured and the reading was given in mm. The experiment was done in triplicate to increase the significance of the result.

3.7 Summary of methodology

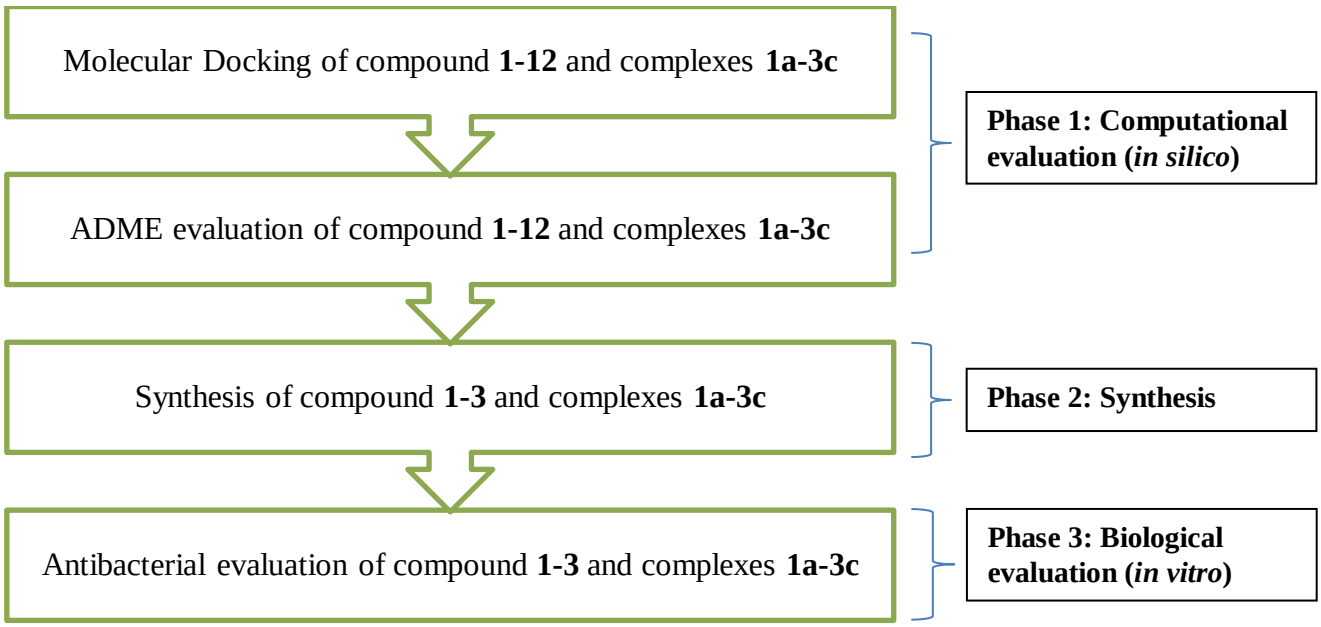

CHAPTER 4

RESULTS AND DISCUSSION

4.1 Molecular docking studies of thiourea and metal complexes

Preliminary dockings were done before any experimental set up were carried out to predict thiourea derivatives with the highest inhibitory activities. Twelve thiourea derivatives were designed and subjected with molecular docking simulation which include the cinnamoyl, palmitoyl, furoyl and dimethyl carbamoyl thiourea derivatives. Eventually, only one group of derivative with the highest docking score will be selected. In this study, AutoDock Vina software was selected as the docking tool of choice due to several advantages such as user-friendly interface and the generation of better binding pose (Nguyen et al., 2020; Prieto-Martínez et al., 2018). Besides, AutoDock Vina is more superior in such a way that the result is more transparent as docking outputs were presented from the highest docking score to the lowest scores and grid map was auto-generated (Butt et al., 2020). DNA gyrase enzyme **(Protein ID: 1KZN)** was selected as target enzyme in this study. DNA gyrase enzyme can be exploited in search for new potent antibiotics due to its omnipresent in bacterial cell but is absent in mammalian cells (De Smet et al., 2021). It is an enzyme that catalyzes the negative supercoiling in bacteria which play an important role in bacterial cell replication (Gellert et al., 1976). Thus, blocking this enzyme is a key feature in many antibiotics (Yi & Lü, 2019). Ciprofloxacin was selected as the positive control in this study as Ciprofloxacin belongs to a broad-spectrum quinolone-class antibiotic that target DNA gyrase and Topoisomerase IV enzyme and is widely used to treat respiratory tract infections, urinary infections, and enteric infections (Hutchings et al., 2019; Millanao et al., 2021).

Prior to docking, the method was first validated by re-docking of co-crystallized ligand onto the crystallized structure of target protein obtained from PDB. Water is removed from the protein structure as it will interfere with the docking process and contribute to high docking scores (Kumar & Zhang, 2013; Reddy et al., 2024). As for ligand preparation, energy minimization was carried out on the 3D structure of the compounds to obtain the most stable conformation.

4.1.1 Molecular docking studies of thiourea

The results of the docking simulation were presented in Table 4.1. The results were compared based on their docking score which is a scoring function to predict the binding affinities of compound inside the enzyme receptor, taking account of their Gibbs free energy (Pantsar & Poso, 2018). Higher docking score would be considered and selected for future experimental studies as higher scores correlate to more stable conformation and thus greater affinity towards target receptor hence better antibacterial activities (Cournia et al., 2017; Luzhkov, 2017; Safi et al., 2024).

From Table 4.1, it was observed that the binding energies of compound **1-12** range from **-5.1 kJ/mol** to **-7.1 kJ/mol** respectively. Generally, the cinnamoyl thiourea derivatives displayed higher docking scores at **-5.7 kJ/mol** to **-7.1 kJ/mol** respectively compared to the other derivatives. Furthermore, the furan (compound **4-6**), dimethyl carbamoyl (compound **7-9**) and especially the palmitoyl groups (compound **10-12**) were all predicted to be weak inhibitors as seen from the binding energies ranging from **-5.1 kJ/mol** to **-5.9 kJ/mol**. The palmitoyl derivatives, compound **11** had the lowest docking scores when docked inside the enzyme pocket of 1KZN receptor. Longer alkyl chains were considered to exert less disruption to the bacterial membrane which translated to lower binding affinity of molecules with target protein (Shalas et al., 2023). When further analyzed, it was observed that the cinnamoyl derivatives had a very similar molecular structure to the positive control Ciprofloxacin (Figure 4.1) which had binding affinities of **-7.4 kJ/mol**. Both compounds contain an aromatic ring and a -COOH group in their structures. Therefore, it is suggested that these two functional groups could play a huge role in

interacting with bacterial cell membrane. Among twelve compounds, compound **2** had the highest docking score at **-7.1 kJ/mol** which implied that compound **2** may bound tightly inside DNA gyrase enzyme and block the cell replication process in bacteria and therefore could possibly inhibit the growth of bacteria. Among other cinnamoyl thiourea derivatives, compound **1** with methionine side chain and compound **3** with leucine side chain had docking score of **-5.8 kJ/mol** and **-5.7 kJ/mol** respectively.

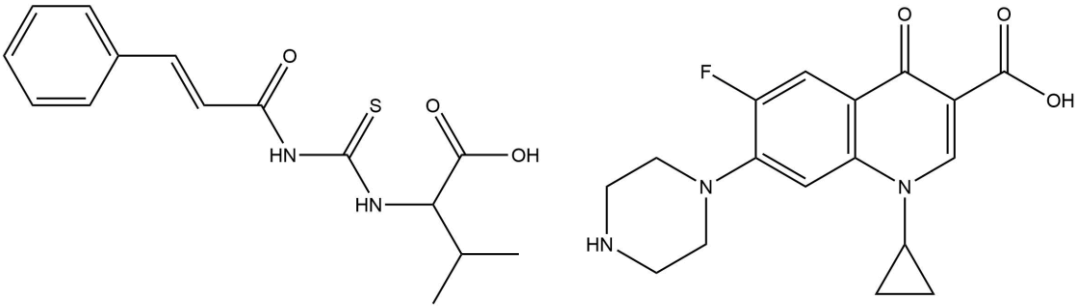

Compound **2** Ciprofloxacin

Figure 4.1: Side by side comparison of molecular structure of compound **2** and Ciprofloxacin

Table 4.1: Docking scores of compound **1-12**

Compound	Molecular Structure	Binding Energies (kJ/mol)
Ciprofloxacin	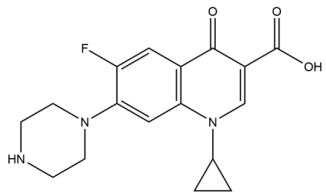	-7.4
1	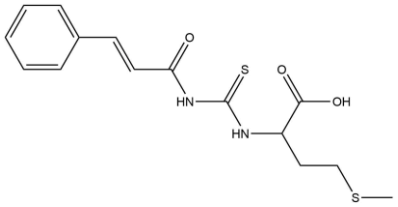	-5.8
2	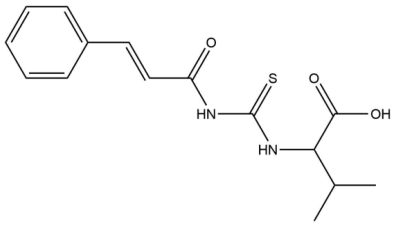	**-7.1**
3	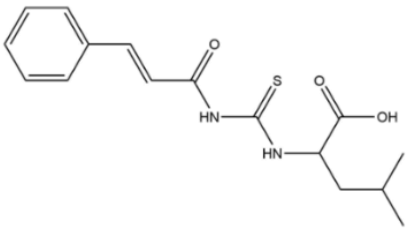	-5.7
4	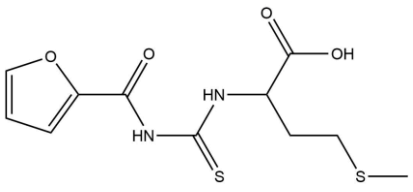	-5.5

Table 4.1 continued

5	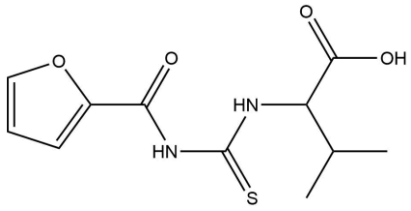	-5.8
6	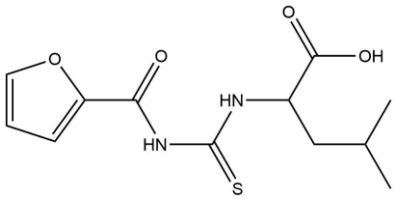	-5.9
7	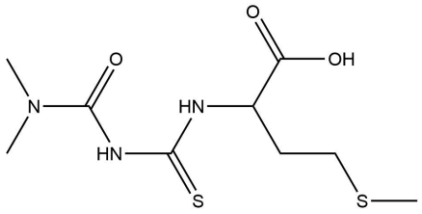	-5.2
8	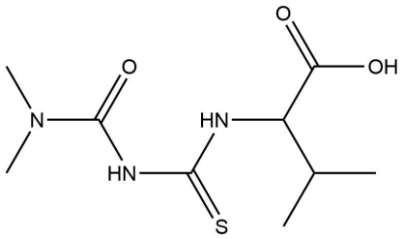	-5.3
9	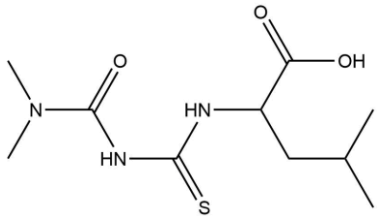	-5.5
10	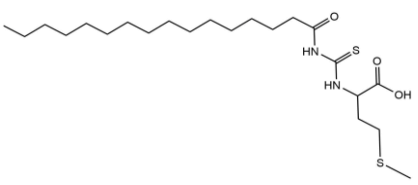	-5.2

Table 4.1 continued

11	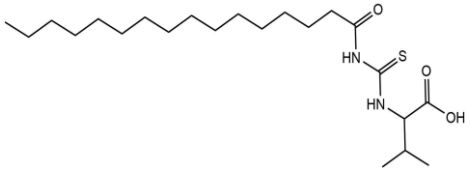	-5.1
12	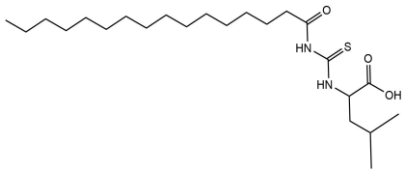	-5.7

For better understanding on the binding interactions, BIOVIA Discovery Studio was used to visualize the interactions of compounds with amino acid residues (Shaweta et al., 2021; Silva et al., 2020). The summary of the interactions of compound **1-12** were presented in Table 4.2. It is crucial to consider the bond length when discussing the interaction of compound with amino acid residues as bond length will give insight on the bond strength and stability. Longer bond length correlates to weaker bond and vice versa. For comparative purposes, the ligand-protein complex interactions will be compared to the positive control Ciprofloxacin. Based on Figure 4.2, Compound **1** was stabilized inside the enzyme pocket of 1KZN receptor by forming one conventional hydrogen bond between the N-H functional group and amino acid **ASN A:46** at a distance 2.90 Å as well as two alkyl interactions between the -CH_3 group with **VAL A:167** and **VAL A:43** at distance 4.68 Å and 5.16 Å respectively. The N-H interactions of urea and thiourea derivatives with amino acids residues were widely reported in literature (Ghorab et al., 2017; Ramaswamy et al., 2022). Besides, pi-alkyl interaction occurred between the aromatic ring of thiourea with **PRO A:79** and **ILE A:90** residues at a distance of 4.06 Å and 5.03 Å each.

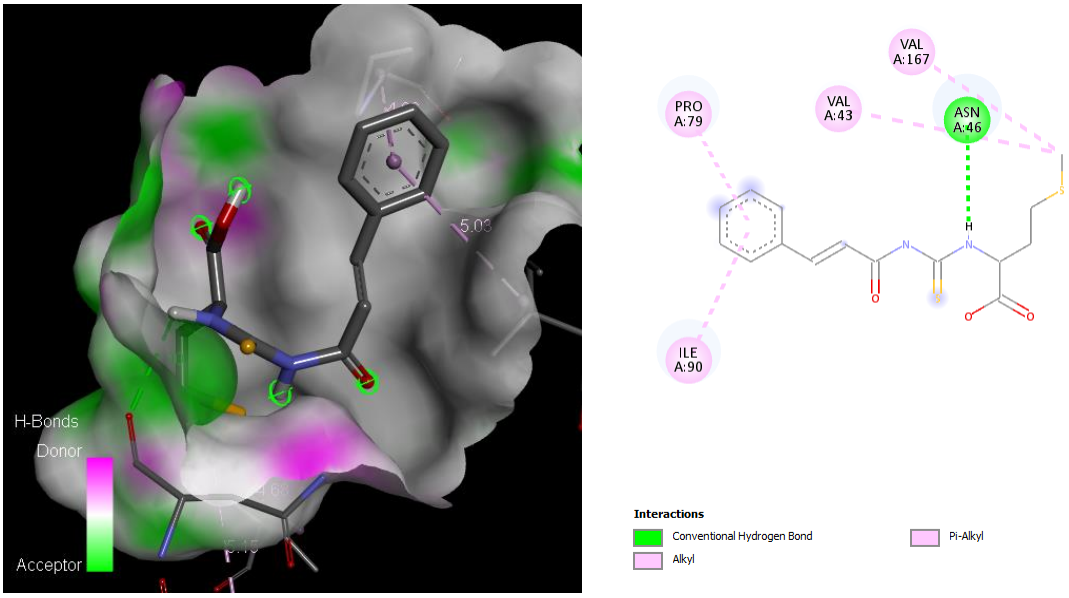

Figure 4.2: 3D (left) and 2D(right) visual representation of docked compound **1** inside 1KZN protein

Table 4.2: Summary of interactions of compound **1-12** inside 1KZN receptor

Compound	Amino acids	Bonds	Distance (Å)
Ciprofloxacin	ILE A:90	Alkyl interaction	4.93
	GLU A:50	Pi-Anion	4.57
	ARG A:76	Unfavourable donor-donor	2.56
	ILE A:78	Pi-Alkyl Interaction	4.72
			4.26
			5.49
	ASN A:46	Amide Pi-Stacked	5.39
	ASP A:73	Halogen (F)	3.12
	ALA A:47	Alkyl Interaction	5.17
	VAL A:43	Conventional Hydrogen Bond	2.76
1	PRO A:79	Pi-Alkyl Interaction	4.06
	ILE A:90		5.03
	VAL A:43	Alkyl Interaction	4.68
	VAL A:167		5.16
	ASN A:46	Conventional Hydrogen Bond	2.90
2	ALA A:47	Pi-Alkyl	4.97
	THR A:165	Conventional Hydrogen Bond	3.13
	GLU A:50		2.17
	ASN A:46	Unfavorable	2.99
3	ASN A:46	Amide Pi-Stacked	5.71
	ILE A:78	Pi-Alkyl	4.46
	ARG A:76	Conventional Hydrogen Bond	5.7
4	GLU A:50	Conventional hydrogen Bond	2.54
	GLY A:77		2.94
	THR A:165		3.01
	ASP A:73	Carbon Hydrogen Bond	3.60
	ILE A:78	Pi-Alkyl	5.29
5	VAL A:120	Alkyl Interaction	4.82
	VAL A:167		5.15
	ILE A:78		4.84
	ILE A:78	Pi-Alkyl Interaction	4.44
	ILE A:90		5.15
	THR A:165	Conventional Hydrogen Bond	3.56
	ASN A:46		2.12
6	ALA A:47	Alkyl Interaction	4.47
	ASN A:46	Conventional Hydrogen Bond	2.73
			2.76
			3.55
	ARG A:76	Pi-Cation	4.62
7	ALA A:47	Alkyl Interaction	4.04
	VAL A:120		4.82
	VAL A:167		5.23

Table 4.2 continued

	ILE A:90		3.78
	ASP A:73	Carbon Hydrogen Bond	3.56
	GLY A:77	Conventional Hydrogen Bond	3.24
	THR A:165		3.04
8	VAL A:120	Alkyl Interaction	5.2
	ALA A:47		4.47
	ILE A:78		4.96
	PRO A:79		4.90
	ASP A:73	Carbon Hydrogen Bond	3.42
	ASN A:46	Conventional Hydrogen Bond	3.25
	ARG A:76		3.13
	GLU A:50		2.36
		Unfavourable	2.89
9	VAL A:120	Alkyl Interaction	4.87
	VAL A:167		5.11
	ALA A:47		4.00
	PRO A:79		5.05
	ASP A:73	Carbon hydrogen bond	3.51
	ASN A:46	Conventional hydrogen bond	3.79
	THR A:165		3.08
10	ALA A:47	Alkyl Interaction	4.10
	ILE A:90	Conventional Hydrogen Bond	5.42
	ILE A:78		4.55/4.62
	PRO A: 79		5.13
	ASP A:49		2.19
	GLY A:117		2.37
11	ILE A:78	Alkyl Interaction	3.87
	ILE A:90		4.69
			4.92
			4.11
	GLY A:117	Conventional Hydrogen Bond	3.06
	ASN A:46		2.91
	HIS A:95		2.82
	ALA A:96		2.50
			2.70
	SER A:121	Unfavourable	1.28
12	PRO A:79	Alkyl Interaction	5.01
	ILE A:78		4.43
			4.76
	ALA A:47		4.21
	ASN A:46	Conventional Hydrogen Bond	2.35
	VAL A:120		2.75
	SER A:121		2.23
			2.71

Compound **2** was made of fewer interaction than compound **1** but more hydrogen bondings were found in the interaction. According to Figure 4.3, compound **2** was nicely embedded inside the active site of 1KZN receptor by two conventional hydrogen bond interactions; one between the oxygen atom of C=O from the amide backbone with the residue **THR A:165** and another one between the N-H functional group of thioamide and amino acid **GLU A:50** at distance 3.13Å and 2.17Å respectively. Hydrogen bonding played a huge role in maintaining protein structure stability (Hung et al., 2021). Thus, it could be deduced that the higher binding energies of compound **2** than compound **1** may be attributed to more hydrogen bond interaction which resulted in more stability of the ligand-protein complex. Additionally, a single pi-alkyl interaction was observed between the aromatic ring and the amino acid residue **ALA A:47** with distance 4.97Å. For comparison purposes, the docking of Ciprofloxacin and DNA Gyrase enzyme revealed many interactions but only one conventional hydrogen bond interaction was found that was between the N-H group and the residue **VAL A:43**. Furthermore, compound **2** resembled Ciprofloxacin as both are interacting with the residues **GLU A:50** and **ALA A:47**. It is also worth mentioning that although Ciprofloxacin consist of one hydrogen bond, it had significantly higher docking scores than any of the thiourea derivatives. This could very well implied that the rest of the interactions such as carbon-hydrogen bond, halogen, alkyl, pi-alkyl, pi-anion and amide-pi stacked interactions may have collectively contributed to the ligand-protein complex stability. Additionally, both compounds were revealed to have one unfavorable bond with amino acid residue. However, according to Wahyuni et al., (2024), the number of unfavorable bond must be <3 in order to maintain stability in which in this case it is still acceptable.

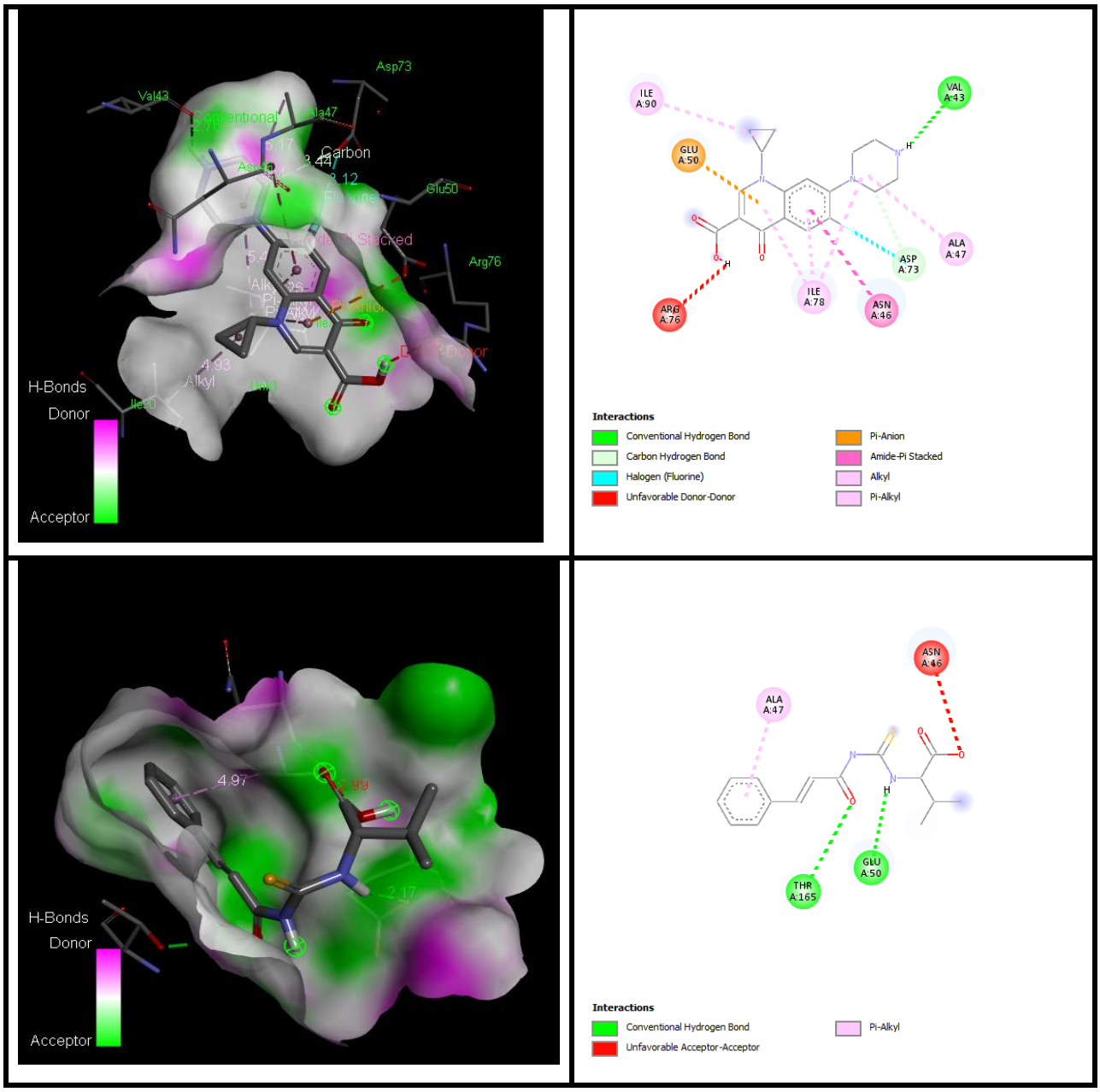

Figure 4.3: 3D (upper left) and 2D (upper right) visual representation of Ciprofloxacin and 3D (bottom left) and 2D (bottom right) visual representation of compound **2** when docked inside the 1KZN protein

Next, compound **3** had a docking score of **-5.7 kJ/mol.** This net binding energy is mostly driven by the formation of one conventional hydrogen bond between C=O of the carboxylic group and the amino acid **ARG A:76** as well as amide-pi stacked with **ASN A:46** and pi-alkyl interaction with **ILE A:78** with the aromatic group as depicted in Figure 4.4. It has been reported that amide-pi interaction contributed to only a significant amount of

energies due to its unfavorable geometrical structure and the energy value were reported to be almost comparable to those of weak hydrogen bond (Breberina et al., 2024). Therefore, the overall low binding energy of compound **3** in this study may arise from the contribution of amide-pi bond which counterbalanced the effect of hydrogen bonding. Furthermore, compared to compound **1** and **2**, compound **3** had the least binding interactions.

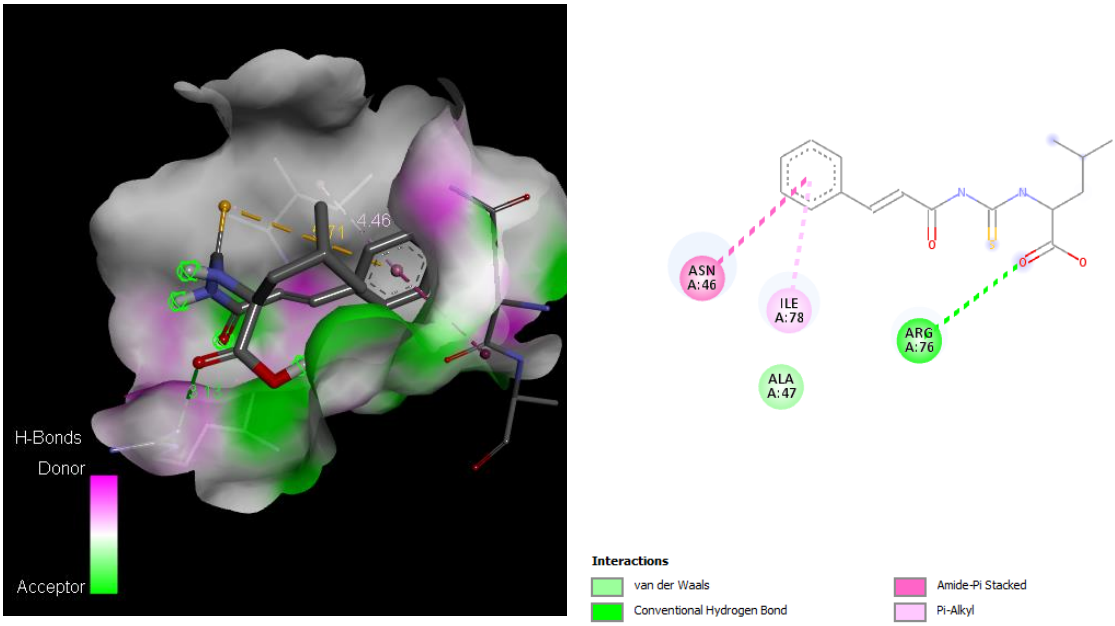

Figure 4.4: 3D (left) and 2D(right) representation of docked compound **3** inside DNA gyrase enzyme pocket

As stated earlier, the docking of the palmitoyl derivatives constituted low docking scores with the highest value at **-5.7 kJ/mol** and the lowest value at **-5.1 kJ/mol**. Li et al. (2013) in their study found that increasing the chain length (CL) from CL16 to CL18 diminished the antibacterial activity of their compound. In this study, the palmitoyl derivatives which consist of long alkyl chain (CL17) were seen to embedded poorly inside the active site of the 1KZN receptor based from the docking results. Therefore, it could be predicted that the palmitoyl derivatives may have poor antibacterial activities based on the

docking simulation. The binding interaction of compound **10** (Figure 4.5) revealed that the compound formed strong hydrogen bond interactions with the residue **ASP A:49** through the N-H group of the thioamide backbone and **GLY A:117** through O-H of the carboxylic group at 2.19 Å and 2.37 Å respectively. Besides, the CH_2 component of the alkyl chains involved actively in forming alkyl interactions with the amino acid residues **ALA A:47**, **ILE A:90**, **ILE A:78** and **PRO A:79** but at a more distance bond length ranging from 4.10 Å to 5.42 Å.

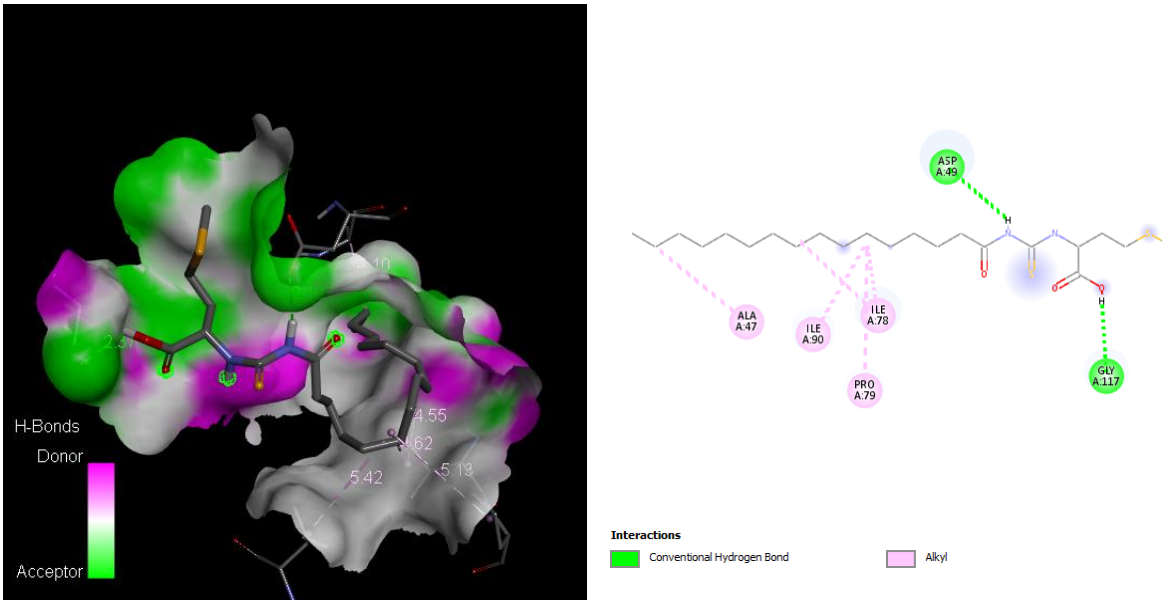

Figure 4.5: 3D(left) and 2D(right) visual representation of compound **10** with 1KZN receptor

Although the formation of hydrogen bond interactions leads to protein stability, it was clearly not sufficient in determining the ligand-protein complex stability. Compound **11** formed a total of five hydrogen bond (as well as four alkyl interactions) to an overall docking score of **-5.1 kJ/mol** which was the lowest score among the twelve compounds. It was observed that compound **11** (Figure 4.6) formed hydrogen bond interactions with various amino acid residues such as **GLY A:117, ASN A:46**, **HIS A:95**, **ALA A:96** and **SER A:121**.

The ethylene component exerted interaction with **ILE A:90** and **ILE A:78** through alkyl interaction. Similarly, the interaction of compound **12** (Figure 4.7) consisting of four hydrogen bond interactions with residues **SER A:121**, **VAL A:120** and **ASN A:46** together with alkyl interactions with **PRO A:79**, **ILE A:78** and **ALA A:47**. The net binding energy of these interactions was **-5.7 kJ/mol**.

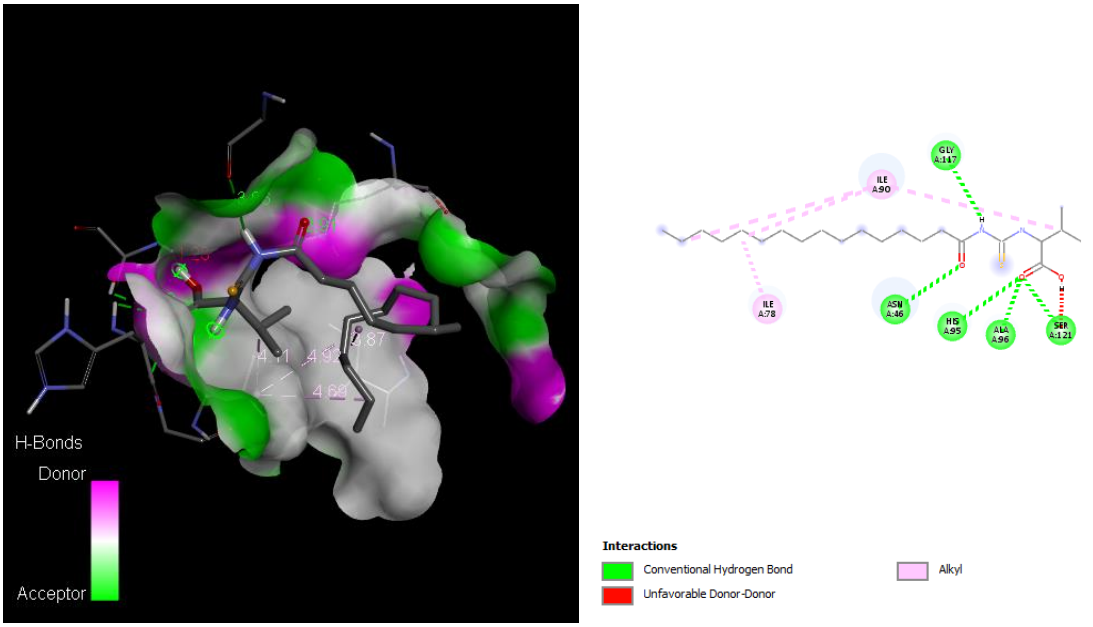

Figure 4.6: 3D(left) and 2D(right) visual representation of docked compound **11** inside 1KZN receptor

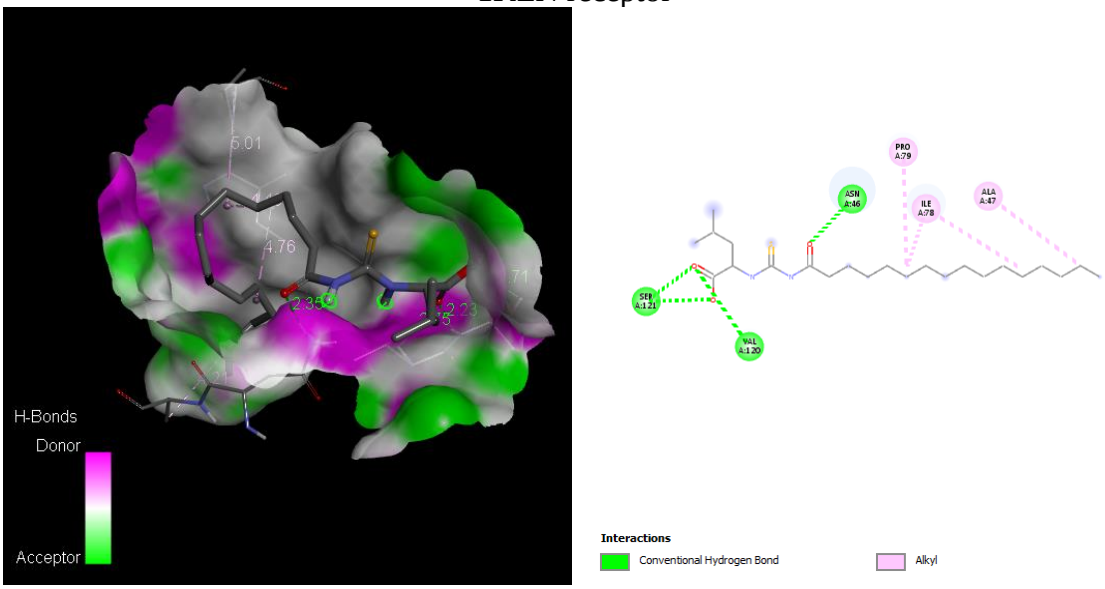

Figure 4.7: 3D(left) and 2D(right) visual representation of docked compound **12** inside 1KZN receptor

For the furan derivatives (compound **4-6**), the docking scores range from **-5.5 kJ/mol** to **-5.9 kJ/mol** and the binding interactions were presented in **Appendix 1-3**. Compound 4 was stabilised inside the 1KZN receptor through hydrogen bonding with **GLU A:50**, **GLY A:77** and **ASP A:73**. Carbon hydrogen bond was also observed between the -COOH backbone with residue **THR A:165** while pi-alkyl interaction was seen with the residue **ILE A:78**. Compound **5** on the other hand made two hydrogen bonding interactions with **THR A:165** and **ASN A:46**, as well as several alkyl interactions with **VAL A:167**, **VAL A:120**, and **ILE A:78**. Pi-alkyl interactions were also observed between the furan rings with ILE **A:90** and **ILE A:78**. The higher binding energies compared to the other derivatives may be contributed by the involvement of two hydrogen bonds. For compound **6,** the binding interaction involved the amino acids **ALA A:47** through alkyl interaction, **ASN A:46** through conventional hydrogen bonds and **ARG A:76** through pi-cation interaction. Likewise, the overall docking scores of dimethyl carbamoyl derivatives range from **-5.2 kJ/mol** to **-5.5 kJ/mol** which is relatively low when compared to the cinnamoyl and furan derivatives. The binding interaction of the each of the compound which was presented in **Appendix 4-6** consists of mainly alkyl and hydrogen bond with an additional carbon-hydrogen interaction. The poor affinities of the compound may be explained by weak alkyl interactions formed with the amino acid residues, which majority occurred at a distance bond length.

To sum up, compound with cyclic and aromatic groups in their structure displayed better docking scores than the dimethyl carbamoyl and long chain thiourea derivatives. This may be due to the rigidity and bulky molecular structure of these compound which contribute to compound stability when binds to the bacteria enzyme. In addition, the cinnamoyl derivative is the most promising candidate for further experimental studies as seen from the

docking score values. Higher docking score suggests that the compound will be bound tightly inside the target enzyme and therefore having the ability to block the cell replication process in bacterial cells.

4.1.2 Molecular docking of thiourea complexes

Motivated by the molecular docking results of compound **1-3,** we sought to run another series of molecular docking simulations using metal complexes of each cinnamoyl compound using three types of metal centers namely the Cu(II), Zn(II) and Co(II) metal centers. These metals were selected due to various studies that have demonstrated their potential as antibacterial as well as the improvement of biological activities after complexation with metals (Khater et al., 2019). Besides, all these metal ions are needed by the body as micronutrients to maintain regular physiological processes therefore they would not be treated as foreign species by the body thus reducing the potential side effects. Table 4.3 depicted the binding energies and the 3D binding pose of the complexes inside the binding cavity of 1KZN enzyme.

Table 4.3: Docking scores and most stable binding pose of thiourea complexes inside 1KZN receptor

Complex	Metal center	Binding Energies (kJ/mol)	3D Binding Pose
1a	Cu	-7.2	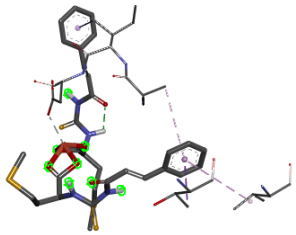
1b	Zn	-7.1	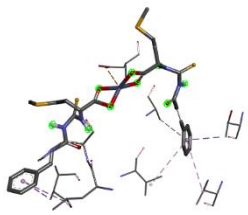
1c	Co	-6.9	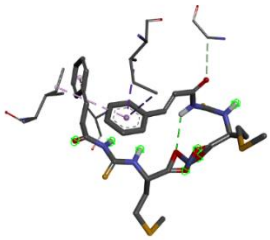
2a	Cu	-8.1	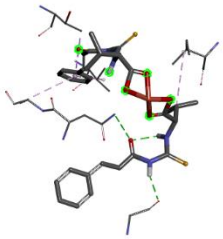

Table 4.3 continued

2b	Zn	-8.0	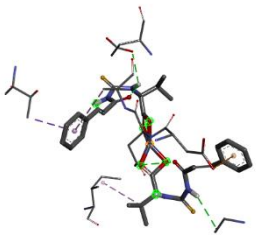
2c	Co	-8.2	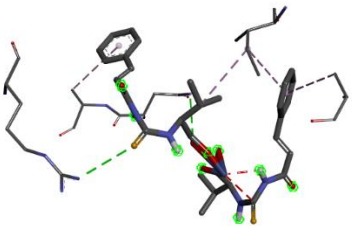
3a	Cu	-8.2	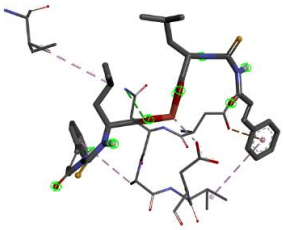
3b	Zn	-8.1	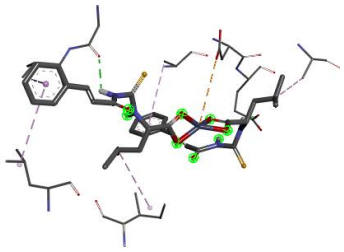
3c	Co	-8.3	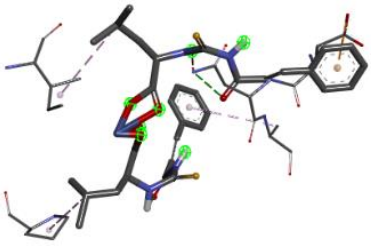

Overall, the metal complexes generally showed higher docking scores than its

ligands counterparts and this observation had been supported in other studies (Refat et al., 2022; Ruswanto et al., 2022; Zabiulla et al., 2023). The binding energies of thiourea complexes ranged from **-6.9 kJ/mol** to **-8.3 kJ/mol** as opposed to results obtained earlier for the free ligands which was between **-5.1 kJ/mol** to **-7.1 kJ/mol**. For compound **1**, the docking scores of its complexes range from **-6.9 kJ/mol** to **-7.2 kJ/mol** respectively. Table 4.4 summarized the overall interactions of thiourea complexes as obtained from docking simulations. Figure 4.8 depicted the binding interaction of complex **1a** while the rest of the interactions of complex **1b** and complex **1c** were shown in **Appendix 7-8**. Figure 4.8 showed several notable interactions with the residues inside the active site of 1KZN receptor including **ASP A:49** (metal-acceptor bond), **ILE A:48** and **THR A:165** (pi-sigma bond) as well as **VAL A:167** and **ALA A:47** (pi-alkyl interactions). Complex **1b** adopted several interactions such as pi-sigma bond with the residues **VAL A:118** and **THR A:165**, attractive charge formed between with **ASP A:49** and zinc metal as well as pi-alkyl interactions with **LEU A:94**, **VAL A:43**, **VAL A:167** and **ALA A:47**. For complex **1c**, there are four amino acid residues involved in the interaction such as **GLY A:119** (carbon-hydrogen bond), **ILE A:90** (Pi-sigma bond) as well as **ILE A:78** and **ALA A:47** (Pi-alkyl interactions). Apparently, the interactions of the complexes of compound **1** did not involve any hydrogen bond probably due to the dominant activities of other types of interaction such as Pi-alkyl and Pi-sigma bond interactions which could reduce the significant of hydrogen bonds in stabilizing the ligand-receptor complex. The docking results also revealed that the aromatic part of the complex were actively involved in forming interactions with the amino acid residues through pi-alkyl and pi-sigma bond. Apart from the Co(II) complex, the metal centers were seen to be involved in compound interactions. This is not surprising since the positively charged metal ions could interact with negatively charged biological molecules as

a result opposite charges.

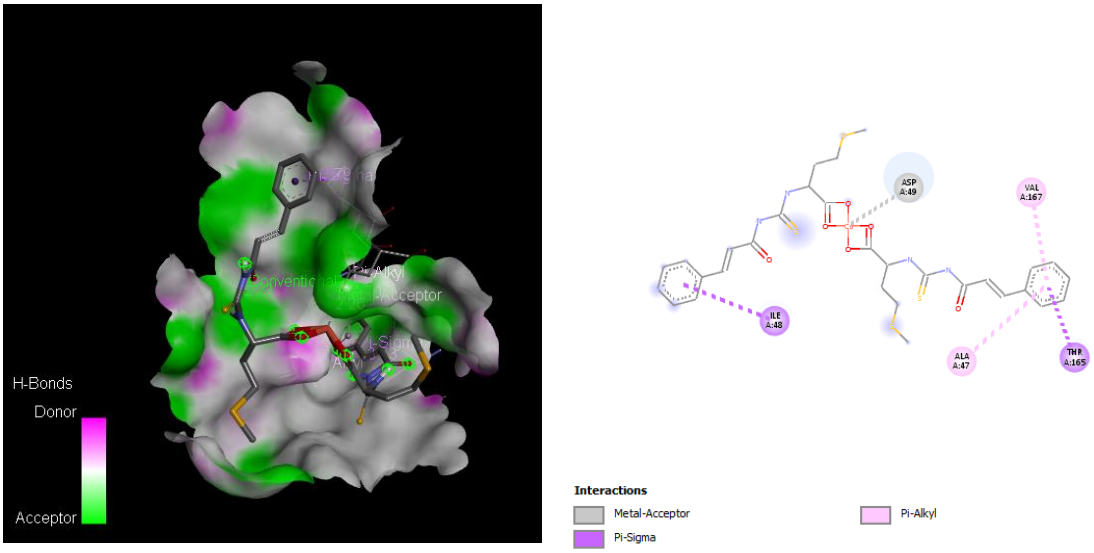

Figure 4.8: 3D(left) and 2D(right) visual depiction of amino acid interaction of complex **1a** inside DNA Gyrase Enzyme

Table 4.4: Summary of amino acid interactions of thiourea complexes

Compound	Amino acids	Bonds	Distance (Å)
1a	ILE A:48	Pi-Sigma	3.79
	THR A:165		3.73
	ASP A:49	Metal acceptor bond	2.26
	ALA A:47	Pi-alkyl	4.70
	VAL A:167		5.13
1b	ASP A:49	Attractive charge	3.99
	VAL A:118	Pi-sigma	3.87
	HIS A:95	Carbon-hydrogen bond	3.15
	LEU A:94	Pi-alkyl	5.24
	ALA A:47		4.67
	VAL A:167		5.12
	VAL A:43		5.42
1c	ILE A:90	Pi-sigma	3.85
	ILE A:78	Pi-Alkyl	4.79
	GLY A:119	Carbon-hydrogen bond	3.79
	ALA A:47	Alkyl	4.94
2a	ASN A:46	Conventional Hydrogen Bond	3.06
	GLY A:117		2.34
	ILE A:90	Alkyl	4.29
	ALA A:47	Pi-alkyl	4.88
	VAL A:167		5.38
	THR A:165	Pi-sigma	3.97
2b	GLU A:50	Conventional hydrogen bond	2.69
	ASN A:46		3.29
	GLY A:117		2.87
	ALA A:47	Pi-Alkyl	5.12
	ILE A:90	Alkyl	4.24
	THR A:165	Pi-Sigma	3.96
	ASP A:45	Pi-Anion	4.39
2c	ASN A:46	Conventional hydrogen bond	4.26
	ARG A:76		3.75
	ALA A:96	Pi-Alkyl	4.65
	ALA A:47		4.98
	ILE A:90		5.22
		Alkyl	4.35
3a	ASN A:46	Conventional hydrogen bond	3.17
	ASP A:45	Pi-anion	3.36
	ASP A:49	Metal acceptor	2.21
	ILE A:48	Pi-alkyl	5.33
	ALA :47	Alkyl	5.00
	ILE A:90		4.70
3b	GLU A:50	Conventional hydrogen bond	1.92
	GLY A:117		2.33

Table 4.4 continued

	ALA A:47	Pi-Alkyl	5.17
	LEU A:94		5.21
	ALA A:58	Alkyl	4.30
	ILE A:90		4.95
	VAL A:118	Pi-Sigma	3.58
	ASP A:49	Attractive charge	4.85
3c	ASN A:46	Conventional Hydrogen Bond	3.26
		Unfavourable bond	2.19
	PRO A:79	Pi-Alkyl	4.67
	ALA A:47		5.05
	PRO A:79	Alkyl	4.67
	ILE A:90		4.94
	ASP A:45		3.83

Complexes of compound **2** exhibited binding energies range from **-8.0** to **-8.2 kJ/mol**. Complex **2a** against DNA Gyrase enzyme adopted key interactions (Figure 4.9) with amino acid **GLY A:117** and **ASN A:46** (hydrogen bond), **THR A:165** (pi-sigma bond), **ALA A:47** and **VAL A:167** (pi-alkyl interactions) and **ILE A:90** (alkyl interactions). These interactions results in high binding energies of **-8.2 kJ/mol.** Complex **2b** (**Appendix 9**) spawned three hydrogen bond interactions with the residues **GLU A:50**, **GLY A:117** and **ASN A:46** which occurred through the N-H group of thiourea and the C=O atom of the amide backbone. Other interactions including pi-sigma bond with **THR A:165**, pi-alkyl interaction between the aromatic group and **ALA A:47**, pi-anion interaction of another aromatic group with **ASP A:45** and alkyl interaction with **ILE A:90** which comes from the methylene group of the valine side chain. Complex **2c** (**Appendix 10**) had three key interactions; Conventional hydrogen bonding was observed with with amino acid **ASNA:46** and **ARG A:76**. The aromatic component of the complex generated pi-alkyl interaction with **ALA A:47** and **ALA A:96** and **ILE A:90**. Another alkyl interaction was also observed between the valine side chain and **ILE A:90**. Compared to its parent ligand, the number of interactions occurred between the amino acid residues with complexes of compound **2** increased significantly. This phenomenon might contribute to higher binding energies; as more interactions may help to stabilise the ligand-protein complex (Soliman et al., 2024).

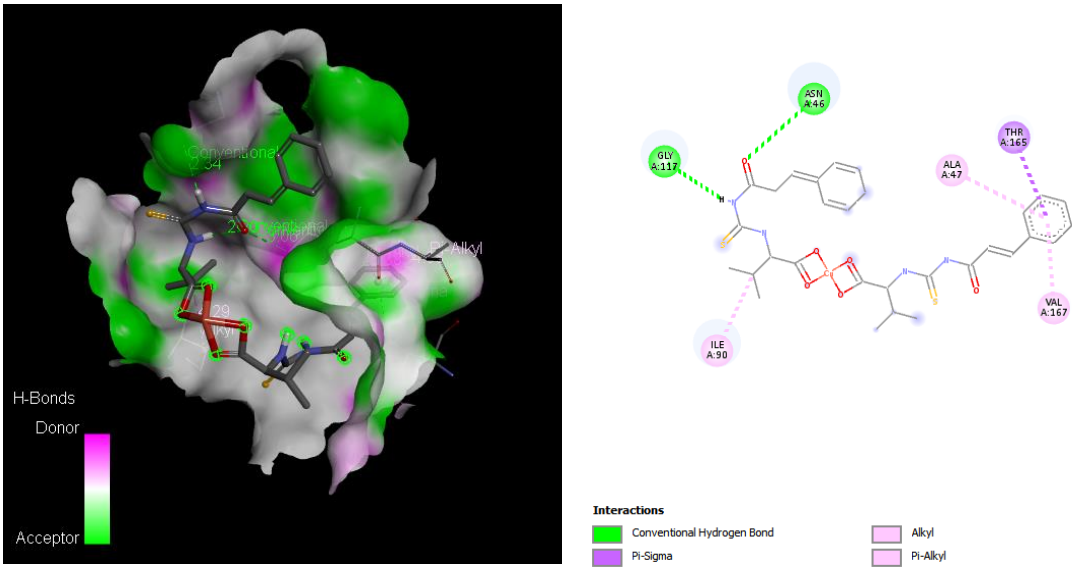

Figure 4.9: 3D(left) and 2D(right) visual depiction of amino acid interaction of complex **2a** inside DNA Gyrase Enzyme

The binding energies of complexes of compound **3** range from **-8.1 kJ/mol** to **-8.3 kJ/mol**. In complex **3a** (Figure 4.10), the compound bound tightly inside the active site of the enzyme through pi-alkyl interactions with **ILE A:48** and **ALA A:47**, alkyl interactions with **ILE A:90**, pi-anion with **ASP A:45**, conventional hydrogen bond with **ASN A:46** as well as metal-acceptor bond with **ASP A:49**. The docking of complex **3b (Appendix 11)** gave insight on two conventional hydrogen bond formed between **GLU A:50** and **GLY A:117** with the NH group, pi-alkyl interactions with **LEU A:94** and **ALA A:47** as well as alkyl interactions with **ILE A:90** and **ALA A:58** residues**.** Besides, pi-sigma bond and attractive charge with **VAL A:118** and **ASP A:49** were also identified from the docking visualization. Last but not least, for complex **3c**, the binding interactions **(Appendix 12)** involved in the active site of the enzyme receptors were pi-anion interaction with **ASP A:45**, conventional bond with **ASN A:46**, alkyl interactions with ILE **A:90** and **PRO A:79**. Another interaction observed is between the residue **ALA A:47** which occurred through pi-alkyl interaction. Notably, there was an unfavourable interaction occurred between the NH

backbone and **ASN A:46**.

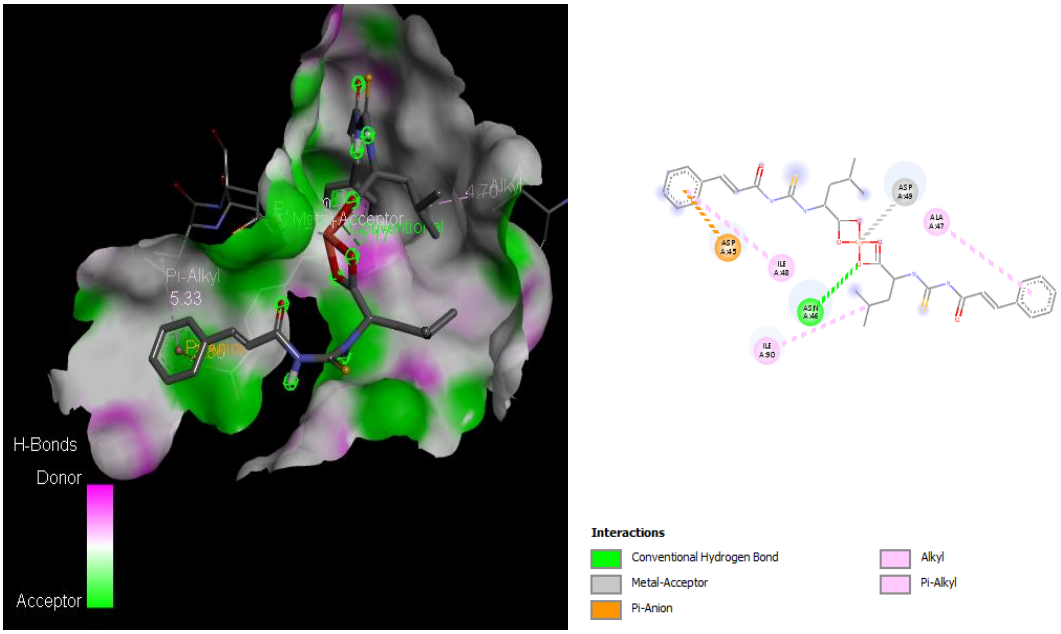

Figure 4.10: 3D(left) and 2D(right) visual representation of docked complex **3a** inside 1KZN receptor

In conclusion, docking simulation allowed us to predict potentially active antimicrobial agent and eliminate the possibly inactive compound. Besides, it gives better understanding on the binding mode which allows medicinal chemist to tweak the chemical structure of the compound to create new compound derivative with even greater efficiency in combating the growth of bacteria. The metal complexes of thiourea demonstrated higher binding affinities against the targeted enzyme receptor, most likely due to the increase in the number of key interactions thus stabilising the positioning of the compound inside the enzyme receptor. Among the complexes, the cobalt(II) complexes had the highest binding energies compared to other complexes with binding energies range from **-8.1 kJ/mol** to **-8.3 kJ/mol**. Therefore, it could be predicted that these complexes may portrayed the highest antibacterial activities against *E. coli* strain. In the next part of the research, an ADME

evaluation were carried out to predict the pharmacokinetic potential of the ligands and its complexes.

4.2 ADME evaluation of thiourea and its metal complexes

4.2.1 ADME evaluation of compound 1-12

While antibiotics are useful for treating bacterial infections, some of the existed common drugs currently warrant unwanted side effects to its patients. In some cases, the side effects are so severe that the drug can no longer be the first-choice treatment despite the efficacy. Ciprofloxacin for instance had been associated with peripheral neuropathy and CNS side effects and had been issued a Boxed Warning by the FDA (Anwar et al., 2024). This is because the drug had lipophilic character therefore possessed ability to cross the BBB and readily penetrate the CNS (Haddad et al., 2022). A compound with the best experimental result and molecular docking interactions does not necessarily become the best drug candidate as it needs to travel the human body to reach its target receptor and in order to do so, the drug has to cross many barriers and membranes. To study the pharmacokinetic profiles of thiourea and its complexes, SwissADME tool was used to predict the pharmacokinetic properties of each compound because it is an open access online webtool and the data are easy to interpret (Daina et al., 2017). The ADME assessment is an important step in drug design and development to screen the best drug candidate as potential medicine with little side effects. Compounds which are predicted with poor pharmacokinetic profiles will be eliminated and were not considered for future studies while compounds with promising pharmacokinetic profiles will be selected for future experimental procedures. The ADME profiles of compound **1-12** are presented in Table 4.5.

Table 4.5: ADME datas of compound **1-12**

Compound	Cipro	1	2	3	4	5	6	7	8	9	10	11	12
Physiochemical Properties													
No. of Heavy Atoms	24	22	21	22	19	18	19	17	16	17	29	28	29
No. arom. heavy atoms	10	8	6	6	5	5	5	0	0	0	0	0	0
Fraction Csp3	0.41	0.27	0.27	0.31	0.36	0.36	0.42	0.67	0.67	0.7	0.86	0.86	0.87
No. rotatable bonds	3	10	8	9	9	7	8	9	7	8	22	20	21
No. H-bond acceptors	5	3	3	3	4	4	4	3	3	3	3	3	3
No. H-bond donors	2	3	3	3	3	3	3	3	3	3	3	3	3
Molar Refractivity	95.25	93.14	85.55	90.36	75.69	68.1	72.91	71.62	64.03	68.84	130.83	123.23	128.04
TPSA	74.57	135.82	110.52	110.52	148.96	123.66	123.66	139.06	113.76	113.76	135.82	110.52	110.52
Lipophilicity (Log P o/w)													
Consensus Log Po/w	1.10	1.92	1.95	2.23	0.91	0.83	1.15	0.38	0.19	0.65	5.33	5.32	5.54
Water solubility													
Class (ESOL)	Very soluble	Soluble	Soluble	Soluble	Soluble	Soluble	Soluble	Very Soluble	Very Soluble	Very soluble	Poorly soluble	Poorly Soluble	Poorly Soluble
Class (Ali)	Highly soluble	Moderately soluble	Moderately soluble	Moderately soluble	Moderately soluble	Moderately soluble	Moderately soluble	Soluble	Soluble	Soluble	Insoluble	Insoluble	Insoluble
Class (SILICOS-IT)	Soluble	Soluble	Soluble	Soluble	Soluble	Soluble	Soluble	Soluble	Soluble	Soluble	Poorly soluble	Poorly Soluble	Poorly Soluble
Pharmacokinetics													
GI absorption	High	High	High	High	Low	High	High	High	High	High	Low	Low	Low
BBB Permeant	No	No	No	No	No	No	No	No	No	No	No	No	No
P-gp substrate	Yes	No	No	No	No	No	No	No	No	No	No	Yes	No
CYP1A2 inhibitor	No	No	Yes	No	No	No	No	No	No	No	Yes	Yes	Yes

Table 4.5 continued

CYP2C19 inhibitor	No	Yes	Yes	Yes	Yes	No	No	No	No	No	Yes	Yes	Yes
CYP2C9 inhibitor	No	Yes	yes	Yes	No	No	No	No	No	No	Yes	Yes	Yes
CYP2D6 inhibitor	No	No	No	No	No	No	No	no	No	No	No	No	No
CYP3A4 inhibitor	No	No	No	No	No	No	No	No	No	No	No	No	No
Log Kp (Skin permeation)	-9.09	-6.22	-5.79	-5.63	-6.73	-6.3	-6.13	-7.33	-6.91	-6.74	-3.16	-2.73	-2.56
Druglikeness													
Lipinski	Yes	Yes	Yes	Yes	Yes	Yes	Yes	Yes	Yes	Yes	Yes	Yes	Yes
Ghose	Yes	Yes	Yes	Yes	Yes	Yes	Yes	Yes	Yes	Yes	No	Yes	No
Veber	Yes	Yes	Yes	Yes	No	Yes	Yes	Yes	Yes	Yes	No	No	No
Egan	Yes	No	yes	Yes	No	Yes	Yes	No	Yes	Yes	No	Yes	No
Muegge	Yes	Yes	Yes	Yes	Yes	Yes	Yes	Yes	Yes	Yes	No	No	No
Bioavailibility score	0.55	0.58	0.58	0.56	0.56	0.56	0.56	0.56	0.56	0.56	0.56	0.56	0.56
Medicinal Chemistry													
PAINS	0	0	0	0	0	0	0	0	0	0	0	0	0
BRENK	0	2	2	2	1	1	1	1	1	1	1	1	1
Leadlikeness	Yes	No	No	No	No	Yes	No	No	No	No	No	No	No
Synthetic accessibility	2.51	3.44	3.19	3.29	3.23	3.03	3.13	3.35	3.05	3.14	4.56	4.22	4.34

As seen from the bioavailability radar (Figure 4.11), compound **1-12** had good scores of drug-likeness parameters except compound **10-12**. Compounds **1-12** generally had satisfying physicochemical properties as there is no violation of five ADME filters namely the Lipinski, Ghose, Veber, Egan and Muegge rules except for compound **1, 4, 7** which violated the Egan rule. Furthermore, the palmitoyl derivatives (compound **10-12**) were seen to violate other rules except for the Lipinski's rule. Nevertheless, only the Lipinski's rule were considered and discussed in this section as it is a general rule of thumb to predict the oral bioavailability of potentially active drug (Roskoski, 2023). From the results tabulated, all compounds obeyed the Lipinski's rule of five (Ro5). According to the Lipinski's rules of five, the molecular weight of a drug should not exceed 500 Dalton (Da) (Lipinski, 2004). This is because higher molecular weight leads to poor water solubility and the aqueous solubility of a molecule influences drug absorption after oral administration (Bhalani et al., 2022; Borgaonkar et al., 2024). The molecular weight of compound **1-12** were between 247-446 g/mol. While Ro5 is an important guideline to predict oral bioavailability of a drug, 16% of oral drugs in reality failed to fulfill at least one of the criteria whilst 6% did not obey two or more criteria. Drugs such as atorvastatin (Lipitor) and montelukast (Singulair) were infamously known to violate more than one of the Lipinski rules (Bickerton et al., 2012). From the values tabulated in Table 4.5, all compounds were predicted to be soluble in water except the palmitoyl derivatives due to the long hydrocarbon chain of the palmitoyl, which are extremely hydrophobic and highly non-polar (Spătaru et al., 2013).

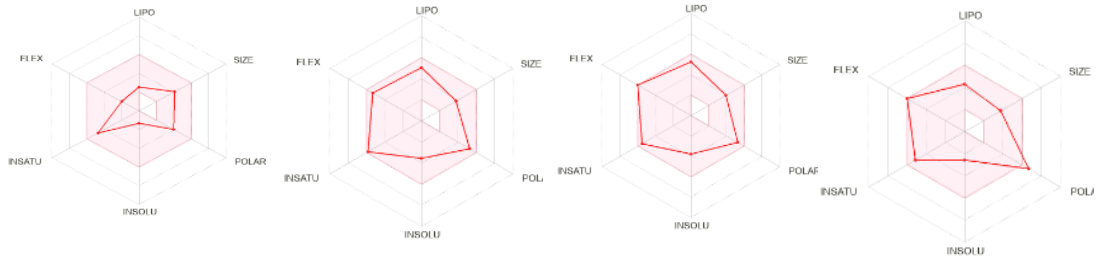

Compound **1** Compound **2** Compound **3** Compound **4**

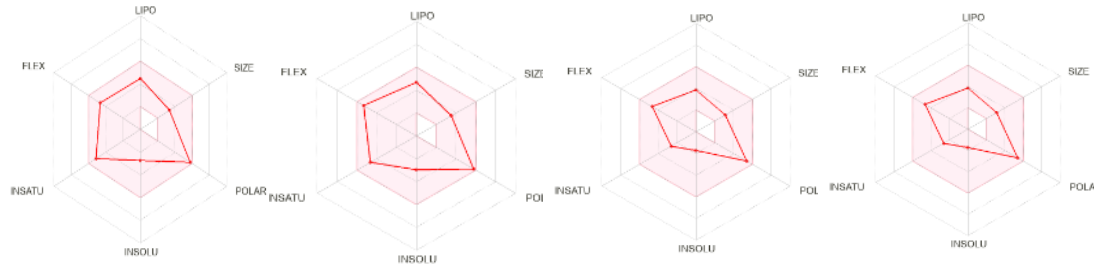

Compound **5** Compound **6** Compound **7** Compound **8**

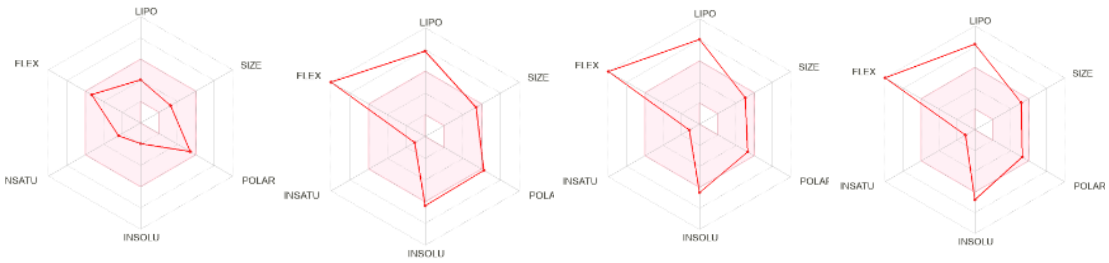

Compound **9** Compound **10** Compound **11** Compound **12**

Figure 4.11: The bioavailibility radar of compound **1-12**

*The pink area in each radar represents the accepted range of molecules for each of the pharmacokinetics evaluation; anything out of the radar indicates that the compound did not fulfill the criteria

Next, compounds **1-12** did not violate the second and third criteria of Lipinski's rules of not having more than five hydrogen bond donors and not more than ten hydrogen bond acceptors (Lipinski, 2004). Hydrogen bonding plays a significant role in ADME as it influences the movement of a molecule to a less polar environment which significantly

affects the permeability and its *in vivo* distribution (Kenny, 2022). A proper balance of lipophilicity and hydrophilicity is required to generate a favorable pharmacokinetic profile (Coimbra et al., 2020). Too many of either the hydrogen bond donor or acceptor would affect the drug's membrane partition and permeability which would cause problem in transportation of drugs across cells later (Alex et al., 2011). Lipophilicity is another important aspect that influences the ADME of a drug. It is expressed as the logarithm of n-octanol partition coefficient (log P) (Lobo, 2020). Similarly, the lipophilicity values suggested the permeability of drug across cell membrane, which would affect the binding of the molecule to the receptor (Czyrski, 2022). The calculated Log P values of the studied compounds are within the accepted range, with values less than five, except for compound **10-12**.

Before a drug enters a tissue or organ, it is distributed by blood supply around the body. However, it first must be absorbed in the GI, and this absorption is largely influenced by the physicochemical properties like water solubility and lipophilicity. Highly polar drug will have difficulty to cross the gut wall membrane while highly lipophilic drug will dissolve in fat globules and become poorly absorbed in the guts hindering drug distribution around the body. All the designed compounds generally shown high GI absorption except for compound **4**, **10**, **11** and **12**. All the palmitoyl derivatives shown poor GI absorption most probably due to its poor water solubility, which is a result of its highly hydrophobic nature. On the other hand, all compounds were predicted to be non-permeable in the blood brain barrier. The blood brain barrier is a semi permeable membrane that surrounds the human central nervous system (Wu et al., 2023). It functions to protect the human brain from blood-borne agent as well as regulating the passage of small molecules and foreign substances or

drugs into the CNS (Kadry et al., 2020). Drugs that are capable to cross the BBB is very likely to induce various CNS side effects such as hallucinations, Parkinson's disease and fatigue and this happened especially due to drugs with highly lipophilic character (Cojocariu et al., 2021). An example of such drug is chlorpheniramine maleate, a first-generation antihistamine drug commonly used to treat allergy and flu symptoms, this drug could induce sedative effects to patients taking this medication (Rizvi et al., 2024). Figure 4.12 illustrated the hard-boiled egg diagram of compound **1-12**. The molecules in the yellow region (if any) are predicted to be BBB permeant while the white region suggested high gastrointestinal absorption.

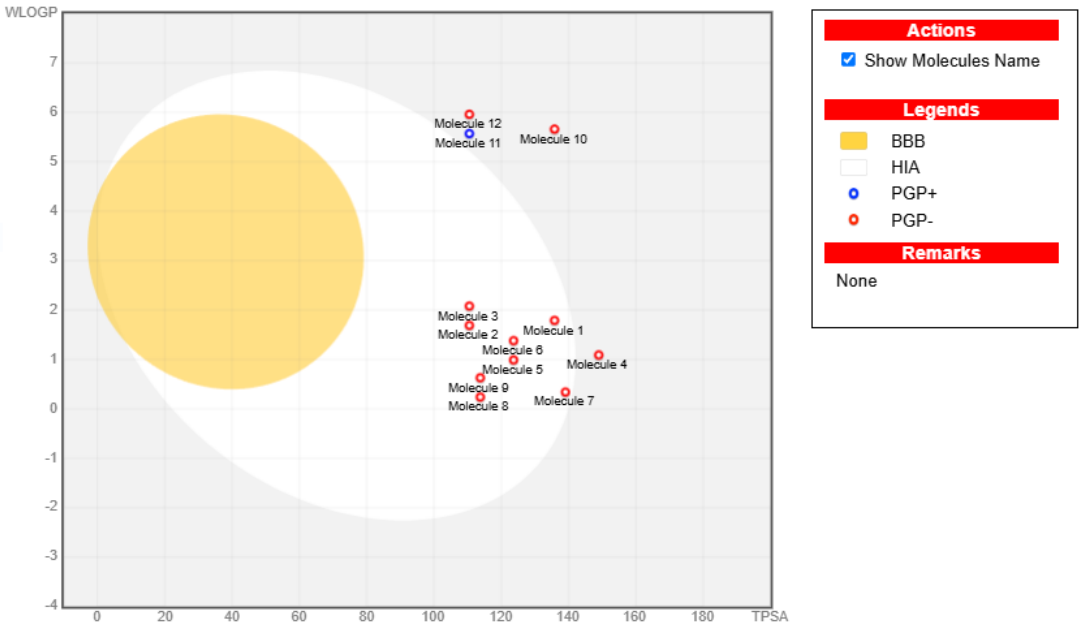

Figure 4.12: Hard-boiled egg diagram of compound **1-12**

Furthermore, compound **1-12** were predicted to be non-P-glycoprotein (P-gp) substrate except for compound **11**. P-gp is a membrane protein transporter that regulates the movement of a drug across a cell membrane, from the uptake to its removal from the cells which give rise to its ADME properties, influencing drug efficacy and bioavailability (Juvale

et al., 2022; Finch and Pillans, 2014). An example of P-gp substrate is an anticoagulant drug, Apixaban (Eliquis) (Zhang et al., 2013). Study shown that when Apixaban was administered alone, the oral bioavailability was 49% but when co-administered with P-gp inducer Rifampin, the oral bioavailability reduced by 25%. This is because the presence of P-gp transporter and CYP3A4 enzyme during the pre-systemic processes reduced the bioavailability of the drug (Vakkalagadda et al., 2016). Therefore, it could be predicted that the compound might have high bioavailability if it not administered together with P-gp inducer. Next, compound **1-12** were expected to be metabolized by P450 enzyme. From the result analysis, compound **1-12** were not the inhibitors of CYP2D6 and CYP3A4 protein. Lastly, the compounds had lower negative log K_p value when compared to the standard Ciprofloxacin. This indicates that the compounds had more penetration in the skin barrier therefore would work well as a topical antibiotic (Daina et al., 2017).

To conclude, most of the thiourea derivatives have good ADME properties except for the palmitoyl derivatives. By taking account both the docking scores and ADME values, cinnamoyl derivatives make a great candidate as potential antibiotic agent due to good binding affinity with DNA gyrase enzyme and satisfying pharmacokinetic profiles. Therefore, the cinnamoyl thiourea compound were selected for future experimental set up to evaluate its *in vitro* biological property**.**

4.2.2 ADME evaluation of metal complexes

Meanwhile, for the assessment of the ADME profiles of metal complexes, the results demonstrated that the complexes generally obeyed the Lipinski's rule of 5 although the molecular weight is more than 500 Da. For complexes of compound **1-3**, each of the metal complex had molecular weight range from 746 - 1110 g/mol. It was worth noted that metal complex drug often violates the general rule applied to common organic molecules (Anthony et al., 2020). In this case, the coordination of a metal with more than one ligand resulting in a complex molecular structure and consequently large molecular weight. Auranofin is an example of metal complex drug which exceed the Lipinski's requirement with molecular weight of 678.49 g/mol. This scenario is commonly observed in natural product (NP) derived drugs where NPs often do not meet the Lipinski's criteria (Doak et al., 2014). In fact, the increase in molecular mass of approved drugs in the last 20 years implied that more and more drugs are exceptional to this rule (Shultz, 2019). From 2013 to 2019, 60 out of 154 (39.9%) new chemical entities (NCEs) oral drugs were found to violate at least one of the Ro5 descriptor (39.9%), up from 21.9% of total NCEs from 1994 to 1997 (Stegemann et al., 2023).

Besides, metal complexes were predicted to have poor water solubility. This observation is expected as metal complexes had high molecular weight, thus difficult to dissolve in water. To overcome the limitation of poor solubility in oral administration, metal complexes would often be given intravenously to the patients (Mjos & Orvig, 2014; Tchounwou et al., 2021). Therefore, the study on efficient drug delivery of metal complexes such as encapsulation with nanocarrier is actively being conducted to improve water

solubility (Dantas et al., 2022; Pearson et al., 2015; Xu et al., 2024).

Although higher molecular weight and lipophilic value is often associated with poor pharmacokinetic profiles (Wang et al., 2019), the lipophilic values of complexes of compound **1-3** were found to be within the accepted range and did not violate the Lipinski's Rule of Five. As a result, the complexes were found to be non-BBB permeant therefore the drugs would not cross the BBB and induce CNS side effects. On the other hand, the complexes were predicted to be poorly absorbed in the intestine. It is expected as higher molecular weights leads to poor oral absorption and thus poor GI absorption and finally leads to low bioavailability of the drugs. Poor bioavailability would cause the active compounds not reaching the systemic circulation in desired quantities to form interaction with targeted receptor. Consequently, data from docking simulation would not be relevant as expected interaction of active compound with targeted active site would not be achieved (Dey, 2021).

Additionally, our SwissADME data revealed that the metal complexes are P-gp substrate. P-gp protein is also known as multi-drug resistance protein that actively pump out foreign species from the cells and is widely distributed in human kidneys, liver, pancreas and the brain (Ferreira et al., 2015; Nguyen et al., 2021). Being a P-gp substrate means that the oral bioavailability of metal complexes will be reduced when co-administered with P-gp inducer, preventing the drug from reaching its full potential. This information allow the experts to consider the possible drug interactions that may arised before prescribing medication to their patients. Last but not least, these metal complexes were expected to be metabolized in the liver. It is predicted that the enzymes involved in the metabolic processes of these metal complexes are **CYP1A2**, **CYP2C9** and **CYP2D6**. Meanwhile, the log K_p

values of the metal complexes suggested that the complexes would make a great candidate as a topical antibiotic rather than as an oral drug. The skin permeation or log K_P values of the metal complexes falls within the range of -4.85 to -6.09 cm/s, which is less negative than the value of Ciprofloxacin (-9.09 cm/s). These values suggested that the complexes had more skin permeability than Ciprofloxacin therefore would work well as a topical antibiotic (Daina et al., 2017). The results of the ADME properties of thiourea complexes were summarized in Table 4.6 and the bioavailability radar was shown in Figure 4.13.

Table 4.6: ADME datas of thiourea complexes

Complex	**1a**	**2a**	**3a**	**1b**	**2b**	**3b**	**1c**	**2c**	**3c**
Physiochemical Properties									
No. of Heavy Atoms	45	43	45	45	43	45	45	43	45
No. arom. heavy atoms	12	12	12	12	12	12	12	12	12
Fraction Csp3	0.27	0.27	0.31	0.27	0.27	0.31	0.27	0.27	0.31
No. rotatable bonds	20	16	18	20	16	18	20	16	18
No. H-bond acceptors	6	6	6	6	6	6	6	6	6
No. H-bond donors	4	4	4	4	4	4	4	4	4
Molar Refractivity	182.19	168.01	177.62	183.19	168.01	177.62	183.19	168.01	177.62
TPSA	249.64	199.04	199.04	249.64	199.04	199.04	249.64	199.04	199.04
Lipophilicity (Log P o/w)									
Consensus Log Po/w	3.08	3.06	3.6	3.08	3.06	3.6	3.08	3.05	3.59
Water solubility									
Class (ESOL)	Poorly Soluble	Poorly soluble	Poorly Soluble	Poorly soluble	Poorly soluble	Poorly soluble	Poorly Soluble	Poorly Soluble	Poorly Soluble
Class (Ali)	Insoluble	Insoluble	Insoluble	Insoluble	Insoluble	Insoluble	Insoluble	Insoluble	Insoluble
Class (SILICOS-IT)	Poorly Soluble	Poorly soluble	Poorly Soluble	Poorly soluble	Poorly soluble	Poorly soluble	Poorly soluble	Poorly soluble	Poorly soluble
Pharmacokinetics									
GI absorption	Low	Low	Low	Low	Low	Low	Low	Low	Low
BBB Permeant	No	No	No	no	No	No	No	No	No
P-gp substrate	yes	Yes	Yes	Yes	Yes	Yes	Yes	Yes	Yes
CYPA142 inhibitor	No	No	No	No	No	No	No	No	No
CYP2C19 inhibitor	No	No	No	No	No	No	No	No	No

Table 4.6 continued

CYPC8 inhibitor	Yes	Yes	Yes	Yes	Yes	Yes	Yes	Yes	Yes
CYP2D6 inhibitor	No	No	No	No	No	No	No	No	No
CYP3A4 inhibitor	No	Yes	No	No	No	No	No	No	No
Log Kp(Skin permeation) (cm/s)	-6.08	-5.22	-4.88	-6.09	-5.23	-4.89	-6.05	-5.19	-4.85
Druglikeness									
Lipinski	Yes	Yes	Yes	Yes	Yes	Yes	Yes	Yes	Yes
Ghose	No	No	No	No	No	No	No	No	No
Veber	No	No	No	No	No	No	No	No	No
Egan	No	No	No	No	No	No	No	No	No
Muegge	No	No	No	No	No	No	No	No	No
Bioavailibility score	0.55	0.55	0.55	0.55	0.55	0.55	0.55	0.55	0.55
Medicinal Chemistry									
PAINS	0	0	0	0	0	0	0	0	0
BRENK	2	2	2	3	3	3	2	2	2
Leadlikeness	No	No	No	No	No	No	No	No	No
Synthetic accessibility	6.6	6.51	6.72	6.59	6.45	6.68	6.55	6.4	6.64

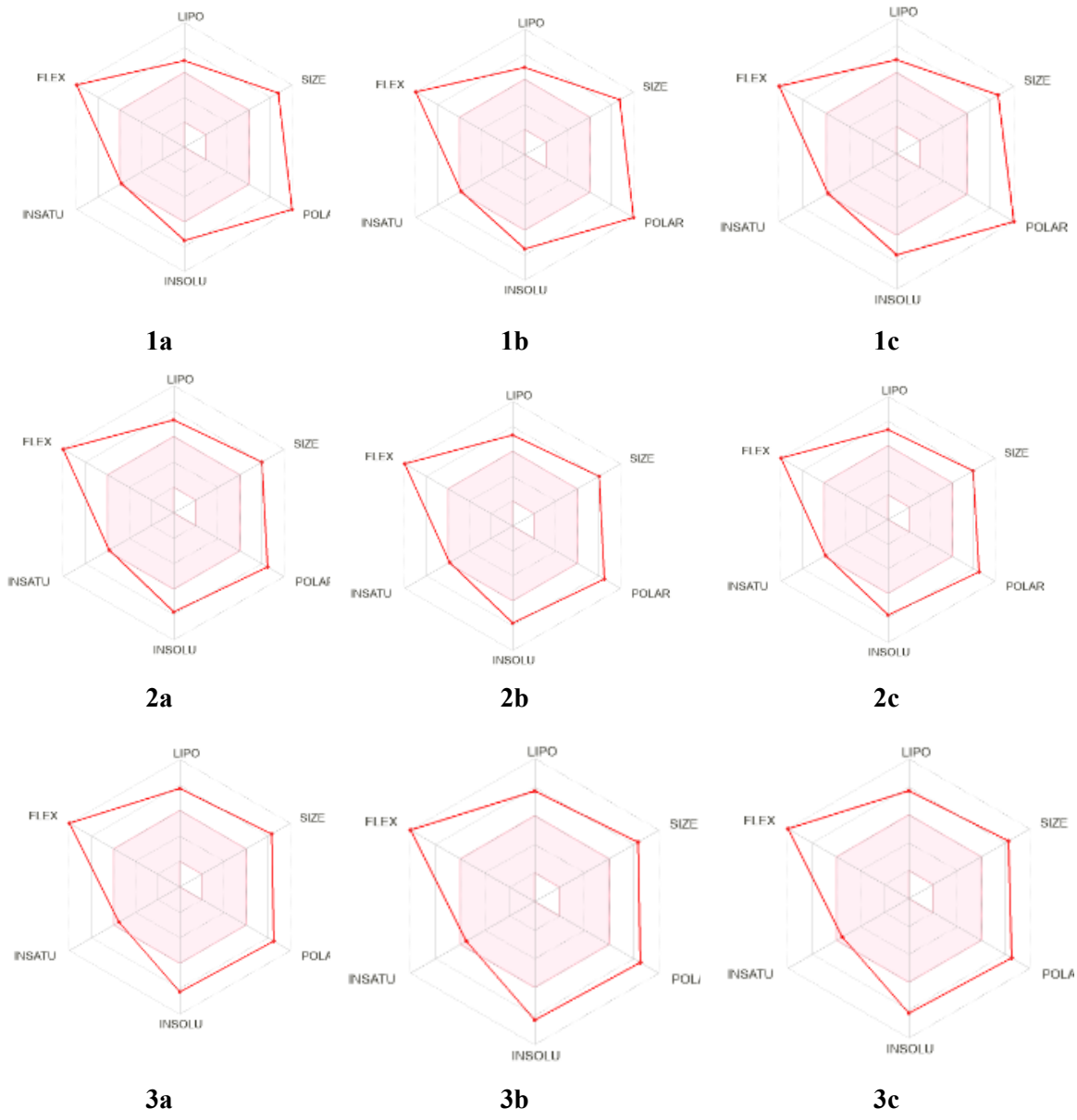

Figure 4.13 The bioavailability radar of thiourea complexes **1a-3c**

4.3 Synthesis of compound 1-3

Based on the screening results from section 4.1 and 4.2, the top ranked thiourea compound based on molecular docking energy scores along with highly promising pharmacokinetic profiles (**compound 1-3**) were selected for experimental study Hence, the synthetic route for the synthesis of thiourea was depicted in Figure 4.14. During the first step, a condensation reaction took place between cinnamoyl chloride and KSCN in dry acetone at room temperature (Roman et al., 2023). This reaction yielded an intermediate and by-products potassium chloride, KCl which appeared as white solid (Abd Halim & Ngaini, 2016). When KSCN was added, the thiocyanato group, due to its nucleophilic character attacked the carbon atom adjacent to the chlorine atom of cinnamoyl chloride. Being a good leaving group, chlorine atom was unstable and eventually replaced by the thiocyanato group forming the isothiocyanate intermediate bearing NCS group. The chlorine atom subsequently reacted with the positively charged potassium ion of KSCN resulting in the formation of KCl which later being removed and filtered off the mixture.

The second step of the reaction involved a nucleophilic addition reaction between amino acid methionine, valine and leucine with the isothiocyanate intermediate to yield compound **1-3** (Ellithy et al., 2023). The reaction was carried out under reflux at 60 °C for 18 hrs due to low reactivity of the amino acid and stirred continuously overnight to allow the completion of reaction. Subsequently, the resulting mixture was filtered and the filtrate was allowed to evaporate at room temperature for few days until solid was formed. The resulting solids were purified through slow recrystallization method using mixture of DCM and ethanol or methanol to obtain their purest form.

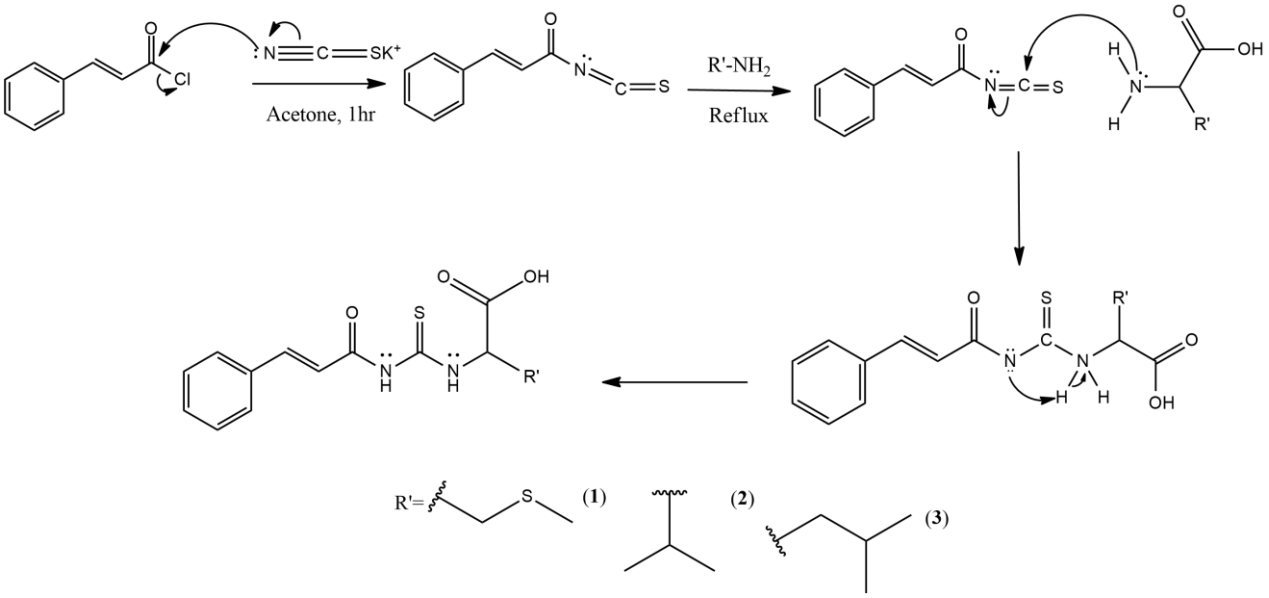

Figure 4.14: Synthesis scheme of compound **1-3**

Compound **1** and **2** were obtained as yellowish solid while compound **3** appeared as white solid with respectable yield between 74.3-83.1%, suggesting the viability of the synthesis method. Compound **1** and **2** were recrystallized in a mixture of DCM and ethanol at 1:1 ratio while compound **3** was recrystallized using a mixture of DCM and methanol in 1:1 ratio. The compounds demonstrated excellent solubility in various organic solvent such as DMSO, methanol and acetone. In ethanolic solution, the compounds dissolved upon heating. On the contrary, the compounds were insoluble in DCM, water and tetrahydrofuran (THF). Hence, ethanol and DCM mixture were selected to recrystallize the compound as the most polar solvent was used to dissolve the compound along with its impurities at high temperature while non-polar solvent was used to initiate nucleation and concentrate the compound out of the solvent, yielding pure crystallized compound. In addition, all compounds were observed to be relatively stable at room temperature. The melting points range from 160-192 ℃ respectively. Each compound displayed sharp melting points in between range of 1 – 5℃. Typically, sharp melting point i.e less than 5 ℃ indicates the

purity of the compound (Dent, 2006). Table 4.7 summarized the physical data of compound **1-3**. A CHNS elemental analysis was also carried out and Table 4.8 showed that the obtained values are in good agreement with the theoretical values suggesting the purity and the successful synthesis of the compounds.

Table 4.7: Physical properties of compound **1-3**

Compound	Molecular formula	m.p (°C)	Yield (%)	Physical appearance
1	$C_{15}H_{18}N_2O_3S_2$	160-163	75.3	Yellowish solid
2	$C_{15}H_{18}N_2O_3S$	155-158	83.1	Yellowish solid
3	$C_{16}H_{20}N_2O_3S$	190-192	74.3	White solid

Table 4.8: CHNS data of compound **1-3**

Compound	Molecular formula	Molecular weight	Elemental Analysis Data			
			% Carbon	% Hydrogen	% Nitrogen	% Sulphur
1	$C_{15}H_{18}N_2O_3S_2$	338.45	52.94 [53.23]	5.56 [5.36]	6.86 [8.28]	17.30 [18.95]
2	$C_{15}H_{18}N_2O_3S$	306.10	59.06 [58.08]	5.96 [5.92]	8.23 [9.14]	10.08 [10.45]
3	$C_{16}H_{20}N_2O_3S$	320.12	60.39 [59.98]	6.33 [6.29]	8.52 [8.74]	10.14 [10.01]

*Theoretical values are indicated in the square brackets

4.4 Synthesis of Cu(II), Zn(II) and Co (II) complexes of thiourea

The synthesis of complexes of thiourea was depicted in Figure 4.15. It was done by adding metal salt solution to the ligand in a ratio of 1:2. Initially, KOH was added so it could act as a strong base to deprotonate the hydrogen ion from the carboxylic group -COOH of thiourea ligand (Karthik et al., 2020). The deprotonation of hydrogen atom at the carboxylic group of thiourea allows it to coordinate to the metal ions in order to form a complex metal. Although NH group and the OH were both present in the compound, the OH group was strongly deprotonated due to its more acidic nature.

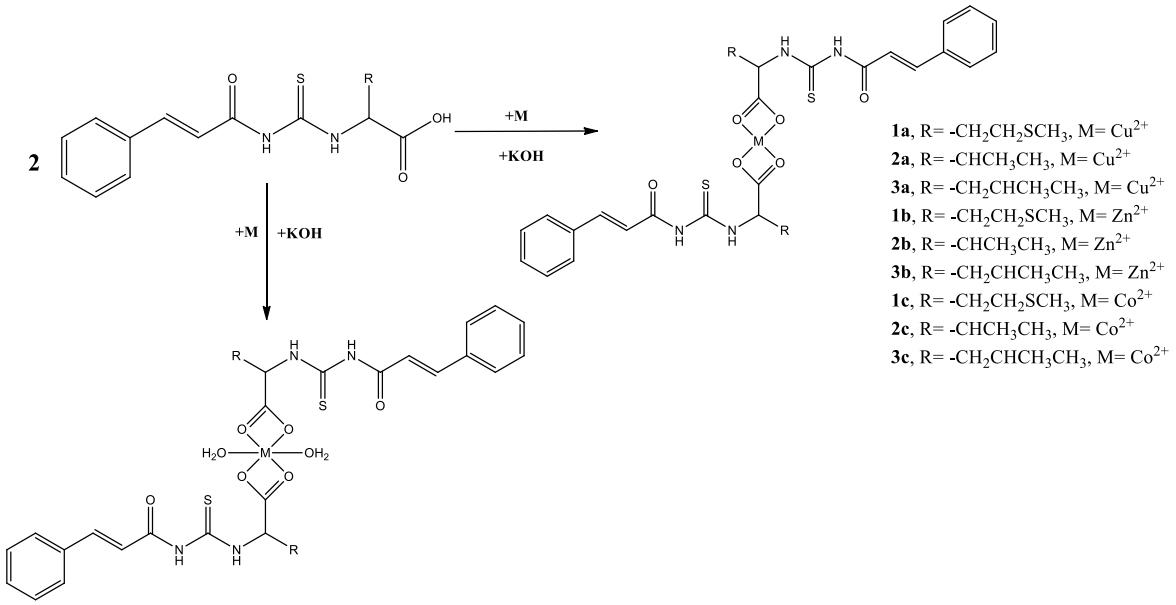

Figure 4.15: Synthesis pathway of metal complexes of thiourea

Metal complexes of thiourea were synthesized with product yield ranging from 24.67-89.76%. It was observed that the complexes demonstrated poor solubility in all organic solvents even upon heating except in DMSO. For compound **3a,** it was insoluble in all tested solvents. However, all compounds were observed to be relatively stable at room

temperature. The melting points of the complexes range from 166-258 ℃ respectively which were relatively higher than their respective ligands. Higher melting point of the metal complexes may be attributed to the increase in its molecular weight as a result of complexation (Gopichand et al., 2023). Hence, the elevation in the melting points were the initial indicator for the formation of metal complexes (Pal et al., 2019). Furthermore, sharp melting points range also indicated the purity of the complexes (Dent, 2006). The physical properties of complex **1a-3c** were summarized in Table 4.9.

Table 4.9: Physical properties of thiourea complexes

Complex	Molecular formula	mp (℃)	Yield (%)	Appearance
1a	$C_{30}H_{36}N_4O_6S_4Cu•2H_2O$	166-168	40.56	Green solid
2a	$C_{30}H_{36}N_4O_6S_2Cu•4H_2O$	198	41.00	Green solid
3a	$C_{32}H_{40}N_4O_6S_2Cu•5H_2O$	205	37.7	Dark green solid
1b	$C_{30}H_{36}N_4O_6S_4Zn•2H_2O$	224-227	34.14	White solid
2b	$C_{30}H_{36}N_4O_6S_2Zn•7H_2O$	211-213	89.76	White solid
3b	$C_{32}H_{40}N_4O_6S_2Zn•7H_2O•5CH_3OH$	237-242	26.39	White solid
1c	$C_{30}H_{36}N_4O_6S_4Co$	255-258	39.7	Purple solid
2c	$C_{30}H_{36}N_4O_6S_2Co•3H_2O•4EtOH$	253-256	24.67	Purple solid
3c	$C_{32}H_{40}N_4O_6S_2Co•5H_2O$	211-215	30.72	Purple solid

The formation of metal complexes were indicated by its color changes after metal salt solution was added. In this experiment, the formation of metal complex is a labile reaction as the complexes formed instantly after the addition of metal salt solution, without giving heat to the reaction. The presence of vacant d-orbital allows the metal and its complexes to appear colorful due to the occurrence of d-d transition of electrons because of the excitation of electrons from low-energy orbital to high-energy orbital which occurred after overcoming the energy difference between the two orbitals in the visible light regions (Kale et al., 2021).

The formation of Cu(II) thiourea complex was indicated by the formation of green or dark green colored compound which is consistent with numerous studies in literature (Drzewiecka-Antonik et al., 2020; Meena & Adusumilli, 2023; Trung et al., 2024). Meanwhile, zinc(II) complex appeared as white solid and cobalt(II) complexes appeared as purple complex. Zinc(II) complexes appeared as white because of lower band gap energy and fully filled d-orbital of zinc(II) ion which corresponds to shorter wavelengths and zero visible light absorption. (Buvaneswari et al., 2015; Kale et al., 2021). Furthermore, Kale et al., (2021) added that weak field ligands appeared as blue-green, blue and indigo because they absorbed low-energy yellow, orange or red-light. Thus, the formation of green and purple colored complex indicated that thiourea is a weak field ligand.

The synthesis of metal complexes were then subjected for CHNS elemental analysis (Table 4.10). The calculated and the obtained values suggested the presence of hydrated water molecules in the complexes which were common in the synthesis of metal complexes

(Abendrot et al., 2020; Carcelli et al., 2020). For compound **3b** and **2c**, the CHNS data implied the presence of solvent in the complex while traces of SO_4^{2-} were also detected in compound **3b**. Furthermore, the obtained result suggested that the geometrical structure of the complexes were in good agreement with the proposed structure except for complex **1c**. In line with previous studies, the structures of Cu(II) and Zn(II) complexes were proposed as square planar (Venkatesh et al., 2024). Instead of the typical six-coordinated cobalt(II) complex (El-Zahed et al., 2023), complex **1c** were found to be four-coordinated or square planar based on the CHNS data. According to the CHNS data, the difference in percentage of carbon atom was 2.17% if the structure was six-coordinated while less than 0.1% difference was obtained if the structure of the complex was four-coordinated therefore it was strongly suggested that the cobalt(II) metal may have formed a square planar complex with ligand **1** (Venkatesh et al., 2024; Saeed and Jasim, 2024).

Table 4.10: CHNS elemental data of thiourea complexes

Compound	Molecular formula	Elemental values			
		%C	%H	%N	%S
1a	$C_{30}H_{36}N_4O_6S_4Cu•2H_2O$	46.48 [46.49]	4.17 [4.65]	7.43 [7.23]	16.76 [16.56]
2a	$C_{30}H_{36}N_4O_6S_2Cu•4H_2O$	48.08 [48.24]	4.17 [4.82]	7.65 [7.51]	8.39 [8.59]
3a	$C_{32}H_{40}N_4O_6S_2Cu•5H_2O$	48.09 [48.46]	4.98 [5.05]	7.04 [7.07]	7.71 [8.09]
1b	$C_{30}H_{36}N_4O_6S_4Zn•2H_2O$	46.40 [46.38]	2.67 [4.64]	5.16 [7.22]	16.11 [16.52]
2b	$C_{30}H_{36}N_4O_6S_2Zn•7H_2O$	45.68 [44.88]	3.89 [4.49]	6.95 [6.98]	5.85 [7.99]
3b	$C_{32}H_{40}N_4O_6S_2Zn•7H_2O•5CH_3OH$	35.29 [35.35]	3.75 [3.68]	5.35 [5.16]	6.51 [5.90]
1c	$C_{30}H_{36}N_4O_6S_4Co$	48.97 [49.06]	3.02 [4.91]	7.61 [7.64]	17.43 [17.48]
2c	$C_{30}H_{36}N_4O_6S_2Co•3H_2O•4EtOH$	39.67 [39.65]	3.71 [3.96]	5.78 [5.73]	3.26 [7.06]
3c	$C_{32}H_{40}N_4O_6S_2Co•5H_2O$	48.73 [48.75]	5.55 [5.08]	6.95 [7.11]	4.78 [8.14]

*theoretical values are indicated in square brackets

4.5 Characterization of compound 1-3 and complexes 1a-3c by FTIR

ATR- FTIR spectroscopy was utilized to determine the important functional groups that were present in the synthesized compounds. Subsequently, the IR spectra of compound **1-3** and complex **1a-3c** were recorded in the IR region between 500 cm^{-1} and 4000 cm^{-1}. Generally, a successful reaction for the synthesis of thiourea was marked by the presence of the following distinctive functional groups: *ν*(N-H), *ν*(C=O) of the carboxylic group, *ν*(C=O) of the amide group, *ν*(C=C) as well as *ν*(C=S) and *ν*(C-N) functional groups. The IR spectrum of compound **1** was shown in Figure 4.16 while the IR spectra of compound **2-3** and complex **1a-3c** was shown in **Appendix 13-22.**

The successful formation of thiourea was indicated by the presence of the N-H stretching which appeared at 3165-3056 cm^{-1}. This observation was consistent with a recent work done by Oleiwi et al., (2023) where the N-H band was assigned at 3404-3164 cm^{-1}. As mentioned earlier, the reaction between cinnamoyl chloride and KSCN formed an isothiocyanate intermediate compound bearing NCS bond. The formation of thiourea compound was indicated by another unique characteristic that was the absence of the NCS vibration, which typically exist at 2140-1990 cm^{-1} according to Ngaini et al., (2017). The addition of amino acid to the isothiocyanate intermediate caused the NCS group to disappear and eventually being replaced by the formation of -NH groups. A similar observation was also observed for the formation of metal complexes such that *ν*(N-H) stretchings were assigned to the absorption frequencies between 3207-3060 cm^{-1} (Figure 4.17).

Furthermore, the formation of synthesised compounds were supported by the absorption at 1732-1716 cm^{-1} which were attributed to the carbonyl group of carboxylic

acid. A significant change from the IR spectra of the metal complexes revealed the shifting of the C=O of the carboxylate group from 1732-1716 cm^{-1} to a lower frequency 1660-1681 cm^{-1} which may have overlapped with the C=O vibration of the amide group. The downward shifting was previously observed in the complexation of carboxylate ligand in a study by Paris et al., (2021) where the stretching of the C=O of the carboxylate group shifted from 1675 cm^{-1} to 1507 cm^{-1} in its complex. It appeared that the addition of KOH salt deprotonated the hydrogen of the carboxylic group, which subsequently allowed the formation of metal complex through the coordination with the COO^- group. Therefore, it was confirmed that the formation of thiourea complexes occurred through the coordination at the COO^- group of thiourea group. This observation is in good agreement with earlier studies (Ghazal et al., 2019; Khan et al., 2020). A comparison between IR spectra of compound **1** and its complexes were represented in Figure 4.18

Subsequently, an intense band was observed for the amide carbonyl group at 1659-1681 cm^{-1} for thioureas and its respective metal complexes (Khalid et al., 2022; Obradović et al., 2020). In addition, the absorption of the aromatic carbons were identified at the region 1593-1496 cm^{-1} (Saeed et al., 2018). Then, the bands at 1293-1220 cm^{-1} were identified as the absorption of the *ν*(C=S) group (Bielenica et al., 2018; Khan et al., 2018; Khan et al., 2020). No changes in this band indicated that the coordination with metal did not occur through this site. Lastly, the *ν*(C-N) group were found in the region 1187-1143 cm^{-1}.

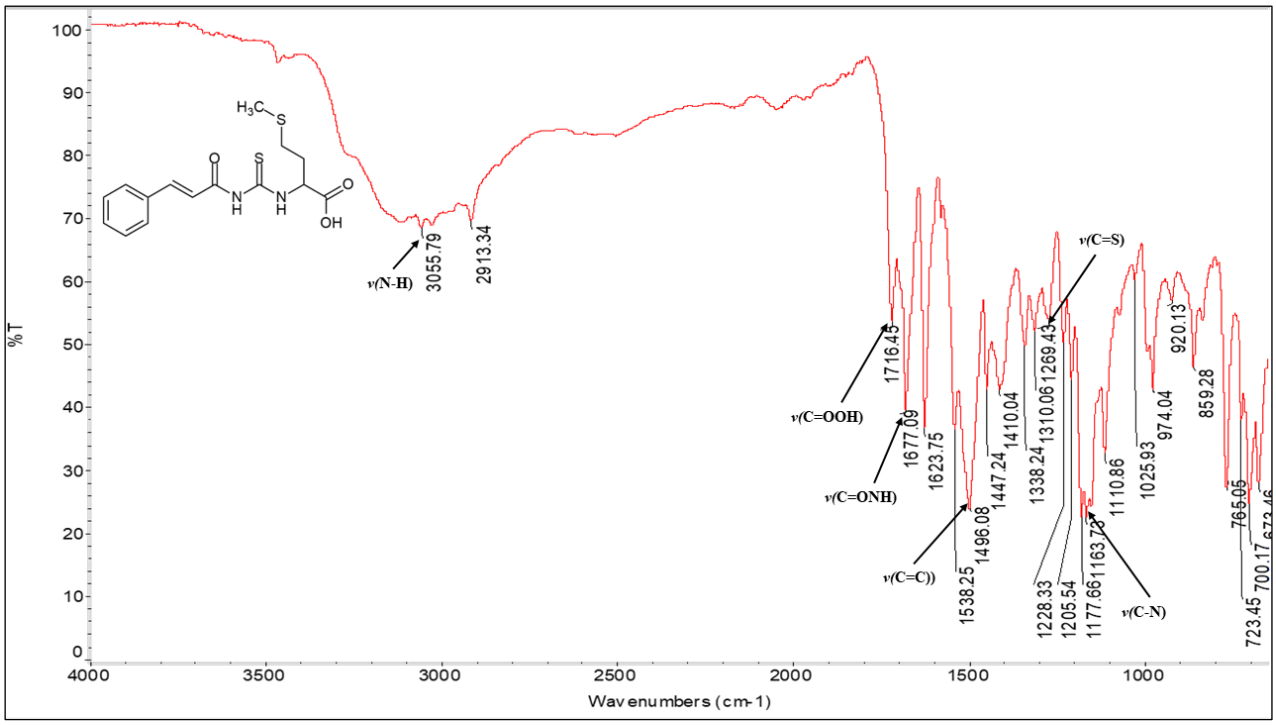

Figure 4.16: IR spectrum of compound **1**

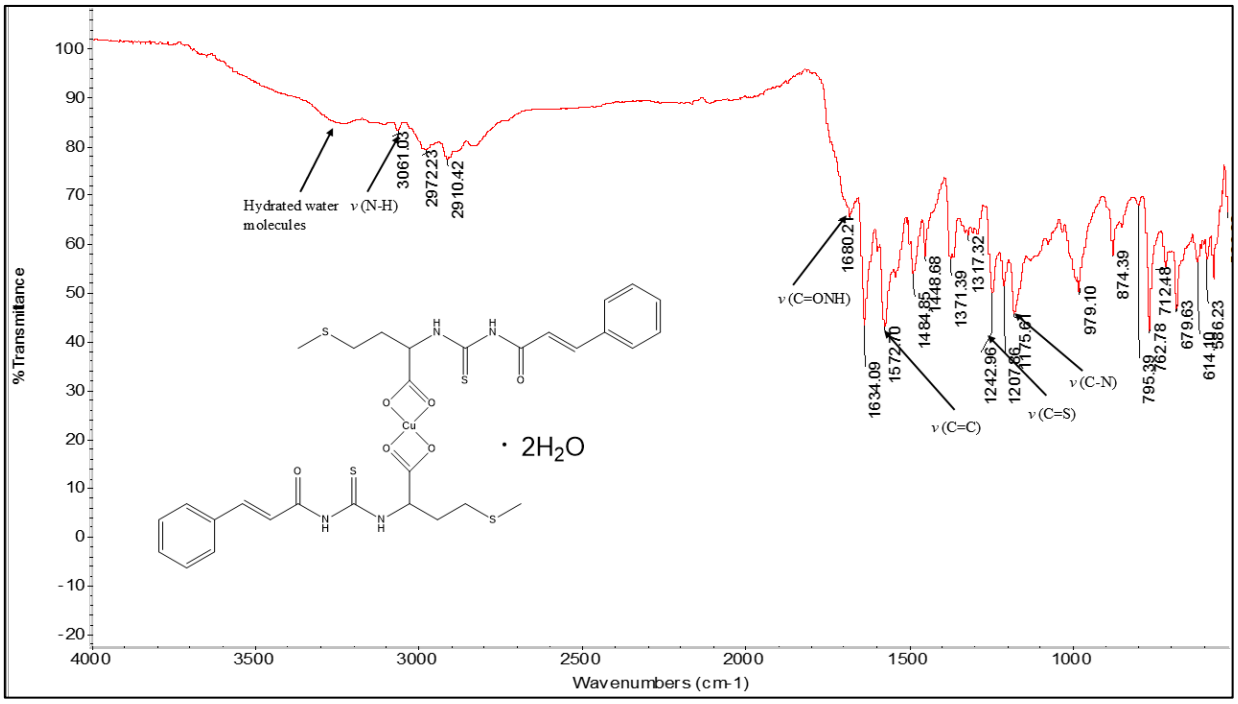

Figure 4.17 Absorption band in IR spectrum of complex **1a**

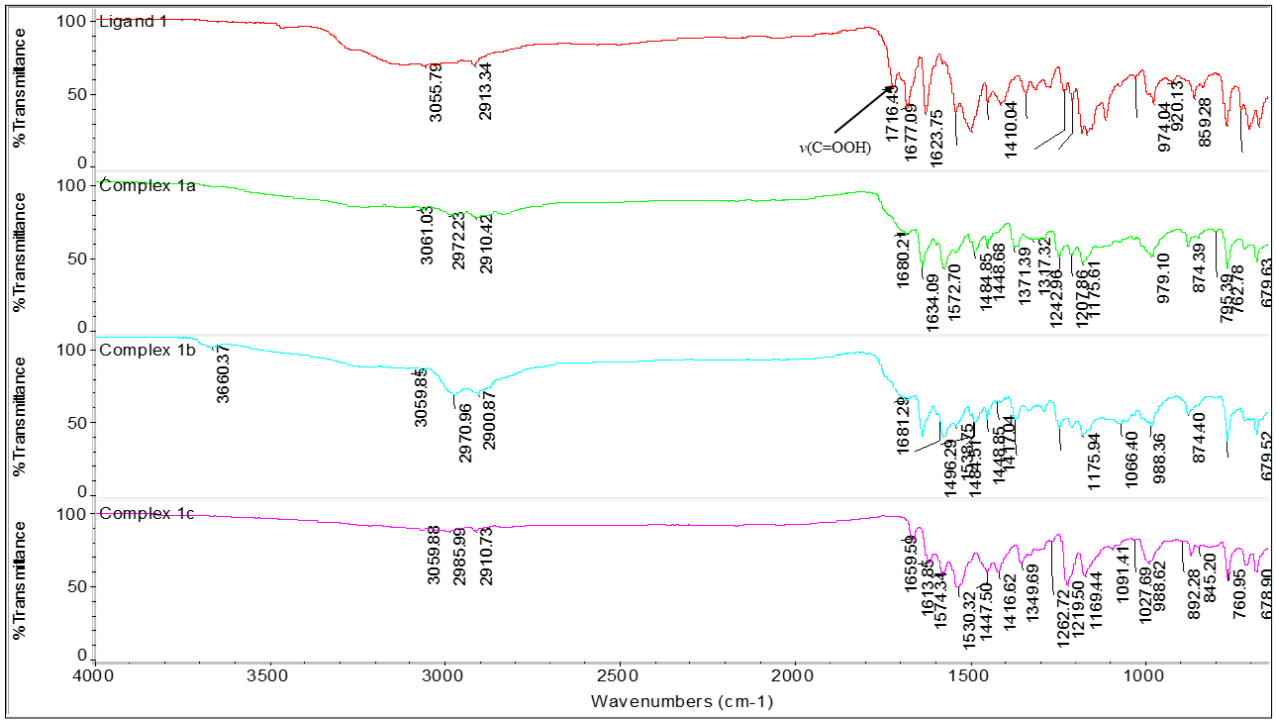

Figure 4.18: Comparison of IR spectra of compound **1** and complex **1a, 1b, 1c**

4.6 UV-Vis spectra of thiourea complexes versus its ligand

The electronic spectra of compound **1-3** and its respective metal complexes were recorded in ethanolic solution and the absorbance reading were taken in the wavelength of 250 – 400 nm. The electronic spectrum of the ligands demonstrated a strong band absorption at λ_{max} 287-295 nm respectively. This band was assigned to the intra-ligand charge transfer π-π^* transition of the free electrons of the C=S chromophores of thiourea (Khairul et al., 2016b). Nevertheless, the broad band suggested the mixture of π-π^* and n-π^* transition which may arised due to the presence of the aromatic rings of the cinnamoyl (Kadir et al., 2016). In metal complexes, the band shifted to longer wavelength to signify that coordination with metal centers have taken place (Tyagi et al., 2015). In Cu(II) complexes, the absorption band shifted to longer wavelength for complex **1a** (290→294 nm). Among Zn(II) complexes, complex **1b** experienced a red shift by 4 nm from 290→294 nm while complex **3b** experienced a little red shift by 1 nm from 295→296nm. A notable red shift was also observed for complex **2b** from 287→294 nm. For cobalt(II) complexes, only complex **1c (**290→295) and **2c (**287→295) experienced a red shift while there were no significant changes in the electronic spectra of complex **3c**. This transition involving red or batrochromic shift is often associated with ligand-metal charge transfer (LMCT) during the formation of metal complexes (Hernández et al., 2024). This transition occurs as a result of the presence of electron deficient metal centers with strongly donating ligand groups which donates electron to the empty orbitals of the metal centers (Chábera et al., 2021; Carter, 1997). However, for complex **3a**, blue shift (295→287 nm) was observed while for complex **2a** and **3c**, no significant changes were observed for the UV-Vis spectra likely because the the charge transfer occuring at the same intensity with the intra ligand bands (Hernández et al., 2024). The comparison of electronic spectra of compound **1** and complex **1a** was shown

in Figure 4.19 while the rest of the spectra will is shown in the **Appendix 23-30.**

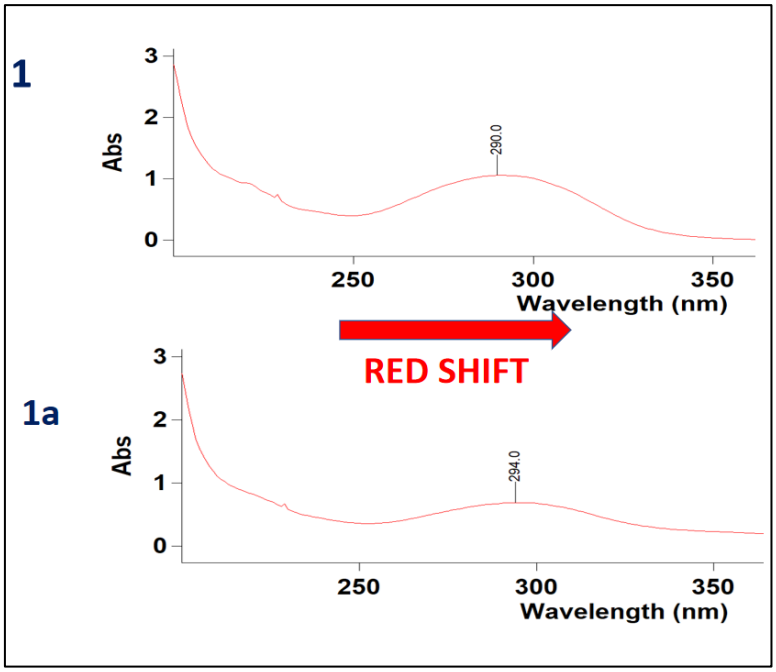

Figure 4.19: Electronic spectra of compound 1 vs complex 1a

4.7 Characterization of compound 1-3 by ^{1}H and ^{13}C NMR

The structures of compound **1-3** were further elucidated by ^{1}H and ^{13}C NMR spectroscopy. NMR aimed to confirm the types and the number of protons present in the synthesized compounds. While FTIR generally provides insight of the functional groups present in the compound, NMR could accurately provide the molecular structure of the compounds using the types and the number of protons present in the sample.

Figure 4.20 illustrated the ^{1}H NMR spectrum of compound **1** while the ^{1}H NMR spectra of compound **2-3** is be shown in **Appendix 31-32**. The formation of thiourea were represented by two distinct -NH signals observed between δ_H11.47-11.13 ppm which were attributed to -CONH signals and -CSNH signal, respectively (Al-Amily & Hassan, 2019; Khan et al., 2018). Both of these signals appeared downfield due to intramolecular hydrogen bonding as well as the surroundings and molecule conformation (Rahamathullal et al., 2013; Yusof et al., 2010). The signal of -CONH proton appeared as a broad singlet peak, with the integral value of one. It resonated more downfield than the -CSNH proton due to the oxygen atom attached being more electronegative than the sulphur atom which subsequently created more deshielding effects and contributed to larger chemical shifts (Saeed et al., 2010). On the other hand, the -CSNH proton appeared as a doublet signal due to the splitting of the neighbouring -CH proton. Furthermore, the multiplet signals for the aromatic protons of cinnamoyl thiourea were observed between δ_H7.72-7.43 ppm collectively with integral values of five (Díaz et al., 2019). The resonance of the -CH_3 protons of compound **1** was observed at δ_H2.02 ppm while for compound **2-3** the resonance were observed between δ_H 0.92-0.88 ppm (Nordin et al., 2017). The downfield effect of the methyl group of compound **1** was expected due to deshielding effect of the neighbouring sulphur atom in the methionine

derivative.

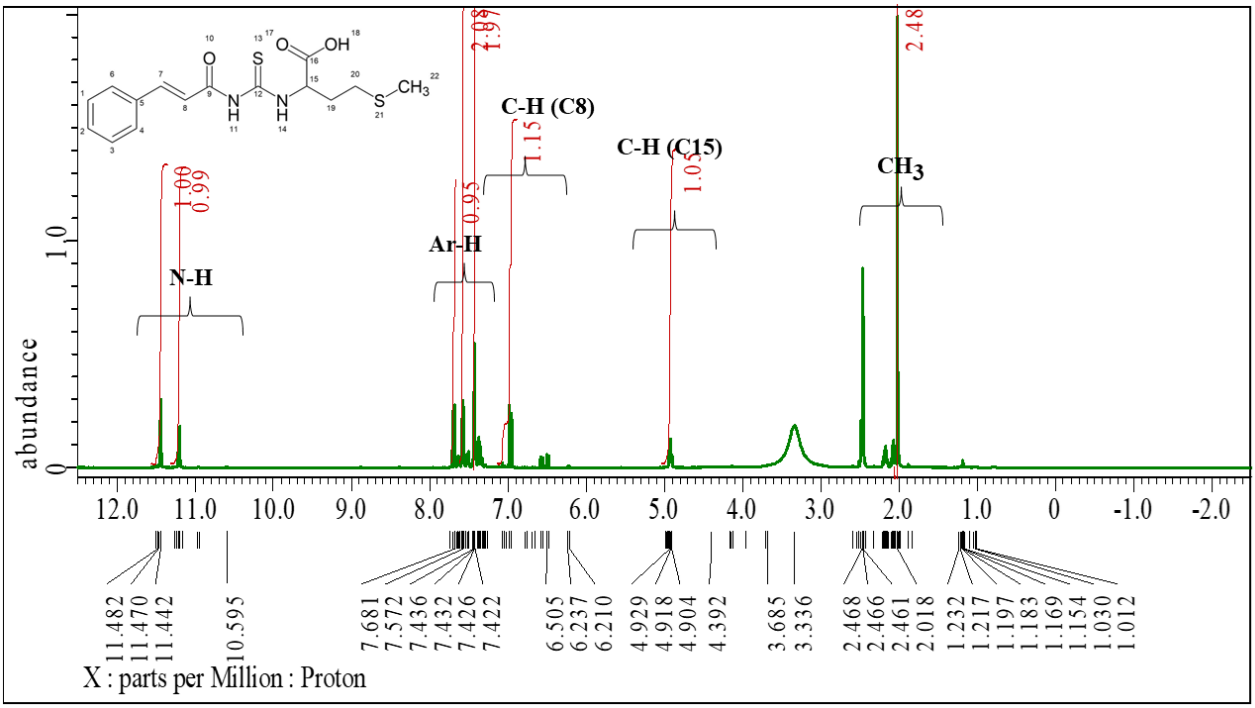

Figure 4.20: ^{1}H spectrum of compound **1**

Next, the formation of thioureas were determined by the assessment of ^{13}C chemical shifts. The ^{13}C spectra of compound **1** was shown in Figure 4.21 while the spectra for compound **2-3** is shown in **Appendix 33-34**. Some of the important signals that can be deduced from the NMR spectra are CSNH, COOH, CONH, Ar-C, CH CH_2 and CH_3 signals. The CSNH peak of compound **1-3** were observed at δ_C 181.35-180.86 ppm (Obradović et al., 2020). Next, the C=ONH carbon resonated at δ_C167.06-166. 76 ppm, which is consistent with the work of Ghazal et al., (2019). The difference in sizes between C and S atom as well as C and O atom causes the overlapping of the p orbital to be less efficient in C=S, creating more deshielding effects (Saeed et al., 2024). Furthermore, the peak at δ_C 173.11-171.99 ppm was attributed to the C=OOH carbon signal. The present of another one more electronegative oxygen atom caused C=OOH to be resonated at higher frequency than C=ONH signal, due to greater deshielding effects.

In addition, the presence of aromatic rings were indicated by multiple carbon signals between 145.10- 120.35 ppm which were consistent for all the compounds (Rasheed et al., 2022). The signals for -CH on the other hand appeared at δ_C 62.89-56.49 ppm (Omotola et al., 2018). For compound **1,** the presence of -CH_2 carbon signals appeared at two different environments at δ_C 39.85 and δ_C 39.68 ppm respectively (Fakhar et al., 2018; Omotola et al., 2018). Finally, a -CH_3 carbon signal was observed at δ_C 15.21 ppm for compound **1** whereby the same signal was observed at two different environments at δ_C 19.26 and δ_C18.38 ppm in compound **2**. For compound **3**, the signals appeared at δ_C 25.22 and δ_C 22.51 ppm respectively (González et al., 2020). Although the -CH_3 carbon was attached to S atom in compound **1**, we noticed that the signal was more upfield compared to that of compound **2** and **3**. The presence of oxygen atoms from the solvent DMSO may have contributed to the shifting of these signals to more upfield.

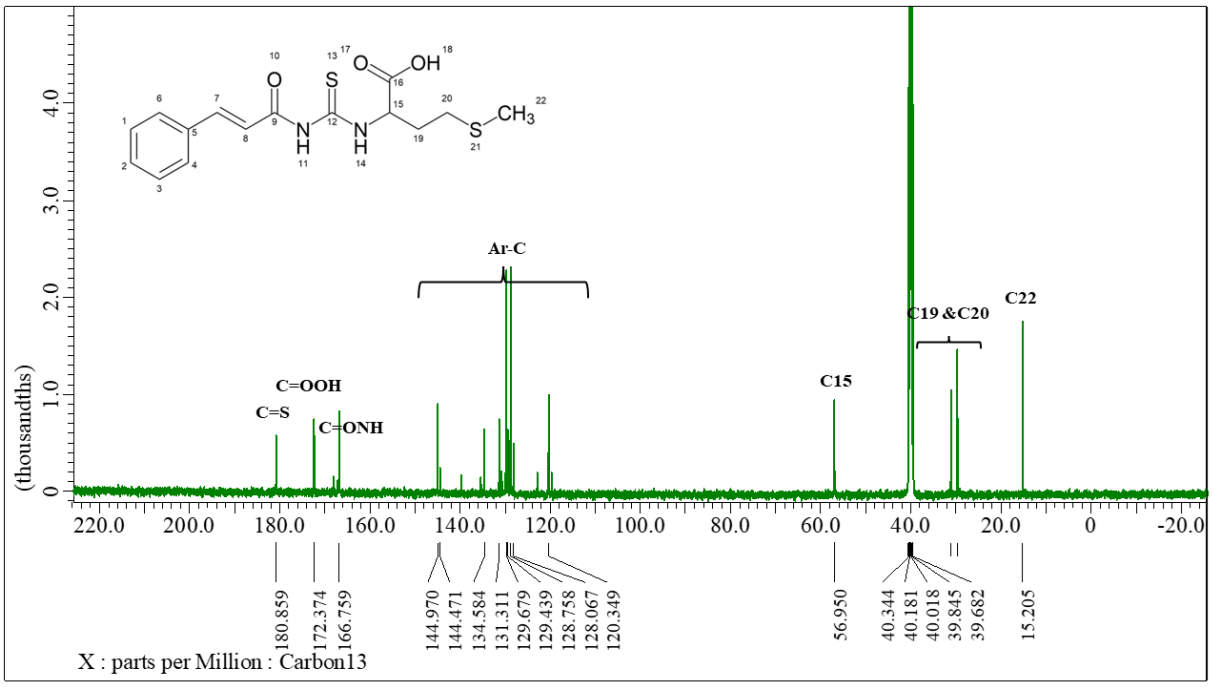

Figure 4.21: ^{13}C NMR spectrum of compound **1**

4.8 Antibacterial evaluation of thiourea and its complexes

Due to rising of resistance of *E. coli* towards fluoroquinolones, it was selected for biological evaluation of thiourea and its complexes (Spellberg & Doi, 2015; Stapleton et al., 2020). Furthermore, due to its versatility and stability in various growth media, *E. coli* was selected as bacteria of choice (Blount, 2015). The ligands (compound **1-3**) and their respective complexes (compound **1a-1c**, **2a-2c** and **3a-3c**) were subjected for antibacterial evaluation against *E. coli* ATCC25922 strain by agar-well diffusion method. The compounds were prepared in standard solution at three different concentrations which were 150 ppm, 250 ppm and 500 ppm respectively. DMSO was chosen as the standard solvent for the dissolution of the compounds because it was a universal solvent for all compounds. The antibacterial activity of the ligands was discussed chronologically, starting with ligands followed by their metal complexes.

4.8.1 Agar-well diffusion method

The antibacterial activity of the compounds against the standard *E. coli* strain was evaluated using agar-well diffusion method. It is a common method employed in microbiology to test the antibacterial action of a compound. In this experiment, DMSO was chosen as the negative control because it is a polar aprotic solvent capable of dissolving polar and non-polar compounds (Verheijen et al., 2019). Ciprofloxacin, antibiotic belongs to the fluoroquinolone group was the positive control of this study. The data is tabulated as zone of inhibition (mm) as presented in Table 4.11.

Table 4.11: Zone of inhibition (mm) of thiourea and its complexes against *E. coli* ATCC25922 strain

Concentration / Compound	150 ppm	250 ppm	500 ppm
1	-	-	-
1a	-	10	11
1b	-	-	-
1c	-	-	-
2	-	13	11
2a	-	-	11
2b	-	-	-
2c	-	-	-
3	-	-	-
3a	ND	ND	ND
3b	-	-	-
3c	-	-	-
Ciprofloxacin	35		
Negative control	-	-	-

*ND indicates no data as compound is insoluble in DMSO
"-" indicates zero zone of inhibition

Based on Table 4.11, only compound **1a**, **2** and **2a** displayed pronounced antibacterial activities with rather weak zone of inhibition ranging from 10 mm - 13 mm. On the other hand, the reference drug Ciprofloxacin had much better inhibition at 35 mm suggesting that

cinnamoyl thiourea and its complexes displayed relatively weak antibacterial potential according to Clinical and Laboratory Standards Institute, (2020). Among the ligands, only compound **2** exerted pronounced antibacterial effect. It was found to inhibit the *E. coli* strain at 250 ppm and 500 ppm with inhibition zone of 13 mm and 11 mm, respectively. Furthermore, it was observed that the antibacterial effect at 250 ppm was higher than that of 500 ppm suggesting that this might be the optimum concentration for the antibacterial activity. On the other hand, no activities were observed for compound **1** and **3**, respectively. This finding showed that valine derivatives were more active than methionine and leucine derivatives which was in good agreement with the docking data. According to data of the docking simulation, compound **2** displayed the highest binding affinities when docked into DNA gyrase enzyme (PDB ID:1KZN) with binding energy of **-7.1 kJ/mol**. Therefore, it is possible that the inhibitory effect of compound **2** may be driven by the interaction with the enzyme receptor such as two conventional hydrogen bond interactions with **THR A:165** and **GLU A:50** as well as pi-alkyl interaction with the amino acid residue **ALA A:47**.

Among the complexes, only the Cu(II) complexes displayed antibacterial potential. Complex **1a** had a zone of inhibition of 10 mm at 250 ppm and 11 mm at 500 ppm, respectively. Previous study showed that the inclusion of copper could enhance the antimicrobial properties of a ligand. For instance, Kumar et al., (2019) examined the antibacterial properties of levoflorxacin and its Cu(II) complexes and they found out that the inclusion of metals significantly enhanced the antibacterial properties against nine tested bacteria including *E. coli*. Similarly, in this work, it was observed that the antibacterial activity of compound **1** was improved significantly after complexation with Cu(II) metal. There was no activity displayed by the free ligand but after complexation with copper, the

complex exerted antibacterial activity at 250 ppm and 500 ppm with zone of inhibition at 10 mm and 11 mm respectively. This result correlated to the previous docking simulation data where complex **1a** demonstrated higher binding affinity than its ligand counterparts suggesting stronger enzyme interaction. The increase in the antibacterial properties of Cu(II) complexes compared to its ligand could also be explained by chelation theory. According to this theory, chelation process reduces the polarity of the central metal atom because of π-electron delocalization within the ring and the partial sharing of its positive charge with the donor groups. Thus, increases its lipophilicity and contributed to better penetration towards the bacterial cell membrane (Abd-Elzaher, 2004). In contrast, for compound **2**, complexation with copper slightly reduced the antibacterial activity. At 250 ppm, the complex compound did not inhibit the bacteria growth despite zone of inhibition was recorded to be at 13 mm for the free ligand. At 550 ppm however, the zone of inhibition remained the same.

As for Co(II) and Zn(II) complexes, none of the complexes portrayed any antibacterial action. In fact, the complexation of compound **2** with zinc(II) and cobalt(II) metal diminished its antibacterial properties as evidenced by its zero inhibition. This study suggested that the choice of metal might influenced the antibacterial effect of a compound. The difference in the antibacterial activity of each complexes may be attributed to the electronegativity of the metal. From this experiment, the electronegativity of the metal may be ranked as Cu>Co>Zn. Comparing the results with the previous findings by Vaidya et al., (2017), the authors observed that the metal with greater electronegativity demonstrated greater antibacterial potential, likely due to stronger interaction with negatively charged bacterial membrane. In the current study, copper(II) was the most electronegative metal which explained the highest antibacterial property.

The antibacterial activities of the Zn(II) and Co(II) complexes were unsatisfactory despite the encouraging docking results. None of the Zn(II) or Co(II) complexes were found to inhibit bacteria despite it was predicted earlier that the complexes may bound tightly inside the active site of the enzyme receptor. It could be plausible that the binding to this enzyme may not be correlated to the inhibitory effect of these complexes. Furthermore, the drawback of this experiment was that the complexes were insoluble at higher concentration. In one finding, Shalas et al., (2023) found that the inhibitory activities of the compound did not match the docking data. However, when the experiment was done by increasing the concentration, the compounds shown some inhibitory activities at higher concentration. Furthermore, according to Mohanty et al., (2023), the docking results may not always complement the experimental data due to several factors such as molecules flexibility, different force field parametrization and the possible involvement of hydrated water molecules in the compound system.

CHAPTER 5

CONCLUSION AND RECOMMENDATIONS

5.1 Conclusion

In this study, the virtual screening of twelve thiourea compounds had been carried out based on molecular docking and ADME evaluation to select the most promising compound as potent DNA gyrase enzyme inhibitors. Out of twelve compounds, the cinnamoyl derivative have shown the most promising potential with compound **2** displaying binding energy of -7.1 kJ/mol as seen from the docking results. Subsequently, Cu(II), Zn(II) and Co(II) complexes of cinnamoyl thiourea derivatives have been designed and docked using the same software which demonstrated higher binding energies than its free ligand with binding energies range between -6.9 kJ/mol to -8.3 kJ/mol. The ADME evaluation revealed that the thiourea derivatives have good pharmacokinetic profiles by obeying the Lipinski's Rule of Five, high gastrointestinal absorption and poor permeability against the blood brain barrier. Due to its complex molecular structures, the metal complexes generally showed poor pharmacokinetic profiles, although good lipophilicity values were observed.

Thus, cinnamoyl thiourea derivatives compound **1-3** and its Cu(II), Zn(II) and Co(II) complexes were selected and successfully synthesized in the lab. Thiourea and its complexes were characterized with various method such as FTIR, ^{1}H NMR, ^{13}C NMR, UV-Vis spectra and CHNS elemental analysis. The formation of thioureas were confirmed by the disappearance of ν(N=C=S) bond at 2140-1990 cm^{-1} as well as the presence of common functional groups such as ν(N-H) band at 3165-3056 cm^{-1} and ν(C=ONH) band at 1732-1716 cm^{-1}as observed from the FT-IR spectra. Meanwhile, two N-H signals were identified

at δ_H 11.47-11.13 ppm from the NMR spectra which were commonly observed in the synthesis of thioureas. The synthesis of thioureas were also supported by CHNS data which saw good agreement between the experimental and theoretical values. The formation of complexes had been confirmed by the downwards shifting of *v*(COOH) absorption in the IR spectra from 1732-1716 $cm^{-1}$to 1660-1681 cm^{-1} . The UV-Vis data suggested there were ligand to metal charge transfer (LMCT) while elevation in melting points indicated the formation of metal complexes. The antibacterial study of the synthesized compounds were conducted by agar-well diffusion method against standard *E. coli* ATCC 25922 strains. The results showed that compound **2** and the Cu(II) complexes, namely complex **1a** and **2a** displayed the most promising antibacterial activities with zone of inhibitions 10 – 13 mm although the antibacterial activities were considerably weak when compared to the standard Ciprofloxacin. The results were correlated to the docking simulation done prior to the experimental activities which predicted compound **2** as the most promising antibacterial agent as seen from its higher docking score. Besides, this research proved that complexation with Cu(II) center metal enhanced the antibacterial properties of a compound and the choice of metal is important in determining the antibacterial activity. For Zn(II) and Co(II) complexes however, the docking scores did not actually represent the actual antibacterial activities as these complexes did not display any antibacterial action despite higher docking scores than most compounds.

5.2 Recommendation

For recommendation, molecular dynamic simulation could be proposed as future studies to investigate the physical movement of atoms and molecules over a period of time, which is another important aspect in virtual drug screening. Furthermore, the

toxicity of compounds should also be considered in drug-design process to select the best compound as lead molecule. It is also important to note that although computer software had been an integral part in drug design process, the experimental studies is still pivotal to confirm the screening results and that computer software only act as a preliminary screening tool to identify potential molecule as drug.

.

REFERENCES

Abendrot, M., Chęcińska, L., Kusz, J., Lisowska, K., Zawadzka, K., Felczak, A., & Kalinowska-Lis, U. (2020). Zinc (II) complexes with amino acids for potential use in dermatology: Synthesis, crystal structures, and antibacterial activity. *Molecules*, *25*(4), 1-17.

Abd-Elzaher, M. M. (2004). Synthesis, characterization, and antimicrobial activity of cobalt(II), nickel(II), copper(II) and zinc(II) complexes with ferrocenyl Schiff bases containing a phenol moiety. *Applied Organometallic Chemistry*, *18*(4), 149–155.

Abd Halim, A.N. & Ngaini, Z. (2016). Synthesis and bacteriostatic activities of bis(thiourea) derivatives with variable chain length. *Journal of Chemistry, 2016*, 1-7.

Agili, F. A. (2024). Biological Applications of Thiourea Derivatives: Detailed Review. *Chemistry*, *6*(3), 435–468.

Ahamad, N. M., Iman, K., Raza, M. K., Kumar, M., Ansari, A., Ahmad, M., & Shahid, M. (2020). Anticancer properties, apoptosis and catecholase mimic activities of dinuclear cobalt(II) and copper(II) Schiff base complexes. *Bioorganic Chemistry*, *95*, 1-15.

Alsalhi, M. S., & Chan, K. A. (2022). Amino acid hydrotropes to increase the solubility of indomethacin and carbamazepine in aqueous solution. *International Journal of Pharmaceutics*, *617*, 1-11.

Al-Amily, D. H., & Hassan, M. (2019). Design, synthesis, and docking study of acyl thiourea derivatives as possible histone deacetylase inhibitors with a novel zinc binding group. *Scientia Pharmaceutica*, *87*(4), 1-15.

Alex, A., Millan, D. S., Perez, M., Wakenhut, F., & Whitlock, G. A. (2011). Intramolecular hydrogen bonding to improve membrane permeability and absorption in beyond rule of five chemical space. *Medicinal Chemistry Communications*, *2*(7), 669-674.

Al-fagieh, E. A., Abukhattala, E. M., & Salah, K. S. B. (2023). The assessment of serum zinc, testosterone concentration and sperm quality in infertile males. *Journal of Academic Research (Health Sciences)*, *24*, 29-33.

Al-Salim, Y. M., & Al-Asadi, R. H. (2023). Synthesis, anti-breast cancer Activity, and molecular docking studies of thiourea benzamide derivatives and their complexes with copper Ion. *Tropical Journal of Natural Product Research*, *7*(6), 3158–3167.

Anthony, E. J., Bolitho, E. M., Bridgewater, H. E., Carter, O. W. L., Donnelly, J. M., Imberti, C., Lant, E. C., Lermyte, F., Needham, R. J., Palau, M., Sadler, P. J., Shi, H., Wang, F. X., Zhang, W. Y., & Zhang, Z. (2020). Metallodrugs are unique: Opportunities and challenges of discovery and development. *Chemical Science*, *11*(48), 12888–12917.

Antypenko, L., Meyer, F., Kholodniak, O., Sadykova, Z., Jirásková, T., Troianova, A., Buhaiova, V., Cao, S., Kovalenko, S., Garbe, L. A., & Steffens, K. G. (2019). Novel acyl thiourea derivatives: Synthesis, antifungal activity, gene toxicity, drug-like and molecular docking screening. *Archiv Der Pharmazie-Chemistry in Life Sciences*, *352*(2), 1-14.

Anwar, A. I., Lu, L., Plaisance, C. J., Daniel, C. P., Flanagan, C. J., Wenger, D. M., McGregor, D., Giustino, V., Kaye, A.M., Ahmadzadeh, S., Cornett, E.M., Shekoohi, S., & Kaye, A. D. (2024). Fluoroquinolones: Neurological complications and side effects in clinical practice. *Cureus*, *16*(2), 1-7.

Aprajita, & Choudhary, M. (2022). Design, synthesis and characterization of novel Ni(II) and Cu(II) complexes as antivirus drug candidates against SARS-CoV-2 and HIV virus. *Journal of Molecular Structure*, *1263*, 1-14.

Abdul Rassip, M. N. A., Puteh, S. E. B. W., Ibrahim, R., Rahman, M. M., Karim, Z. A., Ali, F. Z. B., & Bakhtiar, N. F. B. (2025). Antimicrobial resistance in Malaysia: a cross-sectional study analysing trends and economic impacts. *British Medical Journal*

Open, *15*(2), 1-8.

Arshad, N., Saeed, A., Perveen, F., Ujan, R., Farooqi, S. I., Ali Channar, P., Shabir, G., El-Seedi, H. R., Javed, A., Yamin, M., Bolte, M., & Hökelek, T. (2021). Synthesis, X-ray, Hirshfeld surface analysis, exploration of DNA binding, urease enzyme inhibition and anticancer activities of novel adamantane-naphthyl thiourea conjugate. *Bioorganic Chemistry*, *109*, 1-14.

Babgi, B. A., Domyati, D., Abdellattif, M. H., & Hussien, M. A. (2021). Evaluation of the anticancer and DNA-binding characteristics of dichloro(diimine)zinc(II) complexes. *Chemistry (Switzerland)*, *3*(4), 1178–1188.

Babines-Orozco, L., Balbuena-Alonso, M. G., Barrios-Villa, E., Lozano-Zarain, P., Martínez-Laguna, Y., Rocha-Gracia, R. D. C., & Cortés-Cortés, G. (2024). Antimicrobial resistance in food-associated *Escherichia coli* in Mexico and Latin America. *Bioscience of Microbiota, Food and Health*, *43*(1), 4-12.

Balouiri, M., Sadiki, M., & Ibnsouda, S. K. (2016). Methods for in vitro evaluating antimicrobial activity: A review. *Journal of Pharmaceutical Analysis*, *6*(2), 71-79.

Bassani, D., & Moro, S. (2023). Past, present, and future perspectives on computer-aided drug design methodologies. *Molecules*, 28(9), 1-20.

Batool, M., Ahmad, B., & Choi, S. (2019). A structure-based drug discovery paradigm. *International Journal of Molecular Sciences, 20*(11), 1-18.

Beer, T. M., Armstrong, A. J., Rathkopf, D., Loriot, Y., Sternberg, C. N., Higano, C. S., Iversen, P., Evans, C. P., Kim, C. S., Kimura, G., Miller, K., Saad, F., Bjartell, A. S., Borre, M., Mulders, P., Tammela, T. L., Parli, T., Sari, S., van Os, S., … Tombal, B. (2017). Enzalutamide in men with chemotherapy-naïve metastatic castration-resistant prostate cancer: Extended analysis of the Phase 3 PREVAIL Study. *European Urology*,

71(2), 151–154.

Bernama (2024). *Malaysia To Face 87,000 Deaths Due to Antimicrobial Resistance by 2030 without intervention—Dzukefly*. [online]. Available at:

https://www.bernama.com/en/news.php?id=2365212 [Assessed on 15 July 2025]

Bhalani, D. V., Nutan, B., Kumar, A., & Singh Chandel, A. K. (2022). Bioavailability enhancement techniques for poorly aqueous soluble drugs and therapeutics. *Biomedicines, 10*(9), 1-33

Bickerton, G. R., Paolini, G. V., Besnard, J., Muresan, S., & Hopkins, A. L. (2012). Quantifying the chemical beauty of drugs. *Nature Chemistry, 4*(2), 90–98.

Bielenica, A., Drzewiecka-Antonik, A., Rejmak, P., Stefańska, J., Koliński, M., Kmiecik, S., Lesyng, B., Włodarczyk, M., Pietrzyk, P., & Struga, M. (2018). Synthesis, structural and antimicrobial studies of type II topoisomerase-targeted copper(II) complexes of 1,3-disubstituted thiourea ligands. *Journal of Inorganic Biochemistry, 182*, 61–70.

Bisht, N., & Singh, B. K. (2018). Role Of Computer aided drug design in drug development and drug discovery. *International Journal of Pharmaceutical Sciences and Research, 9*(4), 1405-1415.

Biswas, S., Das, R., & Banerjee, E. R. (2017). Role of free radicals in human inflammatory diseases. *Aims Biophysics, 4*(4), 596-614.

Blair, J. M., Webber, M. A., Baylay, A. J., Ogbolu, D. O., & Piddock, L. J. (2015). Molecular mechanisms of antibiotic resistance. *Nature Reviews Microbiology, 13*(1), 42-51.

Blount, Z. D. (2015). The unexhausted potential of *E. coli*. *ELife, 4*, 1-12.

Bocci, G., Carosati, E., Vayer, P., Arrault, A., Lozano, S., & Cruciani, G. (2017). ADME-Space: A new tool for medicinal chemists to explore ADME properties. *Scientific Reports, 7*(1), 1-13.

Bordeleau, E., Stogios, P. J., Evdokimova, E., Koteva, K., Savchenko, A., & Wright, G. D. (2021). ApmA is a unique aminoglycoside antibiotic acetyltransferase that inactivates apramycin. *MBio*, *12*(1), 1–11.

Borgaonkar, V. B., Jain, C. M., Jaiswal, A. R., Irache, P., Yelane, A. H., & Tattu, H. P. (2024). A review on solubility enhancement technique for pharmaceutical drugs. *GSC Biological and Pharmaceutical Sciences*, *26*(2), 239-253.

Boros, E., Dyson, P. J., & Gasser, G. (2020). Classification of metal-based drugs according to their mechanisms of action. *Chem*, *6*(1), 41-60.

Boulsourani, Z., Geromichalos, G. D., Katsamakas, S., Psycharis, V., Raptopoulou, C. P., Hadjipavlou-Litina, D., Sahpazidou, D., & Dendrinou-Samara, C. (2019). Mononuclear copper(II) complexes with 2-thiophene carboxylate and N-N donors; DNA interaction, antioxidant/anti-inflammatory and antitumor activity. *Materials Science and Engineering C*, *94*, 493–508.

Breberina, L. M., Zlatović, M. V., Stojanović, S. Đ., & Nikolić, M. R. (2024). Amide–π interactions in the structural stability of proteins: Role in the oligomeric phycocyanins. *Computation*, *12*(9), 1-12.

Bruna, J. E., Peñaloza, A., Guarda, A., Rodríguez, F., & Galotto, M. J. (2012). Development of MtCu 2+/LDPE nanocomposites with antimicrobial activity for potential use in food packaging. *Applied Clay Science*, *58*, 79–87.

Buckley, L. F., Agha, A. M., Dorbala, P., Claggett, B. L., Yu, B., Hussain, A., Nambi, V., Chen, L. Y., Matsushita, K., Hoogeveen, R. C., Ballantyne, C. M., & Shah, A. M. (2023). MMP-2 associates with incident heart failure and atrial fibrillation: The ARIC study. *Circulation: Heart Failure*, *16*(11), 966-974.

Burch, H. B., & Cooper, D. S. (2018). Antithyroid drug therapy: 70 years later. *European*

Journal of Endocrinology, 179(5), R261-R274.

Butt, S. S., Badshah, Y., Shabbir, M., & Rafiq, M. (2020). Molecular docking using Chimera and Autodock Vina software for non-bioinformaticians. *Journal of Medical Internet Research Bioinformatics and Biotechnology, 1*(1), 1-25.

Buvaneswari, G., Aswathy, V., & Rajakumari, R. (2015). Comparison of color and optical absorbance properties of divalent ion substituted Cu and Zn aluminate spinel oxides synthesized by combustion method towards pigment application. *Dyes and Pigments, 123*, 413–419.

Caballero, J. (2021). The latest automated docking technologies for novel drug discovery. *Expert Opinion On Drug Discovery, 16*(6), 625-645.

Calderón-Ospina, C. A., & Nava-Mesa, M. O. (2020). B Vitamins in the nervous system: Current knowledge of the biochemical modes of action and synergies of thiamine, pyridoxine, and cobalamin. *CNS Neuroscience & Therapeutics, 26*(1), 5-13.

Carcelli, M., Tegoni, M., Bartoli, J., Marzano, C., Pelosi, G., Salvalaio, M., Rogolino, D., & Gandin, V. (2020). In vitro and in vivo anticancer activity of tridentate thiosemicarbazone copper complexes: Unravelling an unexplored pharmacological target. *European Journal of Medicinal Chemistry, 194*, 1-48.

Carter, R. L. (1997). *Molecular symmetry and group theory*. John Wiley & Sons.

Chábera, P., Lindh, L., Rosemann, N. W., Prakash, O., Uhlig, J., Yartsev, A., ... & Persson, P. (2021). Photofunctionality of iron (III) N-heterocyclic carbenes and related d5 transition metal complexes. *Coordination Chemistry Reviews, 426*, 1-21.

Chalmers, G. (2022). Introducing ligand GA, a genetic algorithm molecular tool for automated protein inhibitor design. *Scientific Reports, 12*(1), 1-20.

Chan, H. C. S., Shan, H., Dahoun, T., Vogel, H., & Yuan, S. (2019). Advancing drug discovery

via artificial intelligence. *Trends in Pharmacological Sciences, 40*(8), 592–604.

Chowdhury, N., Suhani, S., Purkaystha, A., Begum, M. K., Raihan, T., Alam, Md. J., Islam, K., & Azad, A. K. (2019). Identification of AcrAB-TolC efflux pump genes and detection of mutation in efflux repressor *AcrR* from omeprazole responsive multidrug-resistant *Escherichia coli* isolates causing urinary tract infections. *Microbiology Insights, 12*, 1-10.

Cirri, D., Bartoli, F., Pratesi, A., Baglini, E., Barresi, E., & Marzo, T. (2021). Strategies for the improvement of metal-based chemotherapeutic treatments. *Biomedicines, 9*(5), 1-20.

Coimbra, J. T. S., Feghali, R., Ribeiro, R. P., Ramos, M. J., & Fernandes, P. A. (2020). The importance of intramolecular hydrogen bonds on the translocation of the small drug piracetam through a lipid bilayer. *Royal Society of Chemistry Advances, 11*(2), 899–908.

Clinical and Laboratory Standard (2020). Performance standards for antimicrobial susceptibility testing. Clinical and Laboratory Standards Institute, Pennsylvania.

Cojocariu, S. A., Maștaleru, A., Sascău, R. A., Stătescu, C., Mitu, F., & Leon-Constantin, M. M. (2021). Neuropsychiatric consequences of lipophilic beta-blockers. *Medicina, 57*(2), 1-13.

Costales, M. G., Childs-Disney, J. L., Haniff, H. S., & Disney, M. D. (2020). How we think about targeting RNA with small molecules. *Journal of Medicinal Chemistry, 63*(17), 8880-8900.

Cournia, Z., Allen, B., & Sherman, W. (2017). Relative binding free energy calculations in drug discovery: recent advances and practical considerations. *Journal Of Chemical Information And Modeling, 57*(12), 2911-2937.

Cunha, B. N., Colina-Vegas, L., Plutín, A. M., Silveira, R. G., Honorato, J., Oliveira, K. M., Cominetti, M. R., Ferreira, A. G., Castellano, E. E., & Batista, A. A. (2018). Hydrolysis

reaction promotes changes in coordination mode of Ru(II)/acylthiourea organometallic complexes with cytotoxicity against human lung tumor cell lines. *Journal of Inorganic Biochemistry*, *186*, 147–156.

Czyrski, A. (2022). The spectrophotometric determination of lipophilicity and dissociation constants of ciprofloxacin and levofloxacin. *Spectrochimica Acta Part A: Molecular and Biomolecular Spectroscopy, 265*, 1-6.

Daina, A., Michielin, O., & Zoete, V. (2017). SwissADME: A free web tool to evaluate pharmacokinetics, drug-likeness and medicinal chemistry friendliness of small molecules. *Scientific Reports, 7*, 1-13.

Damena, T., Zeleke, D., Desalegn, T., Demissie, T. B., & Eswaramoorthy, R. (2022). Synthesis, characterization, and biological activities of novel vanadium(IV) and cobalt(II) complexes. *American Chemical Society Omega*, *7*(5), 4389–4404.

Dantas, K. C. F., Rosário, J. D. S., & Silva-Caldeira, P. P. (2022). Polymeric nanosystems applied for metal-based drugs and photosensitizers delivery: the state of the art and recent advancements. *Pharmaceutics*, *14*(7), 1-63.

Das, T., Nath, C., Das, P., Ghosh, K., Logno, T. A., Debnath, P., Dash, S., Devnath, H. S., Das, S., & Islam, M. Z. (2023). High prevalence of Ciprofloxacin resistance in *Escherichia coli* isolated from chickens, humans and the environment: An emerging one health issue. *Public Library of Science ONE, 18*(11), 1-16.

Dasari, S., & Tchounwou, P. B. (2014). Cisplatin in cancer therapy: molecular mechanisms of action. *European Journal Of Pharmacology, 740*, 364-378.

Dent, S. (2006). Purity and Identification of Solids Using Melting Points. [online] Available at: https://web.pdx.edu/~wamserc/Labs/StewDentReport.pdf [Assessed on 9 September 2025]

Derafa, W., Elkanzi, N. A., Ali, A. M., & Abdou, A. (2024). Three Co (II), Ni (II) and Cu (II) Schiff base complexes incorporating 2-[(4-{[(4-methylphenyl) sulfonothioyl] oxy} phenyl) methylene] amino} benzoic acid: Synthesis, structural, DFT, biological and molecular docking investigation. *Bulletin of the Chemical Society of Ethiopia*, *38*(2), 325-346.

De Smet, J., Wagemans, J., Boon, M., Ceyssens, P. J., Voet, M., Noben, J. P., Andreeva, J., Ghilarov, D., Severinov, K., & Lavigne, R. (2021). The bacteriophage LUZ24 "Igy" peptide inhibits the *Pseudomonas* DNA gyrase. *Cell Reports*, *36*(8), 1-8.

De Oliveira, M. R. C., de Lima Silva, M. G., de Morais Oliveira-Tintino, C. D., Tintino, S. R., Rocha, J. E., Magalhães, F. E. A., da Costa, R.H.S., Pessoa, R.T., Alcântara, I.S., Martins, A.O.B.P.B, Coutinho, H.D.M, Raposo, A., Carrascosa, C., Jaber, J.D., Saraiva, R.A. & de Menezes, I. R. A. (2023). Antibacterial effect, efflux pump inhibitory (NorA, TetK and MepA) of *Staphylococcus aureus* and *in silico* prediction of α, β and δ-damascone compounds. *Arabian Journal of Chemistry*, *16*(2), 1-15.

Deben, C., Boullosa, L. F., Fortes, F. R., De La Hoz, E. C., Le Compte, M., Seghers, S., Peeters, M., Vanlanduit, S., Lin, A., Dijkstra, K. K., Van Schil, P., Hendriks, J. M. H., Prenen, H., Roeyen, G., Lardon, F., & Smits, E. (2024). Auranofin repurposing for lung and pancreatic cancer: low CA12 expression as a marker of sensitivity in patient-derived organoids, with potentiated efficacy by AKT inhibition. *Journal of Experimental and Clinical Cancer Research*, *43*(1), 1-12.

Denamur, E., Clermont, O., Bonacorsi, S., & Gordon, D. (2021). The population genetics of pathogenic *Escherichia coli*. *Nature Reviews Microbiology*, *19*(1), 37-54.

Dey, P. (2021). Low bioavailability hinders drug discovery against COVID-19, guided by in silico docking. *British Journal of Pharmacology*, *178*(3), 741-742.

Dias, D. A., Jones, O. A., Beale, D. J., Boughton, B. A., Benheim, D., Kouremenos, K. A., Wolfender, J.L & Wishart, D. S. (2016). Current and future perspectives on the structural identification of small molecules in biological systems. *Metabolites*, *6*(4), 1-29.

Díaz, M., de Lucio, H., Moreno, E., Espuelas, S., Aydillo, C., Jiménez-Ruiz, A., Toro, M.A., Gutiérrez, K.J., Martínez-Merino, V., Cornejo, A., Palop, J.A., Sanmartín, C. & Plano, D. (2019). Synthesis and leishmanicidal activity of novel urea, thiourea, and selenourea derivatives of diselenides. *Antimicrobial Agents and Chemotherapy*, *63*(5), 1-16.

DiMasi, J. A. (2020). research and development costs of new drugs. *Journal of the American Medical Association*, *324*(5), 517.

Doak, B. C., Over, B., Giordanetto, F., & Kihlberg, J. (2014). Oral druggable space beyond the Rule of 5: insights from drugs and clinical candidates. *Chemistry & Biology*, *21*(9), 1115-1142.

Dorahy, G., Chen, J. Z., & Balle, T. (2023). Computer-aided drug design towards new psychotropic and neurological drugs. *Molecules*, *28*(3), 1-22.

Drzewiecka-Antonik, A., Rejmak, P., Klepka, M., Wolska, A., Chrzanowska, A., & Struga, M. (2020). Structure and anticancer activity of Cu(II) complexes with (bromophenyl)thiourea moiety attached to the polycyclic imide. *Journal of Inorganic Biochemistry*, *212*, 1-14.

Dutescu, I. A., & Hillie, S. A. (2021). Encouraging the development of new antibiotics: Are financial incentives the right way forward? A systematic review and case study. *Infection and Drug Resistance*, *14*, 415–434.

Eberhardt, J., Santos-Martins, D., Tillack, A. F., & Forli, S. (2021). AutoDock Vina 1.2.0: New docking methods, expanded force field, and python bindings. *Journal of Chemical Information and Modeling*, *61*(8), 3891–3898.

Ellithy, S. A., Abdel-Rahman, A. A. H., Hassan, N. A., Elsawalhy, M., Abou-Amra, E. S., & Hassan, A. A. (2023). Glycosyl thiourea: Synthesis, cyclization, reaction, molecular docking, and evaluation as potential acetylcholinesterase inhibitors. *Egyptian Journal of Chemistry, 66*(13), 1759–1777.

El-Zahed, M. M., Diab, M. A., El-Sonbati, A. Z., Saad, M. H., Eldesoky, A. M., & El-Bindary, M. A. (2024). Synthesis, spectroscopic characterization studies of chelating complexes and their applications as antimicrobial agents, DNA binding, molecular docking, and electrochemical studies. *Applied Organometallic Chemistry, 38*(1), 1-31.

Fakhar, I., Hussien, N. J., Sapari, S., Bloh, A. H., Yusoff, S. F. M., Hasbullah, S. A., Yamin, B. M., Mutalib, S. A., Shihab, M. S., & Yousif, E. (2018). Synthesis, X-Ray diffraction, theoretical and anti-bacterial studies of bis-thiourea secondary amine. *Journal of Molecular Structure, 1159,* 96–102.

FakhriRavari, A., Simiyu, B., Morrisette, T., Dayo, Y., & Abdul-Mutakabbir, J. C. (2022). Infectious disease: how to manage gram-positive and gram-negative pathogen conundrums with dual beta-lactam therapy. *Drugs in Context, 11,* 1-18.

Favre, H. A., & Powell, W. H. (2013). *Nomenclature of organic chemistry: IUPAC recommendations and preferred names 2013*. Royal Society of Chemistry.

FDA (2023). FDA approves enzalutamide for non-metastatic castration-sensitive prostate cancer with biochemical recurrence. [online] Available at https://www.fda.gov/drugs/resources-information-approved-drugs/fda-approves-enzalutamide-non-metastatic-castration-sensitive-prostate-cancer-biochemical-recurrence [Assessed on 12 January 2025]

Feng, M., Tang, B., H Liang, S., & Jiang, X. (2016). Sulfur containing scaffolds in drugs: synthesis and application in medicinal chemistry. *Current Topics in Medicinal*

Chemistry, *16*(11), 1200-1216.

Ferreira, R. J., dos Santos, D. J., & Ferreira, M. J. U. (2015). P-glycoprotein and membrane roles in multidrug resistance. *Future medicinal chemistry*, *7*(7), 929-946.

Finch, A., & Pillans, P. (2014). P-glycoprotein and its role in drug-drug interactions. *Australian Prescriber*, *37*(4), 137-139.

Firdausiah, S., Hasbullah, S. A., & Yamin, B. M. (2020). Synthesis and x-ray crystallographic study of N,N'-bis(2-, 3-, and 4-methoxybenzamidothiocarbonyl) hydrazines. *International Journal of Current Research and Review*, *12*(24), 204–210.

Frei, A., Zuegg, J., Elliott, A. G., Baker, M., Braese, S., Brown, C., Chen, F., G. Dowson, C., Dujardin, G., Jung, N., King, A. P., Mansour, A. M., Massi, M., Moat, J., Mohamed, H. A., Renfrew, A. K., Rutledge, P. J., Sadler, P. J., Todd, M. H., Willans, C.E., Wilson, J.J., Cooper, M.A. & Blaskovich, M. A. T. (2020). Metal complexes as a promising source for new antibiotics. *Chemical Science*, *11*(10), 2627–2639.

Gaillard, T. (2018). Evaluation of AutoDock and AutoDock Vina on the CASF-2013 Benchmark. *Journal of Chemical Information and Modeling*, *58*(8), 1697–1706.

Gajdács, M. (2019). The concept of an ideal antibiotic: implications for drug design. *Molecules*, *24*(5), 1-16.

Gellert, M., Mizuuchi, K., O'Dea, M. H., & Nash, H. A. (1976). DNA gyrase: an enzyme that introduces superhelical turns into DNA. *Proceedings of the National Academy of Sciences*, *73*(11), 3872-3876.

Ghazal, K., Shoaib, S., Khan, M., Khan, S., Rauf, M. K., Khan, N., Badshah, A., Tahir, M. N., Ali, I., & Rehman, A. ur. (2019). Synthesis, characterization, X-ray diffraction study, in-vitro cytotoxicity, antibacterial and antifungal activities of nickel(II) and copper(II) complexes with acyl thiourea ligand. *Journal of Molecular Structure*, *1177*, 124–130.

Ghazy, O. A., El-Hadedy, D. E., Saleh, H. H., & Bekhit, M. (2021). Antimicrobial activity and cytotoxicity of radiation synthesized cu nanoparticles compared with antibiotics. *BioNanoScience*, *11*(3), 878–883.

Ghorab, M. M., Alsaid, M. S., El-Gaby, M. S. A., Elaasser, M. M., & Nissan, Y. M. (2017). Antimicrobial and anticancer activity of some novel fluorinated thiourea derivatives carrying sulfonamide moieties: Synthesis, biological evaluation and molecular docking. *Chemistry Central Journal*, *11*(1), 1-14.

Ghosh, A. K., & Brindisi, M. (2020). Urea derivatives in modern drug discovery and medicinal chemistry. *Journal of Medicinal Chemistry*, *63*(6), 2751–2788.

González, D. L. N., Saeed, A., Shabir, G., Flörke, U., & Erben, M. F. (2020). Conformational and crystal structure of acyl thiourea compounds: The case of the simple (2, 2-dimethyl-propionyl) thiourea derivative. *Journal of Molecular Structure*, *1215*, 1-8.

Gopichand, K., Mahipal, V., Rao, N. N., Ganai, A. M., & Rao, P. V. (2023). Co (II), Ni (II), Cu (II), and Zn (II) complexes with benzothiazole schiff base ligand: preparation, spectral characterization, DNA binding, and in vitro cytotoxic activities. *Results in Chemistry*, *5*, 1-10.

Haddad, N., Carr, M., Balian, S., Lannin, J., Kim, Y., Toth, C., & Jarvis, J. (2022). The blood–brain barrier and pharmacokinetic/pharmacodynamic optimization of antibiotics for the treatment of central nervous system infections in adults. *Antibiotics*, *11*(12), 1-37.

Haley, E., Luke, N., Mathur, M., Festa, R., Wang, J., Jiang, Y., Anderson, L., & Baunoch, D. (2024). The prevalence and association of different uropathogens detected by M-PCR with infection-associated urine biomarkers in urinary tract infections. *Research and Reports in Urology*, *16*, 19–29.

Hashem, H. E., Amr, A. E. G. E., Nossier, E. S., Elsayed, E. A., & Azmy, E. M. (2020).

Synthesis, antimicrobial activity and molecular docking of novel thiourea derivatives tagged with thiadiazole, imidazole and triazine moieties as potential DNA gyrase and topoisomerase IV inhibitors. *Molecules*, *25*(12), 1-18.

Hassan, G. S., Abou-Seri, S. M., Kamel, G., & Ali, M. M. (2014). Celecoxib analogs bearing benzofuran moiety as cyclooxygenase-2 inhibitors: design, synthesis and evaluation as potential anti-inflammatory agents. *European journal of medicinal chemistry*, *76*, 482-493.

Hassan Ali M, E. Z. I. W. K. M. (2020). Synthesis, characterization, biological and antitumor activity of Co(II) , Ni (II) , Cu(II) and Zn (II) complexes of N-(2-chlorophenyl)-N'-benzoyl thiourea. *Organic & Medicinal Chemistry International Journal, 9*(4), 112-124.

Hassuna, N. A., Rabea, E. M., Mahdi, W. K. M., & Abdelraheem, W. M. (2024). Biofilm formation and antimicrobial resistance pattern of uropathogenic *E. coli* ST131 isolated from children with malignant tumors. *Journal of Antibiotics*, *77*(5), 324–330.

Henderson, J. C., Zimmerman, S. M., Crofts, A. A., Boll, J. M., Kuhns, L. G., Herrera, C. M., & Trent, M. S. (2016). The power of asymmetry: architecture and assembly of the gram-negative outer membrane lipid bilayer. *Annual Review of Microbiology*, *70*(1), 255-278.

Herbst, C., Endres, S., Würz, R., & Sotriffer, C. (2024). Assessment of fragment docking and scoring with the endothiapepsin model system. *Archiv Der Pharmazie-Chemistry in Life Sciences, 357*(6), 1-15.

Hernández, J. G., Aguilar, C. A. H., Narayanan, J., Flores, E. D. T., Thangarasu, P., Ramírez, A. H., Shanmugam, K. & Martinez, M. M. L. (2024). Effect of metal ions in the electron-transfer mechanism on the photovoltaic performance of SALPHEN-based DSSC: experimental and theoretical studies. *Materials Advances, 5*(8), 3257-3280

Hou, Y., Zhu, S., Chen, Y., Yu, M., Liu, Y., & Li, M. (2023). Evaluation of antibacterial

activity of thiourea derivative td4 against methicillin-resistant *Staphylococcus aureus* via destroying the NAD+/NADH homeostasis. *Molecules*, *28*(7), 1-13.

Hudzicki, J. (2009). Kirby-Bauer disk diffusion susceptibility test protocol. *American Society For Microbiology, 15*(1), 1-23.

Hung, C. L., Kuo, Y. H., Lee, S. W., & Chiang, Y. W. (2021). Protein stability depends critically on the surface hydrogen-bonding network: A case study of bid protein. *Journal of Physical Chemistry B, 125*(30), 8373–8382.

Hussain, A., AlAjmi, M. F., Rehman, M. T., Amir, S., Husain, F. M., Alsalme, A., Siddiqui, M. A., AlKhedhairy, A. A., & Khan, R. A. (2019). Copper(II) complexes as potential anticancer and nonsteroidal anti-inflammatory agents: In vitro and in vivo studies. *Scientific Reports, 9*(1), 1-17.

Hussain, Z., Iqbal, J., Mumtaz, A., Mahmood, A., Shah, Q., Imran, A., Mughal, E. U., Khan, W., & Baig, A. (2022). Synthesis and evaluation of amide and thiourea derivatives as carbonic anhydrase (ca) inhibitors. *American Chemical Society Omega, 7*(50), 47251–47264.

Hussein, R. R. S., Rabie, A. S. I., Shaman, M. Bin, Shaaban, A. H., Fahmy, A. M., Sofy, M. R., Lattyak, E. A., Abuelhana, A., Naguib, I. A., Ashour, A. M., & Aldeyab, M. A. (2022). Antibiotic consumption in hospitals during COVID-19 pandemic: a comparative study. *Journal of Infection in Developing Countries, 16*(11), 1679–1686.

Hutchings, M. I., Truman, A. W., & Wilkinson, B. (2019). Antibiotics: past, present and future. *Current Opinion in Microbiology, 51*, 72-80.

Ibrahim, M. A., Husin, A., Ngah, N., & Zakaria, N. H. (2021). Antibacterial activity of benzoyl and halobenzoyl thiourea bearing α- and β-alanine. *Journal CleanWAS, 5*(1), 35–38.

Idrees, M., Mohammad, A. R., Karodia, N., & Rahman, A. (2020). Multimodal role of amino

acids in microbial control and drug development. *Antibiotics*, *9*(6), 1-33.

Institute for Medical Research (2024). National Antibiotic Resistance Surveillance Report 2024. Institute for Medical Research, Malaysia.

Institute for Health Metrics and Evaluation (n.d.). The burden of antimicrobial resistance (AMR) in Malaysia. Institute for Health Metrics and Evaluation, Seattle.

Ivanova, L., & Karelson, M. (2022). The impact of software used and the type of target protein on molecular docking accuracy. *Molecules*, *27*(24), 1-20.

Juvale, I. I. A., Hamid, A. A. A., Abd Halim, K. B., & Has, A. T. C. (2022). P-glycoprotein: New insights into structure, physiological function, regulation and alterations in disease. *Heliyon*, *8*(6), 1-12.

Kaczmarek, M. E., Wełniak, A., & Czajkowski, R. (2023). The role of zinc in skin physiology–relevance for the pathogenesis and treatment of vitiligo. *Dermatology Review/Przegląd Dermatologiczny*, *110*(2), 142-150.

Kadir, M. A., Ramli, R., Yusof, M. S. M., Ismail, N., & Ngah, N. (2016). Synthesis, spectroscopic studies and antibacterial activity of new lauroyl thiourea amino acid derivatives. *Asian J. Chem*, *28*, 596-600

Kadry, H., Noorani, B., & Cucullo, L. (2020). A blood–brain barrier overview on structure, function, impairment, and biomarkers of integrity. *Fluids and Barriers of the CNS*, *17*, 1-24.

Kale, M., Rathod, D. V, & Deshmukh, S. B. (2021). The Colours of Complexes. *Cosmos Multidisciplinary Research E-Journal*, *VI*(II), 242-247.

Kamalov, S., Babaev, B., Ibragimov, A., Eshimbetov, A., Ashurov, J., Normamatov, A., Tilyakov, Z., Usmanov, S., Tashpulatov, J. & Ibragimov, B. (2024). Antimicrobial activity enhancement and acute toxicity lowering of benzamide through preparation of

metal complexes. *Journal of Molecular Structure*, *1303*, 1-14

Karthik, A., Shakila, D., Geetha, K., & Muthuvel, I. (2020). Green approach to synthesize, spectral investigation and biological applications of potentially active ternary schiff base copper(II) complexes. *Materials Today: Proceedings, 43,* 2389–2396.

Kennedy, D. O. (2016). B vitamins and the brain: mechanisms, dose and efficacy—A review. *Nutrients*, *8*(2), 1-29.

Kenny, P. W. (2022). Hydrogen-bond donors in drug design. *Journal of Medicinal Chemistry*, *65*(21), 14261-14275.

Khairul, W. M., Zuki, H. M., Hasan, M. F. A., & Daud, A. I. (2016a). Pyridine acyl thiourea as ionophore for the detection of copper(II) in aqueous phase. *Procedia Chemistry*, *20*, 105–114.

Khairul, W. M., Ariffin, A. A., Ismail, N., & Daud, A. I. (2016b). Synthesis, spectroscopic studies, and biological activities of acylthiourea derivatives as potential anti-bacteria agents. *EDUCATUM Journal of Science, Mathematics and Technology*, *3*(1), 13-19.

Khalid, A., Arshad, N., Channar, P. A., Saeed, A., Mir, M. I., Abbas, Q., Ejaz, S. A., Hökelek, T., Saeed, A., & Tehzeeb, A. (2022). Structure and surface analyses of a newly synthesized acyl thiourea derivative along with its in silico and in vitro investigations for RNR, DNA binding, urease inhibition and radical scavenging activities. *Royal Society of Chemistry Advances*, *12*(27), 17194–17207.

Khan, A., Khan, M. S., Iqbal, A., Tahir, M. H., Rizvi, M. B., & Murtaza, M. A. (2023). Compare the effectiveness of carbimazole single dose and divided dose regimens for euthyroid induction in hyperthyroid patients. *Pakistan Journal of Medical and Health Sciences*, *17*(2), 439–441.

Khan, M. R., Zaib, S., Rauf, M. K., Ebihara, M., Badshah, A., Zahid, M., Nadeem, M. A., &

Iqbal, J. (2018). Solution-phase microwave assisted parallel synthesis, biological evaluation and in silico docking studies of 2-chlorobenzoyl thioureas derivatives. *Journal of Molecular Structure*, *1164*, 354–362.

Khan, U. A., Badshah, A., Tahir, M. N., & Khan, E. (2020). Gold(I), silver(I) and copper(I) complexes of 2,4,6-trimethylphenyl-3-benzoylthiourea; synthesis and biological applications. *Polyhedron*, *181*, 1-11.

Khater, M., Ravishankar, D., Greco, F., & Osborn, H. M. (2019). Metal complexes of flavonoids: Their synthesis, characterization and enhanced antioxidant and anticancer activities. *Future Medicinal Chemistry*, *11*(21), 2845-2867.

Khosravi, F., & Mansouri-Torshizi, H. (2018). Antibacterial combination therapy using Co3+, Cu2+, Zn2+ and Pd2+ complexes: Their calf thymus DNA binding studies. *Journal of Biomolecular Structure and Dynamics*, *36*(2), 512–531.

King, R. P., Cairns, K. R., Denman, C., Levason, W., Light, M. E., & Reid, G. (2024). Structural Diversity of Sn (II) Phosphine Oxide Complexes with Weakly Coordinating Anions and Comparisons with Related Ge (II) and Pb (II) Species. *European Journal of Inorganic Chemistry*, *27*(23), 1-11.

Kirishnamaline, G., Magdaline, J. D., Chithambarathanu, T., Aruldhas, D., & Anuf, A. R. (2021). Theoretical investigation of structure, anticancer activity and molecular docking of thiourea derivatives. *Journal of Molecular Structure*, *1225*, 1-24.

Klein, E. Y., Van Boeckel, T. P., Martinez, E. M., Pant, S., Gandra, S., Levin, S. A., Goossens, H., & Laxminarayan, R. (2018). Global increase and geographic convergence in antibiotic consumption between 2000 and 2015. *Proceedings of the National Academy of Sciences of the United States of America*, *115*(15), E3463–E3470.

Kumar, A., & Zhang, K. Y. J. (2013). Investigation on the effect of key water molecules on

docking performance in CSARdock exercise. *Journal of Chemical Information and Modeling*, *53*(8), 1880–1892.

Kumar, B., Devi, J., Dubey, A., & Kumar, M. (2024). Exploration of newly synthesized transition metal (II) complexes for infectious diseases. *Future Medicinal Chemistry*, *16*(20), 2087-2105.

Kumar, M., Kumar, G., Dadure, K. M., & Masram, D. T. (2019). Copper(II) complexes based on levofloxacin and 2N-donor ligands: Synthesis, crystal structures and: In vitro biological evaluation. *New Journal of Chemistry*, *43*(38), 15462–15481.

Kumar, N. R., Balraj, T. A., Kempegowda, S. N., & Prashant, A. (2024). Multidrug-resistant sepsis: A critical healthcare challenge. *Antibiotics*, *13*(1), 1-38.

Kumar, P., Kaur, J., Kumari, S., Paliwal, S., Berry, S., Pinnaka, A. K., & Bhalla, A. (2023). Aroyl-isothiocyanates/isoselenocyanates as precursors to obtain novel cis-3-aroyl-thiourea/urea-β-lactams: design, synthesis, docking and biological evaluation. *New Journal of Chemistry*, *48*(1), 67–78.

Kuo, C. J., Ke, J. N., Kuo, T., Lin, C. Y., Hsieh, S. Y., Chiu, Y. F., Wu, H. Y., Huang, M. Z., Bui, N. N., Chiu, C. H., Chiu, C. T., & Lai, C. H. (2023). Multiple amino acid substitutions in penicillin-binding protein-1A confer amoxicillin resistance in refractory *Helicobacter pylori* infection. *Journal of Microbiology, Immunology and Infection*, *56*(1), 40–47.

LaBute, M. X., Zhang, X., Lenderman, J., Bennion, B. J., Wong, S. E., & Lightstone, F. C. (2014). Adverse drug reaction prediction using scores produced by large-scale drug-protein target docking on high-performance computing machines. *PloS one*, *9*(9), 1-13.

Lalhmangaihzuala, S., Laldinpuii, Z., Lalthanpuii, P. B., Pachuau, Z., Vanlaldinpuia, K., & Lalchhandama, K. (2024). Screening of novel carbohydrate-derived thioureas for

antibacterial activity. *Journal of Applied Pharmaceutical Science, 14*(8), 094-102.

Lalosevic, J., Gajic-Veljic, M., Lalosevic Misovic, J., & Nikolic, M. (2023). Serum zinc concentration in patients with alopecia areata. *Acta Dermato-Venereologica, 103*, 1-4.

Lateef, H. M., Ali, A. M., Khalaf, M. M., & Abdou, A. (2024). New Iron(III), Cobalt(II), Nickel(II), Copper(II), Zinc(II) mixed-ligand complexes: Synthesis, structural, DFT, molecular docking and antimicrobial analysis. *Bulletin of the Chemical Society of Ethiopia*, *38*(1), 147–166.

Lee, S. Y., Modzelewski, K. L., Law, A. C., Walkey, A. J., Pearce, E. N., & Bosch, N. A. (2023). Comparison of propylthiouracil vs methimazole for thyroid storm in critically ill patients. *Journal of American Medical Association Network Open*, *6*(4), 1-10.

Li, F., Weir, M. D., & Xu, H. H. K. (2013). Effects of quaternary ammonium chain length on antibacterial bonding agents. *Journal of Dental Research, 92*(10), 932-938.

Li, J. H., Wang, Y., Wu, Y. P., Li, R. H., Liang, S., Zhang, J., Zhu, Y. G., & Xie, B.J. (2021). Synthesis, herbicidal activity study and molecular docking of novel pyrimidine thiourea. *Pesticide Biochemistry and Physiology*, *172*, 1-8.

Li, S., Smith, K. D., Davis, J. H., Gordon, P. B., Breaker, R. R., & Strobel, S. A. (2013). Eukaryotic resistance to fluoride toxicity mediated by a widespread family of fluoride export proteins. *Proceedings of the National Academy of Sciences of the United States of America*, *110*(47), 19018–19023.

Limban, C., Missir, A. V., Caproiu, M. T., Grumezescu, A. M., Chifiriuc, M. C., Bleotu, C., Marutescu, L., Papacocea, M. T., & Nuta, D. C. (2018). Novel hybrid formulations based on thiourea derivatives and core@shell Fe3O4@C18 nanostructures for the development of antifungal strategies. *Nanomaterials*, *8*(1), 1-14.

Lipinski, C. A. (2004). Lead-and drug-like compounds: the rule-of-five revolution. *Drug*

discovery today: Technologies, *1*(4), 337-341.

Liu, Y., Li, Q., Xu, Y., Chen, Y., & Men, Y. (2023). Comparison of the safety between propylthiouracil and methimazole with hyperthyroidism in pregnancy: A systematic review and meta-analysis. *Public Library of Science ONE*, *18*(5), 1-13.

Lobo, S. (2020). Is there enough focus on lipophilicity in drug discovery? *Expert Opinion on Drug Discovery*, *15*(3), 261-263.

Luo, Y., Fu, Y., Huang, Z., & Li, M. (2021). Transition metals and metal complexes in autophagy and diseases. *Journal of Cellular Physiology*, *236*(10), 7144-7158.

Luzhkov, V. B. (2017). Molecular modelling and free-energy calculations of protein–ligand binding. *Russian Chemical Reviews, 86*(3), 211–230.

M Honório, K., L Moda, T., & D Andricopulo, A. (2013). Pharmacokinetic properties and in silico ADME modeling in drug discovery. *Medicinal Chemistry*, *9*(2), 163-176.

Maalik, A., Rahim, H., Saleem, M., Fatima, N., Rauf, A., Wadood, A., Malik, M. I., Ahmed, A., Rafique, H., Zafar, M. N., Riaz, M., Rasheed, L., & Mumtaz, A. (2019). Synthesis, antimicrobial, antioxidant, cytotoxic, antiurease and molecular docking studies of N-(3-trifluoromethyl)benzoyl-N′-aryl thiourea derivatives. *Bioorganic Chemistry*, *88*, 1-9.

Makeen, H. A., & Albratty, M. (2023). 2D-QSAR, Molecular Docking, and in silico Pharmacokinetics Analysis on N-substituted Urea and Thiourea Derivatives as Tankyrase Inhibitors for Implication in Cancer. *Indian Journal of Pharmaceutical Education and Research, 57*(3), 838–853.

Malis, G., Geromichalou, E., Geromichalos, G. D., Hatzidimitriou, A. G., & Psomas, G. (2021). Copper(II) complexes with non–steroidal anti–inflammatory drugs: Structural characterization, in vitro and in silico biological profile. *Journal of Inorganic Biochemistry*, *224*, 1-14.

Malpani, S.G., Chandrawanshi, M. J., Dharashive,V. M., Kore, S.S. & Shinde, N. N. (2020). Molecular docking: A novel appliance for structure based drug discovery. *International Journal of Pharmacy and Pharmaceutical Research, 19*(1), 285-299.

Mariani, D., Ghasemishahrestani, Z., Freitas, W., Pezzuto, P., Costa-da-Silva, A. C., Tanuri, A., Kanashiro, M. M., Fernandes, C., Horn, A., & Pereira, M. D. (2021). Antitumoral synergism between a copper(II) complex and cisplatin improves *in vitro* and *in vivo* anticancer activity against melanoma, lung and breast cancer cells. *Biochimica et Biophysica Acta - General Subjects, 1865*(10), 1-13.

Martinez, V. R., Martins Lima, A., Stergiopulos, N., Velez Rueda, J. O., Islas, M. S., Griera, M., Calleros, L., Rodriguez Puyol, M., Jaquenod de Giusti, C., Portiansky, E. L., Ferrer, E. G., De Giusti, V., & Williams, P. A. M. (2023). Effect of the structural modification of candesartan with zinc on hypertension and left ventricular hypertrophy. *European Journal of Pharmacology*, *946*, 1-47.

Mayito, J., Dhikusooka, F., Kibombo, D., Busuge, A., Andema, A., Yayi, A., ... & Kakooza, F. (2024). Antibiotic resistance related mortality, length of hospital stay, and disability-adjusted life years at select tertiary hospitals in Uganda: A retrospective study. *medRxiv*, 1-19.

McDevitt, C. A., Ogunniyi, A. D., Valkov, E., Lawrence, M. C., Kobe, B., McEwan, A. G., & Paton, J. C. (2011). A molecular mechanism for bacterial susceptibility to zinc. *Public Library of Science ONE Pathogens, 7*(11), 1-9.

Meena, A., & Adusumilli, U. K. (2023). Antimicrobial studies of copper (II) sesame urea and thiourea complex against *Staphylococus aureus*. *International Journal of Scientific Research in Science, Engineering and Technology*, 78–88.

Meier-Menches, S. M., Gerner, C., Berger, W., Hartinger, C. G., & Keppler, B. K. (2018).

Structure–activity relationships for ruthenium and osmium anticancer agents–towards clinical development. *Chemical Society Reviews*, *47*(3), 909-928.

Meng, X. Y., Zhang, H. X., Mezei, M., & Cui, M. (2011). Molecular docking: a powerful approach for structure-based drug discovery. *Current Computer-Aided Drug Design*, *7*(2), 146-157.

Micoli, F., Bagnoli, F., Rappuoli, R., & Serruto, D. (2021). The role of vaccines in combatting antimicrobial resistance. *Nature Reviews Microbiology*, *19*(5), 287-302.

Millanao, A. R., Mora, A. Y., Villagra, N. A., Bucarey, S. A., & Hidalgo, A. A. (2021). Biological effects of quinolones: a family of broad-spectrum antimicrobial agents. *Molecules*, *26*(23), 1-42

Mitrea, D. G., & Cîrcu, V. (2021). Synthesis and characterization of novel acylthiourea compounds used in ions recognition and sensing in organic media. *Spectrochimica Acta - Part A: Molecular and Biomolecular Spectroscopy*, *258*, 1-8.

Mjos, K. D., & Orvig, C. (2014). Metallodrugs in medicinal inorganic chemistry. *Chemical Reviews*, *114*(8), 4540-4563.

Mohamed, N. A., Abd El-Ghany, N. A., & Abdel-Aziz, M. M. (2021). Synthesis, characterization, anti-inflammatory and anti-*Helicobacter pylori* activities of novel benzophenone tetracarboxylimide benzoyl thiourea cross-linked chitosan hydrogels. *International Journal of Biological Macromolecules*, *181*, 956–965.

Mohammed, H. A., Mohammed, P. A., & Aziz, S. B. (2025). Investigation of optical band gap in PEO-based polymer composites doped with green-synthesized metal complexes using various models. *RSC advances*, *15*(29), 23319-23341.

Mohanty, M., & Mohanty, P. S. (2023). Molecular docking in organic, inorganic, and hybrid systems: a tutorial review. *Monatshefte für Chemie-Chemical Monthly*, *154*(7), 683-707.

Mohapatra, R. K., Das, P. K., Pradhan, M. K., El-Ajaily, M. M., Das, D., Salem, H. F., Mahanta, U., Badhei, G., Parhi, P.K., Maihub, A.A. & -E-Zahan, M. K. (2019). Recent advances in urea-and thiourea-based metal complexes: biological, sensor, optical, and corroson inhibition studies. *Comments on Inorganic Chemistry*, *39*(3), 127-187.

Monisha, B.A., Sugantha Bharathy, L., Premkumar, K., & Sathiyamurthy, K. (2022). Antibiotic resistance and biofilm development of *Escherichia coli* on different surfaces. *Journal of Pure and Applied Microbiology*, *16*(3), 1884–1892.

Morais, C., Costa, S. S., Leal, M., Ramos, B., Andrade, M., Ferreira, C., Abrantes, P., Pomba, C., & Couto, I. (2023). Genetic diversity and antimicrobial resistance profiles of *Staphylococcus pseudintermedius* associated with skin and soft-tissue infections in companion animals in Lisbon, Portugal. *Frontiers in Microbiology*, *14*, 1-15.

Munita, J. M., & Arias, C. A. (2016). Mechanisms of antibiotic resistance. *Microbiology Spectrum*, *4*(2), 1-24.

Murray, C. J., Ikuta, K. S., Sharara, F., Swetschinski, L., Robles Aguilar, G., Gray, A., Han, C., Bisignano, C., Rao, P., Wool, E., Johnson, S. C., Browne, A. J., Chipeta, M. G., Fell, F., Hackett, S., Haines-Woodhouse, G., Kashef Hamadani, B. H., Kumaran, E. A. P., McManigal, B., … Naghavi, M. (2022). Global burden of bacterial antimicrobial resistance in 2019: A systematic analysis. *The Lancet*, *399*(10325), 629–655.

Nanayakkara, A. K., Boucher, H. W., Fowler, V. G., Jezek, A., Outterson, K., & Greenberg, D. E. (2021). Antibiotic resistance in the patient with cancer: Escalating challenges and paths forward. *CA: A Cancer Journal for Clinicians*, *71*(6), 488–504.

Naureen, B., Miana, G. A., Shahid, K., Asghar, M., Tanveer, S., & Sarwar, A. (2021). Iron (III) and zinc (II) monodentate Schiff base metal complexes: Synthesis, characterisation and biological activities. *Journal of Molecular Structure, 1231*, 1-12.

Naz, S., Zahoor, M., Umar, M. N., Alghamdi, S., Sahibzada, M. U. K., & Ulbari, W. (2020). Synthesis, characterization, and pharmacological evaluation of thiourea derivatives. *Open Chemistry*, *18*(1), 764–777.

Ngaini, Z., Wan Zulkiplee, W. S. H., & Abd Halim, A. N. (2017). One-pot multicomponent synthesis of thiourea derivatives in cyclotriphosphazenes moieties. *Journal of Chemistry*, *2017*, 1-7.

Nguyen, N. T., Nguyen, T. H., Pham, T. N. H., Huy, N. T., Bay, M. Van, Pham, M. Q., Nam, P. C., Vu, V. V., & Ngo, S. T. (2020). Autodock Vina adopts more accurate binding poses but autodock4 forms better binding affinity. *Journal of Chemical Information and Modeling*, *60*(1), 204–211.

Nguyen, T. T. L., Duong, V. A., & Maeng, H. J. (2021). Pharmaceutical formulations with P-glycoprotein inhibitory effect as promising approaches for enhancing oral drug absorption and bioavailability. *Pharmaceutics*, *13*(7), 1-48.

Niazi, S. K., & Mariam, Z. (2023). Computer-aided drug design and drug discovery: A prospective analysis. *Pharmaceuticals*, *17*(1), 1-22.

Nomura, R., Nakaminami, H., Takasao, K., Muramatsu, S., Kato, Y., Wajima, T., & Noguchi, N. (2020). A class A β-lactamase produced by borderline oxacillin-resistant *Staphylococcus aureus* hydrolyses oxacillin. *Journal of Global Antimicrobial Resistance*, *22*, 244–247.

Nordin, N. A., Chai, T. W., Tan, B. L., Choi, C. L., Abd Halim, A. N., Hussain, H., & Ngaini, Z. (2017). Novel synthetic monothiourea aspirin derivatives bearing alkylated amines as potential antimicrobial agents. *Journal of Chemistry*, *2017*(1), 1-7.

Obradović, D., Nikolić, S., Milenković, I., Milenković, M., Jovanović, P., Savić, V., Roller, A., Đorđić Crnogorac, M., Stanojković, T., & Grgurić-Šipka, S. (2020). Synthesis,

characterization, antimicrobial and cytotoxic activity of novel half-sandwich Ru(II) arene complexes with benzoylthiourea derivatives. *Journal of Inorganic Biochemistry*, *210*, 1-9.

Oleiwi, A. Q., Al-Jeilawi, O. H. R., & Dayl, S. A. (2023). Synthesis, characterization of some thiourea derivatives based on 4- methoxybenzoyl chloride as antioxidants and study of molecular docking. *Iraqi Journal of Science*, *64*(1), 1–12.

Omer, R. A., Ahmed, K. M., Othman, K. A., Hamad, W. M., Faraj, R. K., Muhialdin, A. J., & Salih, S. K. (2024). New thiazole derivatives. *Aro-The Scientific Journal of Koya University*, *12*(2), 10-22.

Omotola, M. F., Shaâ, R., Wuana, A., John, O. I., Moodley, V., & Werner, E. V. Z. (2018). Spectroscopic and antibacterial studies of some nitro-substituted N-(benzoylcarbamothioyl) amino acids: the crystal structure of N-(3-nitro-benzoylcarbamothioyl)-glycine. *Journal of Chemical Society of Nigeria*, *43*(2), 119-132.

O'neill, J. I. M. (2014). Antimicrobial resistance: tackling a crisis for the health and wealth of nations. *The Review on Antimicrobial Resistance*, *2014*, 1-16.

Pace, N. J., & Weerapana, E. (2014). Zinc-binding cysteines: diverse functions and structural motifs. *Biomolecules*, *4*(2), 419-434.

Padole, S. S., Asnani, A. J., Chaple, D. R., & Katre, S. G. (2022). A review of approaches in computer-aided drug design in drug discovery. *GSC Biological and Pharmaceutical Sciences*, *19*(2), 075-083.

Pagadala, N. S., Syed, K., & Tuszynski, J. (2017). Software for molecular docking: a review. *Biophysical reviews*, *9*, 91-102.

Pakbin, B., Brück, W. M., Brück, T. B., Allahyari, S., & Ashrafi Tamai, I. (2023). A quantitative prevalence of *Escherichia coli* O157 in different food samples using real-

time qPCR method. *Food Science and Nutrition*, *11*(1), 228–235.

Pal, T. K., Alam, M. A., Paul, S., & Sheikh, M. C. (2019). Spectral, magnetic, thermal, antioxidant and biological studies on new mixed ligand complexes. *Journal of King Saud University-Science*, *31*(4), 445-451.

Pantsar, T., & Poso, A. (2018). Binding affinity via docking: fact and fiction. *Molecules*, *23*(8), 1-11.

Pantaleão, S. Q., Fernandes, P. O., Gonçalves, J. E., Maltarollo, V. G., & Honorio, K. M. (2022). Recent advances in the prediction of pharmacokinetics properties in drug design studies: a review. *ChemMedChem*, *17*(1), 1-13.

Paris, J. A., Salvador Rocchi, A. J., Biagioni, B. T., Cavicchioli, M., Amaral Machado, R. T., Pavan, F. R., Corbi, P. P., Lustri, W. R., Pereira, D. H., & Massabni, A. C. (2021). Chemical, spectroscopic characterization, molecular modeling and antibacterial activity assays of a silver (I) complex with succinic acid. *Ecletica Quimica*, *46*(2), 26–35.

Parmar, D. R., Soni, J. Y., Guduru, R., Rayani, R. H., Kusurkar, R. v., Vala, A. G., Talukdar, S. N., Eissa, I. H., Metwaly, A. M., Khalil, A., Zunjar, V., & Battula, S. (2021). Discovery of new anticancer thiourea-azetidine hybrids: design, synthesis, in vitro antiproliferative, SAR, in silico molecular docking against VEGFR-2, ADMET, toxicity, and DFT studies. *Bioorganic Chemistry*, *115*, 1-20.

Pavan, M., Menin, S., Bassani, D., Sturlese, M., & Moro, S. (2022). Implementing a scoring function based on interaction fingerprint for Autogrow4: Protein Kinase CK1δ as a case study. *Frontiers in Molecular Biosciences*, *9*, 1-17.

Pearson, S., Lu, H., & Stenzel, M. H. (2015). Glycopolymer self-assemblies with gold(I) complexed to the core as a delivery system for auranofin. *Macromolecules*, *48*(4), 1065–1076.

Pelkonen, T., Urtti, S., dos Anjos, E., Cardoso, O., de Gouveia, L., Roine, I., Peltola, H., von Gottberg, A., & Kyaw, M. H. (2020). Aetiology of bacterial meningitis in infants aged <90 days: Prospective surveillance in Luanda, Angola. *International Journal of Infectious Diseases*, *97*, 251–257.

Pesingi, P. V., Singh, B. R., Pesingi, P. K., Bhardwaj, M., Singh, S. V., Kumawat, M., Sinha, D. K., & Gandham, R. K. (2019). MexAB-OprM efflux pump of *Pseudomonas aeruginosa* Offers Resistance to Carvacrol: A herbal antimicrobial agent. *Frontiers in Microbiology*, *10*, 1-7.

Petkar, P. A., & Jagtap, J. R. (2021). A review on antimicrobial potential of sulfonamide scaffold. *International Journal of Pharmaceutical Sciences and Research*, *12*(5), 2535–2547.

Pingaew, R., Prachayasittikul, V., Anuwongcharoen, N., Prachayasittikul, S., Ruchirawat, S., & Prachayasittikul, V. (2018). Synthesis and molecular docking of N,N′-disubstituted thiourea derivatives as novel aromatase inhibitors. *Bioorganic Chemistry*, *79*, 171–178.

Plackett, B. (2020). No money for new drugs. *Nature*, *586*, S50-S52.

Poggio, C., Colombo, M., Arciola, C. R., Greggi, T., Scribante, A., & Dagna, A. (2020). Copper-alloy surfaces and cleaning regimens against the spread of SARS-CoV-2 in dentistry and orthopedics. From fomites to anti-infective nanocoatings. *Materials*, *13*(15), 1-12.

Porchia, M., Pellei, M., Del Bello, F., & Santini, C. (2020). Zinc complexes with nitrogen donor ligands as anticancer agents. *Molecules*, *25*(24), 1-41.

Powaleny, A. (2018). *New report and resources put cancer in context, showing more than 1,100 medicines and vaccines in development.* [online] Available at: https://www.phrma.org/blog/new-report-and-resources-put-cancer-in-context-showing-

more-than-1100-medicines-and-vaccines-in-development [Assessed on 8 September 2025]

Pramilla S, Kuldeep S. Synthesis and evaluation of antioxidant activity (In-vitro) of some N-phthalyl-[{(3-nitro anili-no)-4" aryl substituted}]-1, 3, 4 thiadiazoles. *International Journal of Current Research and Review 2015,7*(14),1-6.

Prieto-Martínez, F. D., Arciniega, M., & Medina-Franco, J. L. (2018). Molecular docking: current advances and challenges. *TIP. Revista especializada en ciencias químico-biológicas*, *21*, 65-86.

Puzari, M., & Chetia, P. (2017). RND efflux pump mediated antibiotic resistance in Gram-negative bacteria *Escherichia coli* and *Pseudomonas aeruginosa*: A major issue worldwide. *World Journal of Microbiology and Biotechnology*, *33*, 1-8.

Puzzarini, C. (2012). Molecular Structure of Thiourea. *The Journal of Physical Chemistry A*, *116*(17), 4381–4387.

Qaiser, S., Mubarak, M. S., Ashraf, S., Saleem, M., Ul-Haq, Z., Safdar, M., Rauf, A., Abu-Izneid, T., Qadri, M. I., & Maalik, A. (2021). Benzilydene and thiourea derivatives as new classes of carbonic anhydrase inhibitors: an in vitro and molecular docking study. *Medicinal Chemistry Research*, *30*(3), 552–563.

Quan, G., Xia, P., Lian, S., Wu, Y., & Zhu, G. (2020). Zinc uptake system ZnuACB is essential for maintaining pathogenic phenotype of F4ac+enterotoxigenic *E. coli* (ETEC) under a zinc restricted environment. *Veterinary Research*, *51*(1), 1-10.

Rasheed, S., Aziz, M., Saeed, A., Ejaz, S. A., Channar, P. A., Zargar, S., Abbas, Q., Alanazi, H., Hussain, M., Alharbi, M, Kim, A.J., Wani, T.A. & Raza, H. (2022). Analysis of 1-aroyl-3-[3-chloro-2-methylphenyl] thiourea hybrids as potent urease inhibitors: synthesis, biochemical evaluation and computational approach. *International Journal of Molecular*

Sciences, *23*(19), 1-17.

Rahamathullal, R., Khairul, W. M., Salleh, H., Adli, H. K., Isa, M. I. N., & Tay, M. G. (2013). Synthesis, characterization and electrochemical analysis of V-shaped disubstituted thiourea-chlorophyll thin film as active layer in organic solar cells. *International Journal of Electrochemical Science*, *8*(3), 3333-3348.

Rajakumari, K., Aravind, K., Balamugundhan, M., Jagadeesan, M., Somasundaram, A., Devi, P. B., & Ramasamy, P. (2024). Comprehensive review of DNA gyrase as enzymatic target for drug discovery and development. *European Journal of Medicinal Chemistry Reports*, *12*, 1-10.

Rakhshani, S., Rezvani, A. R., Dušek, M., & Eigner, V. (2018). Design and synthesis of novel thiourea metal complexes with controllable antibacterial properties. *Applied Organometallic Chemistry*, *32*(6), 1-13.

Ramaswamy, S., Kongara, D., Dwarampudi, L. P., & Gade, R. (2022). Synthesis, spectral characterization, anti-bacterial, cytotoxic evaluation and docking studies of new urea and thiourea derivatives. *Indian Journal of Biochemistry and Biophysics (IJBB)*, *59*(7), 767-776.

Rana, P., Parupalli, R., Akhir, A., Saxena, D., Maitra, R., Imran, M., ... & Nanduri, S. (2024). Synthesis and biological evaluation of new naphthalimide–thiourea derivatives as potent antimicrobial agents active against multidrug-resistant Staphylococcus aureus and Mycobacterium tuberculosis. *RSC Medicinal Chemistry*, *15*(4), 1381-1391.

Rani, M., Devi, J., & Kumar, B. (2023). Thiosemicarbazones-based Co(II), Ni(II), Cu(II) and Zn(II) complexes: synthesis, structural elucidation, biological activities and molecular docking. *Chemical Papers*, *77*(10), 6007–6027.

Reddy, J. M., Verma, P., Agrawal, I., Vyas, M., & Sahu, S. K. (2024). Molecular docking

studies of chemical constituents of *Rauwolfia serpentina* on hypertension. In *BIO Web of Conferences*, (Vol. 86, pp. 1-10).

Refat, M. S., Gaber, A., Althobaiti, Y. S., Alyami, H., Alsanie, W. F., Shakya, S., Adam, A. M. A., Kobeasy, M. I., & Asla, K. A. (2022). Spectroscopic and molecular docking studies of Cu(II), Ni(II), Co(II), and Mn(II) complexes with anticonvulsant therapeutic agent gabapentin. *Molecules*, *27*(13), 1-19.

Rilak, A., Puchta, R., & Bugarčić, Ž. D. (2015). Mechanism of the reactions of ruthenium(II) polypyridyl complexes with thiourea, sulfur-containing amino acids and nitrogen-containing heterocycles. *Polyhedron*, *91*, 73–83.

Rizvi, S. A., Ferrer, G., Khawaja, U. A., & Sanchez-Gonzalez, M. A. (2024). Chlorpheniramine, an old drug with new potential clinical applications: a comprehensive review of the literature. *Current Reviews in Clinical and Experimental Pharmacology Formerly Current Clinical Pharmacology*, *19*(2), 137-145.

Roman, R., Pintilie, L., Căproiu, M. T., Dumitrașcu, F., Nuță, D. C., Zarafu, I., Ioniță, P., Chifiriuc, M. C., Chiriță, C., Moroșan, A., Popa, M., Bleotu, C., & Limban, C. (2023). New N-acyl thiourea derivatives: Synthesis, standardized quantification method and in vitro evaluation of potential biological activities. *Antibiotics*, *12*(5), 1-29.

Ronchetti, R., Moroni, G., Carotti, A., Gioiello, A., & Camaioni, E. (2021). Recent advances in urea-and thiourea-containing compounds: focus on innovative approaches in medicinal chemistry and organic synthesis. *Royal Society of Chemistry Medicinal Chemistry*, *12*(7), 1046-1064.

Roope, L. S., Smith, R. D., Pouwels, K. B., Buchanan, J., Abel, L., Eibich, P., ... & Wordsworth, S. (2019). The challenge of antimicrobial resistance: what economics can contribute. *Science*, *364*(6435), 1-42.

Roskoski Jr, R. (2023). Rule of five violations among the FDA-approved small molecule protein kinase inhibitors. *Pharmacological Research*, *191*, 1-12.

Ross, D. S., Burch, H. B., Cooper, D. S., Greenlee, M. C., Laurberg, P., Maia, A. L., Rivkees, S. A., Samuels, M., Sosa, J. A., Stan, M. N., & Walter, M. A. (2016). 2016 American Thyroid Association guidelines for diagnosis and management of hyperthyroidism and other causes of thyrotoxicosis. *Thyroid*, *26*(10), 1343–1421.

Rostas, A. M., Badea, M., Ruta, L. L., Farcasanu, I. C., Maxim, C., Chifiriuc, M. C., Popa, M., Luca, M., Korosin, N. C., Korosec, R. C., Bacalum, M., Raileanu, M., & Olar, R. (2020). Copper(II) complexes with mixed heterocycle ligands as promising antibacterial and antitumor species. *Molecules*, *25*(17), 1-22.

Ruswanto, R., Nofianti, T., Mardianingrum, R., Kesuma, D., & Siswandono. (2022). Design, molecular docking, and molecular dynamics of thiourea-iron (III) metal complexes as NUDT5 inhibitors for breast cancer treatment. *Heliyon*, *8*(9), 1-10.

Saeed, A., Larik, F. A., Jabeen, F., Mehfooz, H., Ghumro, S. A., El-Seedi, H. R., Ali, M., Channar, P. A., & Ashraf, H. (2018). Synthesis, antibacterial and antileishmanial activity, cytotoxicity, and molecular docking of new heteroleptic copper(I) complexes with thiourea ligands and triphenylphosphine. *Russian Journal of General Chemistry*, *88*(3), 541–550.

Saeed, A., Ahmed, A., Haider, M. B., Ismail, H., Hayat, K., Shabir, G., & El-Seedi, H. R. (2024). Novel pyrazoline linked acyl thiourea pharmacophores as antimicrobial, urease, amylase and α-glucosidase inhibitors: design, synthesis, SAR and molecular docking studies. *Royal Society of Chemistry Advances*, *14*(2), 1018–1033.

Saeed, F. T., & Jasim, Z. U. (2024). Synthesis and characterization of new Mn (II), Co (II), Ni (II), Cu (II), Zn (II) and Cd (II) complexes with [(z)-3 ((6-aminopyridine-2-yl) imino)

indolin-2-one] ligand. *Kimya Problemleri*, *22*(1), 103-114.

Saeed, S., Rashid, N., Ali, M., Hussain, R., & Jones, P. G. (2010). Synthesis, spectroscopic characterization, crystal structure and pharmacological properties of some novel thiophene-thiourea core derivatives. *European Journal of Chemistry*, *1*(3), 221-227

Safi, A. N., Behrad, M. S., Mosawi, S. H., & Bayan, A. M. (2024). Integrating molecular docking and molecular dynamics simulation approaches for investigation of the affinity and interactions of Berberine with Class C β-Lactamase. *Afghanistan Journal of Infectious Diseases*, 17–24.

Santos, A. F., Brotto, D. F., Favarin, L. R., Cabeza, N. A., Andrade, G. R., Batistote, M., Cavalheiro, A.A., Neves, A., Rodrigues, D.C.M. & Anjos, A. D. (2014). Study of the antimicrobial activity of metal complexes and their ligands through bioassays applied to plant extracts. *Revista Brasileira de Farmacognosia*, *24*, 309-315.

Satoh, T., Isozaki, O., Suzuki, A., Wakino, S., Iburi, T., Tsuboi, K., Kanamoto N., Otani, H., Furukawa, Y., Teramukasi, S. & Akamizu, T. (2016). 2016 Guidelines for the management of thyroid storm from The Japan Thyroid Association and Japan Endocrine Society. The Japan Thyroid Association and Japan Endocrine Society Taskforce Committee for the establishment of diagnostic criteria and nationwide surveys for thyroid storm. *Endocrine journal*, *63*(12), 1025-1064.

Scarperi, A., Carignani, E., Martini, F., Embs, J. P., Wąsicki, J., Barcaro, G., Geppi, M., & Pajzderska, A. (2023). Different dynamic behavior of methyl groups in crystalline carbimazole as revealed by a multitechnique experimental and theoretical approach. *Journal of Physical Chemistry C*, *127*(10), 5186–5196.

Scher, H. I., Anand, A., Rathkopf, D., Shelkey, J., Morris, M. J., Danila, D. C., Larson, S., Humm, J., Fleisher, M., Sawyers, C. L., Beer, T. M., Alumkal, J., Higano, C. S., Yu, E.

Y., Taplin, M. E., Efstathiou, E., Hung, D., Hirmand, M., & Seely, L. (2010). Antitumour activity of MDV3100 in castration-resistant prostate cancer: A phase 1-2 study. *The Lancet*, *375*(9724), 1437–1446.

Scher, H. I., Fizazi, K., Saad, F., Taplin, M.-E., Sternberg, C. N., Miller, K., de Wit, R., Mulders, P., Chi, K. N., Shore, N. D., Armstrong, A. J., Flaig, T. W., Fléchon, A., Mainwaring, P., Fleming, M., Hainsworth, J. D., Hirmand, M., Selby, B., Seely, L., & de Bono, J. S. (2012). Increased survival with enzalutamide in prostate cancer after chemotherapy. *New England Journal of Medicine*, *367*(13), 1187–1197.

Scott, K. A., & Njardarson, J. T. (2019). Analysis of US FDA-approved drugs containing sulfur atoms. *Sulfur Chemistry*, 1-34.

Scott, L. J. (2018). Enzalutamide: a review in castration-resistant prostate cancer. *Drugs*, *78*(18), 1913-1924.

Shah, R., & Verma, P. K. (2019). Synthesis of thiophene derivatives and their anti-microbial, antioxidant, anticorrosion and anticancer activity. *BioMed Central Chemistry*, *13*(3). 1-13.

Shalas, A. F., Winarsih, S., Ihsan, B. R. P., Kharismawati, A., Firdaus, A. I., & Wiloka, E. (2023). Molecular docking, synthesis, and antibacterial activity of the analogs of 1-allyl-3-benzoylthiourea. *Research in Pharmaceutical Sciences*, *18*(4), 371-380.

Shaweta, S., Akhil, S., & Utsav, G. (2021). Molecular docking studies on the anti-fungal activity of *Allium sativum* (Garlic) against *Mucormycosis* (black fungus) by BIOVIA discovery studio visualizer 21.1.0.0. *Annals of Antivirals and Antiretrovirals*, 028–032.

Shawky, A. M., Ibrahim, N. A., Abourehab, M. A. S., Abdalla, A. N., & Gouda, A. M. (2021). Pharmacophore-based virtual screening, synthesis, biological evaluation, and molecular docking study of novel pyrrolizines bearing urea/thiourea moieties with potential

cytotoxicity and CDK inhibitory activities. *Journal of Enzyme Inhibition and Medicinal Chemistry*, *36*(1), 15–33.

Sheel, A., & Pant, D. (2021). Thiourea *Bacillus* combination for gold leaching from waste lithium-ion batteries. *Bioresource Technology Reports*, *15*, 1-7.

Shultz, M. D. (2019). Two Decades under the Influence of the Rule of Five and the Changing Properties of Approved Oral Drugs. *Journal of Medicinal Chemistry*, *62*(4), 1701–1714.

Silva, J. D. de S., Leite, S. da C., Silva, M. T. S. da, Meirelles, L. M. A., & Andrade, A. W. L. (2020). In silico evaluation of the inhibitory effect of antiretrovirals Atazanavir and Darunavir on the main protease of SARS-CoV-2: Docking studies and molecular dynamics. *Research, Society and Development*, *9*(8), 1-17.

Singer, A. C., Kirchhelle, C., & Roberts, A. P. (2020). (Inter) nationalising the antibiotic research and development pipeline. *The Lancet Infectious Diseases*, *20*(2), e54-e62.

Singh, L. P., & Tiwari, O. P. (2018). Synthesis and antimicrobial activity of some methyl 4-(1h-benzo[d] imidazol-2-yl) phenyl carbamodithioate amine derivatives. *International Journal of Pharmaceutical Sciences and Research*, *9*(3), 1194–1200.

Singh, N., Vayer, P., Tanwar, S., Poyet, J.-L., Tsaioun, K., & Villoutreix, B. O. (2023). Drug discovery and development: introduction to the general public and patient groups. *Frontiers in Drug Discovery*, *3*, 1-11.

Siramshetty, V., Williams, J., Nguyễn, Đ. T., Neyra, J., Southall, N., Mathé, E., Xu, X., & Shah, P. (2021). Validating ADME QSAR models using marketed drugs. *Society for Laboratory Automation and Screening Discovery*, *26*(10), 1326–1336.

Sodhi, R. K., & Paul, S. (2019). Metal complexes in medicine an overview and update from drug design perspective. *Cancer Therapy & Oncology International Journal*, *14*(1), 25-32

Sokhn, E. S., Salami, A., El Roz, A., Salloum, L., Bahmad, H. F., & Ghssein, G. (2020). Antimicrobial susceptibilities and laboratory profiles of *Escherichia coli*, *Klebsiella pneumoniae*, and *Proteus mirabilis* isolates as agents of urinary tract infection in Lebanon: Paving the way for better diagnostics. *Medical Sciences, 8*(3), 1-11.

Solano, F. (2018). On the metal cofactor in the tyrosinase family. *International Journal Of Molecular Sciences*, *19*(2), 1-17.

Soliman, A. M., El-sagheir, A. M. K., Thabet, M. M., Abdel Hakiem, A. F., & Aboraia, A. S. (2024). Synthesis, characterization, molecular modeling studies, and biological evaluation of metal piroxicam complexes (M = Ni(II), Pt(IV), Pd(II), Ag(I)) as antibacterial and anticancer agents. *Drug Development Research*, *85*(2), 1-18.

Soomro, S., Sangi, S., & Nayeem, N. (2023). Anti-oxidative burst, cytotoxicity, and ADME studies of thiourea compounds. *Pharmacophore*, *14*(2), 97–105.

Sovari, S.N., & Zobi, F. (2020). Recent studies on the antimicrobial activity of transition metal complexes of groups 6–12. *Chemistry*, *2*(2), 418-452.

Spătaru, C. I., Purcăr, V., Donescu, D., Ghiurea, M., Cinteză, O., & Miclăuş, T. (2013). Preparation of hydrophobic surface based on hybrid silica films by sol-gel process. *Advanced Materials, 5*, 117-128.

Spellberg, B., & Doi, Y. (2015). The rise of fluoroquinolone-resistant *Escherichia coli* in the community: scarier than we thought. *The Journal of infectious diseases*, *212*(12), 1853-1855.

Stapleton, A. E., Wagenlehner, F. M. E., Mulgirigama, A., & Twynholm, M. (2020). *Escherichia coli* resistance to fluoroquinolones in community-acquired uncomplicated urinary tract infection in women: a systematic review. *Antimicrobial Agents and Chemotherapy*, *64*(10), 1-11.

Stegemann, S., Moreton, C., Svanbäck, S., Box, K., Motte, G., & Paudel, A. (2023). Trends in oral small-molecule drug discovery and product development based on product launches before and after the Rule of Five. *Drug Discovery Today*, *28*(2), 1-13.

Tagiling, A. A., Khairul, W. M., Rahamathullah, R., Sevakumaran, V., Mohammed, M., & Saidin, S. (2024). Computational and Experimental Investigation of Antibacterial Properties of Some Fluorinated Thioureas. *Polycyclic Aromatic Compounds*, *44*(9), 5749-5767.

Tang, S., Chen, R., Lin, M., Lin, Q., Zhu, Y., Ding, J., Hu, H., Ling, M., & Wu, J. (2022). Accelerating AutoDock Vina with GPUs. *Molecules*, *27*(9), 1-18.

Tchounwou, P. B., Dasari, S., Noubissi, F. K., Ray, P., & Kumar, S. (2021). Advances in our understanding of the molecular mechanisms of action of cisplatin in cancer therapy. *Journal of Experimental Pharmacology*, *2021* (13), 303-328.

Teillant, A., Gandra, S., Barter, D., Morgan, D. J., & Laxminarayan, R. (2015). Potential burden of antibiotic resistance on surgery and cancer chemotherapy antibiotic prophylaxis in the USA: A literature review and modelling study. *The Lancet Infectious Diseases*, *15*(12), 1429–1437.

Teng, Y., Zhou, Q., & Gao, P. (2019). Applications and challenges of elemental sulfur, nanosulfur, polymeric sulfur, sulfur composites, and plasmonic nanostructures. *Critical Reviews in Environmental Science and Technology*, *49*(24), 2314–2358.

The Pew Charitable Trust. (2019). *Antibiotics Currently in Global Clinical Development*. The Pew Charitable Trust, Philadelphia.

Thomas, P. M., Deming, M. A., & Sarkar, A. (2022). β-lactamase suppression as a strategy to target methicillin-resistant *Staphylococcus aureus*: Proof of concept. *American Society Chemistry Omega, 7*(50), 46213–46221.

Tran, C., Ouk, S., Clegg, N. J., Chen, Y., Watson, P. A., Arora, V., Wongvipat, J., Smith-Jones, P.M., Yoo, D., Kwon, A., Wasielewska, T., Welsbie, D., Chen, C.D., Higano, C.S., Beer, T.M., Hung, D.T., Scher, H.I., Jung, M.E. & Sawyers, C. L. (2009). Development of a second-generation antiandrogen for treatment of advanced prostate cancer. *Science, 324*(5928), 787-790.

Trotsko, N., Kosikowska, U., Paneth, A., Wujec, M., & Malm, A. (2018). Synthesis and antibacterial activity of new (2,4-dioxothiazolidin-5-yl/ylidene)acetic acid derivatives with thiazolidine-2,4-dione, rhodanine and 2-thiohydantoin moieties. *Saudi Pharmaceutical Journal*, *26*(4), 568–577.

Trott, O., & Olson, A. J. (2010). AutoDock Vina: Improving the speed and accuracy of docking with a new scoring function, efficient optimization, and multithreading. *Journal of Computational Chemistry*, *31*(2), 455–461.

Trung, N. Q., Nam, P. T. P., & Van Tuyen, N. (2024). Synthesis, structural characterization and bioactivities of iron(III) and copper(II) complexes containing Schiff base thiourea ligands of 5-(tert-butyl)-2-hydroxybenzaldehyde. *Vietnam Journal of Chemistry*, *62*(S1), 8-14.

Tshibangu-Kabamba, E., & Yamaoka, Y. (2021). *Helicobacter pylori* infection and antibiotic resistance—from biology to clinical implications. *Nature Reviews Gastroenterology & Hepatology*, *18*(9), 613-629.

Tyagi, P., Chandra, S., & Saraswat, B. S. (2015). Ni (II) and Zn (II) complexes of 2-((thiophen-2-ylmethylene) amino) benzamide: Synthesis, spectroscopic characterization, thermal, DFT and anticancer activities. *Spectrochimica Acta Part A: Molecular and Biomolecular Spectroscopy*, *134*, 200-209.

Uddin, M. N., Chowdhury, D. A., Islam, M. T., & Hoque, F. (2012). Evaluation of biological

activity of dioxouranium complexes of some Schiff base and dithiocarbamate ligands. *Orbital: The Electronic Journal of Chemistry*, *4*(4), 273-287.

Ujan, R., Channar, P. A., Bahadur, A., Abbas, Q., Shah, M., Rashid, S. G., Iqbal, S., Saeed, A., Abd-Rabboh, H. S. M., Raza, H., Hassan, M., Siyal, A. N., Mahesar, P. A., Lal, B., Channar, K. A., Khan, B. A., Nawaz, M., Rajoka, M. S. R., & Kim, J. M. (2021). Synthesis, kinetics and biological assay of some novel aryl bis-thioureas: A potential drug candidates for Alzheimer's disease. *Journal of Molecular Structure*, *1246*, 1-8.

Uzzaman, M., Chowdhury, M. K., & Belal Hossen, M. (2019). Thermochemical, molecular docking and ADMET studies of Aspirin metabolites. *Frontiers in Drug, Chemistry and Clinical Research*, *2*(3), 1-5.

Vaidya, M. Y., McBain, A. J., Butler, J. A., Banks, C. E., & Whitehead, K. A. (2017). Antimicrobial efficacy and synergy of metal ions against *Enterococcus faecium*, *Klebsiella pneumoniae* and *Acinetobacter baumannii* in planktonic and biofilm phenotypes. *Scientific Reports*, *7*(1), 1-9.

Vakkalagadda, B., Frost, C., Byon, W., Boyd, R. A., Wang, J., Zhang, D., Yu, Z., Dias, C., Shenker, A., & LaCreta, F. (2016). Effect of rifampin on the pharmacokinetics of apixaban, an oral direct inhibitor of factor Xa. *American Journal of Cardiovascular Drugs*, *16*(2), 119–127.

Vančo, J., Trávníček, Z., Hošek, J., Malina, T., & Dvořák, Z. (2021). Copper(II) complexes containing natural flavonoid pomiferin show considerable in vitro cytotoxicity and anti-inflammatory effects. *International Journal of Molecular Sciences*, *22*(14), 1-26.

Verheijen, M., Lienhard, M., Schrooders, Y., Clayton, O., Nudischer, R., Boerno, S., Timmermann, B., Selevsek, N., Schlapbach, R., Gmuender, H., Gotta, S., Geraedts, J., Herwig, R., Kleinjans, J., & Caiment, F. (2019). DMSO induces drastic changes in human

cellular processes and epigenetic landscape in vitro. *Scientific Reports*, *9*(1), 1-12.

Venkatesh, G., Vennila, P., Kaya, S., Ahmed, S. B., Sumathi, P., Siva, V., Rajendran, P. & Kamal, C. (2024). Synthesis and spectroscopic characterization of Schiff base metal complexes, biological activity, and molecular docking studies. *American Chemical Society Omega*, *9*(7), 8123-8138.

Villumsen, K.R., Allahghadry, T., Karwańska, M., Frey, J., & Bojesen, A. M. (2023). Quinolone resistance in *Gallibacterium anatis* determined by mutations in quinolone resistance-determining region. *Antibiotics, 12*(5), 1-14.

Vu, T. Y., Le, T. T. H., Pham, T. L., Vo, N. H. H., Pham, T. N. M., Pham, M. Q., & Phung, H. T. T. (2024). Estimation of the binding affinities of glycogen phosphorylase inhibitors by molecular docking to support the treatment of type 2 diabetes. *Physical Chemistry Research, 12*(3), 821–835.

Wahyuni, D. K., Nuha, G. A., Atere, T. G., Kharisma, V. D., Tari, V. S., Rahmawati, C. T., Murtadlo, A. A. A., Syukriya, A. J., Wacharasindu, S., Prasongsuk, S., & Purnobasuki, H. (2024). Antimicrobial potentials of *Pandanus amaryllifolius* Roxb.: Phytochemical profiling, antioxidant, and molecular docking studies. *Public Library of Science ONE, 19*(8), 1-20.

Wang, K., Mishra, M. K., & Sun, C. C. (2019). Exceptionally elastic single-component pharmaceutical crystals. *Chemistry of Materials, 31*(5), 1794-1799.

Wang, S., Dong, G., & Sheng, C. (2019). Structural simplification: an efficient strategy in lead optimization. *Acta Pharmaceutica Sinica B, 9*(5), 880-901.

Wang, Z., Sun, H., Yao, X., Li, D., Xu, L., Li, Y., Tian, S., & Hou, T. (2016). Comprehensive evaluation of ten docking programs on a diverse set of protein–ligand complexes: The prediction accuracy of sampling power and scoring power. *Physical Chemistry Chemical*

Physics, *18*(18), 12964–12975.

Wei, J. J., Xiao, J. J., Yu, J. W., Yi, X. Y., Liu, S., & Liu, G. Y. (2017). Synthesis and structural characterization of silver(I) and gold(I) complexes of N,N′-diisobutyloxycarbonyl-N″,N‴-(1,3-propylene)-bisthiourea. *Polyhedron*, *137*, 176–181.

Wienhausen, G., Dlugosch, L., Jarling, R., Wilkes, H., Giebel, H. A., & Simon, M. (2022). Availability of vitamin B12 and its lower ligand intermediate α-ribazole impact prokaryotic and protist communities in oceanic systems. *International Society for Microbial Ecology Journal*, *16*(8), 2002–2014.

Wittmann, C., Chockley, P., Singh, S. K., Pase, L., Lieschke, G. J., & Grabher, C. (2012). Hydrogen peroxide in inflammation: messenger, guide, and assassin. *Advances in Hematology*, *2012*(1), 1-6.

World Bank Document. (2017). Drug-resistant infections: A threat to our economic future. World Bank, Washington, DC.

WHO. (2019). Prioritization of pathogens to guide discovery, research and development of new antibiotics for drug-resistant bacterial infections, including tuberculosis. World Health Organization, Geneva.

WHO. (2022). Global antimicrobial resistance and use surveillance system (GLASS) report 2022. World Health Organization, Geneva.

WHO. (2024). WHO Bacterial Priority Pathogens List, 2024: Bacterial pathogens of public health importance to guide research, development and strategies to prevent and control antimicrobial resistance. World Health Organization, Geneva.

World Economic Forum. (2020). The Global Risk Report 2020. World Economic Forum, Geneva.

Wu, D., Chen, Q., Chen, X., Han, F., Chen, Z., & Wang, Y. (2023). The blood–brain barrier:

structure, regulation, and drug delivery. *Signal Transduction and Targeted Therapy, 8*(1), 1-27.

Xu, D., Li, Y., Yin, S., & Huang, F. (2024). Strategies to address key challenges of metallacycle/metallacage-based supramolecular coordination complexes in biomedical applications. *Chemical Society Reviews, 53*, 3167-3204.

Xu, K., Ying, L., Ying, T., Wu, Q., Du, L., Yu, Y., Ying, Y., Wei, B., Wang, H. & Yang, Z. (2024). Design, synthesis, and biological evaluation of (thio) urea derivatives as potent *Escherichia coli* β-glucuronidase inhibitors. *Journal of Enzyme Inhibition and Medicinal Chemistry*, *39*(1), 1-9.

Yagi, H., Toyama, T., Kasama, S., Koitabashi, N., Arai, M., Yokoyama, T., Adachi, H., Naito, S., Hoshizaki, H., Oshima, S. & Kurabayashi, M. (2012). Relation between connective tissue growth factor and cardiac sympathetic nerve activity in heart failure in DCM patients. *International Heart Journal*, *53*(5), 282-286.

Yam, E. L. Y., Hsu, L. Y., Yap, E. P. H., Yeo, T. W., Lee, V., Schlundt, J., Lwin, M. O., Limmathurotsakul, D., Jit, M., Dedon, P., Turner, P., & Wilder-Smith, A. (2019). Antimicrobial resistance in the asia pacific region: A meeting report. *Antimicrobial Resistance and Infection Control*, *8*(1), 1-12.

Yee, B. E., Richards, P., Sui, J. Y., & Marsch, A. F. (2020). Serum zinc levels and efficacy of zinc treatment in acne vulgaris: A systematic review and meta-analysis. *Dermatologic therapy*, *33*(6), 1-8.

Yi, L., & Lü, X. (2019). New strategy on antimicrobial-resistance: Inhibitors of DNA replication enzymes. *Current Medicinal Chemistry*, *26*(10), 1761–1787.

Yılmaz, Ü., Tekin, S., Buğday, N., Yavuz, K., Küçükbay, H., & Sandal, S. (2019). Synthesis and evaluation of anticancer properties of novel benzimidazole ligand and their cobalt(II)

and zinc(II) complexes against cancer cell lines A-2780 and DU-145. *Inorganica Chimica Acta*, *495*, 1-45.

Yu, W., & MacKerell, A. D. (2017). Computer-aided drug design methods. *Antibiotics: methods and protocols*, 85-106.

Yu, X. H., Hao, Z. H., Liu, P. L., Liu, M. M., Zhao, L. L., & Zhao, X. (2022). Increased expression of efflux pump norA drives the rapid evolutionary trajectory from tolerance to resistance against Ciprofloxacin in *Staphylococcus aureus*. *Antimicrobial Agents and Chemotherapy*, *66*(12), 1-14.

Yusaini, F. D., & Arif, M. A. M. (2022). Multi-Stimuli-Responsive Organogel Based on Bisthiourea Compounds for The Removal of Selected Organic Dyes. *Borneo Journal of Resource Science and Technology, 12*(1), 106-124.

Yusof, M. S. M., Jusoh, R. T. H., Khairul, W. M., & Yamin, B. M. (2010). Synthesis and characterisation a series of N-(3, 4-dichlorophenyl)-N′-(2, 3 and 4-methylbenzoyl) thiourea derivatives. *Journal of Molecular Structure*, *975*(1-3), 280-284.

Zabiulla, Kouser, S., Joythi, M., Bushra Begum, A., Asha, M. S., Hezam Al-Ostoot, F., Lakshmeesha, D. P., Ramu, R., & Ara Khanum, S. (2023). Molecular docking, synthesis and antimicrobial evaluation of metal complexes with Schiff base. *Results in Chemistry*, *5*, 1-16.

Zhang, D., He, K., Herbst, J. J., Kolb, J., Shou, W., Wang, L., Balimane, P. V., Han, Y. H., Gan, J., Frost, C. E., & Humphreys, W. G. (2013). Characterization of efflux transporters involved in distribution and disposition of apixaban. *Drug Metabolism and Disposition*, *41*(4), 827–835.

Zhang, Y., Li, X., Li, J., Khan, M. Z. H., Ma, F., & Liu, X. (2021). A novel zinc complex with antibacterial and antioxidant activity. *BioMed Central Chemistry*, *15*(1), 1-12.

Zullkiplee, W. S. H., Abd Halim, A. N., Ngaini, Z., Mohd Ariff, M. A., & Hussain, H. (2014). Bis-Thiourea bearing aryl and amino acids side chains and their antibacterial activities. *Phosphorus, Sulfur and Silicon and the Related Elements*, *189*(6), 832–838.

Zullkiplee, W. S. H. W., Rasin, F., Halim, A. N. A., Mortadza, N. A., Ramli, N., Hani, N. I., & Ngaini, Z. (2021). Synthesis, biological properties and comparative molecular docking evaluation studies of 1,3 and 1,4 bis-thiourea derivatives as potential antimicrobial resistant agents. *International Journal of Current Research and Review*, *13*(4), S-23-S-30.

APPENDICES

Appendix 1: 3D (left) and 2D(right) visual representation of docked compound **4** inside 1KZN enzyme

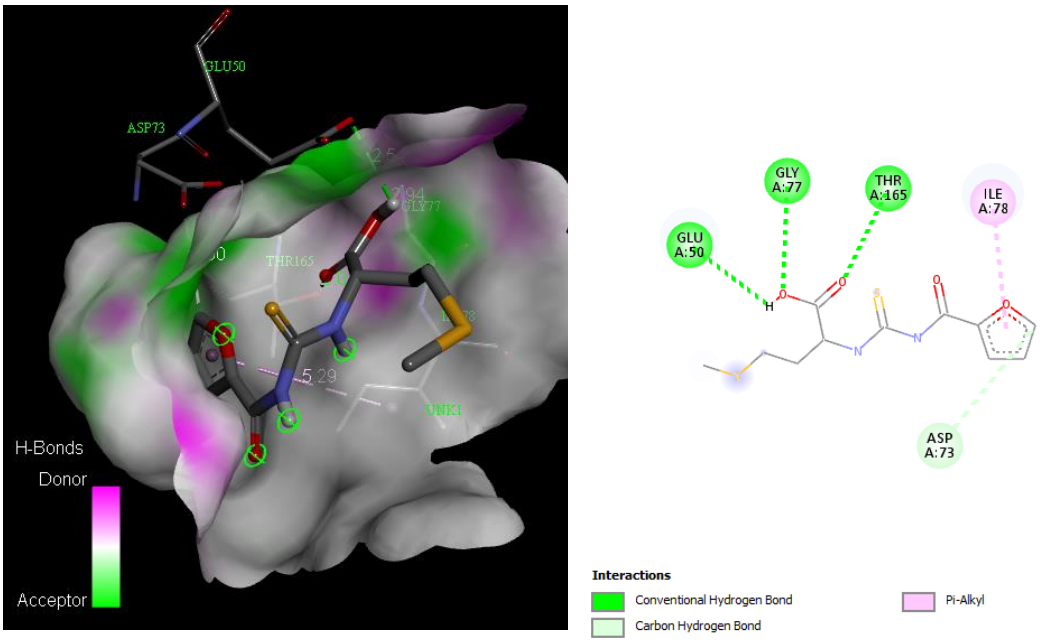

Appendix 2: 3D (left) and 2D(right) visual representation of docked compound **5** inside 1KZN enzyme

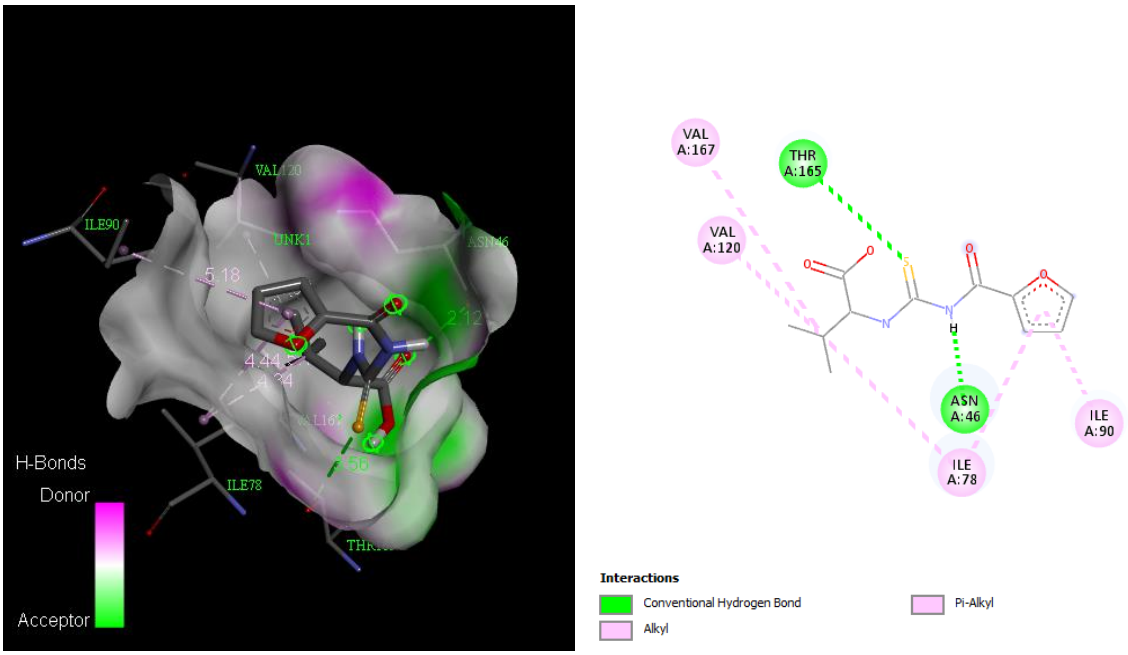

Appendix 3: 3D (left) and 2D(right) visual representation of docked compound **6** inside 1KZN enzyme

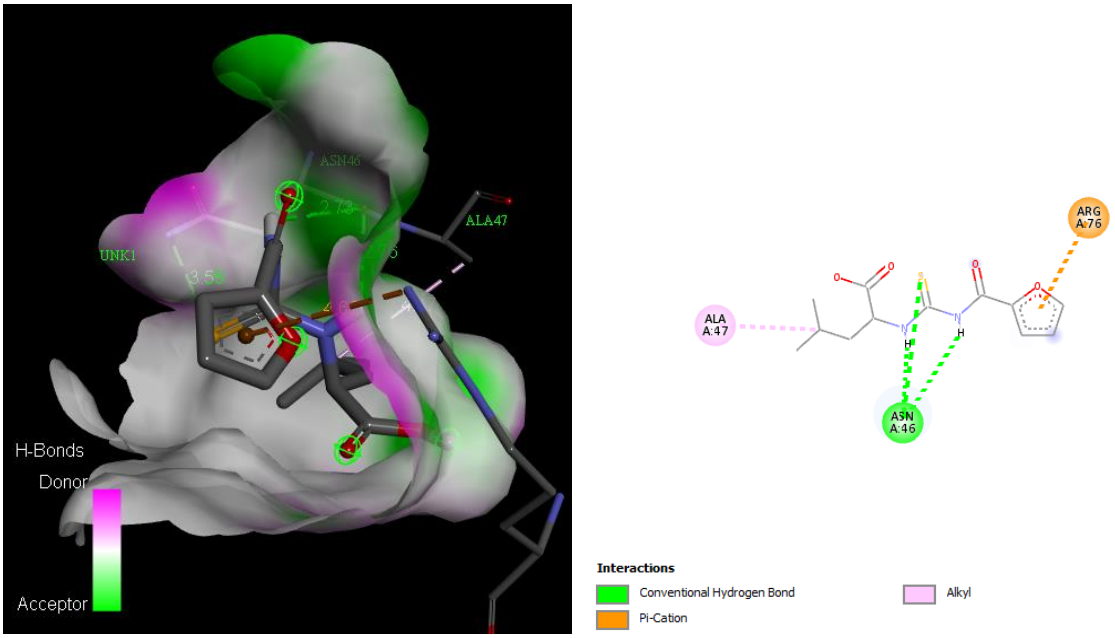

Appendix 4: 3D (left) and 2D(right) visual representation of docked compound **7** inside 1KZN enzyme

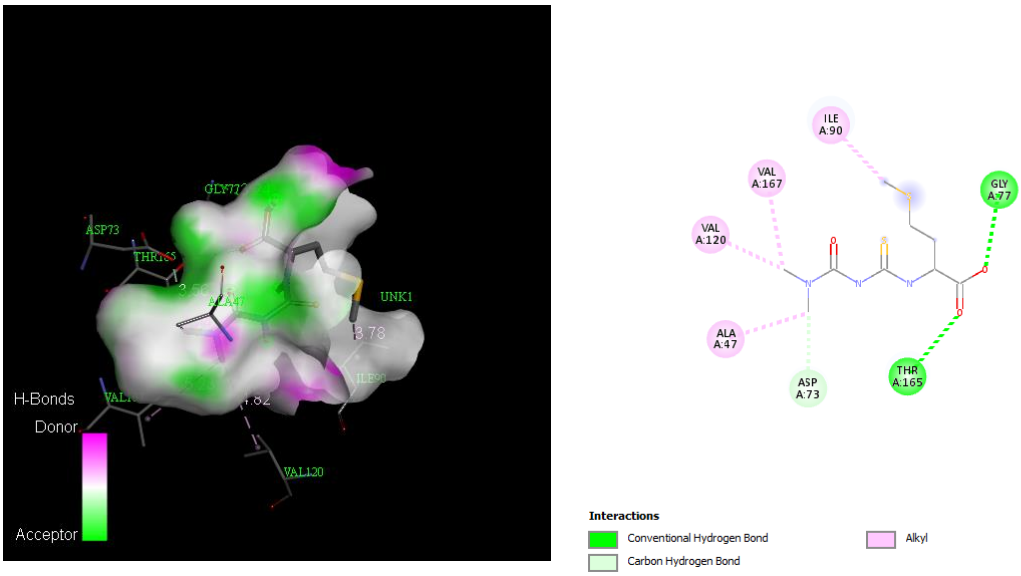

Appendix 5: 3D (left) and 2D(right) visual representation of docked compound **8** inside 1KZN enzyme

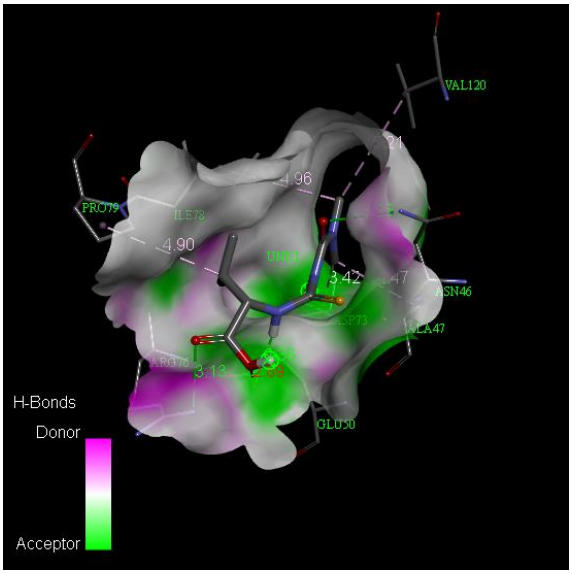

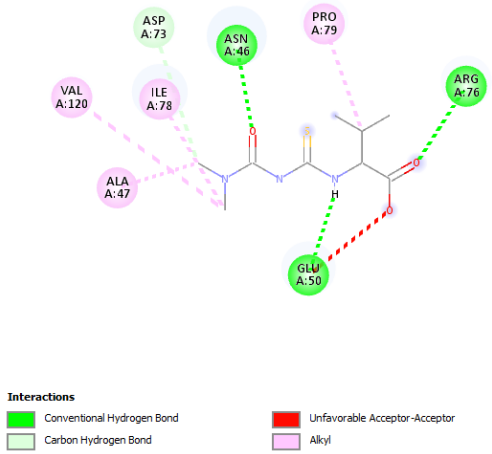

Appendix 6: 3D (left) and 2D(right) visual representation of docked compound **9** inside 1KZN enzyme

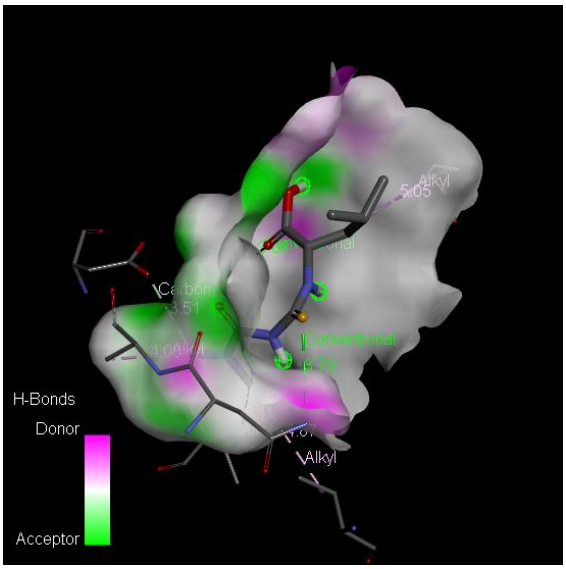

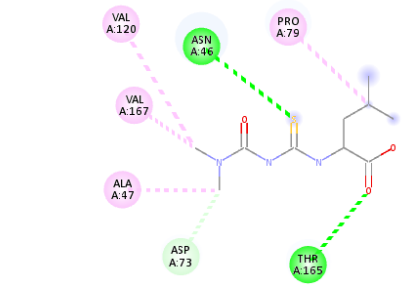

Appendix 7: 3D (left) and 2D(right) visual representation of docked complex **1b** inside 1KZN enzyme

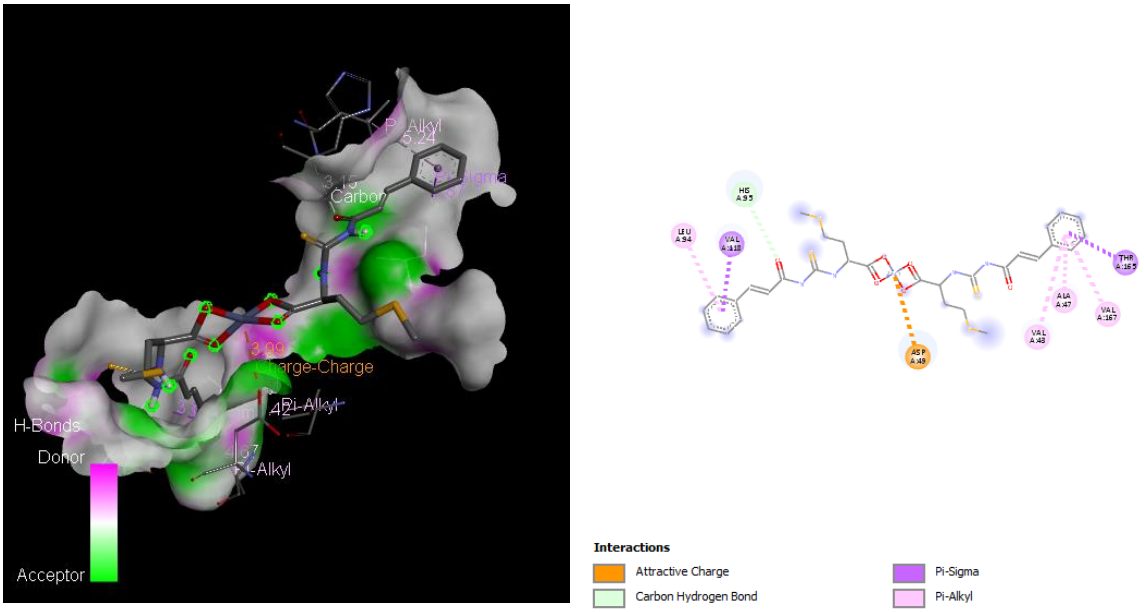

Appendix 8: 3D (left) and 2D(right) visual representation of docked complex **1c** inside 1KZN enzyme

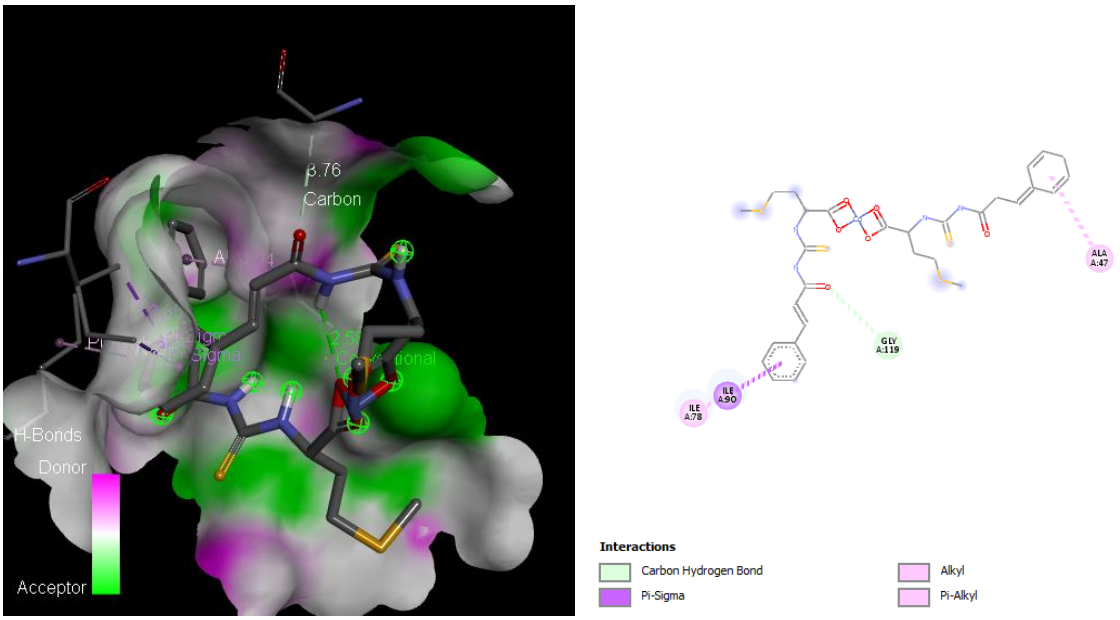

Appendix 9: 3D (left) and 2D(right) visual representation of docked complex **2b** inside 1KZN enzyme

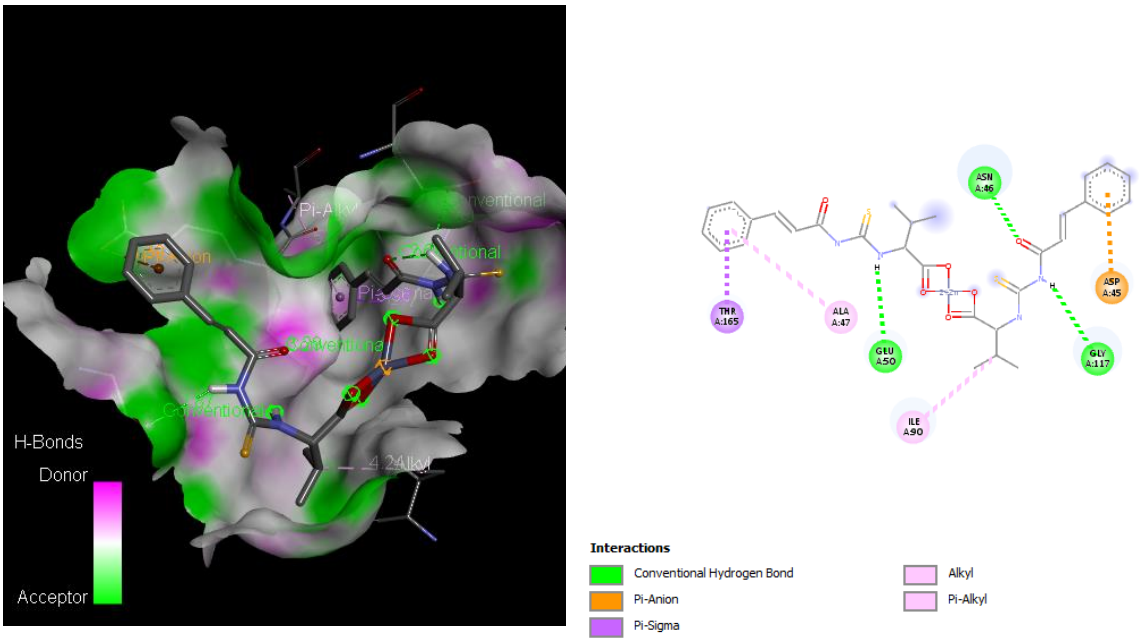

Appendix 10: 3D (left) and 2D(right) visual representation of docked complex **2c** inside 1KZN enzyme

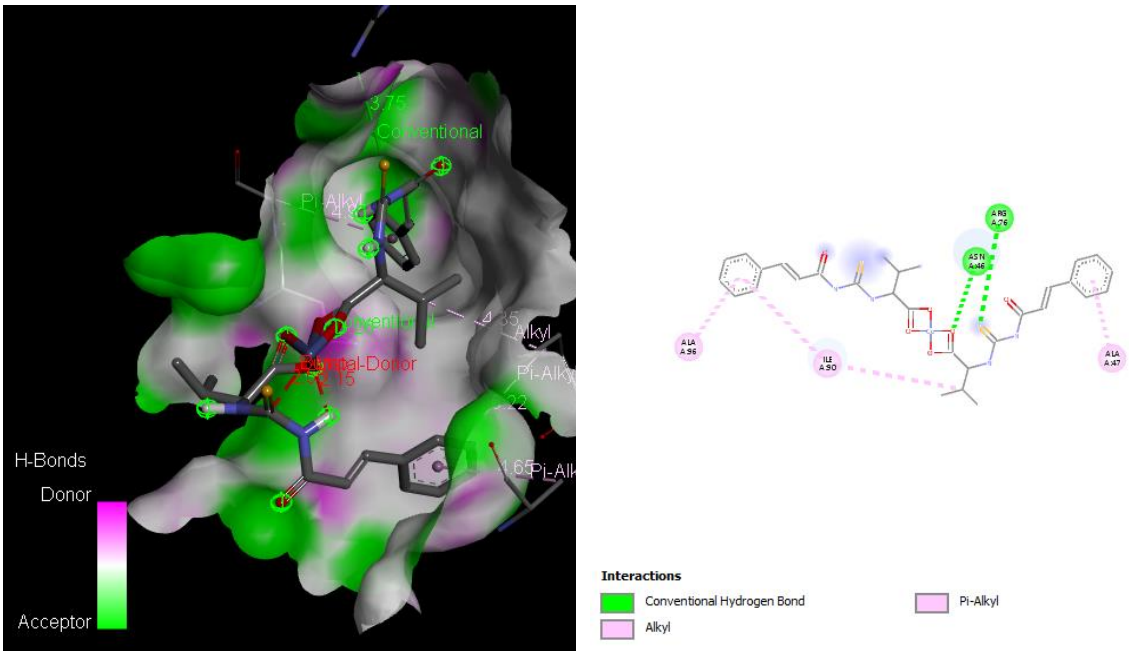

Appendix 11: 3D (left) and 2D(right) visual representation of docked complex **3b** inside 1KZN enzyme

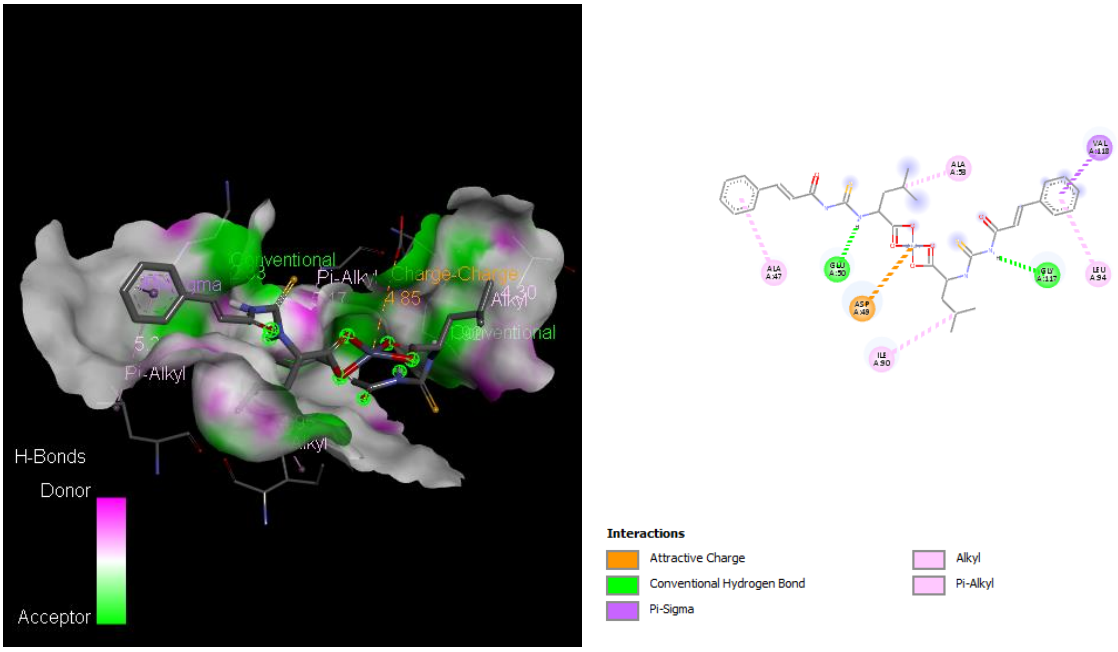

Appendix 12: 3D (left) and 2D(right) visual representation of docked complex **3c** inside 1KZN enzyme

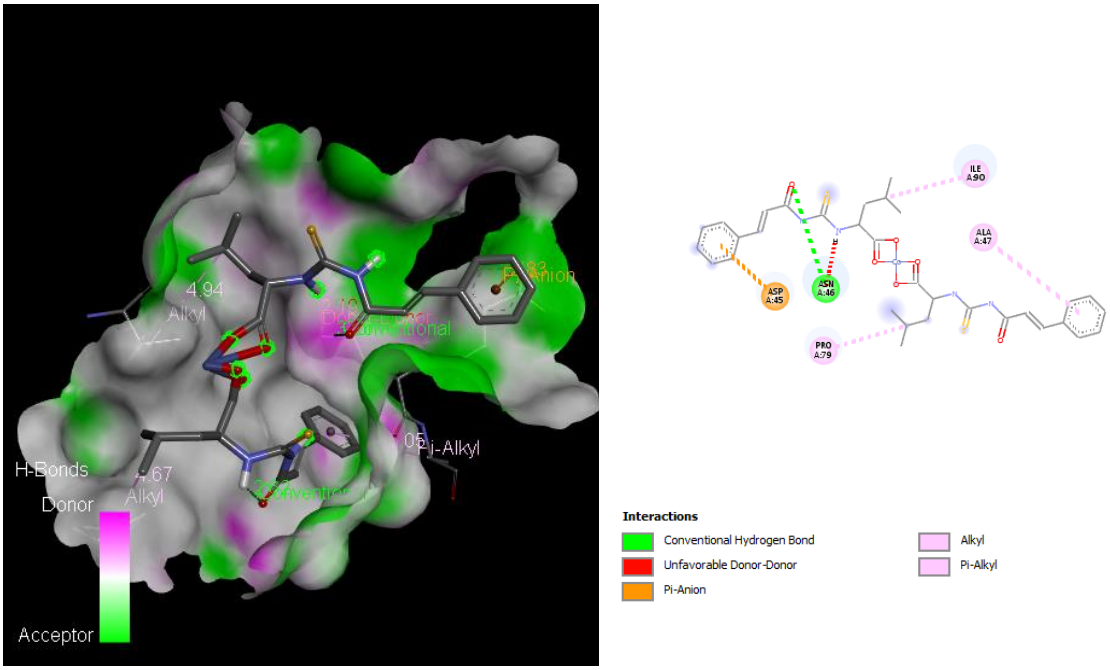

Appendix 13: FTIR spectrum of compound **2**

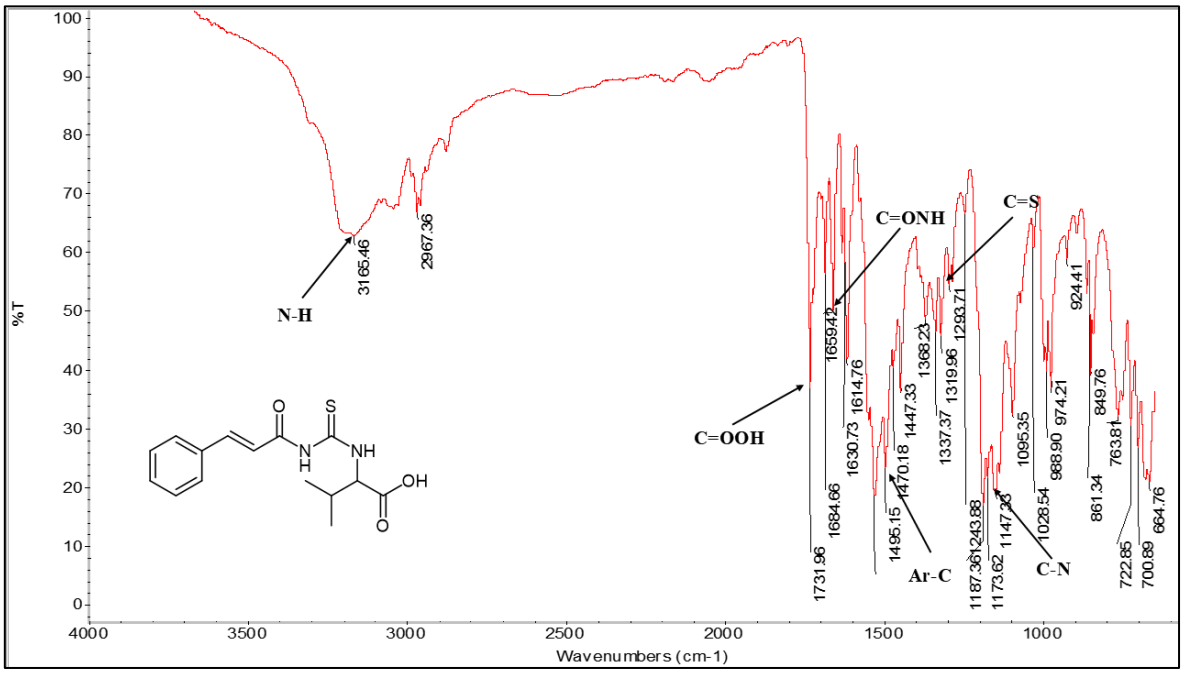

Appendix 14: FTIR spectrum of compound **3**

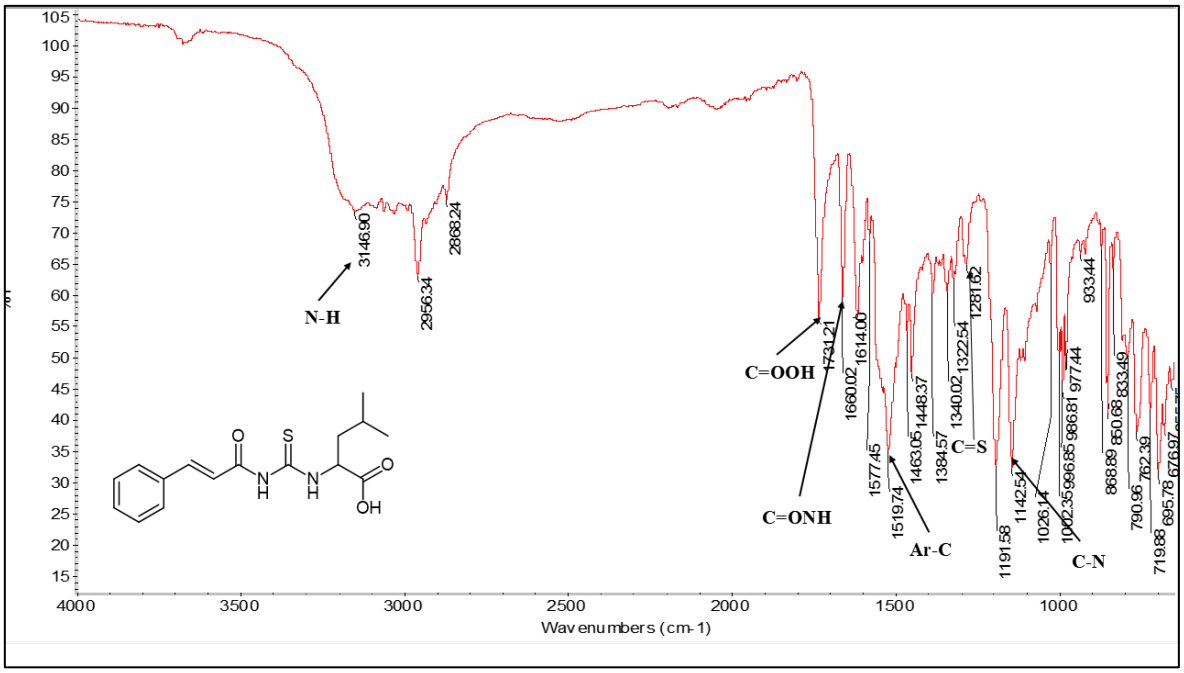

Appendix 15: FTIR spectum of complex **2a**

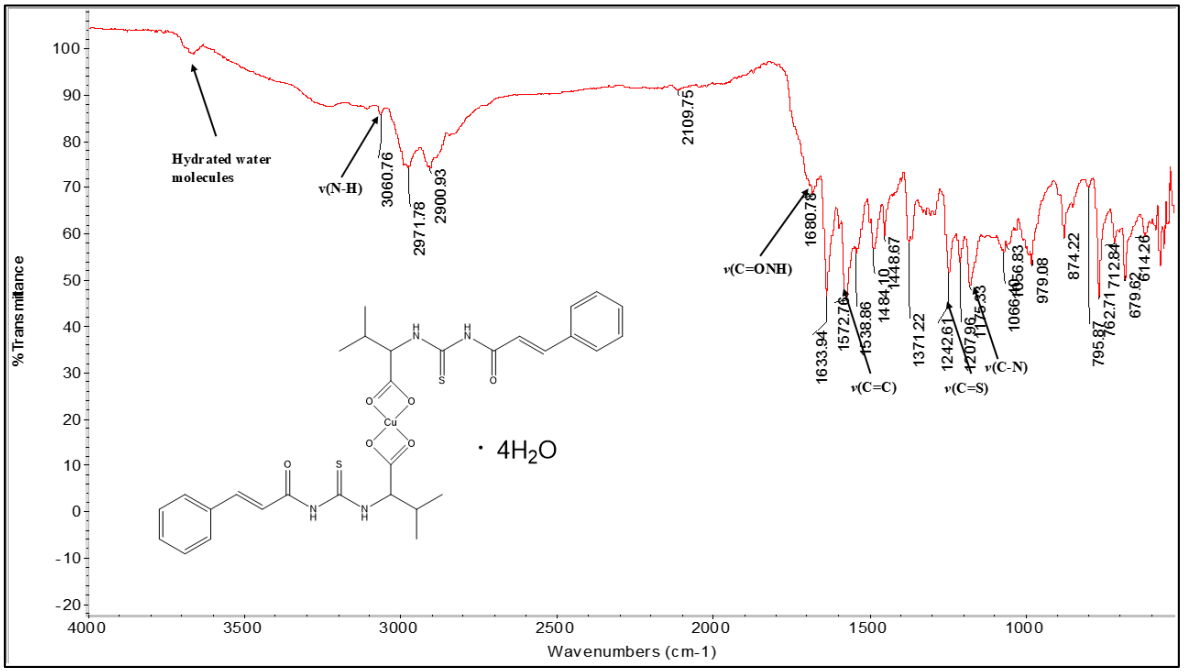

Appendix 16: FTIR spectrum of complex **3a**

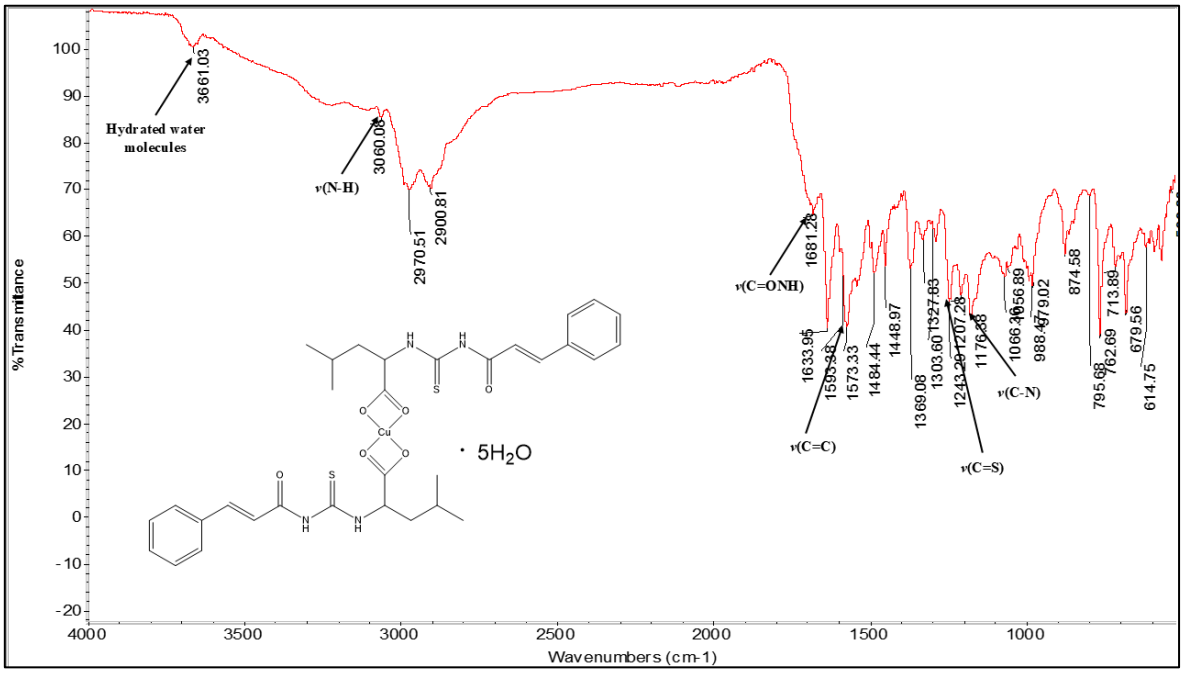

Appendix 17: FTIR spectrum of complex **1b**

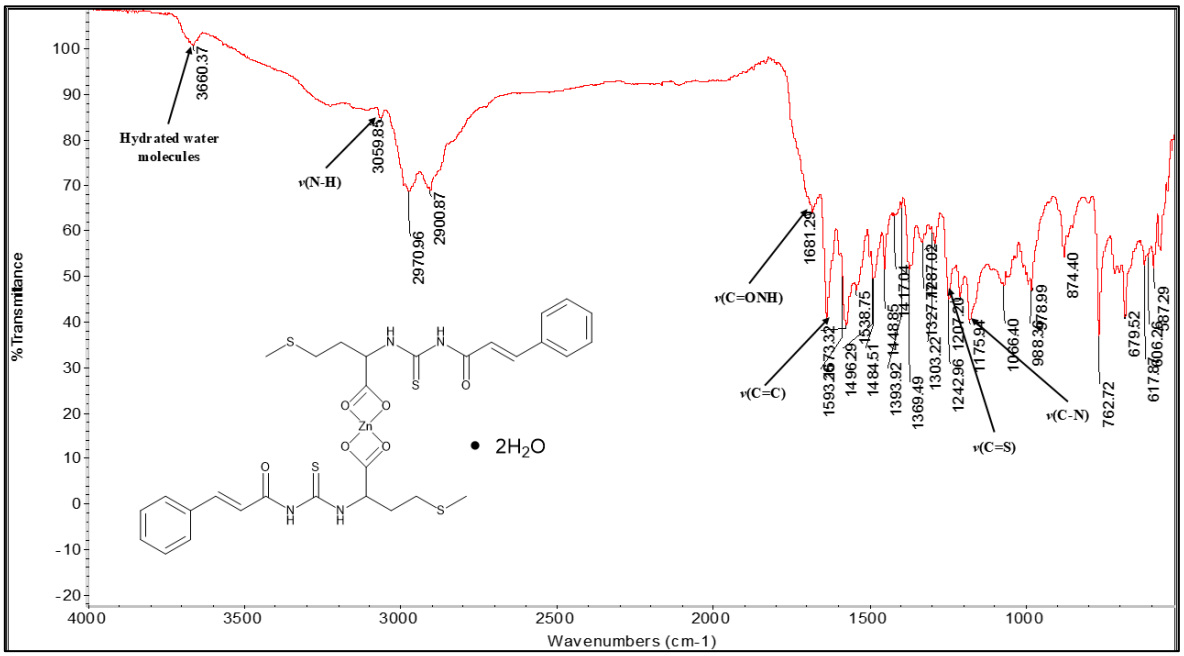

Appendix 18: FTIR spectrum of complex **2b**

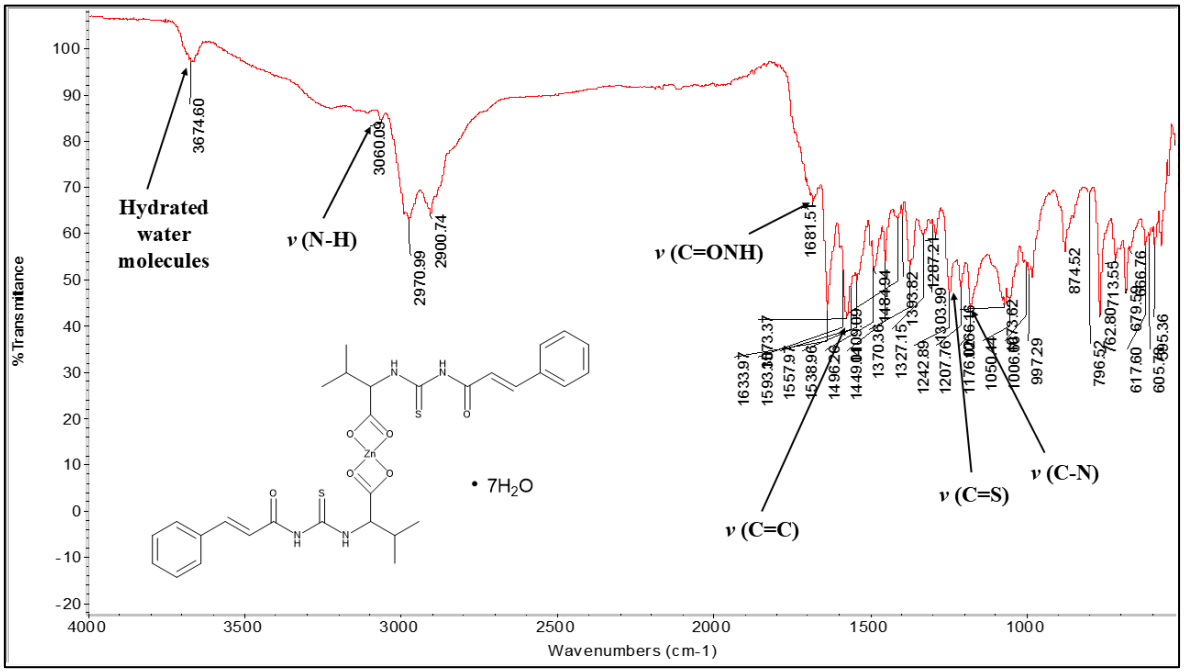

Appendix 19: FTIR spectrum of complex **3b**

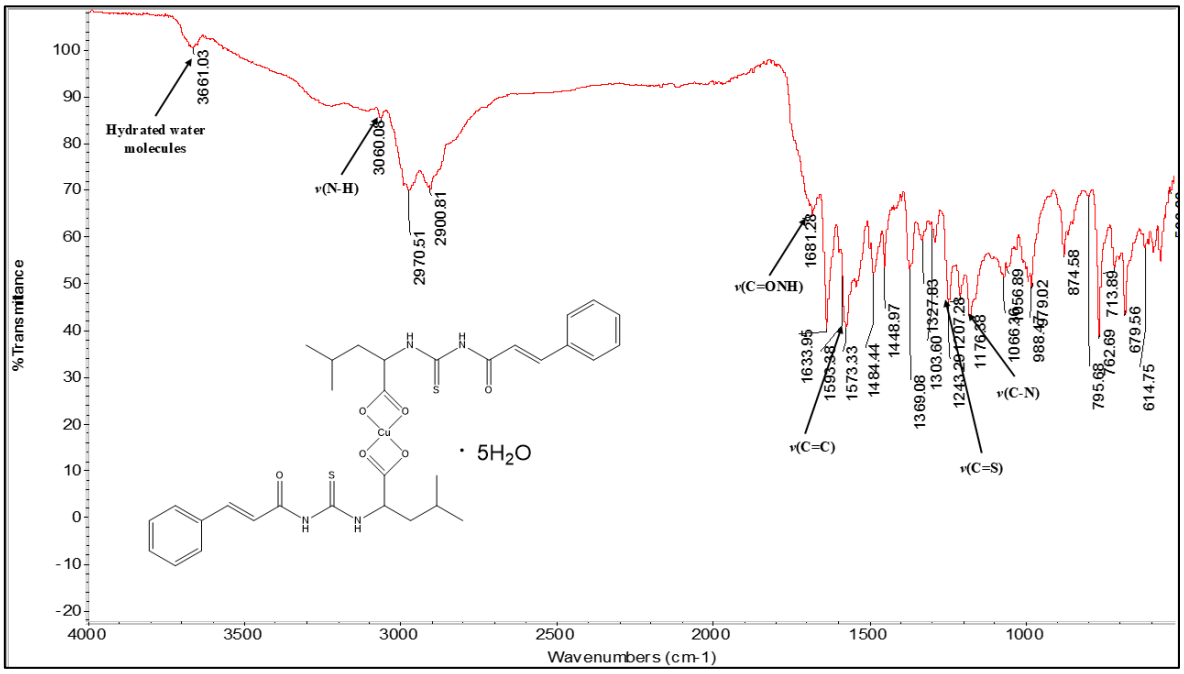

Appendix 20: FTIR spectrum of complex **1c**

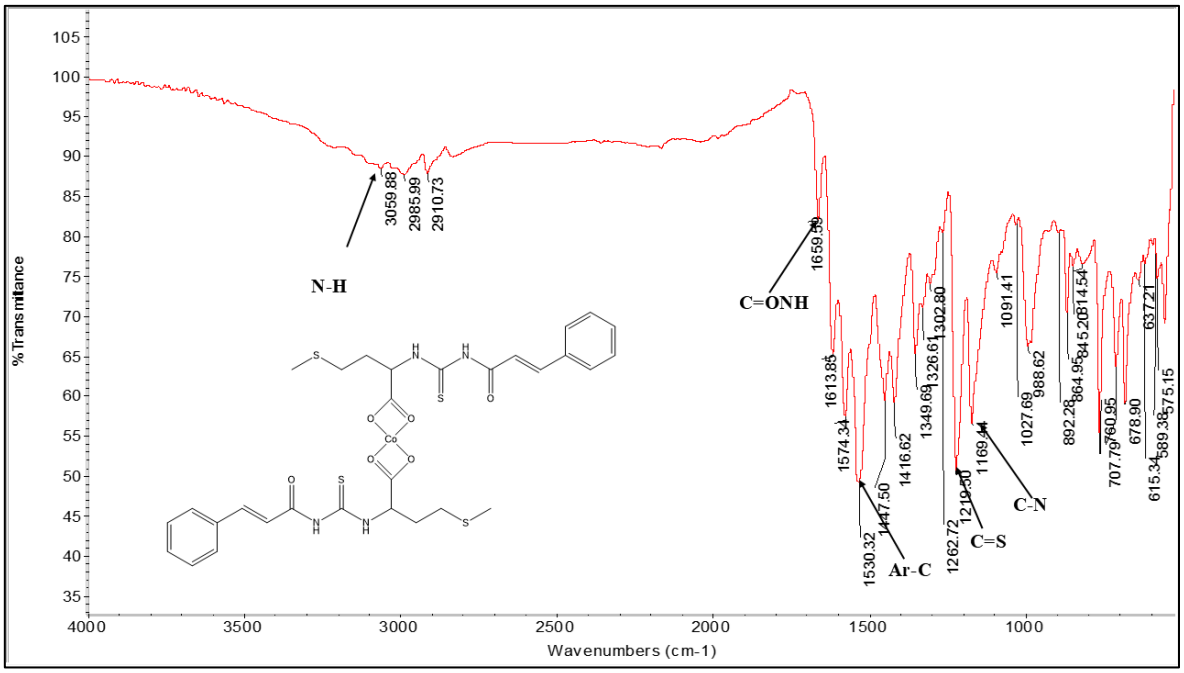

Appendix 21: FTIR spectrum of complex **2c**

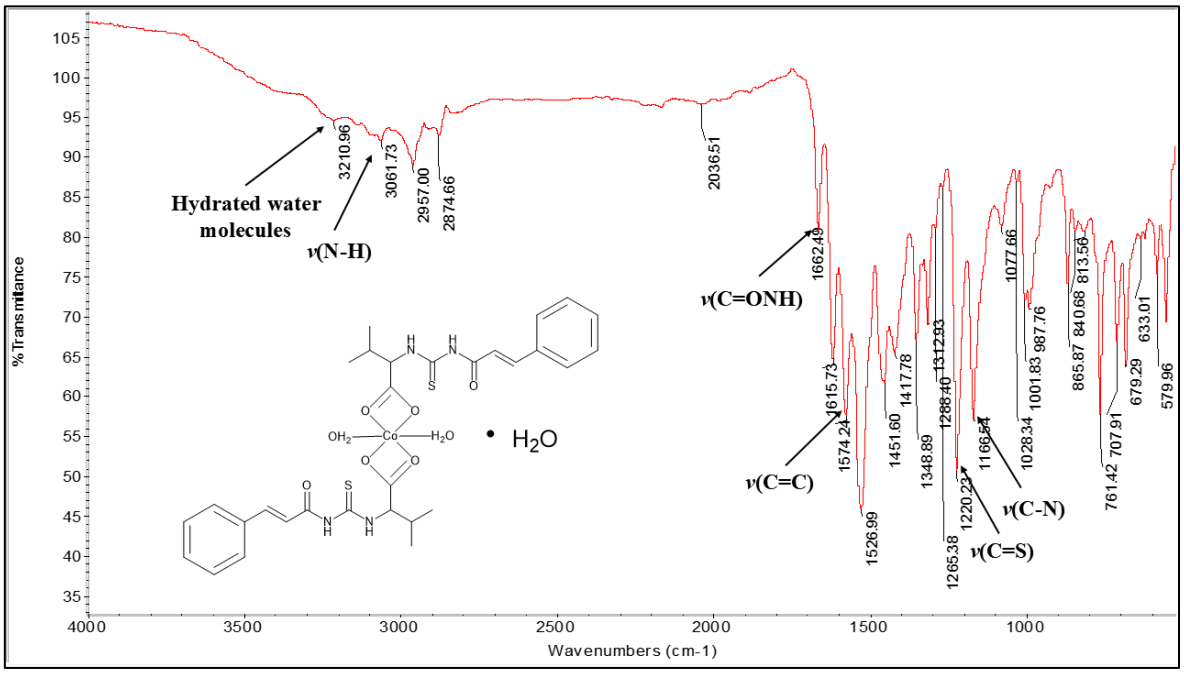

Appendix 22: FTIR spectrum of complex **3c**

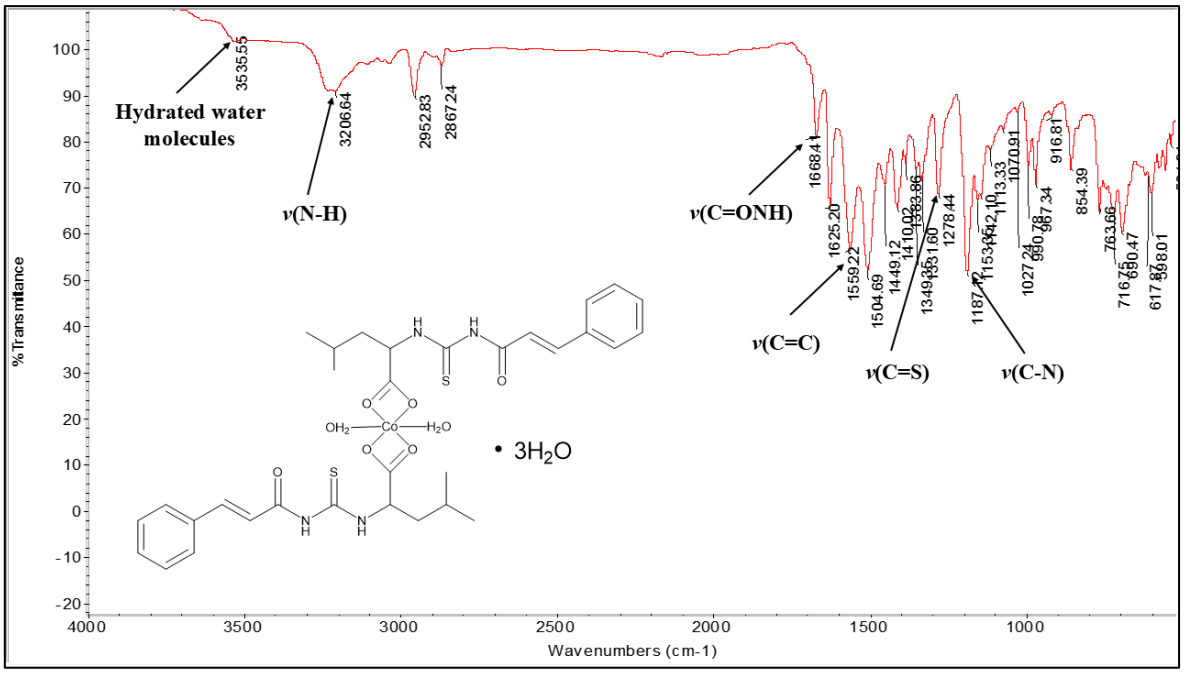

Appendix 23: UV-Vis spectrum of compound **1** vs complex **1b**

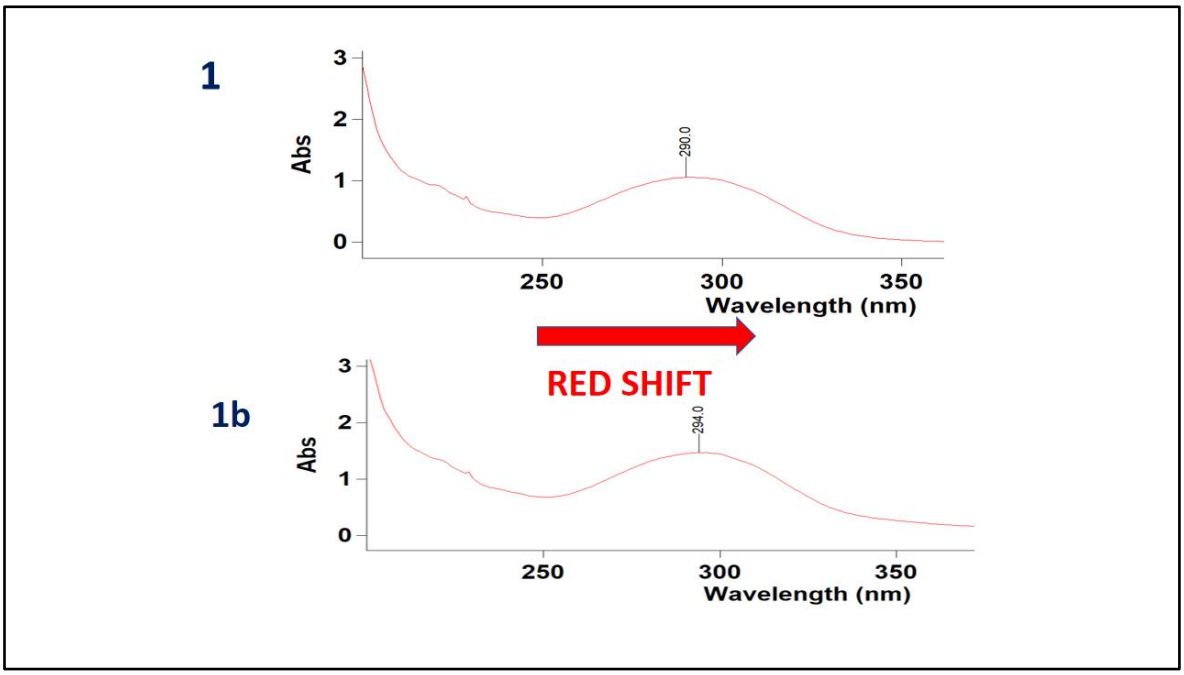

Appendix 24: UV-Vis spectrum of compound **1** vs complex **1c**

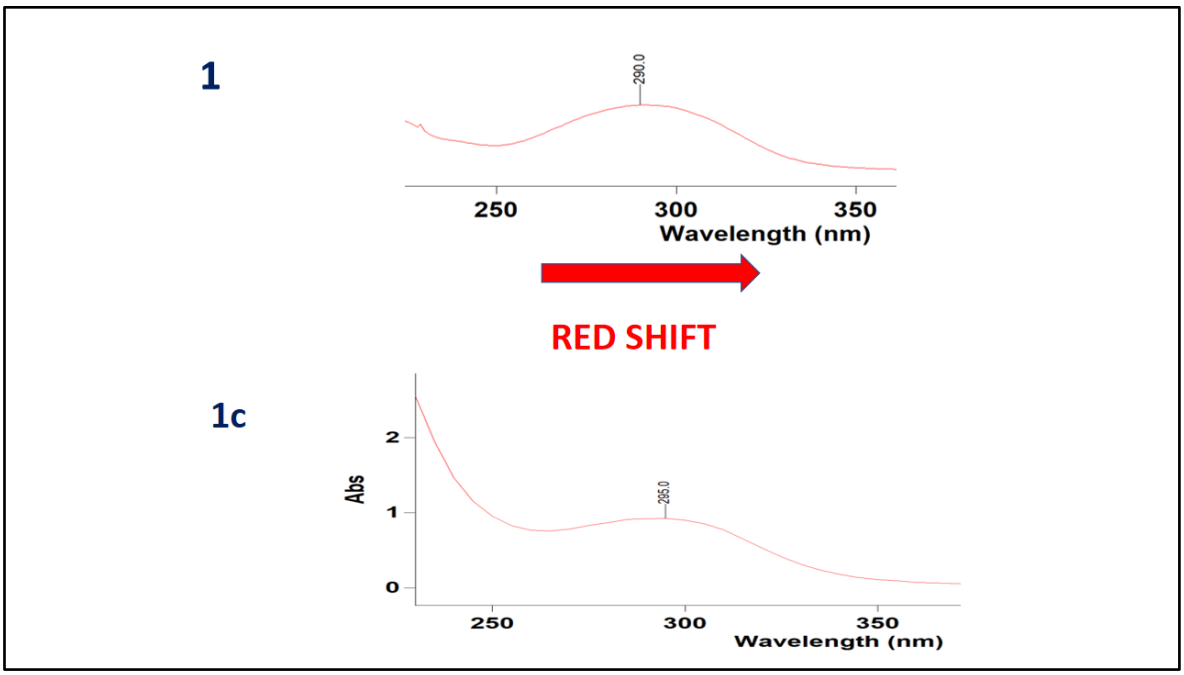

Appendix 25: UV-Vis spectrum of compound **2** vs complex **2a**

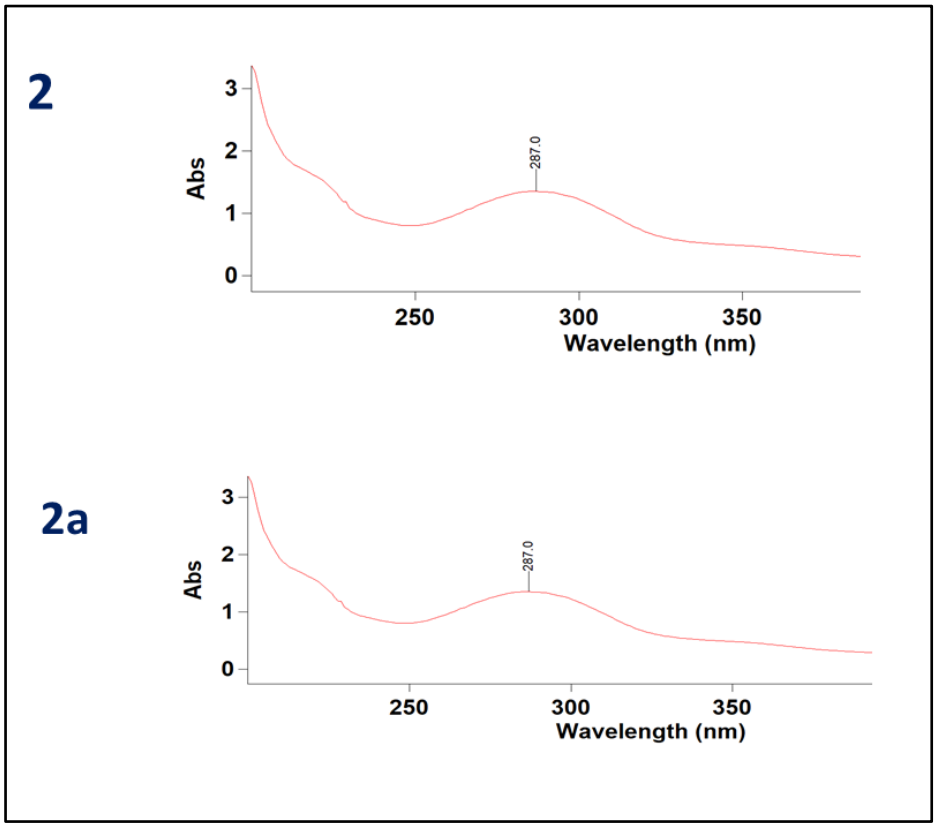

Appendix 26: UV-Vis spectrum of compound **2** and complex **2b**

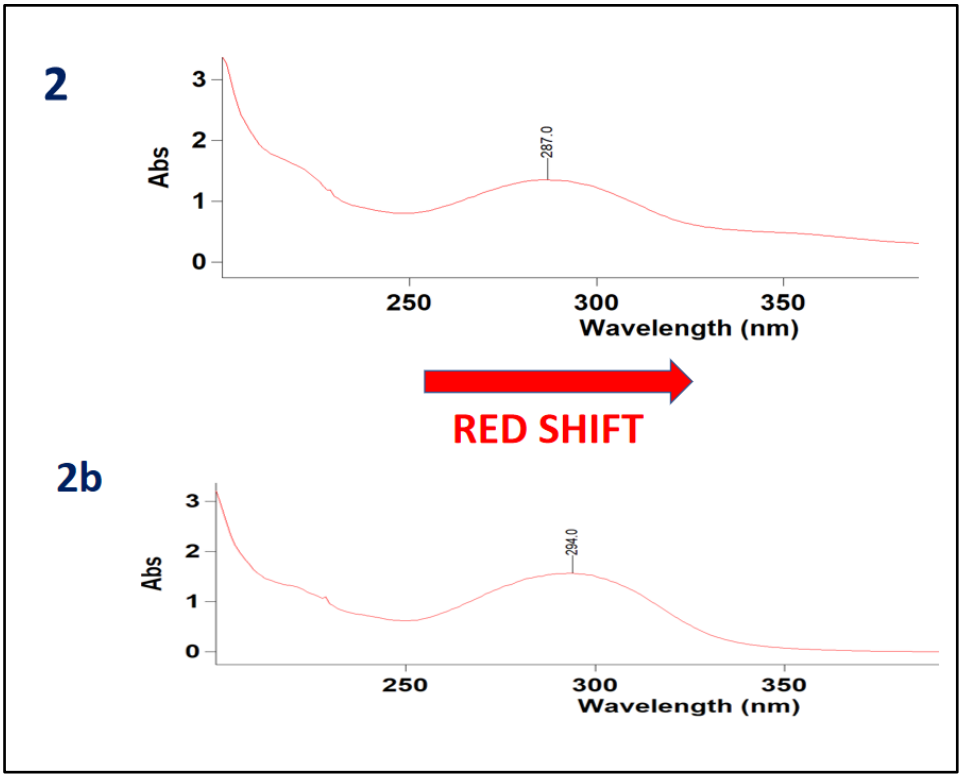

Appendix 27: UV-Vis spectrum of compound **2** vs complex **2c**

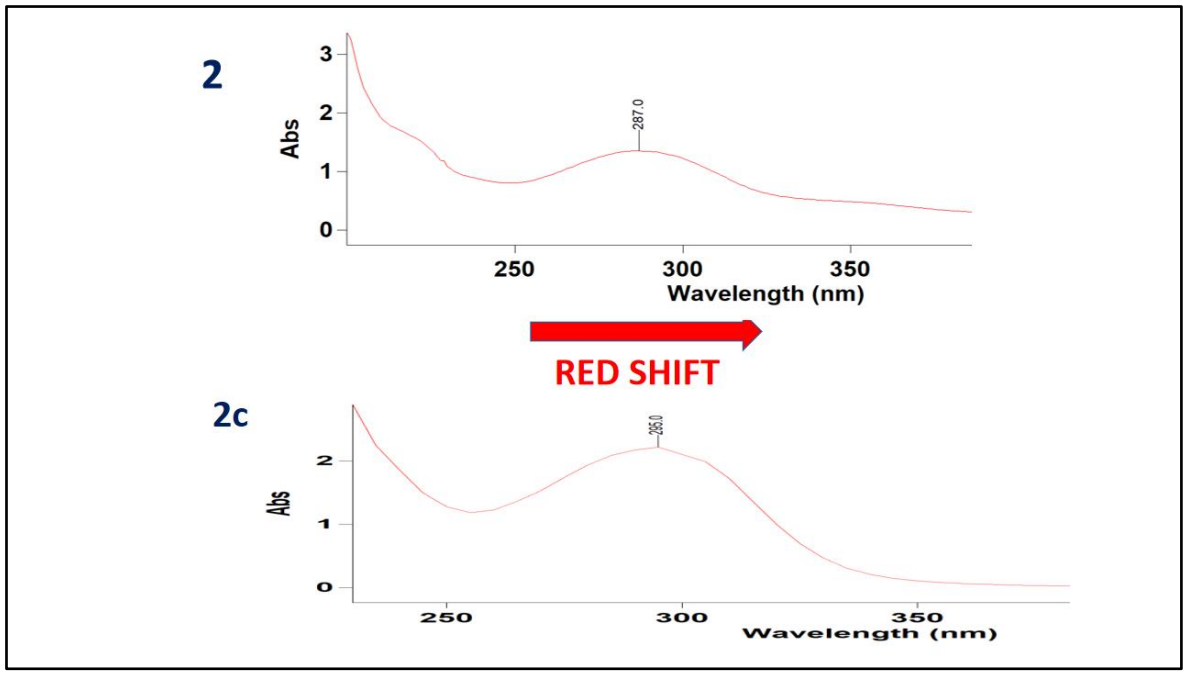

Appendix 28: UV-Vis spectrum of compound **3** vs complex **3a**

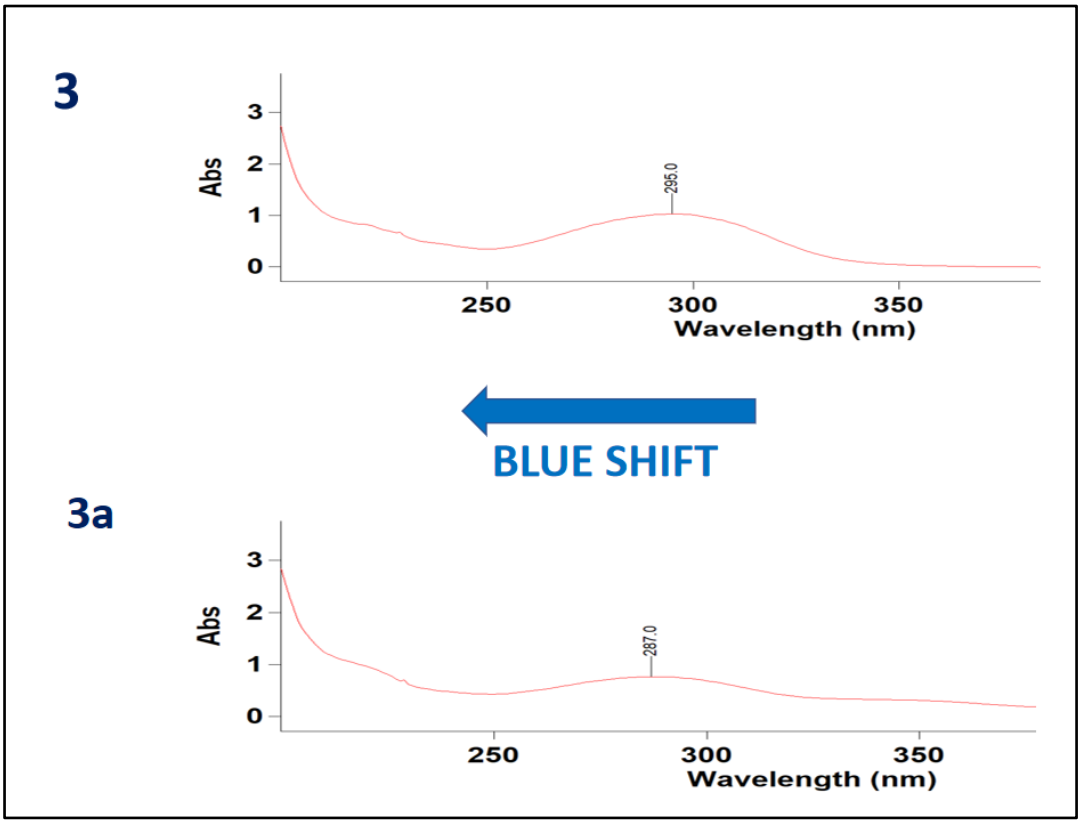

Appendix 29: UV-Vis spectrum of compound **3** vs complex **3b**

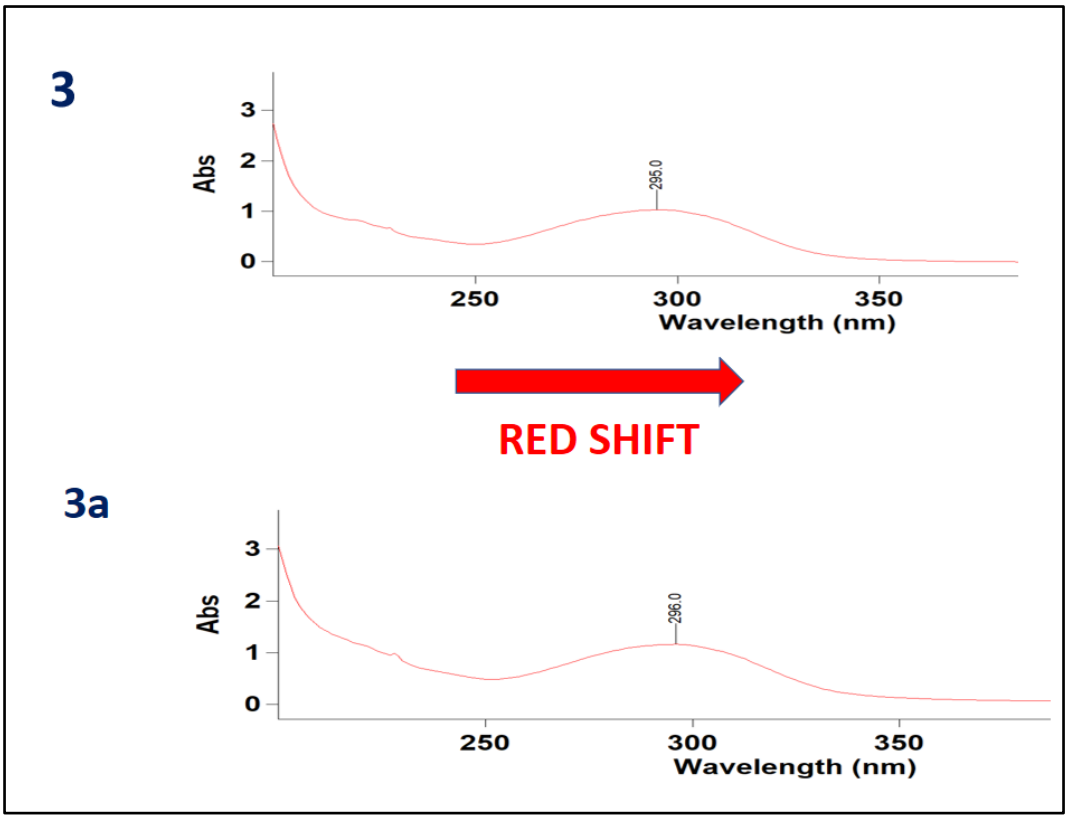

Appendix 30: UV-Vis spectrum of compound **3** vs complex **3c**

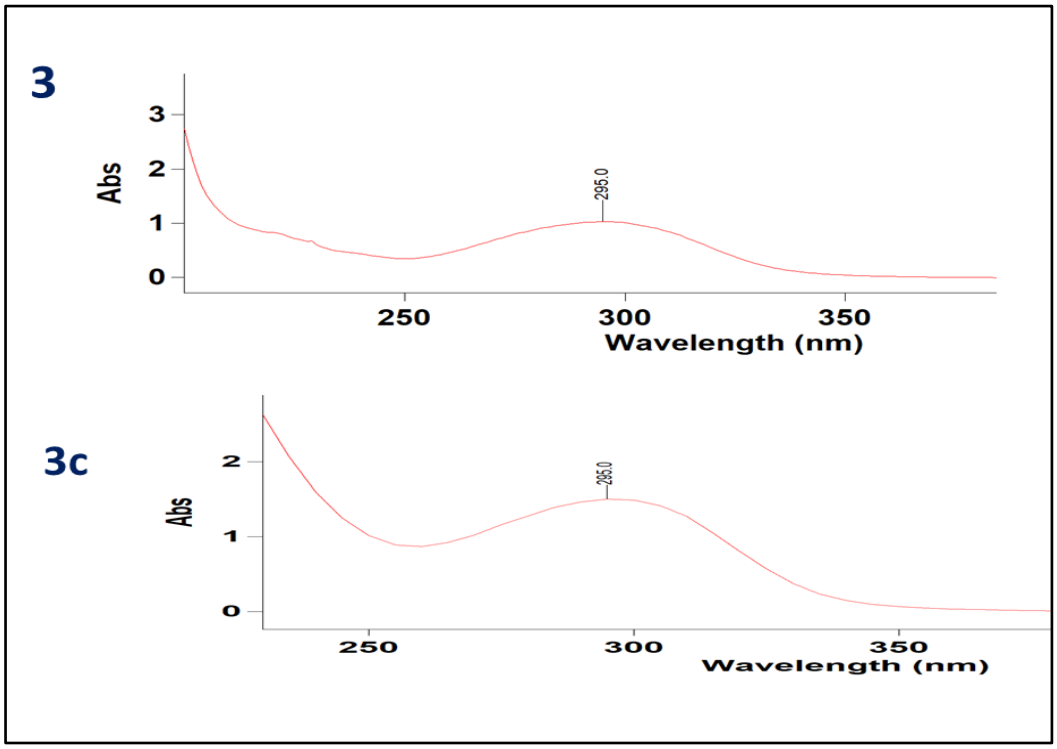

Appendix 31: ^{1}H NMR spectrum of compound **2**

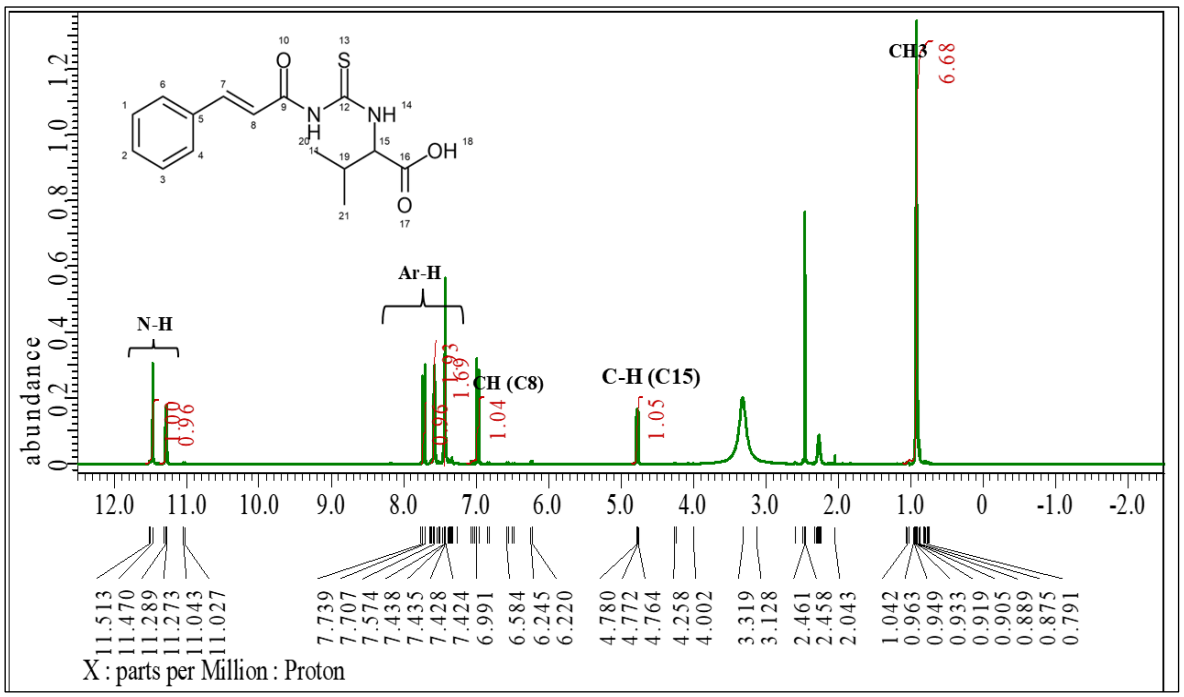

Appendix 32: ^{1}H NMR spectrum of compound **3**

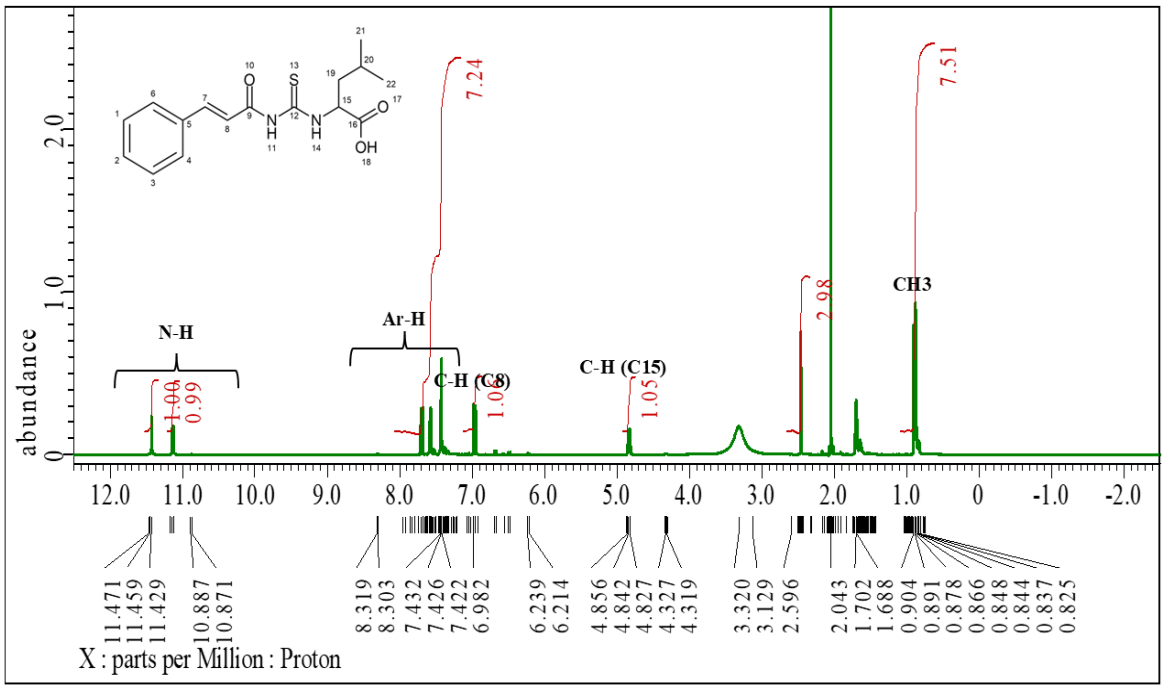

Appendix 33: ^{13}C NMR spectrum of compound **2**

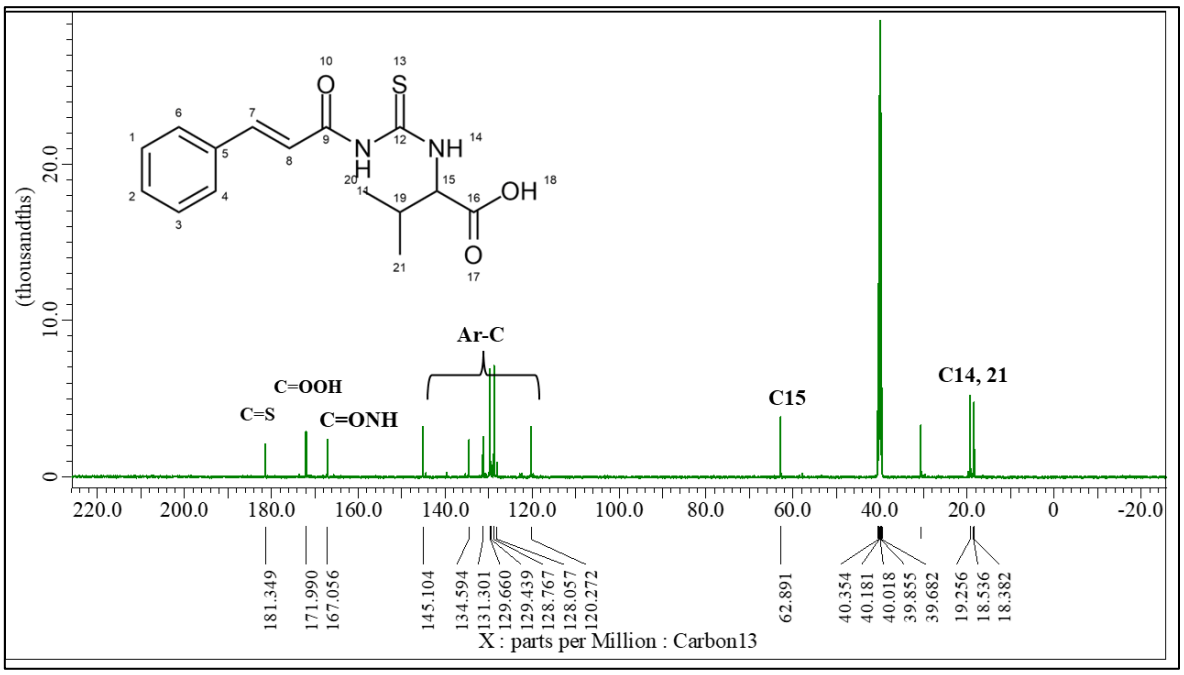

Appendix 34: ^{13}C NMR spectrum of compound **3**